

Production of Caseins Using Extrusion Technology

by

Jaouad Fichtali

Department of Food Science and
Agricultural Chemistry
Macdonald College,
McGill University,
Montreal, Canada

July, 1990

A Thesis submitted to the Faculty of Graduate Studies and Research in Partial fulfillment
of the requirements for the degree of Doctor of Philosophy

©Jaouad Fichtali, 1990

Dedicated to my parents

ABSTRACT

Jaouad Fichtali

Ph.D.

Food Science and
Agricultural Chemistry**Production of Caseins Using Extrusion Technology**

Preliminary experiments indicated that an acid casein co-precipitate could be produced by extrusion from skim milk powder (SMP). In assessing the problems encountered, experiments were designed to model and optimize the coagulation/washing process using response surface methodology (RSM), to minimize residual whey components and losses of fines. This study yielded useful information relative to improving our understanding of the coagulation mechanism and the most important variables affecting the process. In addition, RSM allowed multiresponse optimization of acid casein production using unique and newly developed optimization techniques. In order to simplify the process, an extruder die was designed to assist with the dewheyng process, however, plugging problems occurred due to screw design limitations. Studies were implemented to determine the rheological behaviour of sodium caseinate and to evaluate the extruder performance in terms of energy consumption, and in terms of mixing and conveying through mathematical description of residence time distributions in the extruder. The knowledge gained from these studies was integrated to produce acid casein and sodium caseinate at pilot plant level and to conceive a plant layout of the process for the dairy industry. The process developed has many advantages, including the ability to produce a high quality product.

RESUME

Jaouad Fichtali

Ph.D.

Sciences Alimentaires
et Chimie Agricole

Application de la Technologie d'Extrusion à la Production des Caséines

Des expériences préliminaires ont montré qu'une caséine acide co-précipité peut être produite par extrusion à partir du lait écrémé en poudre (LEP). Pour résoudre les problèmes rencontrés dans le processus, des expériences ont été effectuées selon la méthodologie des surfaces de réponse (MSR). La MSR a permis de caractériser et d'optimiser le processus de coagulation/lavage afin de minimiser les composés résiduels de lactosérum et les pertes en fines particules. Cette étude a généré de nombreuses informations dont l'identification des variables affectant de façon importante la coagulation, élargissant ainsi notre connaissance de ce processus. En plus, la MSR a permis une optimisation à réponses multiples pour la production de la caséine acide, en utilisant des techniques nouvelles d'optimisation. Dans le but de simplifier et d'accélérer le processus de séparation du lactosérum, une filière pour l'extrudeur a été construite. Cependant, un problème d'obstruction de la filière s'est manifesté lors de la production de la caséine. Des études ont été entreprises pour déterminer le comportement rhéologique du caséinate de sodium et évaluer la performance de l'extrudeur en termes d'énergie consommée et de capacité de mélange et de convoyage à l'aide d'une description mathématique des temps de séjour dans l'extrudeur. Les résultats obtenus ont été intégrés pour produire la caséine et le caséinate de sodium à l'échelle pilote et pour établir un schéma du processus pour une industrie laitière. Le processus développé s'avère très avantageux par rapport au processus conventionnel y compris la possibilité d'obtenir un produit de qualité supérieure.

ACKNOWLEDGMENTS

I wish to express my sincere gratitude to my supervisor, Dr. F.R. van de Voort, for his invaluable assistance, encouragement and confidence in conducting this research. The author acknowledges with sincere appreciation the Centre de Recherche et de Développement sur les Aliments (CRDA) for access to its facilities to complete the experimental work and the preparation of the manuscript. I owe a large debt of gratitude to a number of individuals from the CRDA, Technologie de Conservation Section, for their friendship and providing an excellent research atmosphere. Specifically, I wish to thank Dr. C.J. Toupin for accepting to be my co-director at CRDA and for his constructive criticism in reviewing part of this manuscript, Dr. G.J. Doyon, to allow me to work in his section and for his contribution to this research, J. Fortin for her friendship and her help in conducting the pilot plant experiments, and J. Gagnon for the extruder die drawing.

The author also wishes to thank Dr. L.L. Diosady, Department of Chemical Engineering, University of Toronto, who made the arrangement for using the SLOWPOK reactor. A special thank goes to my friend Francis Roebben and my brother Nour-dine for their assistance in the plant layout drawing, and to V. Barraquio for her help in the initial phases of this work.

I owe a large debt of gratitude to my parents whose support and encouragement have made this work possible and finally, I wish to thank all of my family and friends who supported me.

CONTRIBUTIONS TO KNOWLEDGE

The objective of this study was to conceive and design a completely new process to convert surplus skim milk powder (SMP) into added value acid casein and sodium caseinate. The concept of using an extruder for this process emerged from its versatility and flexibility as a continuous reactor and carrying out multiple unit operations. As we were dealing with developing a new process and a complex machine, extensive work was required which contributed to knowledge from a variety of aspects. These included basic milk chemistry, process engineering, product optimization and characterization, each of which are presented below:

- 1) A comprehensive review of flow behaviour, mixing, and residence time distribution in twin screw extruders. The review served to transfer concepts from polymer engineering to food science/food engineering in a manner conducive to the future development, modelling, and process applications of extrusion in the food sector.
- 2) The first application of an extruder for the continuous coagulation of skim milk powder.
- 3) An extensive study of the coagulation/washing process using response surface methodology (RSM) to produce acid casein from SMP. Critical parameters were determined which may help in control and improvement of acid casein manufacture.
- 4) The physico-chemical mechanisms affecting the coagulation efficiency of concentrated milk were investigated as little was known about the coagulation mechanism of concentrated milk.

5) New multiresponse optimization techniques were applied to acid casein production and their performance characteristics compared. This included a newly devised optimization technique developed by the author, namely, Extended Surface Response Procedure (ESRP) for multiresponse optimization. These techniques provide a tool for simulation and modelling of multivariate processes from statistical viewpoint. Their use in process engineering can assist in new product development efforts and optimization.

6) A die was designed and tested for assisting in whey separation from casein using the extruder. This was the first attempt of using the extruder for a separation process in the food sector. Although not successful in this application, indications were that future applications of the extruder in separation technology may be possible.

7) A rheological model for sodium caseinate was developed which would be useful for sodium caseinate manufacturing and applications, whether conventional or extrusion processes.

8) The performance of the extruder for acid casein neutralization was evaluated in terms of energy consumption, and in terms of mixing and conveying using mathematical descriptions of residence time distributions. This study supported the application of the extruder as a chemical reactor in the food sector.

9) Production of acid casein and sodium caseinate were combined at pilot plant scale using all the information gained in this study and the process produced a very satisfactory product. A plant layout was developed which could be used by the dairy industry.

In Summary, through a combination of basic research and engineering concepts a new process of converting SMP to acid casein and sodium caseinate was developed. Taken as a whole the process is a major contribution to dairy technology and extrusion processing.

TABLE OF CONTENTS

		Page
	ABSTRACT	iii
	RESUME	iv
	ACKNOWLEDGEMENTS	v
	CONTRIBUTIONS TO KNOWLEDGE	vi
	NOMENCLATURE	xi
	LIST OF FIGURES	xiv
1	GENERAL INTRODUCTION	1
2	LITERATURE REVIEW	3
2.1	INTRODUCTION	3
2.2	CASEIN/CASEINATE CHEMISTRY AND PRODUCTION	4
2.2.1	Introduction	4
2.2.2	Casein Chemistry	4
2.2.3	Acid Casein Production	6
2.2.4	Caseinates Production	9
2.2.5	Conclusion	13
2.3	TWIN SCREW EXTRUSION: A BASIC UNDERSTANDING	14
2.3.1	Introduction	14
2.3.2	Extruders Types and Their Operational Characteristics	14
2.3.2.1	Single-Screw Extruders	14
2.3.2.2	Twin-Screw Extruders	15
2.3.3	Process Variables and Process Control	19
2.3.4	Rheology	26
2.3.5	Modelling and Optimization	27
2.3.6	Conclusion	30
2.4	FLOW BEHAVIOUR, MIXING AND RESIDENCE TIME DISTRIBUTION IN RELATION TO TWIN SCREW EXTRUSION	31
2.4.1	Introduction	31
2.4.2	General Concepts Related to Flow	33
2.4.3	General Concepts Related to Mixing	41
2.4.3.1	Velocity and Stress Distributions	42

		ix
2.4.3.2	Strain Analysis	44
2.4.3.3	Use of Analytical Procedures	46
2.4.4	Residence Time Distribution	48
2.4.4.1	RTD Basics	49
2.4.4.2	Calculation of Experimental RTD Functions and Tracer Techniques	52
2.4.4.3	Process Variables in Relation to RTD	54
2.4.4.4	Models for RTD	56
2.4.5	Conclusion	65
2.5	CONCLUSION	67
3	RESULTS AND DISCUSSION	68
3.1	ACID COAGULATION OF SKIM MILK POWDER BY EXTRUSION PROCESSING: A PRELIMINARY EXPERIMENT	68
3.1.1	Introduction	68
3.1.2	Materials and Methods	69
3.1.3	Results and Discussion	72
3.1.4	Conclusion	75
3.2	COAGULATION AND WASHING CONDITIONS FOR ACID CASEIN PRODUCTION	77
3.2.1	Introduction	77
3.2.2	Material and Methods	78
3.2.3	Results and Discussion	82
3.2.4	Conclusion	95
3.3	EFFECT OF COAGULATION AND WASHING CONDITIONS ON FINES, WATER HOLDING CAPACITY AND MICROSTRUCTURE OF ACID CASEIN CURD	96
3.3.1	Introduction	96
3.3.2	Material and Methods	97
3.3.3	Results	97
3.3.4	Discussion	107
3.3.5	Conclusion	113
3.4	MULTIRESPONSE OPTIMIZATION OF ACID CASEIN PRODUCTION	115
3.4.1	Introduction	115
3.4.2	Material and Methods	116
3.4.3	Results and Discussion	119
3.4.4	Conclusion	125

3.5	AN EXTRUDER DIE DESIGN FOR WHEY SEPARATION	127
3.5.1	Introduction	127
3.5.2	Material and Methods	128
3.5.3	Results and Discussion	128
3.5.4	Conclusion	131
3.6	RHEOLOGICAL BEHAVIOUR OF SODIUM CASEINATE	132
3.6.1	Introduction	132
3.6.2	Material and Methods	133
3.6.3	Results and Discussion	134
3.6.4	Conclusion	143
3.7	EVALUATION OF THE TWIN SCREW EXTRUDER PERFORMANCE FOR ACID CASEIN NEUTRALIZATION	144
3.7.1	Introduction	144
3.7.2	Material and Methods	145
3.7.3	Results and Discussion	151
3.7.4	General Discussion and Conclusion	168
3.8	PILOT PLANT PRODUCTION OF CASEINS USING EXTRUSION PROCESSING. I. ACID CASEIN PRODUCTION	171
3.8.1	Introduction	171
3.8.2	Material and Methods	172
3.8.3	Results and Discussion	175
3.8.4	Conclusion	186
3.9	PILOT PLANT PRODUCTION OF CASEINS USING EXTRUSION PROCESSING. II. SODIUM CASEINATE PRODUCTION	187
3.9.1	Introduction	187
3.9.2	Material and Methods	188
3.9.3	Results and Discussion	191
3.9.4	Plant Layout Concept	196
3.9.5	Conclusion	199
4	GENERAL CONCLUSION	202
	LITERATURE CITED	204
	APPENDICES	215

NOMENCLATURE

A	Constant in truncation equation
A_n	Cross sectional area in nip zone (m^2)
a	Slope of the estimated tail (semi-log plot)
b	Coefficient of exponent
$C(t)$	Tracer concentration at time t ($Kg\ cm^{-3}$ or counts g^{-1})
$C(\theta)$	Normalized residence time distribution function
C_c	Last measured concentration (counts g^{-1})
D	Screw diameter (m)
D_c	Axial dispersion coefficient ($cm^2\ s^{-1}$)
$F(t)$	Cumulative residence time distribution function
$F(\theta)$	Normalized cumulative residence time distribution
F_d	Drag flow shape factor (dimensionless)
F_p	Pressure flow shape factor (dimensionless)
f_d	Weight fraction of material which delayed in dead space
$E(t)$	Residence time distribution
$E(\theta)$	Normalized residence time distribution
E_a	Activation energy for flow ($Kcal\ g^{-1}\ mol^{-1}$)
E_k	Apparent kinetic factor at infinite time
e	Flight width (m)
h	Height of a slit die (m)
H	Channel depth (m)
i_m	Index of axial mixing
K	Die geometry constant/Constant
L	Barrel length (m)/Die length (m)
M	Product moisture (%)
m	Consistency index
N	Screw speed (revolution s^{-1})
n	Number of CSTRs in series/Flow behaviour index
P	Pressure in screws ($N\ m^{-2}$)/Plug flow time (s)
Pe	Peclet number
p	Number of channels in parallel
Q	Volumetric flow rate ($m^3\ s^{-1}$)
Q_d	Drag flow rate ($m^3\ s^{-1}$)
Q_p	Pressure flow rate ($m^3\ s^{-1}$)
Q_n	Nip flow rate ($m^3\ s^{-1}$)
R	Gas constant ($Kcal\ g^{-1}\ mol^{-1}\ K^{-1}$)
R'	Truncation error
r	Die orifice radius (m)

T	Temperature ($^{\circ}\text{C}$ or K)
T_c	Dimensionless time required for a fluid particle to traverse a streamline in the chamber
Tr	Torque
t	Time (s)
\bar{t}	Mean residence time (s)
t_e	Time of last sample (s)
t_a	Mean residence time in active volume (s)
t_d	Mean residence time in dead volume (s)
u	Average axial velocity (m s^{-1})
V_b	Tangential velocity of the barrel (m s^{-1})
V_r	down channel velocity of the barrel (m s^{-1})
V_x	Cross channel velocity of the barrel (m s^{-1})
V_f	Filled volume of screws (m^3)
v_x	Axial velocity (m s^{-1})
v_z	Down channel velocity (m s^{-1})
v_n	Velocity in the nip zone (m s^{-1})
v_o	Circumferential velocity in Burkhardt et al., (1978) model (m s^{-1})
W	Channel width (m)
w	width of the slit die (m)
x	Cross channel coordinate (m)
y	Channel depth coordinate (m)
z	Down channel coordinate (m)

Greek letters

α	Index of positive displacement
γ	Shear strain (dimensionless)
γ_c	Shear strain over one cycle in the chamber
γ_t	Shear strain per T_c
$\dot{\gamma}$	Shear rate (s^{-1})
$\dot{\gamma}_w$	Shear rate at the die wall (s^{-1})
Δ	Difference operator
ϵ	System phase shift (s)
η	Viscosity coefficient/Apparent viscosity (Pa s)
η^*	Reference apparent viscosity (Pa s)
θ	Normalized time
μ	Newtonian viscosity ($\text{kg m}^{-1} \text{s}^{-1}$)
μ_o	Casson plastic viscosity ($\text{kg m}^{-1} \text{s}^{-1}$)
μ_d	Viscosity at the die ($\text{kg m}^{-1} \text{s}^{-1}$)
σ^2	Variance of residence time distribution (s^2)
σ_g^2	Variance of Gaussian distribution (s^2)
τ	Shear stress (Pa)
τ_o	Yield stress (Pa)

τ_w	Die wall shear stress (Pa)
τ_{yz}	Acting stress perpendicular to y-axis in z direction ($N\ m^{-2}$)
ϕ	Ratio of pressure flow to drag flow
ψ	Helix angle (radians or degrees)

Abbreviations

CCP	Colloidal Calcium Phosphate
CSTR	Continuously Stirred Tank Reactor
ERSP	Extended Response Surface Procedure
GDA	Generalized Distance Approach
HTST	High Temperature Short Time
MR	Multiple Response
RSM	Response Surface Methodology
RTD	Residence Time Distribution
SEC	Specific Energy Consumption
SMP	Skim Milk Powder
SSE	Single Screw Extruder
TSE	Twin Screw Extruder
WPN	Whey Protein Nitrogen
WWR	Wash Water Ratio

LIST OF FIGURES

	Page
Figure 1. Schematic diagram of fully intermeshing counter- and co-rotating extruder screws (a); pressure distribution in counter- and co-rotating extruder (b); and cross sections of the flights in the intermeshing zone of counter- and co-rotating extruder (c).	16
Figure 2. Schematic representation of the process, design and system variables in relation to extruder performance and target variables.	21
Figure 3. Schematic diagram of a feedback control system using a control algorithm.	25
Figure 4. Basic channel geometry.	
Figure 5. Cross-sectional view of a co-rotating twin screw extruder (a); and cross-sectional view of the unwound channel of a co-rotating twin screw extruder (b).	37
Figure 6. Tracer input into extruder and the resulting $E(t)$ and $F(t)$ functions which describe the residence time distributions.	50
Figure 7. Some of the flow models used to describe residence time distributions in an extruder which are: Levich et al. (1967) model (a); GAMMA model with recirculation (b); and CASPAR model (c).	61
Figure 8. Schematic diagram of a data acquisition system used to collect extrusion data during processing.	71
Figure 9. Continuous plots of the data collected during the extrusion run using the data acquisition system illustrated in Figure 8.	73
Figure 10. Experimental set-up for coagulation/washing process.	
Figure 11. A surface response plot of predicted residual ash (%) as a function of coagulation pH and SMP concentration.	85
Figure 12. Contour plot of the predicted residual sodium (mg/g) as a function of coagulation pH and SMP concentration.	86

- Figure 13.** A surface response plot of predicted residual lactose (%) as a function of SMP concentration and washing time. 88
- Figure 14.** A contour plot of predicted residual lactose (%) as a function of coagulation pH and washing temperature. 89
- Figure 15.** A surface response plot of predicted residual WPN (%) as a function of coagulation pH and SMP concentration. 90
- Figure 16.** Superimposed contour plots of predicted percent ash (∇) and percent lactose (\blacktriangledown) as a function of coagulation pH and SMP concentration. 92
- Figure 17.** Effect of the number of washing stages on residual ash, lactose, whey protein nitrogen, and lactose in wash water. 93
- Figure 18.** Titration curves of skim milk powder at 45°C and different concentrations. 100
- Figure 19.** Contour plots of the predicted percent fines as a function of pH and concentration. 101
- Figure 20.** Contour plots of the predicted percent fines as a function of concentration and agitation (rpm) at a fixed pH of 4.42. 102
- Figure 21.** Effect of pH on percent fines at two coagulation temperatures. 104
- Figure 22.** Contour plots of the predicted water holding capacity after the last wash as a function of pH and temperature. 105
- Figure 23.** Contour plots of the predicted water holding capacity after the last wash as a function of pH and concentration. 106
- Figure 24.** Scanning electron micrographs of acid casein obtained at pH of (A) 4.1, (B) 4.9, and (C) 4.5. 108
- Figure 25.** Scanning electron micrographs of acid casein obtained at concentration of (A) 10% SMP and (B) 50% SMP. 109
- Figure 26.** Scanning electron micrographs of acid casein obtained at temperature of (A) 40°C, and (B) 60°C. 109
- Figure 27.** Scanning electron micrographs of acid casein obtained at various conditions of pH, concentration and temperature. 110

Figure 28. Superimposed multiple response contour plots of predicted percent ash (∇), lactose (\blacktriangledown), and fines (\square) as a function of pH and concentration.	120
Figure 29. Schematic diagram of the die used for extrusion dewheying process.	129
Figure 30. Flow curves for sodium caseinate at 13% solid concentration as a function of temperature and shear rate.	136
Figure 31. Flow curves for sodium caseinate at 45°C as a function of concentration and shear rate.	137
Figure 32. Effect of temperature on viscosity of sodium caseinate at various concentrations.	139
Figure 33. Effect of concentration on viscosity of sodium caseinate at various temperatures.	141
Figure 34. Combined effect of temperature and concentration on the logarithmic of viscosity of sodium caseinate.	142
Figure 35. Pressure and temperature control zones, and screw configuration used for casein neutralization.	147
Figure 36. Residence time distribution of caseinate under various conditions.	150
Figure 37. Effect of barrel setting temperature profile (continuous lines) on product temperature profile (dashed lines).	152
Figure 38. Effect of last zones barrel temperature setting on product temperature at the exit, SEC, and pressure at the die.	153
Figure 39. Effect of screw speed on product temperature at the exit, SEC, and pressure at the die.	155
Figure 40. Effect of feed rate on product temperature at the exit, SEC, and pressure at the die.	156
Figure 41. Integral age distribution of caseinate under various conditions.	159
Figure 42. Typical experimental $E(\theta)$ distribution function for casein neutralization process compared to the dispersion model.	161

- Figure 43.** Typical experimental $E(\theta)$ distribution function for casein neutralization process compared to the tanks in series model. 162
- Figure 44.** Experimental $F(\theta)$ distribution functions for the casein neutralization process compared to the Wolf and Resnick model. 164
- Figure 45.** Typical fit of experimental $F(\theta)$ distribution function to the multistage Wolf and Resnick model. 166
- Figure 46.** Screw configuration and barrel temperature profile used for SMP coagulation. 173
- Figure 47.** Effect of separation technique on lactose removal for the whey off stage and each washing stage. 177
- Figure 48.** Effect of separation technique on ash removal for the whey off stage and each washing stage. 178
- Figure 49.** Effect of coagulation pH and SMP concentration (C) on the lactose removal for the whey off stage and each washing stage. 180
- Figure 50.** Effect of coagulation pH and SMP concentration (C) on the ash removal for the whey off stage and each washing stage. 181
- Figure 51.** Lactose concentration in the wash water as a function of contact time using screen for dewatering (solid lines) and centrifuge for dewatering (dashed lines) for each washing stage. 184
- Figure 52.** Screw configuration and barrel temperature profile used for casein neutralization. 190
- Figure 53.** Pilot plant flow diagram used to produce acid casein and sodium caseinate. 192
- Figure 54.** Viscosity curves of sodium caseinates P1, P2 and P4 listed in Table 22 at 25°C and 10 % solids content. 197
- Figure 55.** Scanning electron micrographs of sodium caseinate obtained from SMP using extrusion (A) and its comparison to a commercial roller dried sodium caseinate (C) and commercial spray dried caseinates (B, D, and E). 198
- Figure 56.** Plant layout concept for caseinate production using extrusion technology. 200

1 GENERAL INTRODUCTION

Canada, the United States, and the European Economic Community (EEC) have a chronic oversupply of milk of which substantial amounts are converted into skim milk powder. In 1985-86, 69.9 thousand tonnes of Canada's Skim Milk Powder (SMP) was mostly exported as is, while 11.8 thousands tonnes were exported in the form of whole milk products to reduce surplus butter stocks (Canadian Dairy Commission, 1986). As early as 1978, one option considered in Canada has been the diversion of this oversupply of SMP into casein production (ACP Marketing, 1978). The production of 9.1 million Kg of casein could divert 31.8 million Kg of SMP into a functionally useful food ingredient and save the Canadian Dairy Commission one to three million dollars per year (Canadian Dairy Commission, 1983).

World production of casein is about 150 thousand tonnes from which 70 to 80% is used for food ingredients (Muller, 1982). The largest amounts of casein and caseinates are used in cheese imitation manufacturing (33%) and coffee whitener (10%). The United States imports about 70 thousands tonnes of casein and caseinate annually and uses about 75-80% of this amount in formulated food applications (Gwozdz, 1983).

Casein production is a well developed industry, specifically in the leading producing countries such as New Zealand and Australia, but also in France, Ireland and Argentina. Neutralization of imported casein to form caseinates is carried out in the United States. Competition and increasing sophistication of end-user requirements for industrial casein, including edible grades, has pressured manufacturers to produce improved milk protein products with specific functional properties and closely controlled quality parameters (Muller, 1982). To meet market requirements for cost reduction and

improved product, research was undertaken to introduce more efficient methods of manufacture in plants designed.

In 1986, where this research program was conceived, the Canadian SMP surplus and the lack of caseinate technology in Canada led to the consideration of converting SMP directly to acid casein and sodium caseinate using extrusion processing. Extrusion had the potential of being simpler than the conventional processes in use, could be more economical, flexible, controllable and have the ability of producing new and different products. The aim of this thesis was to conceive and to develop such technology for dairy industry through basic research with the intent of developing a usable application. The steps taken, results obtained, interpretation, discussion of the results, and the conclusions drawn are presented in the form of nine papers, most of which are in press for publication. In addition, two review papers form the backbone of the literature review section, and a general conclusion was developed from the interrelated aspects at the end of this thesis.

2 LITERATURE REVIEW

2.1. INTRODUCTION

The relevant literature related to casein/caseinate production and to twin screw extrusion is reviewed in following three chapters. The first chapter introduces basic casein chemistry and highlights the present status of casein and caseinate production. The second chapter focuses on the understanding of the practical and fundamental aspects of twin screw extrusion required for this work and is based on an invited paper (Fichtali & van de Voort, 1989) published in *Cereal Foods World*. The last chapter is a detailed review article submitted to the *Journal of Food Engineering*, dealing specifically with engineering aspects of twin screw extrusion, such as, flow, mixing, and residence time distribution. This paper updates the theoretical aspects and research findings of extrusion from the polymer engineering side, for which extrusion processing is the most developed, and translates the findings into practical terms for the food scientist and engineer, providing a set of useful tools for evaluating food extrusion processes and their optimization.

2.2 CASEIN/CASEINATE CHEMISTRY AND PRODUCTION

ABSTRACT

Milk proteins are among the most widely consumed human food proteins and consequently, are the best characterized of all food proteins. Acid induced coagulation is an important process in separating and purifying caseins. This chapter introduces casein chemistry and updates casein/caseinate production knowledge in terms of coagulation, washing, dewatering, neutralization and drying.

2.2.1 Introduction

Many of the unique properties of proteins have been exploited in food production since pre-historic times, e.g. the rennet or acid coagulation of the casein of milk in the manufacture of cheese or fermented dairy products. The expansion and increasing sophistication of food processing has led to the development of many fabricated foods and has created the need for purified proteins to perform specific physico-chemical functions in these products. Bovine milk contains ~ 12% solids, which include fat, lactose, protein, and organic and inorganic salts. The first step in the isolation of the casein fraction from milk is the removal of fat to yield a skim milk from which the casein is isolated after coagulation. The mechanism of coagulation of casein involves partial dissociation of the micelle followed by reassociation of caseins into aggregates and rapid precipitation (Kim & Kinsella, 1989).

2.2.2 Casein Chemistry

The basic casein chemistry has been reviewed extensively by numerous authors (Fox, 1982; Swaisgood, 1982; Kinsella et al., 1989; Fox, 1989; Schmidt, 1982). Caseins

are usually defined as those milk proteins insoluble at 20°C and pH 4.6, the isoelectric pH. About 80% of the milk proteins are caseins which exist as coarse colloidal particles, termed micelles, with molecular weights of $\sim 10^8$ and mean diameter of ~ 100 nm (Fox, 1989). Casein micelles are composed of a number of small subunits, commonly referred to as casein submicelles. The micelles consist of about 90% protein and 6% colloidal calcium phosphate (CCP). In spite of its low proportion, CCP plays a key role in maintaining the integrity of the casein micelles.

Isoelectric casein consists of four principal primary proteins (gene products): α_{s1} -, α_{s2} -, β -, and κ -, in an approximate ratio of 40:10:35:12, in addition to several minor proteins which include γ - and λ -casein (Fox, 1989). All the caseins are relatively small molecules, $\sim 20,000$ - $24,000$ daltons and are insoluble around their isoelectric points. The caseins are strongly hydrophobic in the order $\beta > \kappa > \alpha_{s1} > \alpha_{s2}$. The four primary caseins exhibit "microheterogeneity" due to variations in the degree of phosphorylation or glycosylation, disulphide-linked polymerization and genetically-controlled amino acid substitution (genetic polymorphism). The caseins are amphipathic, unstructured, open molecules. This structure in addition to their hydrophobicity are of considerable technological significance. Hydrophobic bonding is probably significant in such functional properties as viscosity, gelation, water sorption, foaming and emulsification. The open structure of the caseins renders them more susceptible to proteolysis than the globular whey proteins and allows them to spread readily at interfaces. Their amphipathic structures facilitate orientation of the hydrophobic residues into the air or oil phases with the hydrophilic residues in the aqueous phase, optimizing their surfactant properties.

Several interactions may occur between casein molecules, such as hydrophobic bonding, hydrogen bonding, electrostatic interactions, disulphide bonding, and calcium bonding. The remarkable colloidal stability of the caseinate system is due to two constituents: κ -casein and CCP. Allied to these and partially arising from them, is a high degree of hydration (~ 2.0 g H₂O/g protein) and a high negative zeta-potential (~ 18 mV). Thus, the mechanism of milk coagulation is primarily concerned with

alterations in the structure of the micelles and their surface properties. Casein micelles can be destabilized by acid, ethanol and other organic solvents, heat, limited proteolysis, Ca^{2+} , or combinations of these. The destabilization results in coagulation or gelation and is exploited in the production of a range of dairy products.

Casein and caseinates can withstand considerable heat treatment before heat flocculation occurs, which probably reflects their open, random-coil quaternary structure and the lack of secondary and tertiary structures. This property is extensively exploited in the dairy industry in evaporation, drying and ultrafiltration processes. Sodium caseinate can withstand heat treatments up to 140°C for >60 min at pH 6.7. Five principal contenders for the primary reaction leading to the heat coagulation of casein are, acidification, dephosphorylation, hydrolysis of κ -casein, general proteolysis and Maillard browning. In the presence of oxygen, lactose is the source of most of the heat-induced acidity which reduces heat stability of caseins and is also involved in Maillard browning, its role in concentrated milk products being particularly significant (Fox, 1982).

Preheating of milk prior to concentration may induce denaturation of whey proteins and precipitation of calcium phosphate. The stability of the calcium-caseinate-phosphate complex to various coagulating agents declines rapidly on concentration. In most respects the stability of concentrated milks is more important commercially than that of milk of standard concentration, but due to its greater complexity it has not been studied extensively. Concentration induces major changes in the milk system such as, close packing of casein micelles, a higher concentration of denaturable proteins and precipitation of calcium phosphate which also causes a significant decrease in the pH. The coagulation mechanism for concentrated milks is much more complex than that of standard milks and the influence of the various compositional and processing factors thereon is not well understood (Fox, 1982).

2.2.3 Acid Casein Production

Casein can be separated from whey components by at least four techniques (Fox, 1989): isoelectric precipitation, rennet induced coagulation, ultracentrifugation, and salting out using $(\text{NH}_4)_2\text{SO}_4$. The latter two techniques are not of industrial importance, while isoelectric precipitation is the most commonly used method for the industrial preparation of casein.

The basic manufacturing processes and uses of edible caseins have been reviewed extensively by numerous authors (Muller, 1971; Richert, 1975; Muller, 1982; Southward, 1985; Southward, 1986; Mulvihill, 1989; Fichtali et al., 1990a). The process generally involves isoelectric precipitation of casein, the removal of whey using inclined screens, horizontal bowl centrifuges or roller presses, washing to remove the residual whey components, followed by dewatering, drying and grinding. The coagulum is produced by mixing skim milk and acid (HCl or H_2SO_4) at 30-35°C to obtain final pH of 4.3-4.6, followed by raising the temperature to 45°C using steam injection. A multi-stage countercurrent washing operation (4-6 stages), with a contact time of 20-30 minutes is usually used to remove the whey components. In general, D-shaped vats are used for washing the curd, although tube based systems (Gwozdz, 1983) and vertical vats (Jordan, 1983) have been reported to provide better washing efficiencies. Washing temperatures range from 30-75°C but are not the same for all washes. A high temperature wash (70-75°C) is generally carried out prior to the last wash to reduce microbial contamination with the final wash at temperatures of 40-45°C to minimize matting of the curd during the dewatering operation. Dewatering is usually done using a continuous press or horizontal centrifuge to attain a residual moisture level between 55-60%. The resulting casein is then dried using vibratory or fluidised bed dryers, although attrition drying is being used in Europe because of apparent improvements in product dispersability and wettability (Muller, 1982; Roeper, 1982; Gwozdz, 1983).

The production of high quality casein depends on the efficiency of the separation of caseins from the whey components and International standards generally require that residual lactose and ash be less than 0.1% and 2% respectively. A high lactose content

can be responsible for Maillard browning during the drying process and subsequent off-flavour development during storage (Cayen & Baker, 1963). In order to produce a caseinate which has low viscosity characteristics, a low calcium (ash) content is required (Southward, 1985). Separation depends to a large extent on the conditions associated with the coagulation process and subsequent washing of the curd. The mode and efficiency of the washing operation has a direct influence on production costs in relation to equipment requirements, water usage, energy inputs and the loss of fines.

The effect of coagulation temperature and pH on casein curd characteristics, including particle size distribution, curd strength and calcium content have been studied from laboratory scale up to commercial production levels by Jablonka & Munro (1985, 1986a, 1986b, 1987). Some theoretical aspects of lactose removal have been studied by Zadow (1971a, 1971b) who considered the efficiency of screen separation for countercurrent and concurrent washing. Hobman (1978) developed a model for predicting the water required to wash casein curd in a continuous multi-stage, countercurrent system. The model requires an accurate estimation of the Murphree Stage Efficiency (MSE) coefficient, an indicator of the approach to equilibrium in each washing stage. Bressan & Hobman (1985) extended this work to study the effects of particle size, curd residence time per washing stage and wash water temperature on MSE. Computer simulation of a continuous four-stage countercurrent washing process (Pearce et al., 1987) has provided additional insight into the relationship of curd lactose concentration to MSE and wash water ratio (WWR). The effects of MSE and WWR were assumed to be independent, however, their interaction may also affect the residual lactose in the curd.

The models noted above have improved lactose removal predictions, but still have some limitations, i.e., particle size, presence of other components and assumed diffusion coefficients. Particle size is assumed to be homogeneous, but can change dramatically with precipitation conditions (Jablonka & Munro, 1985). Most models only consider lactose as the whey component, ignoring whey proteins and minerals, and their diffusion characteristics. Furthermore, the temperature/diffusion coefficient relation developed by

Bressan et al. (1981) for total solids over the range of 25-58°C, used in other studies, may be limiting since the curd shrinks and firms at higher temperatures (O'Meara & Munro, 1982). This behaviour can lead to a decrease in curd porosity and offset any positive temperature effect on the lactose diffusion coefficient.

2.2.4 Caseinates Production

Casein is an insoluble product with limited applications to food formulations and should be neutralized by an alkali and converted into soluble sodium caseinate. Caseinates are widely used in various formulated foods as useful sources of protein because of their physico-chemical, nutritional and functional properties. Their manufacture and food uses have been reviewed by several authors (Muller, 1971; Richert, 1975; Muller, 1982; Segalen, 1982; Southward, 1985; Southward, 1986; Barraquio & van de Voort, 1988; Mulvihill, 1989). They are used in meat products for their emulsion stabilizing and water-binding properties and in baked products to control the water absorption characteristics to have the desired textural and organoleptic properties. They are of excellent supplementary value for cereals because of their high lysine and tryptophan contents, especially for wheat products such as flour which contain a low percentage lysine (Lohrey & Humphries, 1976). They are used as emulsifying, thickening and/or foam-stabilizing agents in coffee whiteners, whipped toppings, desserts, sauces, weaning foods, dietetic foods and others. They are also the common protein ingredients of various simulated cheese products. Besides their food uses, their industrial and pharmaceutical applications are also numerous (Muller, 1982; Southward, 1986). Different caseinates can be produced namely, sodium caseinate, calcium caseinate, magnesium caseinate, potassium caseinate and ammonium caseinate. Sodium caseinate is by far the most commonly used water soluble form of casein. Commercial sodium caseinates are not homogeneous in their physico-chemical properties and may differ substantially from fresh laboratory prepared caseinate (Dagleish & Law, 1988) leading to differences in their functional properties.

Caseinates may be produced from freshly precipitated acid casein curd or from dried casein. The manufacture of caseinate from fresh casein curd gives a blander flavour to the product and furthermore will reduce the production cost associated with drying and storage prior to its conversion to sodium caseinate (Cayen & Baker, 1963; Muller, 1971; Southward, 1985). Casein should have a low calcium content ($<0.15\%$, dry basis) to produce a caseinate solution with low viscosity properties, and a low lactose content ($<0.2\%$, dry basis) to produce sodium caseinate with the best colour, flavour and nutritional characteristics (Southward, 1985).

In general, caseinate is produced by a batch process, wherein the casein is dissolved in heated vats fitted with powerful stirrers by adding an alkali to obtain a pH 6.7-7.0. The most commonly used alkali is sodium hydroxide used in a quantity of ~ 1.7 - 2.2% by weight of the casein solids, however, sodium carbonate has also been used but generally costs more (Southward, 1985). The dissolving time can take up to 3 or 4 hours (Johnson, 1970) and in order to decrease this time, colloid mills are often used to reduce the particle size of casein curd before the addition of alkali to the slurry of about 25% solids. Recirculating the vat contents using high speed centrifugal pumps has also been used as a means to speed up the dissolution of casein (Johnson, 1970; Towler, 1976, Muller, 1982) but requires an increased equipment investment and furthermore the system does not guarantee a good homogeneity of all the solution in the vat (Johnson, 1970). The dissolving time for sodium caseinate is usually 30-60 minutes at a temperature of 60-75°C (Southward, 1985). The conversion rate depends on the particle size, agitation, temperature and concentration (Towler, 1976) all of which affect the viscosity of the slurry. Other factors can also affect the viscosity of the caseinate such as, pH, Ca content of the curd, type of alkali used and seasonal and genetic factors (Southward, 1985), however, pH was found to have a non significant effect within the range 6.7-7.1 (Towler, 1976).

Caseinate can be dried using roller-driers or spray driers equipped with either disc or pressure nozzle atomization. In the spray drying, the solution is generally heated

to 90-95°C to reduce its viscosity before the spray drying and at this temperature the maximum total solid content is usually ~20% (Muller, 1971). Thus the cost of spray drying of sodium caseinate is high and the processing rate is low when compared with the rate of production of SMP in which concentrates containing up to 50% total solids may be dried (Towler, 1978). Higher caseinate concentrations may be tolerated by the atomization system of the spray dryer if the temperature is raised. However, in order to preserve good flavour and functional attributes in the product, one should avoid high temperatures for long periods (Muller, 1971, Southward, 1985). Because of the low solid content of the feed solution, spray dried sodium caseinate has a low bulk density (0.25-0.40 g/ml) resulting in relatively high costs for storage and transport. Generally, pressure driers produce caseinate with a higher bulk density than that from disc atomizer driers (Segalen, 1982). Since the powder is light, the losses from the product cyclones may be rather high and it is therefore considered prudent to install bag filters for improved recovery.

Roller drying of sodium caseinate can be achieved with a relatively higher solids content than spray drying, resulting in a higher bulk density product. The roller drying of sodium caseinate requires a lower capital investment than spray drying, however, a higher level of supervision is needed, the throughput per unit time is usually lower, and its application is generally limited to casein for the meat industry (Segalen, 1982; Southward, 1985). Roller dried caseinates differ from spray dried caseinates in their proportion of casein fractions and they are much more insensitive to the presence of calcium ions (Dagleish & Law, 1988).

The high cost and the problems associated with spray drying have prompted investigators to produce granular sodium caseinate. Towler (1978) produced a granular sodium caseinate by reacting reduced moisture casein curd (>40%) with sodium carbonate at ambient temperature followed by drying using a pneumatic-conveying drier. The resulting product had a higher bulk density (0.65g/ml) and improved dispersability but lower solubility in water at 20°C than the spray dried product. Another alternative

means of producing granular caseinate, specifically used in France, is attrition drying, where milling is incorporated while drying the pulverized particles. The resulting product is very similar to a spray dried product but has a higher bulk density (0.5-0.6 g/cm³) and a lower energy costs (Roepert, 1982; Gwozdz, 1983). The conversion uses casein with minimum 45% total solids and sodium carbonate, mixed at a temperature not exceeding 15°C. The free-flowing mass is easily conveyed to the dryer, however, care is required with granular caseinate when adding the alkali to avoid localized high pH's which may cause the development of off-flavours. Complete conversion is not achieved with granular caseinates and the product is not completely soluble when reconstituted in water at low temperatures, often having poorer flavour stability than to spray dried caseinate.

The major problem associated with sodium caseinate production lies in its high viscous, glue like, characteristics increasing the dissolving time and limiting the maximum concentration for spray drying. The quality of caseinate depends on the temperature-time history associated with conversion of casein and the holding time before and during the drying.

Extrusion technology is a High Temperature Short Time (HTST) process and could be looked at as a means to handle more concentrated solutions, reduce the conversion time, increase the throughput and reduce the drying cost. Furthermore, it is a continuous process which can be readily adjusted, controlled and automated (Fichtali & van de Voort, 1989). Most work related to casein neutralization by extrusion is patented and little information is available in the open literature. Generally dried casein is used as a feed material and an alkali is pumped into the extruder to form a mixture of ~ 10-30% moisture (Southward, 1985). Drying is generally required after extrusion and can be achieved through the use of attrition drying (Boullé, 1987). Tossavainen et al. (1986) have studied the effects of extrusion process variables such as moisture, temperature, sodium bicarbonate concentration on the product characteristics using a twin screw extruder. The moisture levels used were between 20 and 30% and the temperature ranged from 65-112°C with the highest solubilities obtained at high moisture values and highest

expansion ratio obtained at low temperatures. Calcium paracaseinate can be extruded to obtain a porous and fibrous structure through an adequate choice of humidity, temperature and pressure (Szpendowski et al., 1983). The quest for new dairy products via texturization of casein arose from the fact that this material was in a state of over-supply (English, 1981).

2.2.5 Conclusion

Even though the effects of some variables, such as pH and temperature, on the acidic coagulation of casein micelles have been studied extensively, more information is needed to understand the mechanism of coagulation and how the properties of the product are affected. The higher complexity of concentrated milks renders their coagulation mechanism much less known as compared to normal liquid milk. The production of casein from SMP might differ from casein production from liquid milk in many aspects, such as, physico-chemical characteristics of the curd, yield, washing efficiency and functional properties of the end product. Although casein and caseinate production is a well established technology, the processes proposed and used up to now are rather complex and expensive. Problems related to washing efficiency predictions, flavour deterioration and other quality problems due to low efficiency of the neutralization system and/or Maillard browning, are still unsolved in casein industry. By combining the knowledge of casein chemistry, caseinate production technology and extrusion processing, the possibility of converting stable SMP, rather than normal milk to caseinates by extrusion can be explored systematically.

2.3 TWIN SCREW EXTRUSION: A BASIC UNDERSTANDING

ABSTRACT

Extrusion processing has been approached from both a fundamental and practical point of view to provide a basic understanding for non experts. The most important aspects of extrusion, such as, extruder types and their operational characteristics, process variables, process control, rheology, modelling and optimization are discussed.

2.3.1 Introduction

Extrusion technology is increasingly important in the food industry for transforming ingredients into intermediate or finished products. Though generally associated with a screw as a conveying mechanism, higher temperatures and pressures, extrusion is basically a specialized form of a continuous HTST reactor. The extruder is unique in working with relatively dry materials, plasticising the food mass, reducing microbial load, denaturing enzymes, gelatinizing starch, polymerizing proteins and most importantly, texturizing the end product into a desirable form. These combined operations are possible because there are a wide range of operator controllable variables including screw speed, screw profile, temperature, moisture, feed rate and die size/shape. The tremendous flexibility of extruders is both a boon and a bane, and new users must recognize the inherent complexity associated with such a processing system. The purpose of this chapter is to provide a basic understanding of both fundamental and practical aspects of extrusion processing, specifically in relation to the twin screw extruder.

2.3.2 Extruder Types and Their Operational Characteristics

2.3.2.1 Single-Screw Extruders

The main difference between a single and twin screw extruder is the conveying mechanism. The only force in the single screw extruder (SSE) that keeps the material from rotating with the screw and therefore makes it advance, is its friction against the barrel surface. Hence transport is based on the frictional and viscous forces associated with the mass. Thus the surface geometry of the barrel wall and the ratio of the barrel length to the screw diameter (L/D) are important factors in the design of a SSE. Under the same extrusion conditions, friction increases with the surface to volume ratio of the channel and contributes to the propulsive action as does having a grooved barrel surface. The flow in SSE is well understood and is considered as a combination of drag and pressure flow (Levine, 1988). Drag flow results from viscous drag and is proportional to screw speed while pressure flow is caused by increased pressure at the die and opposes drag flow. This flow mechanism explains the strong dependence of SSE operation on barrel design and pressure exerted by the die, which tend to limit its flexibility and operating range. The mixing of ingredients within the screw channel is also limited because laminar flow conditions generally exist, however, this can be minimized through the use of cut-flights screws and/or a grooved barrel. Increased back pressure behind the die can also help in improving mixing performance. One of the main limitations associated with the SSE is surging (variation in mass flow from the die), which is associated with variations in the frictional coefficient of the mass as well as changes in its viscosity.

2.3.2.2 Twin-Screw Extruders

Twin-screw extruders (TSE's) can be divided into co-rotating and counter-rotating types depending on the direction of screw rotation (Figure 1a). These in turn can be subdivided into fully intermeshing, partially intermeshing and non intermeshing screws, with the latter avoiding any protrusion of one screw within the channel of the other. Each of these categories of TSE's has distinct operating principles, functions and applications. The non-intermeshing type of TSE operate basically on the same principle as SSE, with

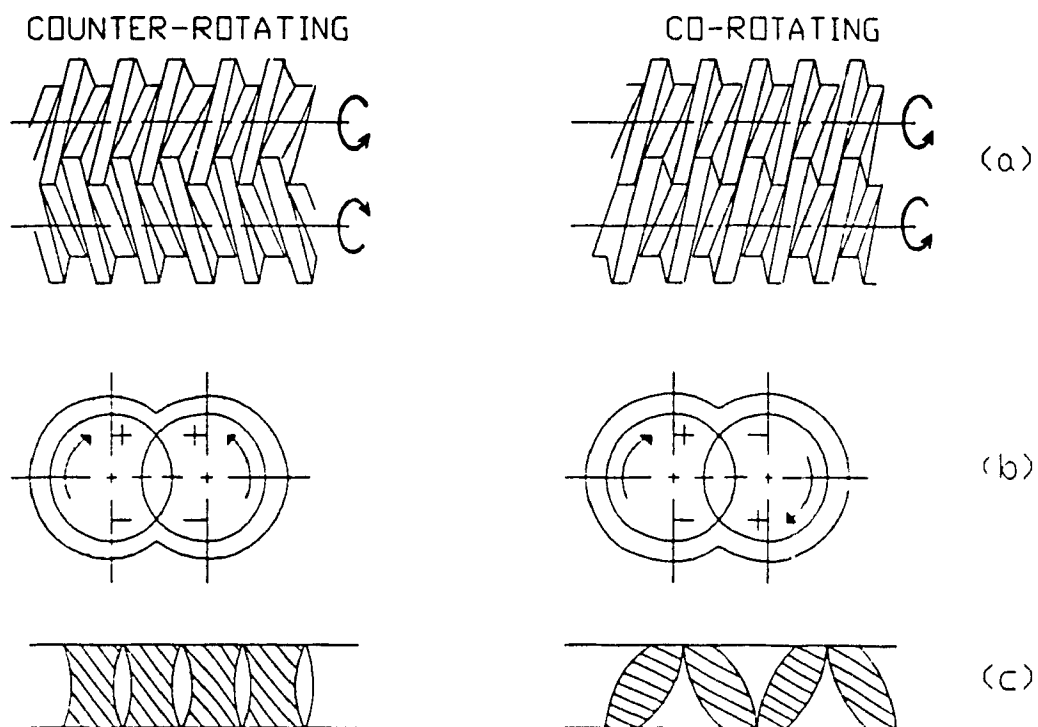


Figure 1. Schematic diagram of fully intermeshing counter- and co-rotating extruder screws (a); pressure distribution in counter- and co-rotating extruder (b); and cross sections of the flights in the intermeshing zone of counter- and co-rotating extruder (c).

the frictional characteristics of the material being the main factor controlling the transport mechanism. These extruders are rarely, if ever, used in food processing and therefore are not discussed further. TSE's with fully intermeshing screws have a geometrical configuration in which the material is enclosed in C-shaped chambers (compartments) formed by the two screws and the barrel. In the counter-rotating system, the closed C-shaped chambers have a small volume preventing material leakage from one screw to the other. Co-rotating screws form axially open channels and allow material exchange lengthwise in the machine. A cross section of the intermeshing zone (Figure 1c) shows the difference in the open area between the screws for the two systems. The differences in flight shape and screw geometry lead to the differences in the operational characteristics of these two groups of machines. These differences are related to conveying, working conditions, output, shear stresses, pressure build up, leakage flow, mixing, flow behaviour, and residence time distribution (RTD). These differences are discussed in general below, with flow, mixing and RTD being treated extensively in the next chapter.

Counter-Rotating Twin-Screw Extruders

Intermeshing counter-rotating TSE's with small gaps essentially form closed channels, which minimize leakage flow between channels, reduce mixing and residence time distribution. Under these circumstances, conditions close to plug flow occur, however, localized pressure builds up at the top of the chambers where the screws converge (Figure 1b), leading to high shear rates and stresses. These stresses can cause a wearing of the system by pressing the screws against the barrel. Since wear increases proportionally with screw speed, counter-rotating extruders are generally operated at lower speeds, resulting in lower throughputs for a given void volume. As a consequence of the general transport mechanism, a large percentage of material inside the channels is not exposed to sufficient uniform shear for good dispersion. The benefits of this design are good pumping action, high output efficiency, and narrow residence time distributions. Conversely, its limitations are poor mixing, lower throughputs, low product homogeneity and highly localized stresses which may lead to a shorter barrel life. To improve mixing and minimize the effects of high local pressures, larger clearances

between the screws is an option often considered but at the expense of pumping action due to increased backflow, making the machine more sensitive to variations in head pressure. Extruder performance can be improved by either reducing flight-tip width and/or increasing screw clearance, however such changes should be limited to the mixing zone and maintaining narrow gaps in the pumping zone. Counter-rotating extruders are used when high positive conveying action, low overall shear rates and narrow residence time distributions are required as in the case of thermally sensitive materials. These extruders are especially useful for running low viscosity materials, slurries or rapidly solubilizing sugars and gums.

Co-Rotating Twin-Screw Extruders

In co-rotating TSE's, closed chambers are not formed and the combined flights produce passages that allow material to move from the channel of one screw to the channel of the other. Hence there is no tangential pressure buildup and when the pressure is high for one screw, it is low for the other (Figure 1b). The material itself keeps the screws centred in the barrel, allowing small clearances to be used between the screws and the barrel, and between the screws, which gives them a self-cleaning action. There are no zones of localized high shear as in the case of counter-rotating screws, thereby reducing overall machine wear. The self-cleaning action of the screws is of practical importance as it prevents material from sticking to the screw which could lead to the scorching of heat sensitive material. In addition, the self-cleaning action leads to a more homogeneous velocity profile, which in turn results in a narrowing of the residence time distribution. Increasing throughput and decreasing screw speed can narrow the velocity distribution considerably, allowing more uniform shear stresses to be obtained with a consequent improvement in material homogeneity. In contrast, the velocity and shear stress distributions for a counter-rotating system are strictly a function of screw geometry. Co-rotating extruders with self-wiping screws allow significant amounts of back leakage along the screws, thus these extruders have a lower degree of positive conveying action but better mixing capabilities. This leakage flow minimizes the auger/barrel wear and allows these extruders to be run at speeds of up to 500 rpm. In terms of throughput, the

superior conveyance characteristics of counter-rotating extruders are offset by the high speeds and throughputs offered by co-rotating extruders. Overall, co-rotating extruders are considered to be one of the more useful general extrusion systems available because of their flexibility, good mixing characteristics, decreased wear, high shear rates and throughput.

Beyond the direction of rotation or degree of intermeshing, screws can have various flight geometries and channel depths which can further affect the operating characteristic of a twin screw extruder. In general, screws come in sections which may have specific functions, such as feeding, melting, mixing, pumping or shearing. Traditionally, extruders have been considered to have three basic zones, feeding, melting and metering, however, by changing the screw profile new combined functions can be obtained. The screw configuration selected can have a drastic effect on the process, process stability, energy consumption and the residence time distribution. Unfortunately there are no basic rules which can assure that one has chosen the optimal screw profile in terms of section length, location of each function or their sequence. The choice of a screw configuration which assures the best conditions for a given process is not always easy to achieve and the arrangement is still a function of experience or trial and error.

2.3.3 Process Variables and Process Control

The quality of extrudates is readily affected by extrusion process variables and therefore all process conditions require proper monitoring, adjustment and control. Once the optimum conditions for a product are established, these conditions must be maintained to assure a consistent product quality.

Batch processes, as opposed to continuous processes, rely more on stepwise evaluation to control product variables such as flavour, colour and texture, and therefore do not lend themselves to rapid responses to changes in product or process variables (Stults, 1978). As a continuous process, extrusion cooking has the potential for

automation and feedback control which has been successfully used in plastics extrusion, and could improve both product quality and yield (Olkku et al., 1980a). More sophisticated instrumentation and process control systems are being integrated into TSE's as applications became more complex.

The *process variables* which one can control during the extrusion run are also commonly termed independent or control variables and include; screw speed, feed rate, water and/or steam addition, barrel temperature and cutter speed. A modern twin screw extruder should be equipped with monitoring devices to measure and control these variables. Beyond these variables, the extruder *design variables* can also be brought into play such as; screw configuration, die size and shape, barrel length and diameter (L/D). Both the process variables and the extruder design variables can considerably affect the *system variables* which in turn are called dependent variables or response variables related to the system, which may include the product temperature profile, pressure at the die, torque and degree of screw fill. A last set of variables, termed *target variables*, also require consideration, which in turn can be sub-categorized as product characteristic or economic response variables. Depending on the process to be achieved, the desired target variables must be defined and optimized. Extruder performance is generally analyzed in terms of throughput, energy consumption, flow behaviour and RTD and this information should be obtained to have a sound understanding of the process. Figure 2 summarizes the all input, output and system variables associated with the extrusion process.

Only the process and system variables (except the degree of fill) of the extrusion system can be monitored with any degree of ease. Monitoring of these variables is important not only to detect any fluctuations in the system during operation but in addition these variables can be used to develop the process, evaluate extruder performance and predict subsequent product quality. Furthermore, the behaviour of some of these variables can be used as useful tools for developing a picture of what is occurring in the extruder and their assessment and function are described below.

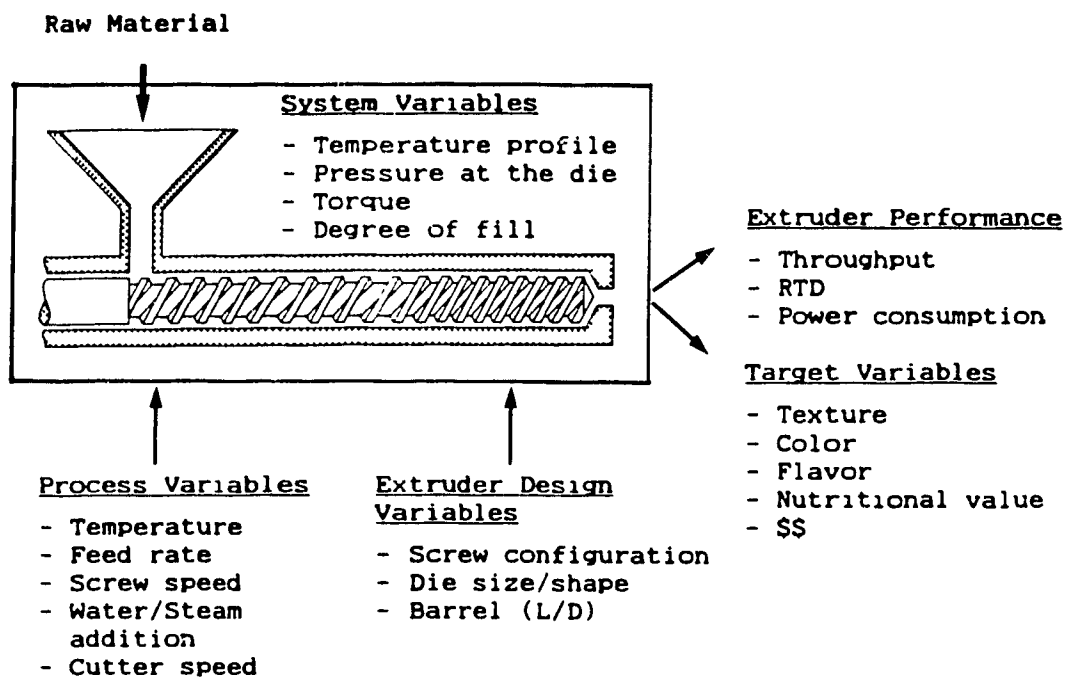


Figure 2. Schematic representation of the process, design and system variables in relation to extruder performance and target variables.

The pressure drop at the die can be used to determine the shear stress at the die using the following relations (Harper, 1981):

for a die with circular orifice:

$$\tau_w = r\Delta P/2L \quad (1)$$

for a die with slit orifice:

$$\tau_w = h\Delta P/2L \quad (2)$$

where τ_w is the wall shear stress, r is the die orifice radius, ΔP is the pressure drop across the die, L is the die length, and h is the height of the slit. Torque provides a direct indication of the energy absorbed by the material due to the shear exerted by the extruder screw and die orifice, and the specific mechanical energy (SME) input can be determined by the relation:

$$\text{SME} = \text{Tr} N/Q \quad (3)$$

where Tr is the torque, N is the screw speed, and Q is the throughput. Fluctuations in energy input indicate erratic feeding, surging or plugging and is a very sensitive indicator during extruder operation.

Throughput is generally determined by weighing the exiting material over some discrete time interval during steady state operation. Continuous monitoring is also possible using a nuclear sensor, a weight belt or a tachometer device (Harper, 1978; Antila et al., 1984), however, either the expense of instrumentation (nuclear sensor) or the sticky nature of freshly extruded product can make such measurements difficult. Throughput data can be used to determine the shear rate at the die wall using the following relations (Harper, 1981):

for a die with circular orifice:

$$\dot{\gamma}_w = (3n+1/4n) (4Q/\pi r^3) \quad (4)$$

for a die with slit orifice:

$$\dot{\gamma}_w = (2n+1/3n) (6Q/wh^2) \quad (5)$$

where $\dot{\gamma}_w$ is the shear rate at the die wall, n is the flow behaviour index, and w is the width of the slit. Using the calculated shear stress and shear rate (eqns (1) and (4) or (2) and (5)) the viscosity of the mass at the die (μ_d) can be determined via:

$$\mu_d = \tau_w / \dot{\gamma}_w = K(\Delta P / Q) \quad (6)$$

where K is the die geometry constant. On the other hand the viscosity may be predicted and controlled from response variables data using an empirical formula. Meuser & associates (1987) found by experience that product temperature and specific mechanical energy have the most influence on viscosity. Therefore by monitoring these variables and controlling them by adjusting the process parameters, the viscosity was automatically controlled and held constant. The mean residence time in the extruder can be determined by calculating the ratio of filled volume of screws to throughput (Q). The degree of fill can be determined by shutting down the extruder while it is running in a steady state and measuring the portion of the screw which is totally full.

Steam generation in the barrel is a common problem in high temperature extrusion processes and can lead to chaotic fluctuations in process characteristics, output, and product quality. For example, the use of paddles commonly leads to such problems, which can be overcome through the use of either a higher degree of screw fill or inserting pumping screws before the paddle zone to act as steam lock (Roberts & Guy, 1987).

Under some process conditions, a steady state condition, as indicated by stability in pressure and torque, is difficult to obtain. The operating stability of an extruder can be increased (Roberts & Guy, 1986) by (a) reducing the work input (i.e., by increasing the moisture content of the feed mix or reducing the screw speed); (b) reducing the ratio of the length of die cavity to the length of shear zone or (c) reducing the die resistance by increasing the area of the die orifice(s) or decreasing its land length. Such changes may work but may in turn affect the end product and compromises may be required.

Some useful directions as to how operating problems such as surging, plugging, flow variation, mixing, etc., can be overcome, have been given by Rossen & Miller (1973). Periodic instabilities are known to occur in extrusion processes such as the disturbance of a steady state by moisture fluctuations which can cause viscosity and pressure changes in the system. Models have been developed by Roberts & Guy (1986) and by Levine & co-workers (1987) to predict such effects and may have future applications in the dynamic correction of such occurrences.

The most common means of obtaining information about process variables is by obtaining data from the extruder control panel and recording them on an operation chart. This is economical in terms of investment, but is tedious and generally inaccurate given the number of variables to report and also difficult to detect short term fluctuations which can occur as the process proceeds. A better method is the use of a data acquisition/computer system connected to the extruder which allows one to have a continuous record of the process. Such a system has been used by the author (see Chapter 3.1) to monitor variables such as screw speed, barrel temperature profile, moisture addition rate, feed rate, amperage and pressure at the die, and subsequently plotting the data to allow a detailed analysis of the run. The details of these and other devices for measuring process variables are available in the literature (Harper, 1981; Rauwendaal, 1986; Millauer, 1986).

In food industry the use of automatic feedback control systems based on pre-set values is quite common. The automation of such processes follows hierarchical thinking (Olkku et al., 1980a) and is based primarily on an optimized steady state process. Once obtained, the process is maintained by dynamic control, to keep the values of the selected variables within specific bounds to attain a consistent product. The application of a direct digital control system to extrusion has been reported by Olkku et al. (1980a), where the change in the control variable was calculated from actual reading in relation to the set point using a control algorithm (Figure 3). The success of such a control operation depends to a large extent on the reliability of the sensors and on the accuracy

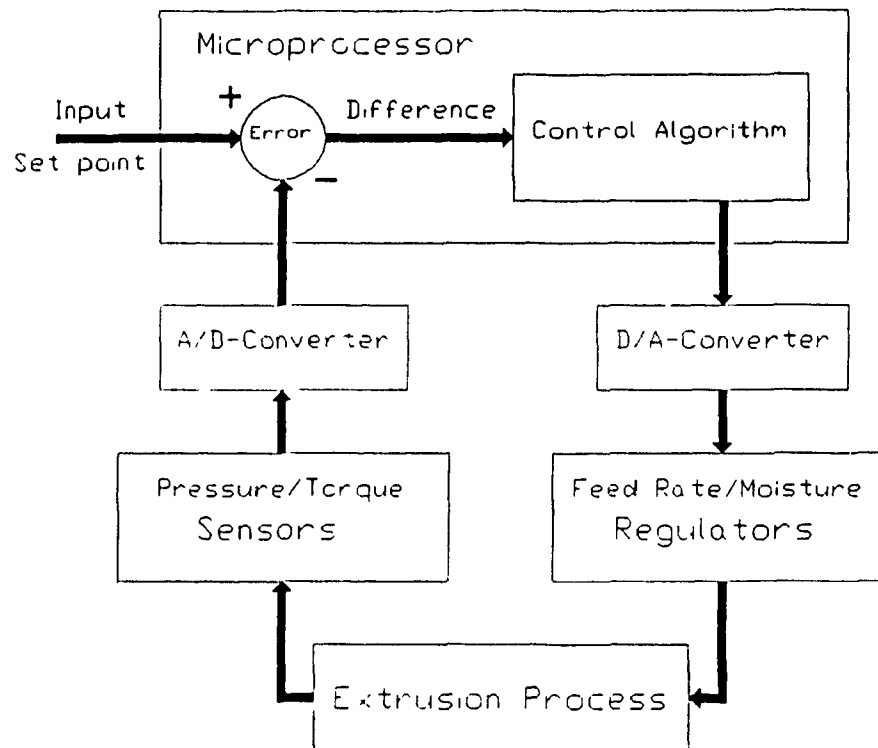


Figure 3. Schematic diagram of a feedback control system using a control algorithm.

of the process model in describing reality. Quite often, such models are not sufficiently accurate and the model may change over time as the machine wears out or the raw material varies. These problems may be solved by applying adaptive control by continuously optimizing the control algorithm constants (Olkku et al., 1980a). Clearly there are many variables and exceptional circumstances which make such control difficult, however such problems require solution to make extrusion a more viable process. Process automation in relation to the extrusion has numerous advantages and the reader is referred to Antila et al. (1984) for further details.

2.3.4 Rheology

When a food material is subjected to heat, shear and pressure, physico-chemical modifications occur which may lead to denaturation and cross linking of proteins, gelatinization of starches, degradation of minor constituents and the formation of new compounds. These changes usually affect the mass viscosity and flow behaviour in the extruder requiring adjustment in operating conditions to obtain the best compromise between control limitations, product quality and economics. Viscosity is an important parameter in characterizing product properties and its value at the die can be determined using the pressure drop and flow rate information as noted earlier. Extensive studies have been carried out on the rheological characteristics of food doughs in relation to extrusion (Remsen & Clark, 1978; Mackey et al., 1989; Morgan et al., 1979; Jasberg et al., 1981; Bhattacharya & Hanna, 1986; Jao & Chen, 1978; Chen et al., 1978; Harper et al., 1971; Clark, 1978). Under normal operating conditions, starchy and proteinaceous materials often exhibit shear thinning which can be characterized by the power law model:

$$\eta = m\dot{\gamma}^{n-1} \quad (7)$$

where η is the apparent viscosity, m is the consistency index, and $\dot{\gamma}$ is the shear rate. In extrusion processing it is important to predict the changes in viscosity as a function of

moisture and/or temperature. In such cases the following relation has been suggested for predicting these effects for viscoelastic biopolymers (Harper, 1981):

$$\eta = \eta^* \gamma^{n-1} \exp(E_a/RT) \exp(KM) \quad (8)$$

where η^* is the reference apparent viscosity, E_a is the energy of activation for flow, R is the gas constant, T is the absolute temperature, K is a constant, and M is the product moisture. The rheological behaviour of food stuffs is generally complex because of physico-chemical changes which occur as extrusion proceeds. Models has been developed to account for these changes considering the effect of time-temperature history (Remsen & Clark, 1978; Morgan et al., 1979; Mackey et al., 1989). Such models may be useful in the mathematical simulation of the extrusion cooking. The model developed by Remsen & Clark (1978) is given by:

$$\eta = \eta^* \gamma^{n-1} \exp(E_a/RT) \exp\left(\int_{t_0}^t k_{\infty} \exp(E_c/RT) dt\right) \quad (9)$$

where k_{∞} is the apparent Kinetic factor at infinite t , and E_c is the activation energy for the cooking reaction.

2.3.5 Modelling and Optimization

Despite the rapidly increasing use of extrusion technology in the food and feed industry, many of the improvements attained to date have been based more on empirical observations than on theoretical predictions. In the extrusion of synthetic polymers, a long standing tradition of modelling and optimization exists which has been used extensively to fine tune and optimize processes. In contrast, biopolymer extrusion is still far from being clearly understood and mathematical modelling is still in its infancy.

The theoretical concepts which have been successfully applied to polymer extrusion can form a useful basis for the study of the more complex field of food extrusion. However this cannot be achieved readily for a host of reasons, which include (a) the more complicated physical variables associated with food extruders (screw and die design, complex screw configurations, grooved barrel etc.), (b) the difficulty in controlling the process because of the more severe operating conditions and non homogeneity of raw materials, (c) the lack of adequate information about the rheological and thermodynamic characteristics of food systems, and (d) the difficulty of predicting physico-chemical changes which occur during the process. These problems explain why many of the processes have initially been approached on an empirical (trial and error) basis rather than scientifically, and the successes to date have ingrained this hit and miss philosophy in the food extrusion sector. However, most of the simple processes have now been exploited and in order to look to the future, more complex applications such as centre filled co-extrusion, reaction flavour and controlled texture development will require a much more detailed understanding of the extrusion process, including further improvements in extruder design.

Modelling and simulation of the extrusion process are means of obtaining a deeper understanding of the processes which may be taking place in the extruder. Although modelling is based on a simplified version of a complex real system, often the predictions obtained from a good model are useful guides in either changing the process or design variables. In a broad sense mathematical modelling includes both the empirical and theoretical aspects of solving problems, which can be viewed as an investigation of how specific variables are related to each other (Singh, 1983). Optimization is used to design or improve efficient processes that will yield a product with defined specifications in minimum time at minimum cost. Stochastic modelling is more used in food processing because of uncertainties and to allow multi-objective optimization. A mathematical model to simulate an extrusion cooking process has to consider physical and chemical data, process variables and extruder design, and relate them to extruder performance and product quality attributes (Figure 2). However, no model describing the interrelation

between process variables, the system and the product characteristics has been developed to date.

Extrusion modelling and optimization can proceed either from a process or a product viewpoint. The first concerns the modelling of extruder performance to predict the total power requirement, temperature/pressure profiles and to describe the flow patterns. This work has mostly been carried out by polymer engineering researchers and has led to the development of mechanistic models capable of predicting flow, mixing and energy consumption for single screw extruders (Griffith, 1962; Pinto & Tadmor, 1970). Similar work has been attempted to relate these concepts to the twin screw extruder, however the predictions were less precise. Chapter 2.4 provides a detailed description of TSE models related to flow, mixing and residence time distribution.

When optimization is approached from a product viewpoint, one seeks to modify the conditions of an existing process in an evolutionary manner so that product quality is optimized. This area is generally the scope of the food scientist, who usually uses statistical tools such as response surface methodology (RSM) to predict and optimize the product quality attributes. This approach is used in systems engineering and is called the "black box" system, where the output variables are generated from the input variables without specific knowledge of the process itself. The model derived by this approach has some important limitations, i.e., it cannot be extrapolated to other extruder types or raw material, cannot be used for scale-up and is limited to processing conditions within the range investigated. Even so, RSM can play a major role in understanding the relationships which exist between product characteristics and the process variables (Barraquio et al., 1988; van de Voort et al., 1984; Owusu-Ansah, et al., 1982, 1983, 1984) and thereby reducing the trial and error aspects of extrusion. As a systematic approach to a complex problem, RSM is a useful tool in product development and process optimization when other alternatives are not available, and the reader is referred to Box & Draper (1987) for more information in using this technique.

The systematic study of food extrusion is just a beginning and if fundamental principles can be elucidated in the same way as in the plastics industry, major progress could be made. A link is required between the basic engineering aspects of extrusion processing and the physico-chemical changes occurring in food systems, requiring that process engineers and food scientists collaborate to better define and solve the present problems associated with the twin screw extrusion process. The economic benefits to be gained by processors are sufficient to warrant continued and increased support of basic and applied research to continue laying the foundation for improvements in product quality and process efficiencies.

2.3.6 Conclusion

Most of the important aspects of twin screw extrusion have been described and summarized in this chapter to provide a basic understanding for non experts. Intermeshing, co-rotating twin screw extruders have the features which best suit general food processing needs. There are many variables to consider when dealing with twin screw extruders, some of which can be controlled, measured, or automatically adjusted, while others are physical variables, but must be selected (i.e., screw profile); all with the aim of optimizing desired target variables. The extruder can provide a wealth of data (shear stress, throughput, viscosity etc.,) which can be used to aid in defining the processes taking place. Modelling and optimization are the new frontiers which require development for a deeper understanding of extrusion cooking to be realized.

Since basic information on so many fundamental aspects of extrusion are still lacking and many aspects of extrusion processing still poorly understood, experience still counts heavily in any developmental work and will continue to be important. Models and experience can work together to help solve many of these problems and this iterative process will converge over time to solve the indeterminate state food extrusion presently finds itself.

2.4 FLOW BEHAVIOUR, MIXING AND RESIDENCE TIME DISTRIBUTION IN RELATION TO TWIN SCREW EXTRUSION

ABSTRACT

Despite the progress in the process applications of twin screw food extrusion technology, the engineering aspects are generally not fully understood and theoretical developments are still lacking. This chapter reviews the present status of the flow patterns, mixing characteristics, and concentrates on the residence time distribution (RTD) in relation to process variables (i.e., feed rate, screw speed) and extruder design. Each of these phenomena will be discussed separately and the mechanism behind each will be described in detail. The emphasis will be on developing a thorough understanding and obtaining a quantitative description of the extrusion process from a functional point of view. Food scientists and engineers will find such information an invaluable tool in decision making in terms of the type of extruder to use, evaluating extruder capabilities, modelling and assessing extrusion processes under development.

2.4.1 Introduction

Extrusion has become a very sophisticated science, especially in the plastics industry and is finding ever-increasing applications in the food sector. Today, extrusion is an important process in the food industry and numerous products (i.e., bacon bits, cheese curls, breakfast cereals, pet foods etc.) are produced by extrusion processing. In contrast to plastics extrusion, the theoretical understanding and development of food extrusion is still in its infancy (Fichtali & van de Voort, 1989) and although similar on a superficial level, biopolymer extrusion is fundamentally more complex. Plastics are relatively stable, uniform (chemically/physically) raw materials which are predictable in their behaviour during extrusion. A typical food formulation for extrusion may contain

proteins, carbohydrates and lipid, plus many other minor constituents. Multi-component systems of this nature may react in a manner which is difficult to predict, undergoing many reactions which change the product's physical and chemical characteristics as the extrusion process proceeds (Bruin et al., 1978; Luxenburg et al., 1985). Beyond the complexity of the food system itself, there are additional complications, including extruder design (i.e., single/twin, co-/counter-rotating) and the effect of the wide variety of process variables which can affect the process (Fichtali & van de Voort, 1989).

Empirical modelling has been extensively used in food extrusion such as the use of Surface Response Methodology (RSM) to generally predict the effect of operating conditions on product quality attributes (Owusu-Ansah et al., 1983; Barraquio et al., 1988; Meuser et al., 1987; Meuser & Wiedmann, 1989). As a systematic approach to a complex problem, RSM is a useful tool in product development and process optimization and has been enhanced by the availability of new routines to solve complex multiresponse optimization problems (Fichtali et al., 1990c). However, models derived by RSM have some important limitations (see section 2.3.5). As the system is not considered, any screw configuration or raw material can be assessed using RSM, however it has the drawback of providing one little about the basic phenomena occurring inside the extruder. Thus, there is a need to integrate a rational knowledge within this empirical development of food extrusion.

In order to be able to evaluate twin screw extruders (TSE's) from an engineering viewpoint, mathematical expressions are required to define and calculate a variety of parameters such as flow rate, power requirements, pressure, temperature and velocity distributions. Ideally, these relations should include pertinent physical characteristics (e.g., flow and thermal properties), design variables of the screws, the barrel and the die, and overall operating conditions. Considering the complexity of the screw and barrel on one hand and the variable nature of the food material on the other, it is obvious that deriving workable mathematical relationships for a food system is a very formidable task, but one which has to be tackled to advance the applications of TSE's to food systems.

Although food extrusion is complex, some of the basic models developed in the plastics sector can be used as a foundation on which to build more specific models related to food systems. With this concept in mind, this chapter reviews and analyses the models available for describing flow behaviour, mixing and residence time distribution in TSE's with more emphasis on co-rotating TSE's which dominate food extrusion. The basic differences between single screw extruders (SSE's) and TSE's, and between co-rotating and counter-rotating TSE's have been already discussed in chapter 2.3 and also by numerous authors (i.e., Janssen & Smith, 1980; Martelli, 1983; Rauwendaal, 1986; Fichtali & van de Voort, 1989).

2.4.2 General Concepts Related to Flow

Modelling flow in SSE's is simpler than in TSE's because flow can be considered fully developed in a continuous channel (Bruin et al., 1978). This approach provides a basis for analytical and numerical solutions for flow equations, an approach precluded in twin screw extrusion because of the intermeshing nature of the screws. Flow in SSE has been investigated by Griffith (1962), McKelvey (1962), Schenkel (1966), Pinto & Tadmor (1970), Bigg & Middelman (1974) and Stevens (1985). Flow modelling is generally less advanced in TSE's with more complications arising in co-rotating than counter-rotating TSE's. In counter-rotating screws, screw geometry permits one to consider product being transported in closed C-shaped chambers, an approach which has advanced theoretical developments for this type of screws (Janssen, 1978).

To characterize the flow in a SSE or TSE, some basic assumptions are required and the geometry of screw channel requires simplification. To date, most models have been developed to describe product flow behaviour considering the following assumptions; (a) the fluid is Newtonian, isothermal and has a constant density, (b) flow is fully developed and uniform, (c) gravitational and inertial effects can be neglected, (d) fluid flow is laminar (i.e., $Re \ll 1$), steady and, (e) zero leakage flow occurs. Deviations

from these assumptions for SSE can be accounted for in certain circumstances, which have been discussed by Stevens (1985).

A basic knowledge of flow in SSE is required to understand flow in TSE. For a SSE, in most models, determinations of the velocity profile of the material being extruded are based on a parallel plate model formed by the barrel surface and the unwound channel of the screw. In this approach, the barrel becomes an infinite plate moving at a constant velocity, V_b , at an angle ψ (the helix angle) relative to the down channel direction z . Figure 4 illustrates the basic channel geometry, and the velocity profile in the down channel direction is given by (Pinto & Tadmor, 1970):

$$v_z = V_z \frac{Y}{H} (1 + 3\phi - 2\frac{Y}{H}\phi) \quad (10)$$

where y is the channel depth coordinate, H is the channel depth, and ϕ is the ratio of pressure to drag flow and is equal to:

$$\phi = -\frac{H^2}{6\mu V_z} \frac{\partial P}{\partial z} \quad (11)$$

in which μ is the viscosity. The velocity profile in the cross channel direction x is:

$$v_x = V_x \frac{Y}{H} (2 - 3\frac{Y}{H}) \quad (12)$$

The down channel and cross channel velocity components of the barrel, V_z and V_x , can be determined as follows:

$$V_z = \pi N D \cos \psi \quad (13)$$

$$V_x = \pi N D \sin \psi \quad (14)$$

where N is the screw speed, D is the screw diameter, and ψ is the helix angle. The velocity profile in the axial direction can be determined from eqns (10) and (12) to give:

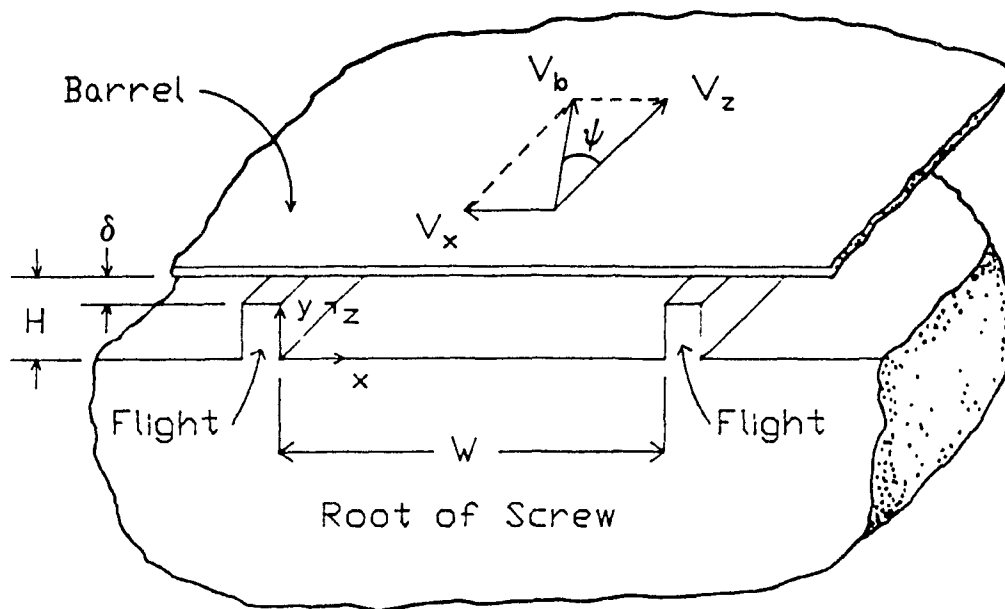


Figure 4. Basic channel geometry. V_b is the barrel velocity; V_x and V_z are the down channel and cross channel barrel velocity components, respectively; ψ is the helix angle; δ is the flight clearance; and H is the channel depth.

$$v_1 = 3V_b \frac{Y}{H} \left(1 - \frac{Y}{H}\right) (1 + \phi) \sin\psi \cos\psi \quad (15)$$

Here v_1 is parallel to the screw axis, while v_2 is parallel to the screw channel walls, which wrap helically around the axis of the screw. Once v_2 is found, it can be used to estimate the volumetric flow rate (Q):

$$Q = p \int_0^H \int_0^W v_z \, dy \, dx \quad (16)$$

where p is the number of channels in parallel and W is the channel width. Solving eqn (16) gives:

$$Q = p \frac{WH}{2} v_z + p \frac{WH^3}{12\mu} \frac{\partial P}{\partial z} \quad (17)$$

Under these circumstances, the flow rate in eqn (17) for a SSE is a summation of two terms, the first termed drag flow (Q_d) which is proportional to screw speed (N), and the second, termed pressure flow (Q_p), proportional to the pressure gradient ($\partial P/\partial z$) down the screw channel. Eqn (17) can therefore be rewritten as:

$$Q = Q_d + Q_p \quad (18)$$

In the case of the TSE, the geometry is substantially more complicated and some additional simplifying assumptions are required to develop a flow model. To visualize the system (Figure 5a), one screw is considered stationary while the barrel and the other screw rotates around it (Wyman, 1975). Due to the intermeshing nature of the two screws, the second screw must turn on its axis with the same rotational speed as the barrel so that it will not be forced to move axially. By unwinding the stationary screw and the barrel, one is left with two parallel flat plates and the flight walls of the rotating screw (Figure 5b). By neglecting the curvature of the mobile second screw lands, they can be regarded as flat plates which extend at regular intervals through the barrel wall and

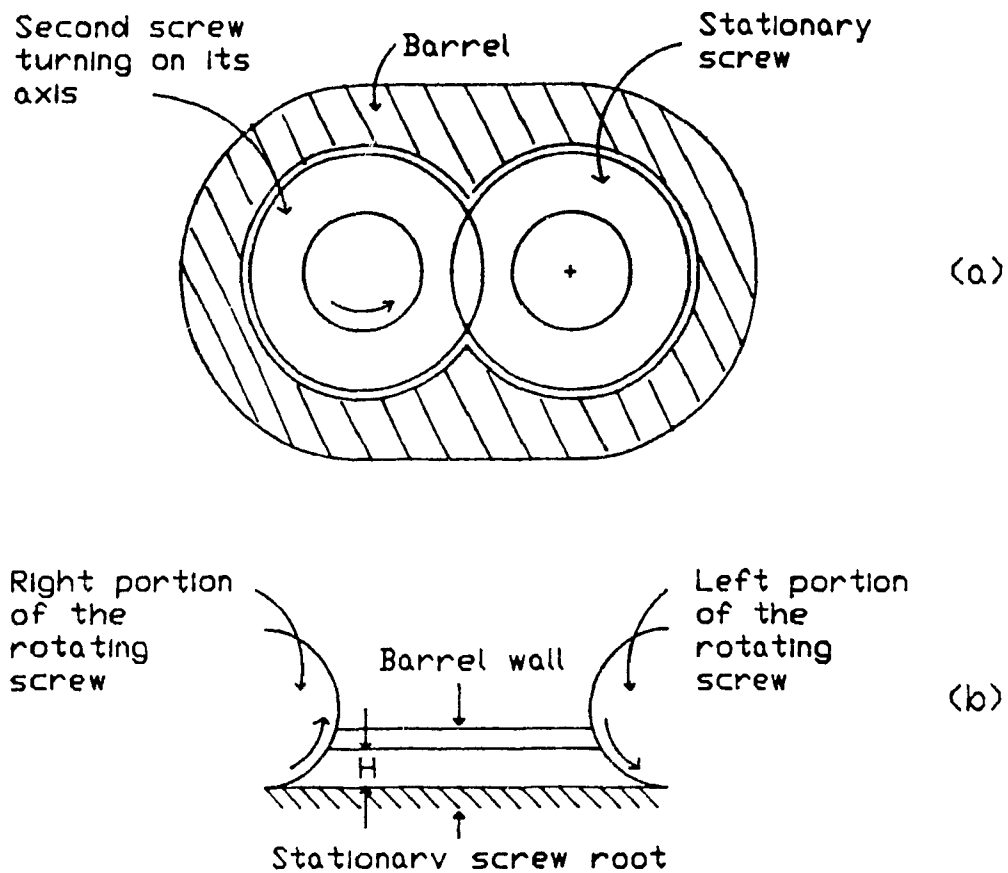


Figure 5. Cross-sectional view of a co-rotating twin screw extruder perpendicular to the screw axis with the barrel and the second screw rotating around the stationary screw and with the second screw rotating on its axis (a); and cross-sectional view of the unwound channel of a co-rotating twin screw extruder (b).

contact the stationary screw root and flight. A detailed description of these and other geometric considerations are given by Booy (1978).

Several attempts have been made to develop workable models for describing flow behaviour in TSE's. However, there is some disagreements in the published literature related to flow mechanism assumptions and boundary conditions. The coordinate system can be placed on the stationary screw (Wyman, 1975) as in the case of SSE to maintain a steady state of boundary conditions. However, Burkhardt et al. (1978) reported that doing so, the periodic gliding velocity of the second screw, which rotates with the barrel as well as the wedge area, would result in changing the boundary conditions. To overcome the problem, the coordinate system were placed in the inner barrel surface and then moved parallel to the screw axis. The model given by Wyman (1975) was for an ideal leak-proof TSE having a rectangular channel and considers axial pressure gradient, channel depth, but not the channel width. Wyman's analysis illustrated that the drag flow terms were identical to those for a SSE, while the pressure flow terms were also identical in magnitude but opposite in sign. Although Burkhardt et al. (1978) and Herrmann & Burkhardt (1978), took a totally different approach than that of Wyman, the model had similar limitations, however, more realistic expressions were derived for co-rotating and counter-rotating screws.

Werner & Eise (1979) considered the actual channel geometry for a self wiping co-rotating TSE and obtained expressions for the velocity as a function of both the channel depth and width based on three-flighted (three-tip) screw element geometry. They restricted their analysis to the case where the axial pressure gradient was zero (i.e., open discharge), concerning themselves with the effect of degree of fill (ratio of the product volume to the free channel volume) on flow behaviour and the flow in kneading discs.

A more sophisticated approach extending the work of Werner & Eise has been presented by Denson & Hwang (1980), where the motion equation was solved through

the use of finite element analysis. The actual channel geometry was considered using Booy's results (1978) and a three-tip screw element was used as a base to develop a flow model in fully filled channels. Only down channel flow was considered and an expression of the dimensionless flow rate as a function of the axial pressure gradient was obtained, which might be useful in scale-up and predicting extruder performance. Furthermore, shape factors (dimensionless functions of the channel geometry) were calculated to allow the application of the general form of SSE flow equation to self-wiping co-rotating TSE's. This work was further extended by Szydłowski & White (1987) to include the contribution of the intermeshing region of the screws. The effect of the intermeshing region on flow rate/axial pressure distribution relationship depended on the ratio of the flight width to the channel width (e/W). When this ratio is small ($e \ll W$) the effect of intermeshing region can be neglected, however, this effect becomes important when e is comparable to W , because of increased pressure losses. The computed flow rate values at open discharge were in good agreement with the data obtained by the Werner & Eise (1979) and Denson & Hwang (1980) models.

Booy (1980) used a different approach to derive a flow model for a co-rotating screws with fully filled channels and the total flow rate was given as a function of drag flow (Q_d), pressure flow (Q_p) and nip flow (Q_n), with the later occurring in the nip (intermeshing) zone, by:

$$Q = Q_d + Q_n - Q_p \quad (19)$$

where Q_d , Q_p , and Q_n are given respectively by:

$$Q_d = p \frac{WH}{2} F_d V_z \quad (20)$$

$$Q_p = p \frac{WH^3}{12\mu} F_p \frac{\partial p}{\partial z} \quad (21)$$

$$Q_a = v_a A_a \quad (22)$$

where F_d is the drag flow shape factor, F_p is the pressure flow shape factor, A_n is the cross sectional area in the nip zone, and v_n is the axial velocity in the nip zone. For partially filled channels, flow transition from one channel to another was not smooth, and the pattern indicated that product produced a bulge ahead of the flight as it was pushed through the flight tips. The axial velocity in this case was found to be proportional to screw speed, but independent on the degree of fill.

The flow modelling in TSE using biopolymers is very scarce in the literature. Yacu (1985) predicted pressure distribution based on Wyman (1975) model for wheat starch extrusion and the results were satisfactory for certain operating conditions. Tayeb and co-workers (1988a), using corn starch as the feed material, presented a means of modelling flow through reverse screw elements having axial slots applying a cylindrical coordinate system. The model was based on a rectangular channel considering both down and cross channel velocities, and a variety of flow rates were computed assuming flow rate conservation at each node of the cut-flight reverse screw element. Their model for the metering zone (Tayeb et al., 1988b) considered only down channel velocity and has the classical form of SSE flow model with shape factors.

All of the models discussed have largely been developed for an ideal material, considering a simplified screw channel and neglecting the effect of mechanical clearances and leakage flow. Thus, their use for a quantitative analysis is limited especially when the rheological and the physico-chemical changes of the food material are not known accurately. Even so, they are still useful for gaining an understanding of the particulate flow path in an extruder, its mixing capabilities, working conditions, design limitations, scale-up, and general performance of an extruder as a reactor.

2.4.3 General Concepts Related to Mixing

In food extrusion as in plastics extrusion, mixing is one of the most important functions the extruder has to perform. It is especially important in situations where the uniform dispersion of minor components (i.e., colours, pigments, additives) and homogeneity of the end product are required. Two kinds of mixing can occur in a TSE, dispersive and distributive mixing (Ess & Hornsby, 1986). Dispersive mixing is defined as operations which are aimed at reducing the agglomerate size of a minor component during mixing to its minimal size, a process which is mainly a function of shear forces, but includes an exposure time effect (Rauwendaal, 1986). Distributive mixing can be defined as operations employed to randomize the spatial distribution of the minor constituent within a bulk, without a change in particle size and can be characterised by how far two fluid particles, initially adjacent, are separated by the mixing process. Dispersive mixing and distributive mixing often cannot be separated, and the two occur in combination during extrusion processing. In dispersive mixing, there will always be distributive mixing, however, the reverse is not always true. In distributive mixing, there can be dispersive mixing only if there is a solid component with a yield stress and if the acting stress exceeds this component yield stress (Rauwendaal, 1986).

A complete characterization of a mixture requires a specification of the size, shape, orientation and spatial location of every element of the minor component. This is impossible in an extruder due to the complex flow patterns which can occur. Even so, models and methods have been developed to assess the extent, uniformity and/or quality of mixing that an extruder can perform. Approaches include (a) determination of velocity and stress distributions, (b) determination of weighted average total strain induced in the material, (c) direct analytical procedures (i.e., microscopic/image analysis techniques) or (d) residence time distribution, each of which are discussed separately.

2.4.3.1 Velocity and Stress Distributions

The relative linear velocities of fluid elements vary according to their position in the screw channel, being higher for layers near the tip of the flights and lower near the root of the screws (Martelli, 1983). The various paths that the material takes and the turbulence within the intermeshing area create conditions for good mixing, however, these flow patterns across the screw channel are very complex. Velocity and stress distribution expressions can be generated from flow models discussed earlier. For conditions of no net flow ($Q = 0$), the Wyman (1975) model predicted velocity and stress distributions which are the inverse of what would be obtained for a SSE, i.e., that the greatest shear occurs near the screw root for a TSE, while it is close to the barrel wall for a SSE. Even though this model indicates a basic difference in mixing behaviour between a SSE's and TSE's, the model is limited by its basic assumptions, i.e., restricted to shallow channels ($W > 10H$) to permit an analytical solution to the flow equation. Such an assumption is generally invalid for TSE's, and as a result, shape factors must be included or the flow should be treated in a three-dimensional manner.

The models developed by Burkhardt et al. (1978), to predict velocity and stress distributions for fully intermeshing counter- and co-rotating extruders, lead to some very interesting equations and conclusions. For a counter-rotating TSE, the velocity and stress distributions are expressed respectively by:

$$\frac{v_z}{v_0} = \frac{1}{\cos \psi} \left\{ 3 \left[\left(\frac{Y}{H} \right)^2 - \frac{Y}{H} \right] (\sin^2 \psi + 1) + \frac{Y}{H} \cos^2 \psi + \sin^2 \psi \right\} \quad (23)$$

$$\frac{\tau_{yz}}{\frac{\mu v_0}{H}} = \frac{1}{\cos \psi} \left[3 \left(2 \frac{Y}{H} - 1 \right) (\sin^2 \psi + 1) + \cos^2 \psi \right] \quad (24)$$

and for a co-rotating one they are expressed as follows:

$$\frac{v_z}{v_0} = \frac{H^2}{2\mu\pi DN} \frac{\partial P}{\partial z} \left[\left(\frac{Y}{H}\right)^2 - \frac{Y}{H} \right] + \frac{Y}{H} \cos\psi + \frac{\sin^2\psi}{\cos\psi} \quad (25)$$

$$\frac{\tau_{yz}}{\mu \frac{v_0}{H}} = -\frac{H^2}{2\mu\pi DN} \frac{\partial P}{\partial z} \left(2\frac{Y}{H} - 1 \right) - \cos\psi \quad (26)$$

where τ_{yz} is the acting stress perpendicular to y-axis in z direction, and v_0 is the circumferential velocity. These relationships predict a basic difference between the two extruder types in terms of intensity, uniformity and location of maximum and minimum shear. The shear stress is greater in counter-rotating screws at the barrel surface and screw root than co-rotating screws, with the later having maximum shear stress at the barrel while the former is at the screw root. More uniform stress distribution occurs with co-rotating screws, resulting in more homogeneous mixing while poor mixing quality can result in counter-rotating TSE's because of localized high shear regions. These localized high shear regions, however, might still be efficient for dispersive mixing situations (Chung, 1983), which justify their use in some polymer and food applications. Furthermore, the shear stress distribution is only dependent on the screw pitch (H) in a counter-rotating system, while in co-rotating systems, it is additionally dependent on throughput and screw speed. This means that with co-rotating screws, the shear stress distribution not only changes with geometry but also with the operating conditions, and this additional flexibility favours homogeneous mixing.

The degree of fill can affect shear velocity, shear deformation (strain) and conveying characteristics in a co-rotating TSE (Werner & Eise, 1979) and can be adjusted to optimize mixing. The degree of fill also affects the conveying characteristics of kneading elements, conveying being based on a positive displacement flow generated by the staggered pressure profiles. Pressure losses in the intermeshing region can be

maximized or minimized depending on screw geometry (Szydlowski & White, 1987) and one can increase pressure losses by choosing a greater e/W ratio, which will result in improved dissipative mixing. Thus, e and W can be chosen to provide a dominant pumping action or a dominant mixing action (Martelli, 1983). In certain situations, left-handed screws (reverse screw elements) are used to improve distributive mixing through flow re-orientation and randomization and such screws can also act as an effective decompression element (Szydlowski & White, 1987), especially useful prior to the die to avoid chaotic fluctuations at the output.

2.4.3.2 Strain Analysis

The analysis of mixing using residence time distribution (RTD), cannot in itself, predict whether elements of a fluid with similar residence times can be considered well mixed. An essential requirement for effective dispersive mixing is to generate sufficient shear stresses to reduce particle size and to ensure all the fluid elements traverse and spend sufficient time in the high shear zone. For solids which deform elastically and having a finite yield stress, it is necessary to exceed this stress to cause permanent deformation or fracture, before distributive mixing can occur. Therefore, it is evident that the total shear strain is an appropriate measure of mixing, as it takes into account both the relative movement and the initial separation state of the particles (Stevens, 1985). In a SSE, strain has been used as a means for estimating local mixing with some success (Mckelvey, 1962; Pinto & Tadmor, 1970; Bigg & Middelman, 1974). The total shear strain is given by the product of shear rate and the time for which it acts, and the average strain can be calculated by weighting the various levels of strain experienced by fluid particles according to the fraction of the flow they comprise, i.e., the RTD. The weighted average total strain (WATS) is given by (Pinto & Tadmor, 1970) as:

$$WATS = \int_{t_0}^{\infty} \gamma E(t) dt \quad (27)$$

where $E(t)$ is the residence time function, γ is the shear strain, and t_0 is the minimum residence time. WATS in itself, does not produce an experimentally measurable quantity to describe mixing and also does not consider the initial orientation of the minor components nor the changes in orientation (Rauwendaal, 1986).

In TSE's the screw chambers are geometrically complex, with additional strain imposed on the material by the intermeshing region of the second screw land. In addition leakage flow is generally neglected, as well as the normal velocity components close to the flight flanks. This constitutes a severe limitation on the validity and applicability of results obtained using strain for mixing analysis. Maheshri & Wyman (1979, 1980) calculated the strain for a leak-proof TSE, finding the total absolute strain by calculating and summing the strains for all successive complementary depths of the channel, with the strain per unit dimensionless residence time period T_c , γ_i , being given by:

$$\gamma_t = \frac{\gamma_c}{T_c} \quad (28)$$

where γ_c is the amount of strain experienced by the particle in one cycle over a dimensionless time period, T_c . γ_i may be multiplied by the dimensionless residence time to give the total strain for an idealized extruder, since all the material in the leak-proof chamber is assumed to have the same residence time. Calculation of product streamlines at various helix angles for both co- and counter-rotating screws produced two circulating zones (Maheshri & Wyman, 1979, 1980). The main zone contains two circulating modes, one clockwise in the lower portion of the chamber, and a second, counter clockwise in the upper area of the chamber, with the later becoming more important as the helix angle increases. The second circulating zone is close to the second screw land and results in a region where the material remains in a small closed loop, with the strain in this region being higher than that of the main zone. Hornsby (1987) was able to physically demonstrate the existence of these two zones by carbon black visualization techniques. Janssen (1978) also reported that a counter-current flow existed within the chambers and a well defined zero velocity contour (unmixed zone) was elucidated based on both theory

and visualization experiments. In co-rotating TSE's, through proper screw design and appropriate processing conditions, it is possible to shift the zero shear strain point of the axial flow component to a point outside of the screw channel (Burkhardt et al., 1978; Eise et al, 1981), eliminating any dead mixing region. It is however difficult to do the same thing in counter-rotating screws, and as a result, more uniform strain distribution is possible with co-rotating devices. This is in contrast with the analysis of Mahsheri & Wyman (1979, 1980) which indicated that the absolute strain distribution across the intermeshing TSE chambers is generally uniform regardless the mode of the screw rotation, and that only the increase in the helix angle was found to increase the strain. They did mention, however, that the calculated strain could only be considered an approximation of mixing, as leakage flow had not been included, the geometry of the second screw land simplified, and the interaction of the two basic flow patterns (cross and down channel flows) was not considered. For a counter-rotating TSE, the leak-proof assumption may be an acceptable first approximation, however, for co-rotating screws significant deviations could be expected using such a simplified analysis.

Kim et al. (1973) predicted the three velocity components of material flow using Stokes equations, assuming the product being far from the intermeshing second screw lands. He calculated the strain by averaging the shear rate components over the channel depth from which the striation thickness in the extruder can be estimated to analyze the extent of mixing in the chambers. The striation thickness is defined as the total volume divided by half the total interfacial surface area (Rauwendaal, 1986). The increase in interfacial area is directly proportional to the total shear strain and can be achieved by inclusion of mixing sections within the screw.

2.4.3.3 Use of Analytical Procedures

The use of velocity and stress distributions, and strain analysis, although theoretically capable of yielding quantitative data related to mixing behaviour, are

generally difficult to verify experimentally. Visualisation experiments are a useful alternative when theoretical concepts are difficult to implement.

Various methods have been considered for assessing dispersive and distributive mixing using combined microscopic/image analysis techniques (Ess et al., 1984; Ess & Hornsby, 1986, 1987). Some of these methods have been applied to the analysis of mixing behaviour for compounding mineral filled thermoplastics using co-rotating TSE's (Ess & Hornsby, 1986, 1987). Werner & Eise (1979) used a microscope photometer, where an output voltage is measured as a function of time (or distance), to study the dispersion capacity of kneading discs through the use of mixtures of carbon black and polyethylene. The degree of voltage fluctuation is indicative of mixing and can be used to calculate the dispersion quality. Striation thickness can be measured and used to obtain a quantitative measure of mixing quality, using an optical microdensitometer (Ess & Hornsby, 1986). The method, however can become limiting if the striation width becomes too small to measure as mixing progress. Hornsby (1987) visualized the flow behaviour in co-rotating system using a carbon black tracer and then examined the material across the C-shaped chambers by microscopy after a shut-down of the extruder. His micrographs physically demonstrated the presence of the two principal circulating flow zones predicted to be present theoretically (Maheshri & Wyman; 1979, 1980). Microwave attenuation sensors have also been used to study mixing in a co-rotating extruder by monitoring changes in the moisture content of food material in the barrel (Chouikhi et al., 1989). The response of such a sensor may be affected by physico-chemical changes occurring during the process and it cannot be used to measure solid-solid mixing, unless one of the components is microwave sensitive (Kudra et al, 1989).

Segmented mixing elements have been shown to enhance distributive mixing through re-orientation and randomisation of fluid elements, however, their effect on dispersive mixing was shown to be very limited (Ess & Hornsby, 1986, 1987). Operating conditions (temperature, screw speed, throughput) were also found by the same authors to have an effect on distributive mixing, but no significant effect on dispersive mixing.

However, Werner & Eise (1979) found that the dispersion quality is proportional to the average shear stress, decreasing with increasing throughput rate and also dropping at higher melt temperatures. The effect of temperature can readily be understood, since decreasing the temperature will increase viscosity and thus increase the frictional forces. Ess & Hornsby (1986, 1987) have indicated that there are no temperature effects, however, it is likely that this result was due to limitations associated with the method used. Dispersion quality is also influenced by the minimum residence time during which the agglomerates are exposed to shear, thus, the longer the residence time, the better the dispersion quality. Using a colour tracer, Burkhardt et al. (1978) showed that with increasing screw speed, homogeneity decreases in the case of counter-rotating screws and increases in the case of co-rotating screws.

A fourth way of evaluating the conveying and mixing performance characteristics of TSE's, is through the determination of the residence time distribution (RTD). As RTD is the most commonly used technique for evaluating mixing behaviour in the extruder and because of its importance, it is treated more extensively in the next section.

2.4.4 Residence Time Distribution

One of the most important properties in the performance of an extruder is the RTD of the material in the barrel. The RTD in an extruder is a useful tool for determining the optimal processing conditions for mixing, cooking and shearing which are factors related to the rate of the chemical reactions taking place during the process. From the RTD functions one can estimate the degree of mixing, the life expectancy of particles, the average total strain exerted on the mass during its transition and provide a clear picture of how an extruder behaves as a chemical reactor.

To understand how the mass moves through the extruder one has to be able to follow all of the mass as it passes through the barrel and this is usually done by obtaining a velocity distribution profile of the material in the extruder. Pinto & Tadmore (1970)

have developed a RTD model for fully filled SSE's with Newtonian systems, which has been extended to power law fluids by Bigg & Middleman (1974) and verified experimentally (Bigg & Middleman, 1974; Wolf & White, 1976). Because of the substantially more complex geometry of the TSE, an adequate mathematical model of the RTD for the TSE has not been developed to date. Although no RTD model is available at present, RTD information can still be obtained experimentally and methods are available by which inferences can be made about the processes taking place in the extruder.

2.4.4.1 RTD Basics

A marker or tracer element instantaneously injected into the feed port of an extruder will exit over a finite and defined period of time because of dispersion, mixing and varying velocities within different parts of the screw channel. The resulting distribution, commonly known as the residence time distribution (RTD), can be described quantitatively using the E- and/or F-function (Figure 6). Danckwerts (1953) defined the residence time distribution $E(t)$ mathematically such that $E(t)dt$ is the fraction of the mass at the exit which has spent a time between t and $(t + dt)$ in the system.

$$E(t) = \frac{C(t)}{\int_0^{\infty} C(t) dt} \quad (29)$$

where $C(t)$ is the tracer concentration at the outlet at time, t . By integrating the $E(t)$ function, the cumulative residence time distribution function $F(t)$ can be obtained.

$$F(t) = \int_{t_0}^t E(t) dt \quad (30)$$

The minimum residence time (t_0) is an important variable which is defined as the time elapsed between instantaneous addition of the tracer to its initial exit at the die. The

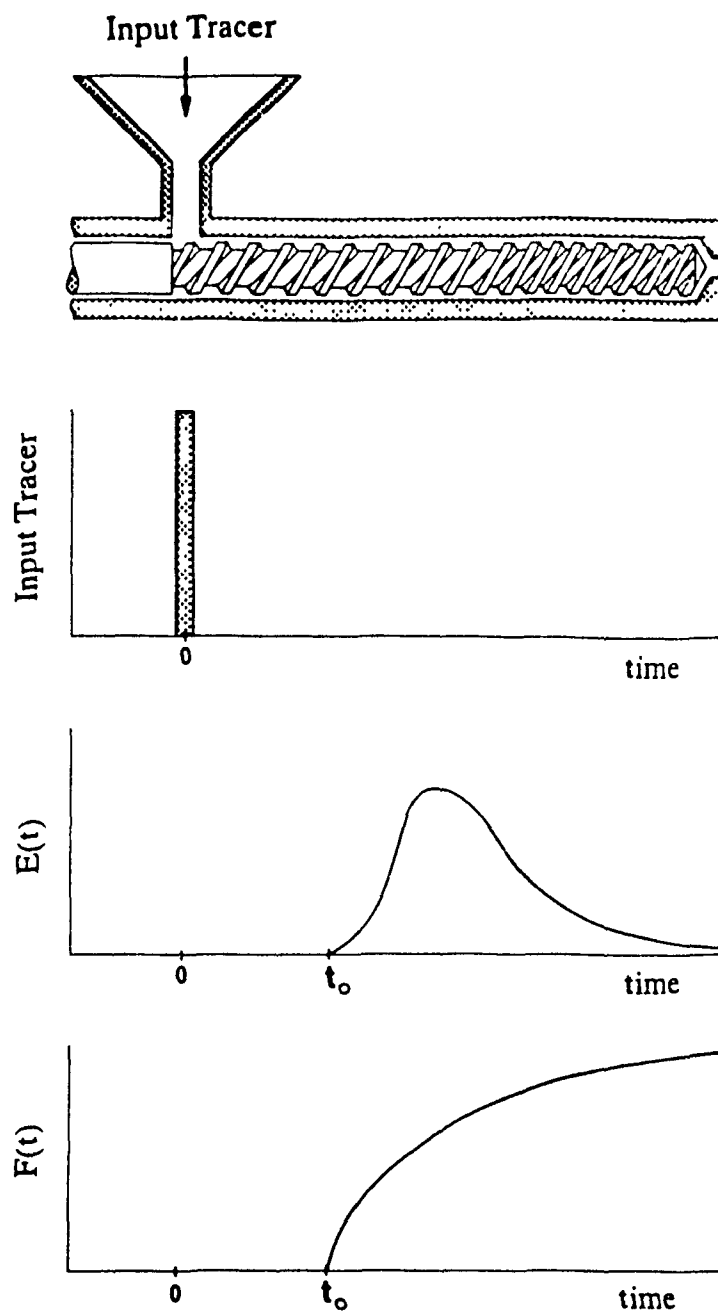


Figure 6. Tracer input into extruder and the resulting $E(t)$ and $F(t)$ functions which describe the residence time distributions.

mean residence time \bar{t} can be obtained from the following relation:

$$\bar{t} = \int_0^{\infty} t E(t) dt \quad (31)$$

Alternatively, the mean residence time can be obtained by measuring extruder parameters such as filled volume of screw (V_f) and volumetric flow rate (Q):

$$\bar{t} = \frac{V_f}{Q} \quad (32)$$

The variance of the residence time can be calculated as:

$$\sigma^2 = \left[\int_0^{\infty} t^2 E(t) dt \right] - \bar{t}^2 \quad (33)$$

It is often useful for comparative purposes to define a dimensionless time variable which measures time directly in units of mean residence time, i.e.,

$$\theta = \frac{t}{\bar{t}} \quad (34)$$

An alternate means of presenting the cumulative distribution is in the form of (1-F) which represents the distribution inside the extruder barrel commonly known as the internal age distribution:

$$1 - F(\theta) = 1 - \int_0^{\theta} E(\theta) d\theta = \int_{\theta}^{\infty} E(\theta) d\theta \quad (35)$$

Any amount of tracer left in the system after the sampling period contributes to truncation error when attempting to normalize the experimental RTD curve. Todd (1975b) suggested a method for estimating this truncation error using a semi-logarithmic plot of concentration against residence time. The straight line portion of this plot, the tail portion, can be expressed as:

$$C = Ae^{-at} \quad (36)$$

where A is a constant, and a is the slope of the straight line portion. If the last measured concentration, C_e , was made at time, t_e , the truncation error (R') can be calculated from

$$R' = \int_{t_e}^{\infty} Ae^{-at} dt = \frac{A}{a} e^{-at_e} \quad (37)$$

since

$$C_e = Ae^{-at_e} \quad (38)$$

then

$$R' = \frac{C_e}{a} \quad (39)$$

thus the truncation error can be estimated by dividing the value of the last point on the curve by the slope of the linear section of the tail.

2.4.4.2 Calculation of Experimental RTD Functions and Tracer Techniques

The experimental RTD can be determined by taking samples at the extruder die, usually every 5 seconds and processing the resultant concentration data using the following equations (Wolf & White, 1976):

$$E(t) = \frac{C(t)}{\sum_0^{\infty} C(t) \cdot \Delta t} \quad (40)$$

$$F(t) = \frac{\sum_0^t C(t) \cdot \Delta t}{\sum_0^{\infty} C(t) \cdot \Delta t} \quad (41)$$

$$\bar{t} = \frac{\sum_0^t t \cdot C(t) \cdot \Delta t}{\sum_0^{\infty} C(t) \cdot \Delta t} \quad (42)$$

The experimental method generally used to define the RTD may be classed as a stimulus-response technique. The stimulus is usually a concentrated tracer introduced "instantaneously" to the extruder with the response being the quantity of tracer leaving the system over time. Analyzing the concentration in terms of $E(t)$ and $F(t)$ provides useful information about the residence time distribution in the system. Harper (1981) provided a typical sample calculation for a laboratory Brabender extruder using flour dough.

Numerous techniques for obtaining RTD functions have been cited in the literature, of which the two more common methods are radioactive tracers and dyes. A radioactive technique using MnO_2 was developed by Wolf & White (1976) to study the RTD in a SSE, and has since been used by others for both SSE's (Davidson et al, 1983) and TSE's (Janssen et al., 1979; Wolf et al., 1986). This technique can be used in two ways, using labelled material directly or by activating the tracer in the extrudate after the process. Both methods have the advantage of being capable of measuring low concentrations and hence provide a better estimate of the trailing portion of the distribution. The later method avoids the use of radioactive materials in the extruder while the former allows measurements at various locations along the barrel, so that the effect of selected screw sections can be investigated (Olkku et al., 1980b; Wolf et al., 1986). Drawbacks to these methods are the requirement for either a scintillation counter and/or a nuclear source (i.e., SLOWPOKE reactor) to activate the sample. Zuilichem et al. (1973) used Cu^{64} to study the effect of process variables on the RTD in a single screw extruder. This method has recently been improved with the introduction of a coincidence detection system which significantly increases the accuracy of the measurements through improved resolution and the advantage of an absence of background radiation interference (Zuilichem et al., 1988a). The method has since been applied to SSE (Zuilichem et al., 1988b) and to a conical counter-rotating TSE (Zuilichem et al., 1988c; Jager et al., 1988, 1989). K^{42} has also been used by Mangé et al. (1987) in co-rotating extruders having different throughput capacities.

Dyes have also been used widely to study the effect of process variables on the RTD and as means to fit extrusion results with theoretically proposed models (Biral, 1979; Mosso et al, 1982; Lim et al., 1985; Colonna et al, 1983; Kao & Allison, 1984; Guzman-Tello & Cheftel, 1987; Ferry-Wilczek et al., 1988). The use of dyes has the advantage of visually allowing one to monitor the output as the extrusion run is in progress and provides one with simplicity in terms of analysis. Other approaches, such as the use a soluble salts (KNO_3 or $NaNO_3$) or a metal oxide (ZnO) have also been used, which in turn were subsequently analyzed by conductivity (Todd, 1975a,b) or atomic absorption (Bounie & Cheftel, 1986), respectively.

2.4.4.3 Process Variables in Relation to RTD

Process variables may have an effect on the extruder RTD in terms of the minimum residence time, mean residence time and/or the shape of the distribution. Increasing the feed rate will significantly decrease the mean RTD, narrow the distribution curve, but have a relatively minor effect on the minimum RTD in a co-rotating system (Biral, 1979; Mosso et al, 1982; Altomare & Ghossi, 1986; Kao & Allison, 1984; Agur, 1986; Boissonat et al., 1986; Zuilichem et al., 1988c; Jager et al., 1988, 1989) Screw speed has a significant effect on both the minimum RTD and the mean RTD (Mosso et al, 1982; Altomare & Ghossi, 1986; Kao & Allison, 1984; Zuilichem et al., 1988c; Jager et al., 1988, 1989), but does little to alter the shape of the RTD, even though screw speed influences both temperature and viscosity (Altomare & Ghossi, 1986; Bounie & Cheftel, 1986). Combining all of these factors, it becomes obvious that for a given screw configuration, it is impossible to achieve a long residence time in the extruder (implying a low screw speed) with a very narrow distribution (implying a high feed rate), because these conditions are not compatible with extruder throughput. The best positive conveying characteristics for either co- or counter-rotating TSE's are obtained at high throughput rates and low screw speeds (Rauwendaal, 1981).

A fluid mechanical model of flow in partially filled rectangular channels has been used to explain the dependence of the mean residence time on feed rate and screw speed (Kao & Allison, 1984). Their relation to mean residence time is given by:

$$\bar{\tau} = \frac{V_f}{Q} = 2 \frac{V_f}{\pi D N \cos \psi W H F_d} \quad (43)$$

Screw configuration also affects the mean residence time (Altomare & Ghossi, 1986; Kao & Allison, 1984; Boissonat et al., 1987; Zuilichem et al., 1988c; Jager et al., 1988, 1989) with an uninterrupted screw configuration being a more efficient means of conveying than one which includes mixing or reverse screw elements. The inclusion of these elements brings about a substantial broadening of the RTD through its interruption of smooth flow and mixing action. Based on the work by Olkku et al. (1980b), using radioactive tracers to dynamically measure RTD along the extruder barrel and at the die exit, the final portion of the extruder screw profile for a co-rotating system appears to have the greatest overall effect on the RTD. However, Wolf et al. (1986) didn't observe any differences in RTD for different sections for a counter-rotating TSE. Axial mixing was found to occur also in the feed zone and the compression zone for a counter-rotating TSE (Zuilichem et al., 1988c; Jager et al., 1988, 1989). Axial mixing, on the other hand, has been shown to be affected more by screw design (helix angle, screw configuration) than by overall operating conditions (Todd & Irving, 1969; Todd, 1975a,b).

Temperature has an effect on viscosity, and would intuitively be expected to affect the minimum residence time, however, Kao & Allison (1984) & Altomare and Ghossi (1986) have shown that temperature in general has little or no effect on the RTD. Lower levels of moisture do not appear to have a significant effect on the RTD (Altomare & Ghossi, 1986), however, higher levels or large variations appear to have an effect according to Bounie & Cheftel (1986). Die size and shape appear to have little effect on RTD for a co-rotating system (Altomare & Ghossi, 1986; Boissonat et al., 1987) and since pressure is related to the die size, it may be inferred that the effect of pressure

on RTD is not significant. In counter-rotating system, the effect of die opening was not always observed and depended on moisture content and screw configuration (Jager et al., 1989). Generally, similar effects were observed with a single screw extruder (Zuilichem et al., 1973; Davidson et al., 1983; Zuilichem et al., 1988b), however, a significant die effect has been observed by Zuilichem et al. (1988b). In general, screw speed has a greater effect on the minimum residence time, while feed rate tends to affect the dispersion of the residence time curve (axial mixing). This has also been predicted based on a theoretical model for co-rotating system (Tayeb et al., 1988a,b). Table 1, summarizes the general trends associated with the effect of process variables on minimum RT, mean RT and degree of dispersion (Fichtah & van de Voort, 1989).

Table 1. General trends associated with the effect of process parameters on minimum residence time (t_0), mean residence time (\bar{t}), and degree of dispersion.

Variables	t_0	\bar{t}	Dispersion
Feed rate	m	M(-)	M(-)
Screw speed	M(-)	M(-)	m
Temperature	m	m	m
Moisture	m	m	m
Screw severity ^a	M(+)	M(+)	M(+)

m = minor effect, M = major effect, + = Positive effect, - = Inverse effect

^a The severity of screws can be increased by including mixing elements such as paddles, kneading discs, or cut-flight screws

2.4.4.4 Models for RTD

The theoretical analysis of RTD's are normally based on the ideal assumption of either plug flow or perfect mixing conditions expressed by, for plug flow:

$$\begin{aligned}
 F(t) &= 0; & t < \bar{t} \\
 F(t) &= 1; & t \geq \bar{t}
 \end{aligned}
 \tag{44}$$

and for perfect mixing:

$$F(t) = 1 - e^{-t/\bar{t}} \tag{45}$$

The required condition for plug flow is for the residence time in the reactor to be identical for all the elements of fluid, leading to a constant velocity profile. In a mixed flow model the fluid inside the reactor is so well mixed and uniform throughout, that the exit stream from the vessel has the same composition as the mass within the reactor. However, the conditions in an extruder are neither that of plug flow nor perfect mixing. Many models have been suggested to characterize the non ideal flow patterns within reactors, with two useful ones having been described by Levenspiel (1972); the "dispersion model" and the "tanks in series model", both of which may be applicable to the extruder, and are discussed below along with other models.

Dispersion model and tanks in series model

In the dispersion model, one considers plug flow upon which is superimposed axial mixing diffusivity without the presence of dead space, bypassing or short-circuiting. By considering the plug flow model plus Fick's law of diffusion, the concentration distribution function for a tracer impulse can be derived (Levenspiel, 1972):

$$c(\theta) = \frac{1}{2\sqrt{\pi(D_e/uL)}} \exp\left[-\frac{(1-\theta)^2}{4(D_e/uL)}\right] \tag{46}$$

where D_e is the axial dispersion coefficient, u is the average axial velocity, and L is the vessel (i.e. extruder) length. D_e/uL is called the reactor dispersion number, varying from

zero for plug flow, to infinity for back mix flow and is the inverse of the axial Peclet number (Pe) for mass transfer. Since the integration of $C(\theta)$ between zero and infinity is unity, $C(\theta)$ also represents the residence time distribution $E(\theta)$, and $F(\theta)$ can therefore be obtained by the integration of the $E(\theta)$ function. By associating the D_z/uL value with the corresponding theoretical curve which most closely matches the experimental E or F -curve, the behaviour of the extruder as a reactor can then be predicted (Todd & Irving, 1969; Levenspiel, 1972). This model is satisfactory when the flow does not deviate too greatly from plug flow behaviour, a condition which counter-rotating system approaches more than the co-rotating one.

The tanks in series model is an alternative approach to the dispersion model for dealing with small deviations from plug flow (Levenspiel, 1972). In this model one considers the system to be represented by a series of n Continuously Stirred Tank Reactors (CSTR). The E function in this case is:

$$E(\theta) = \frac{n^n \theta^{n-1}}{(n-1)!} e^{-n\theta} \quad (47)$$

A perfectly mixed vessel is represented when n is equal to unity and if n approaches infinity plug flow conditions are being met. This model is generally known as CASCAD model and was not found to be satisfactory in describing the RTD in a co-rotating system (Bounie, 1988).

An alternative approach in developing the dispersion model is proposed by Todd & Irving (1969) to fit the experimental data of the RTD using a co-rotating TSE. Here the concentration distribution function, $C(\theta)$, was given by:

$$C(\theta) = \sqrt{\frac{Pe}{\pi\theta}} \exp\left[-\frac{Pe}{4} \frac{(1-\theta)^2}{\theta}\right] - \frac{Pe}{2} e^{Pe} \left[\operatorname{erfc} \sqrt{\frac{Pe}{4} \frac{1-\theta}{\theta}} \right] \quad (48)$$

where Pe is the Peclet number which can be related to the variance of the residence time, in the case of closed vessel, by (Levenspiel, 1972):

$$\left[\frac{\sigma}{\bar{t}} \right]^2 = 2 \frac{Pe - 1 + e^{-Pe}}{Pe^2} \quad (49)$$

The model given by eqn (48) was used to study axial mixing in a TSE having various arrangements of staggered paddles and/or screws (Todd & Irving, 1969; Todd, 1975a,b). The extent of axial mixing was assessed in terms of the Peclet number, which is a measure of the spread of distribution curves. The cumulative RTD plotted as a log-probability graph produces a straight line, its slope giving a first estimation of Pe (Todd & Irving, 1969; Todd, 1975a,b). A deviation from linearity may suggest that other phenomena, than just simple axial mixing such as stagnant zones or backflow, are occurring. Such RTD studies indicate that high Pe (narrow RTD's) can be achieved with very low helix angle screws or with relatively straight paddles, the later having the advantage of increasing new surface generation.

The dispersion model was also used to simulate axial mixing in a conical counter-rotating TSE (Zuilichem et al., 1988c; Jager et al., 1988, 1989). Each C-shaped chamber of the extruder screw was considered to be a CSTR and the leakage flow between the chambers was accounted for. A plug flow time was introduced into the RTD model to account for axial mixing effect due to kneading elements.

Mixed models

In many situations when dealing with real flow systems, the dispersion model or the CSTR model cannot satisfactorily characterize the flow in a reactor because of large deviations from plug flow. The concept of using mixed models is a means of overcoming these limitations by dividing the reactor into distinct regions. Commonly designated regions used in the construction of mixed models include, plug flow regions, backmix

flow regions, dispersed plug flow regions and deadwater regions (Levenspiel, 1972). Various mixed models have been assessed as means of fitting extrusion RTD data (Bounie, 1988). The model used by Davidson et al. (1983) consists of n stages of active and dead space regions with a low cross flow of material between them (Figure 7a). This model was derived by Levich et al. (1967) and demonstrates that the RTD can be approximated by combining a Gaussian and exponential decay curve for large values of n . The general form of this RTD model is (Davidson et al, 1983):

For $t < t_d$

$$E(t) = (1-f_d) \frac{1}{\sqrt{2\pi\sigma_g^2}} \exp\left[-\frac{(t - t_a)^2}{2\sigma_g^2}\right] + \frac{f_d}{4t_d} \left[1 - \operatorname{erf}\left(\frac{t_d - t}{\sqrt{2} t_d}\right)\right] \quad (50)$$

and for $t > t_d$

$$E(t) = (1-f_d) \frac{1}{\sqrt{2\pi\sigma_g^2}} \exp\left[-\frac{(t - t_a)^2}{2\sigma_g^2}\right] + \frac{f_d}{t_d} \exp\left[-\frac{t}{t_d}\right] \quad (51)$$

where t_a is the mean residence time in the active region, t_d is the mean residence time in the dead space region, f_d is the fraction of the material delayed in the dead space, and σ_g^2 is the variance of the Gaussian distribution.

Such distributions can be interpreted as an indication of two distinct mechanisms being associated with the passage of the material through the extruder. The first set of terms, which the two equations have in common, are responsible for the Gaussian aspect of the distribution characteristically observed for the majority of the material undergoing extrusion. The remaining terms describe the exponentially decaying portion of distribution with the term in eqn (51) being the most important, while it may be neglected in eqn (50). Regardless of the fact that the second term represents only a small fraction of the

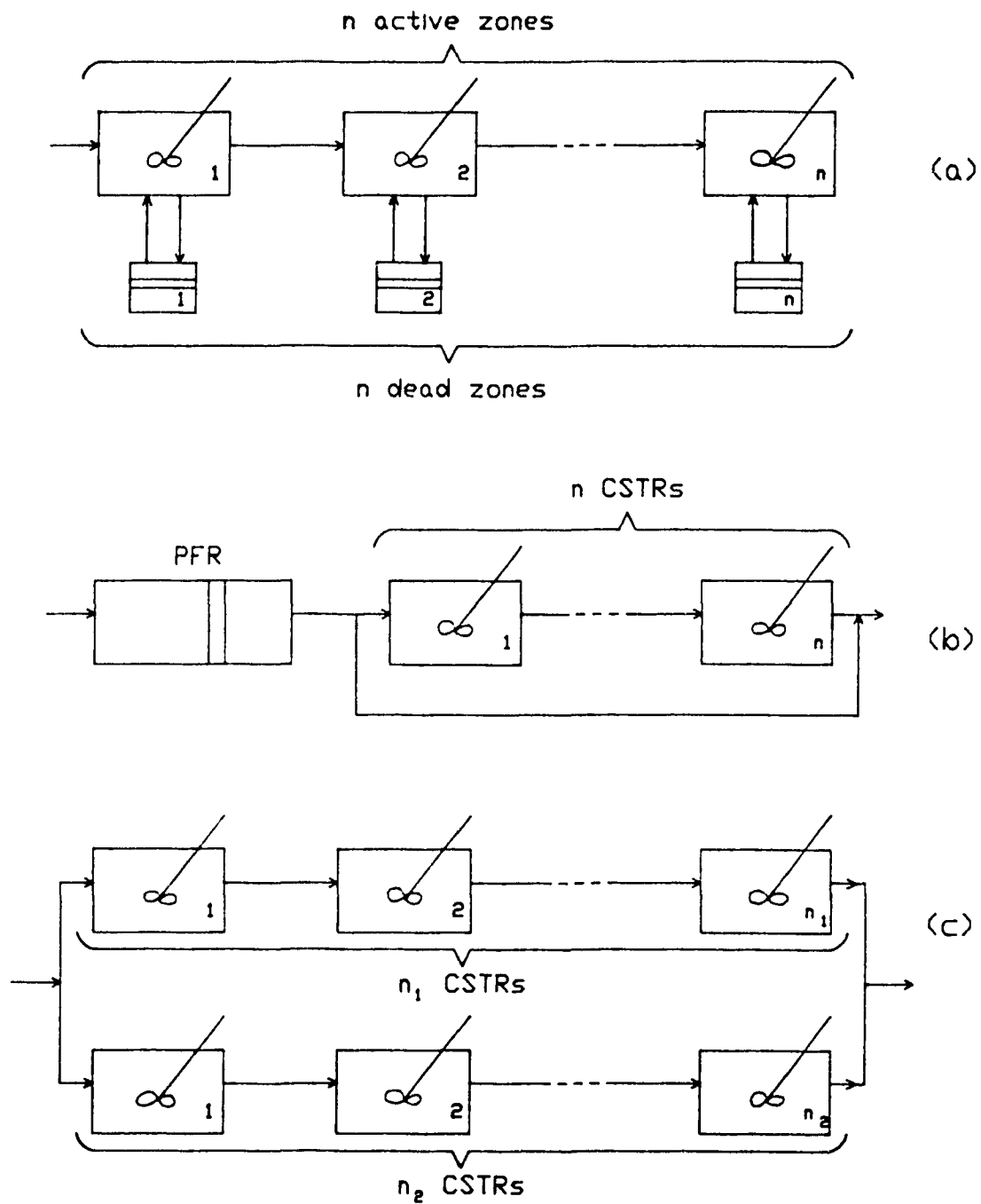


Figure 7. Some of the flow models used to describe residence time distributions in an extruder which are: Levich et al. (1967) model (a); GAMMA model with recirculation (b); and CASPAR model (c). PFR=Plug Flow Reactor, CSTR=Continuously Stirred Tank Reactor.

material comprising the overall distribution, it is crucial because the decay component of the distribution may be slow, and thereby contribute extensively to the tail portion of the distribution.

Wolf & Resnick (1963) considered the perfect mixing model and included within it, additional parameters to account for non ideal phenomena; i.e., plug flow, dead space, bypassing and short circuiting, error in average residence time and lags in response. The general equation developed by them is expressed as follows:

$$F(\theta) = 1 - \exp\left[-b(\theta - \epsilon/\bar{\tau})\right]; \quad \theta \geq \epsilon/\bar{\tau}$$

$$F(\theta) = 0; \quad 0 < \theta < \epsilon/\bar{\tau}$$
(52)

where b is the coefficient of the exponent and ϵ is the system phase shift. The term b can be considered as a measure of the efficiency of mixing, being equal to 1 for perfect mixing and tends toward infinity for plug flow. Thus deviations of b from unity are an indication of extent of imperfect mixing. For a combination of plug flow and perfect mixing, eqn (52) becomes (Wolf & Resnick, 1963):

$$F(\theta) = 1 - \exp\left[-\left[\frac{1}{1-P}\right](\theta - P)\right]; \quad \theta \geq P$$

$$F(\theta) = 0; \quad 0 < \theta < P$$
(53)

where P is the fraction of material in plug flow and is equal to the normalized delay time (in plug flow). Thus, the value of P can be viewed as an indication of the conveying performance, while the $(1-P)$ value can be related to the mixing performance of the extruder (Agur, 1986). This model was successfully used by Wolf & White (1976) to describe the RTD in a single screw extruder. It was also shown by Walk (1982) that was the most adequate model from these tested to fit the data for a counter-rotating, non-

intermeshing twin screw extruder and has since been used to study the RTD of co-rotating twin screw extruders (Altomare & Ghossi, 1986; Balke, 1985; Agur, 1986). The Wolf & Resnick model for multistage systems could be useful when the model given by eqn (52) is not satisfactory. With the assumption that the values of b and ϵ are equal for each stage, The multistage wolf & Resnick (1963) model for n identical stages in series, is given by:

$$F(\theta) = 1 - e^{-b(\theta - n\epsilon/\bar{\epsilon})} \left\{ 1 + b \left[\frac{\theta - n\epsilon}{\bar{\epsilon}} \right] + \dots + \frac{b}{(n-1)!} \left[\frac{\theta - n\epsilon}{\bar{\epsilon}} \right]^{n-1} \right\} \quad (54)$$

This model has been used by Davidson et al. (1983) to interpret single screw extrusion data and has been shown to be very adequate in describing RTD in a co-rotating system (Fichtali et al., "unpublished data").

A model considering plug flow in series with 2 perfectly mixed tanks was used by Zuilichem et al (1973) in their interpretation of experimental results for a single screw extruder. This model was valid only for lower moisture contents (< 16.5%) and he suggested that for higher values a model using more tanks would be needed to fit the experimental residence time curve. This model is commonly known as the GAMMA model (i.e., plug flow plus n CSTR in series), where the number of CSTR can be calculated to best fit a given distribution curve. Other phenomena such as recirculation (Figure 7b) or dead volume can be included to improve the fit. The GAMMA model has been shown to be very adequate for a co-rotating extruder (Biral, 1979; Bounie, 1988), and as a consequence flow in a co-rotating extruder can be considered as a combination of plug flow related to conveyance performance and perfect mixing related to the mixing performance. To quantify the positive displacement and the axial mixing using the GAMMA model, Bounie (1988) used the following formulae:

$$\alpha = \frac{t_0^*}{\bar{t}^*} \quad (55)$$

$$1 - \alpha = \frac{\bar{t}^* - t_0^*}{\bar{t}^*} \quad (56)$$

$$i_m = \sqrt{\left[\frac{(\bar{t}^* - t_0^*)^2}{n} \right]} = \sqrt{(\sigma^{*2})} \quad (57)$$

where α is the positive displacement index, $1-\alpha$ represents the relative mean time of mixing, and i_m represents the intensity of axial mixing, assessed as the square root of the variance of the fitted RTD curve (σ^2).

Another mixed model, represented by two parallel CASCAD's of perfectly mixed tanks, termed the CASPAR model (Figure 7c), has been shown to be useful in describing the RTD in a co-rotating system (Boissonnat et al., 1987). This model permits the division of the flow into two separate circulating modes with one flow fraction remaining in the C-shaped chamber and having a shorter residence time than the second flow passing from one screw channel to the other in a figure 8-shaped path.

Developing equations for mixed flow models can be achieved through the use of the transfer function concept in the Laplace form or in Fourier form (Wolf & Resnick, 1963; Biral, 1979; Bounie, 1988). The transfer function permits the calculation of the intrinsic flow function of a system and has the advantage of obtaining the model serial moments, which can express the characteristic shape of any RTD curve. As a consequence, more complex mixed models can be studied.

Describing RTD by fitting the experimental data to any of the models discussed above is still the only available way when dealing with TSE's. Predictions of RTD from theoretical flow models for TSE's are very rare in literature and are only as accurate as the velocity profiles that form the basis of the calculation. Werner & Eise (1979) used a theoretical model based on a cascade of ideal mixers (chambers) to quantify axial mixing in a kneading disc section of an extruder. Using a series of equations and solving them numerically, gives a residence time spectrum which depends on the axial mixing coefficient (ratio of backflow in kneading disc combination to volumetric throughput rate) based on the total number of ideal mixers. Increasing the number of ideal mixers narrows the residence time spectrum, while increasing the axial mixing coefficient, broadens the spectrum and increases its tail portion. The axial mixing coefficient decreases with an increased conveying factor (ratio of average conveying velocity in axial direction to average conveying velocity in circumferential direction), which corresponds with increasing the degree of fill. This coefficient can be determined experimentally by matching the experimental results to the theoretical curves of RTD. The flow model through reverse screw elements developed by Tayeb et al. (1988a), allows the computation of the RTD by summing the particles arriving at the die over a specified time for a range of flow paths. To determine the RTD in the whole extruder, plug flow was assumed in the conveying and in pumping zones (Tayeb et al., 1988b).

2.4.5 Conclusion

Flow, mixing and RTD all are basic phenomena very important in extruder and process evaluation. Developing models for flow behaviour is very fundamental from the perspectives of computing extruder throughput, deriving expressions for velocity and shear distributions, obtaining flow pattern maps, analyzing mixing and modelling RTD's. Developing models to predict the extent and uniformity of mixing is also useful in determining screw design and overall screw configuration. In co-rotating TSE's one can more readily tailor the dispersive and the distributive mixing effects by the virtue of a wide choice of screw designs and operating conditions. Counter-rotating extruders

generally have narrower RTD's and better dispersive mixing capabilities, but less product homogeneity. The RTD provides a general picture of the mixing and subsequent thermal history of a product. Using the RTD as a basis, any changes in extrusion parameters (i.e. screw profile, temperature, screw speed, feed rate, etc.) can be evaluated in terms of optimizing the process. The velocity profile and the RTD are also useful means for comparing extruder types, design, scale-up in relation to a given process, and troubleshooting (i.e. surging, plugging, non uniformity problems). In relation to these factors, screw design is a key parameter, which include helix angle, clearances, channel depth, plus the additional complications introduced by the use of mixing elements, all of which have to be balanced against throughput, mixing, power, new surface generation, obtaining uniform residence times and maintaining temperature control. Users of extruders for food applications generally have a very poor understanding of these aspects and the rationale for the choice of any particular screw configuration.

It is quite clear that the theoretical understanding of food extrusion lags far behind the knowledge accrued for plastics applications, although some interesting modelling work has been published in relation to food extrusion (i.e., Yaku, 1985; Tayeb et al., 1988a,b; Bounie, 1988). There is an ongoing need for a more systematic and scientific investigation of twin screw extrusion in the food sector. This chapter has attempted to summarize much of the basic information related to flow behaviour, mixing and residence time distribution, which might be useful to the process engineer and food scientist carrying out research and development, or applications work in food extrusion. The models described and discussed, although largely related to plastics extrusion, provide a set of useful tools for evaluating food extrusion processes and may assist in their optimization. Judicious selection and application of some of these basic concepts would assist in reducing the more empirical aspects of food extrusion, leading to a better understanding of the cause and effect relations in any process undertaken.

2.5 CONCLUSION

The literature provides a substantive information base from which to draw on in terms of casein/caseinate chemistry and production, basic information about twin screw extrusion in general, plus specific detail related to the flow behaviour, mixing and residence time distribution of the twin screw extrusion process. The research results described in the thesis draw heavily on the knowledge and concepts described in this literature review.

3 RESULTS AND DISCUSSION

3.1 ACID COAGULATION OF SKIM MILK POWDER BY EXTRUSION PROCESSING: A PRELIMINARY EXPERIMENT

ABSTRACT

Using the extruder as a continuous reactor, skim milk powder (SMP) was mixed with acid to produce a coagulum. The effect of process variables on selected extrudate properties was studied using response surface methodology. No effect was observed using high heat SMP, while total protein and lactose levels were significantly affected by temperature when medium heat SMP was used. Washing the coagulum turned out to be more difficult than anticipated in terms of removing lactose and resulted in high losses of fines. Extrusion processing was determined to be a potential means of preparing an acid coagulated product from SMP as a preliminary step to the production of sodium caseinate, however, more investigation is required to understand and control the process.

3.1.1 Introduction

Extrusion is a suitable process when the raw material is a powder which should be processed under specified conditions of moisture, shear, pressure, and time-temperature history. Extrusion has many advantages (Harper, 1981) such as versatility, product homogeneity, high productivity and other features discussed in detail in Chapters 2.3 and 2.4. These advantages could be put to use in producing a quality casein from surplus SMP and also neutralizing acid casein to sodium caseinate.

This preliminary study was undertaken to determine the feasibility of using the extruder for the acid coagulation of SMP and the effectiveness of the process unit operations, including coagulation, washing and neutralization, and as a prelude to future studies designed to understand, control and optimize the process.

3.1.2 Materials and Methods

Commercially available high and medium heat SMP were obtained from Fedeco (Cooperative Fédérée du Québec, Montreal) which had the following proximate analysis (Table 2):

Table 2. Proximate analysis of high and medium heat SMP (as is basis).

	Protein (%)	Lactose (%)	Fat (%)	Moisture (%)	Ash (%)
High heat SMP	31.0	52.1	0.8	5.8	8.2
Medium heat SMP	30.6	54.0	4.2	4.2	8.0

Extruder

A Creusot-Loire model BC 45 fitted with intermeshing, co-rotating twin screws and a barrel heated by an electrical induction system was used in this study. The extruder was rated at 25HP and the maximum allowable torque set at 50 m.kg for the 15 Kw motor drive. A screw profile was assembled, consisting of approximately three equal feeding, mixing, and metering sections, respectively. Cut-flight reverse screw elements were used just before the die to increase the filled length of the screws and avoid fluctuations at the output. A special, multi-orifice die (Barraquio et al., 1988) was assembled to reduce the pressure and increase the surface area of the resultant product.

Process control

The extruder was equipped with 3 thermocouples (one in each section), a pressure transducer, plus sensors to follow screw speed, amperage (load), and pump flow rate. All the sensors were calibrated and tested and were connected to a Campbell CR7 data logger for continuous monitoring of the data which were recorded on magnetic tape. The data were transferred to an IBM PC via a program written in Basic (Appendix 1A), and analyzed using an APL program (Appendix 1B). A schematic diagram of the setting used for process control is given in Figure 8.

Coagulation

Two extrusion runs were conducted. The first, with high heat SMP using a central composite $2^4 + 2k + 1$ design (Cochran & Cox, 1957) consisted of 25 treatment combinations which included three levels of temperature (50, 70, 90 °C), screw speed (50, 70, 90 rpm), feed rate (8.58, 12.24, 15.9 Kg/hr), and moisture (0.2 M HCl solution) levels (25, 30, 35%). Based on the results of the first extrusion run, a $2^4 + n$ factorial design of seven treatment combinations was followed for the extrusion of medium heat SMP. In this case, only temperature (74, 84, 94°C) and moisture (26, 32, 38%) were tested while screw speed and feed rate were maintained at 70 rpm and 12.24 Kg/hr, respectively.

Representative extrudate samples were collected from each extrusion run and analyzed for fat, lactose, total protein, soluble protein, and non protein nitrogen (Barraquio et al., 1988). Other analysis included electrophoresis to determine whether heat and/or shear altered the proteins in any significant manner and statistical analysis were used to generate the regression estimates for each response.

Washing

A portion of the curd from high heat SMP (~30% moisture) was ground to coarse particles using a colloid mill and then washed in an agitated tank for 20 min at 45-46°C and a wash water ratio (water weight to original SMP weight) of 4.1. The washing

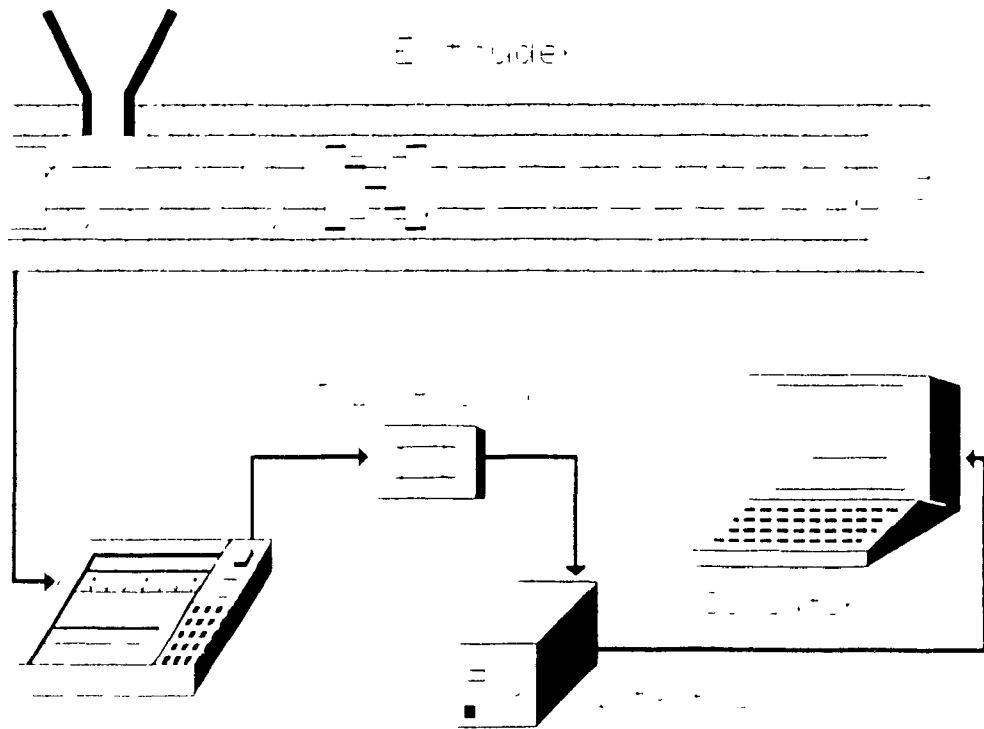


Figure 8. Schematic diagram of a data acquisition system used to collect extrusion data during processing.

operation was repeated 3 times and the curd was separated from the wash water after each washing step using a Kason vibrating 100 mesh screen separator. The efficiency of washing was determined by analyzing lactose after each washing step by the Multispec MK1 infrared milk analyzer (van de Voort, 1980).

Neutralization

The washed casein (~75% moisture) was neutralized in the same extruder used for the coagulation step using the same screw configuration, but with a single orifice slit die. The operating conditions were 50 rpm for screw speed, feed rate of 22 kg/hr, flow rate of 3 l/hr and temperature ranges from 55 to 150°C. Sodium hydroxide was used for neutralization to obtain a pH close to neutral and the moisture content of the end product averaged 78%.

3.1.3 Results and discussion

Process control

The operating conditions as a function of time are plotted in Figure 9; with Figure 9a showing temperature at each zone, which are the feed zone (curve T1), the mixing zone (curve T2), and the metering zone (curve T3). Each curve represents three stages which corresponds to the setting temperature of 50, 70, and 90°C. The measured temperature at the mixing zone, where the extruder was heated, is identical to the setting temperature at 70 and 90°C and no major fluctuations occurred when changing the other operating conditions. However, at 50°C major temperature fluctuations were encountered, specifically when increasing the screw speed, which corresponds to the two peaks observed at T2 curve of Figure 9a. Thus, the temperature setting is more sensitive to operating conditions changes, specifically screw speed, at lower temperatures. Temperatures at the feed and metering zones are also affected by the changes in operating conditions. At a setting of 50°C, the temperature at the metering zone (curve T3) is higher than the temperature at the mixing zone (curve T2), but is lower at a temperature setting of 90°C. Regression analysis showed that the product temperature at the die exit was

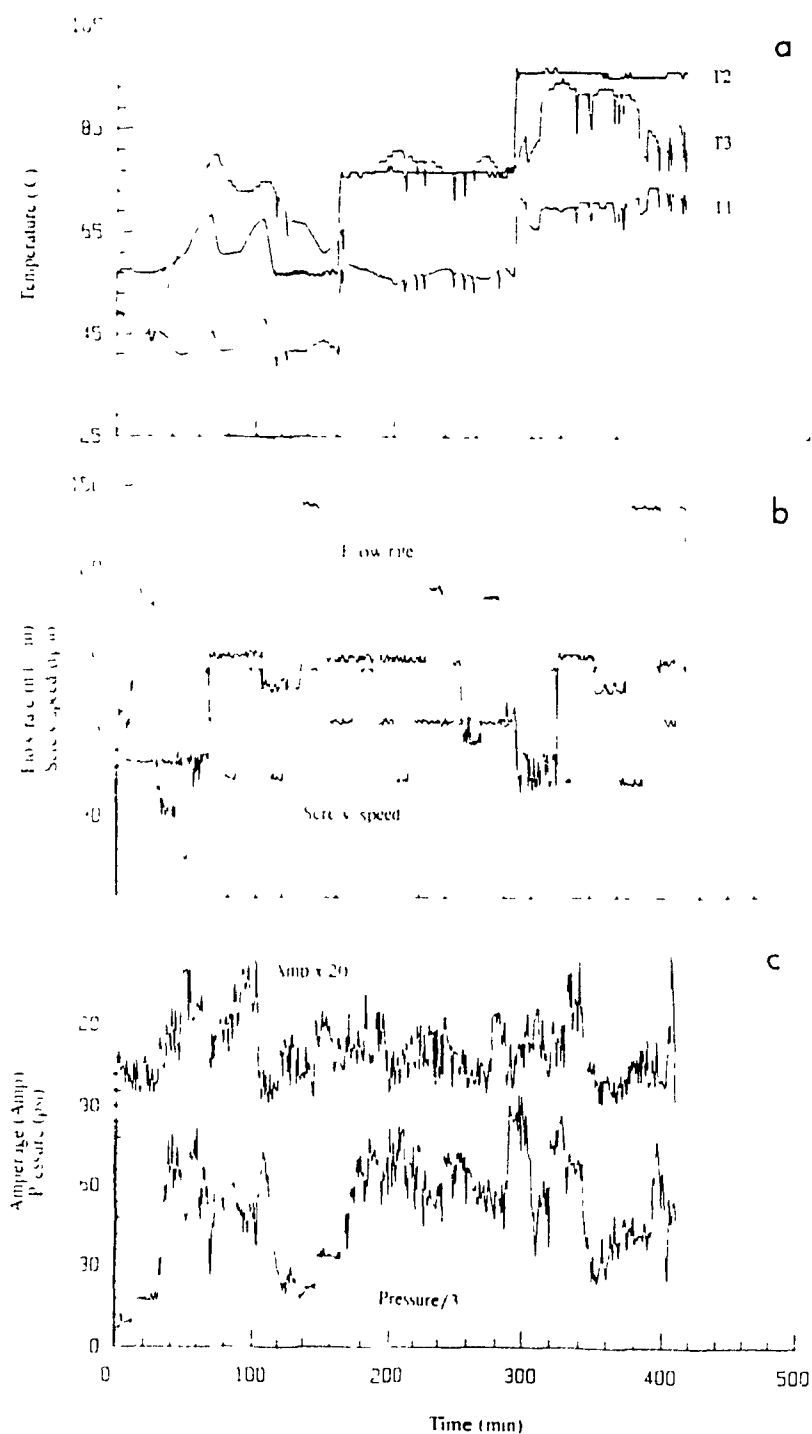


Figure 9. Continuous plots of operating conditions using the data acquisition system illustrated in Figure 8. (a) temperatures at feed zone (T1), mixing zone (T2), and metering zone (T3); (b) flow rate and screw speed; and (c) amperage and pressure at the die.

significantly affected by setting temperature ($p < 0.01$) and by the interaction between moisture and feed rate ($p < 0.05$), with the former having a positive effect and the later having a negative effect.

No major fluctuations were associated with flow rate or screw speed at different settings (Figure 9b). The motor load (amperage) was amplified 20 times (Figure 9c) to detect fluctuations and was mainly affected by the screw speed with an average of about 5.5 amperes. Major variations were observed in the die pressure and regression analysis indicated that is significantly affected by moisture ($p < 0.01$), which has a negative effect on pressure by reducing viscosity. However, fluctuations in die pressure were observed even under constant operating conditions due to surging and plugging of some of the die holes. These fluctuations were less pronounced at higher feed rate because of the increase in the filled volume of the screws.

Coagulation

The extrudate exiting from the die under the extrusion conditions imposed, varied from a dry brittle product to one which was wet, crumbly and showed marked syneresis. The results of the physico-chemical and statistical analysis will be only summarized here as they have been presented elsewhere (Barraquio et al , 1988).

The pH of the extrudates was much higher than the isoelectric point (~ 4.6) and ranged from 5.75 to 5.95. Thus, coagulation can take place at high pH's under high solids concentrations. None of the extrusion parameters (temperature, moisture, screw speed, and feed rate) significantly affected the total protein, soluble protein, NPN or lactose concentration in the coagulum from high heat SMP. However, in the case of extrudates from medium heat SMP, total protein was strongly affected ($p < 0.01$) by temperature as was lactose ($p < 0.05$). The increase of total protein with temperature resulted from whey protein denaturation which was also confirmed by electrophoresis. The negative effect of heat on lactose implies that lactose may be bound to the whey proteins, either physically, via the Maillard reaction or degraded to organic acids such as formic acid as a result of

heating (Blais et al., 1984). Electrophoretic analysis indicated that extrusion conditions did not cause any alteration in the casein fractions relative to the original SMP.

Washing and Neutralization

Washing indicated that the coagulation was not complete and the coagulum was rather rubbery and gelatinous. The lactose content was 15%, 4%, and 2% after the first, second, and third wash, respectively. The high lactose content after the third wash reflects a low washing efficiency which might be due to several factors, including the washing system, washing conditions, coagulation conditions and the structure of the coagulum. Fines were exceptionally high and reached ~15% of the original SMP, reflecting the inadequacy of coagulation conditions. Neutralization by extrusion was possible, however, the high moisture of the curd caused major fluctuations in feeding and caused variations in the pH of the end product. Colour formation due to Maillard browning started to appear when the product temperature reached 82°C and was very pronounced at 150°C.

3.1.4 Conclusion

Preliminary experiments assessing the coagulation of SMP and the neutralization of the acid casein produced by extrusion indicated some potential, however, the process clearly required a more basic approach including: (1) an intensive study on the coagulation of concentrated milks to determine the parameters which affect the structure of the coagulum and the subsequent washing efficiency to remove whey components and minimize losses of fines; (2) A better equipment for coagulation, washing, dewatering, and neutralization, including an extruder having better temperature control and better feeding system; (3) an investigation of extruder performance to characterize the process and understand the basic phenomena occurring in the extruder, specifically related to neutralization of acid casein.

This preliminary study provided a general idea of the process, the difficulties associated with the conversion and the research required to develop the process. The

1
ensuing chapters describe the work undertaken to solve the problems encountered in this preliminary study, which led to improvements in our understanding of coagulation and washing and finally the development of a process to produce casein and caseinate.

3.2 COAGULATION AND WASHING CONDITIONS FOR ACID CASEIN PRODUCTION

ABSTRACT

Response surface methodology was used to study the production of acid casein from skim milk powder and to investigate the effects of pH, concentration and washing conditions (agitation, time, temperature and wash water ratio) on the end product. The washed curd was analyzed for residual ash, minerals, lactose and whey protein nitrogen (WPN). The critical variables were found to be concentration and pH in relation to mineral content, concentration and washing time for lactose, and pH for WPN. Surface response methodology provided a unique insight into the relationships between the variables related to the process and the results were used to explain the observations in terms of milk chemistry. The washing process was further evaluated in term of Murphree Stage Efficiency to elucidate the effect of the number of washing stages on residual whey components in the casein curd. This study also helped in understanding the extrusion process of skim milk powder which uses high milk solids levels.

3.2.1 Introduction

Preliminary work (Chapter 3.1) indicated that an acid co-precipitate could be produced from SMP. However, the washing of the extruded gelatinous coagulum to produce a product meeting international standards proved to be more difficult than anticipated. In assessing the problems encountered, i.e., difficulty in removing lactose and the high loss of fines, it was recognized that the conditions of SMP coagulation and the subsequent washing of the curd would have to be re-evaluated.

The coagulation of SMP and subsequent washing to produce acid casein involves the same variables as conventional acid casein production from liquid skim milk, including pH, temperature (T), time (t), agitation (rpm) and wash water ratio (WWR). One additional variable associated with extrusion processing is concentration (C). To date no work has been published examining the interrelationship between the process variables and the product characteristics related to casein production, largely due to its complexity. Such a multivariate system cannot be handled effectively using a one variable at a time approach, but may be studied by response surface methodology (RSM). Using this method, empirical models can be generated from the independent variables in relation to assessed responses, which in turn provides a means of optimising the process.

This chapter describes a general multivariate SMP acid coagulation/washing system to aid in determining the operating conditions for SMP extrusion and conventional acid casein production, and explains the results in physico-chemical terms.

3.2.2 Material and Methods

Commercial low heat SMP was obtained locally from Crino Ltd. (Agropur, Québec) which had the following proximate composition; 30.6% protein, 54% lactose, 0.8% fat, 4.5% moisture, 7.8% ash and a whey protein index of 7.5 mg/g powder.

Coagulation/Washing

Skim milk powder was reconstituted on a wt/wt basis using pre-heated (45°C) deionised water as required to produce pre-selected concentrations. The solution was placed in a 1 l mixing vessel which was part of the experimental set-up (Figure 10) used for all coagulation/washing operations. The pH of the system was monitored using a Corning Model 140 digital pH meter and the holding temperature controlled using a Haake W13 water bath and D8 controller. A controlled speed, Catramo RZR50 stirrer, fitted with a custom-made agitator consisting of four parallel equidistant blades was used to cut and disperse the curd as it formed (Figure 10).

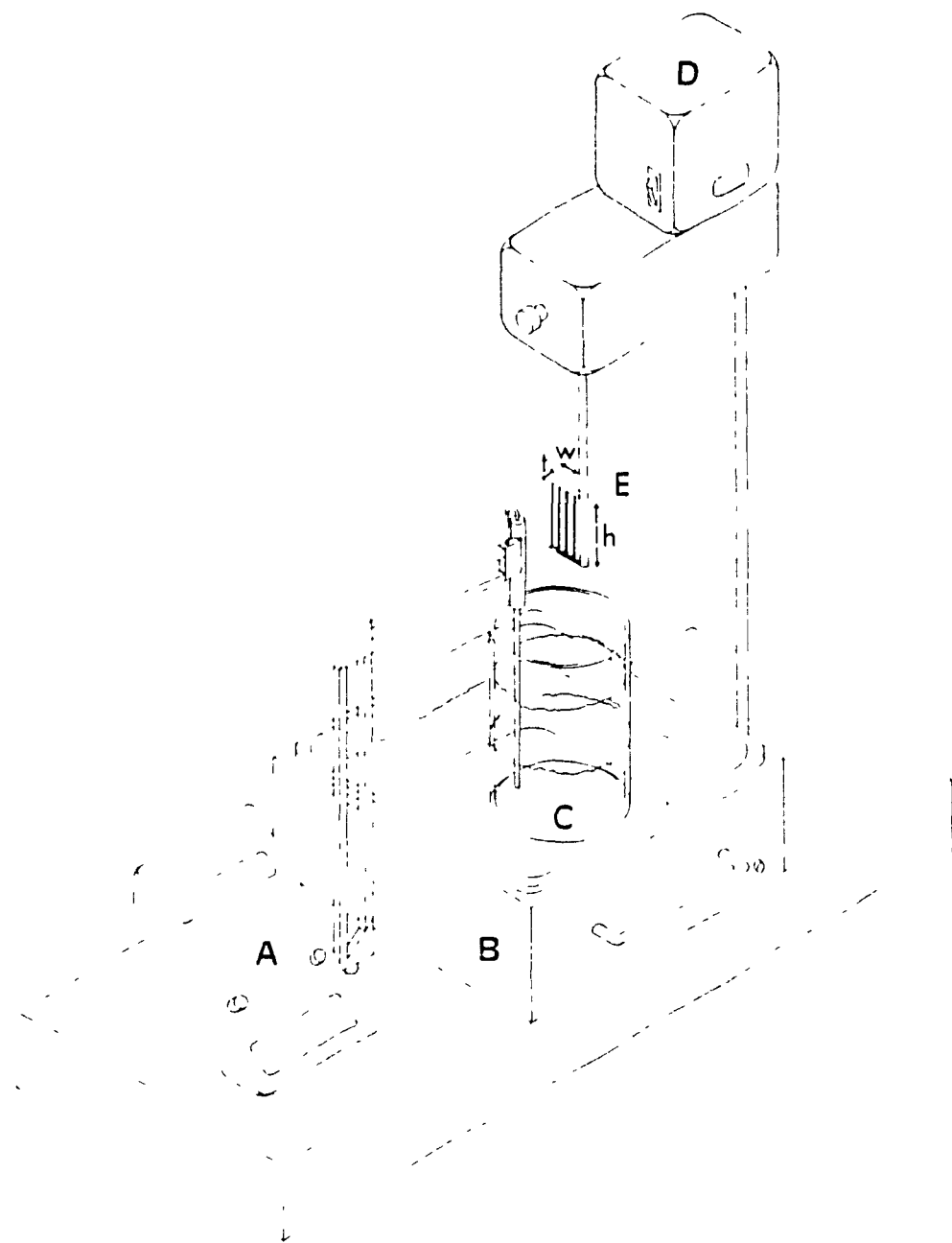


Figure 10. Experimental set-up for coagulation/washing process including (A) pH-meter, (B) water bath, (C) holding vessel, (D) controlled speed stirrer, and (E) mixing blade. The vessel diameter is 10.4 cm and the mixing blade dimensions are: $h=6.8$ cm; $w=3.7$ cm; and $t=0.5$ cm.

A predetermined amount of standardized 1.24 M HCl was added to the SMP solution to produce coagula of a specified pH. The acidified solution was stirred at high speed (400 rpm) for 1 min, followed for 5 min at the speed dictated by the experimental design, and then allowed to rest for 9 min (acidulation time), after which the final pH and temperature were measured. The reproducibility of the pH and temperature measurements were ± 0.02 and ± 0.5 °C respectively.

The coagulum was separated from the whey using a 100 mesh (150 μm) stainless steel screen, the whey set aside and coagulum returned to the holding vessel for the washing procedure. This process was repeated a total of 4 times. The coagulum in the holding vessel was diluted with deionised water acidified to the pH selected for coagulation at a temperature and volume dictated by the experimental design, as were agitation and washing time. Only the temperature of the second and third wash was varied, while the temperature of the first and last wash were kept at the original coagulation temperature (45°C). The resulting curd, which had been washed 4 times, was frozen and subsequently freeze dried for further analysis. Fines, which are important in acid casein production, were also studied, but will be considered in the next chapter.

Analytical Methods

The ash content of the curd was assessed by the standard AOAC (1984) procedure (16.216), its weight recorded and retained for subsequent Inductive Coupled Plasma spectroscopic analysis (ICP). Calcium and sodium were simultaneously determined using ICP with an Applied Research Laboratories Model 3510 spectrophotometer (Date & Gray, 1989). Standards were prepared using mixtures of NaCl/CaCl₂ and the calibration incorporated into the instrument computer. The ash retained from the AOAC ashing process was then dissolved with heat in 15 ml of 3M HCl and filtered into a 100 ml volumetric flask. The crucible was washed three times with 5 ml aliquots of acid and the solution brought to volume with 3M HCl. About 3 ml of the sample was aspirated into the flame.

Lactose was determined using the International Standard phenol-sulphuric acid method specifically developed for acid casein (International Standard, 1980) and is expressed as anhydrous lactose as a percent by mass. A calibration curve was prepared using analytical grade lactose on a Varian Model DMS100 UV-visible double beam spectrophotometer and the samples prepared for analyses according to the standard method. Whey protein nitrogen (WPN) was analyzed using the Harland- Ashworth method (Kuramoto et al., 1959).

Experimental Design

A central composite design with 3 blocks (Box & Draper, 1987) for 6 factors and with 6 centre points was used for this study. The input variables considered in the experiment, their original values and coded levels are presented in Table 3. The design consisted of 50 treatment combinations, including 5 levels for each factor which were fixed to allow the investigation of a wide range of experimental conditions within practical limits. Using the SAS RSREG procedure (SAS; Institute Inc., Cary, North Carolina, 1985), the 50 coded levels were regressed against each of the responses to obtain the coefficients for second order regression equations which describe the contribution of each variable to the selected response. By selecting two of the more important contributing variables and fixing or eliminating the others, a two dimensional contour plot or three dimensional surface response plot could be generated. The general form of a second-order regression model is:

$$Y = \beta_0 + \sum_{i=1}^k \beta_i X_i + \sum_{i=1}^k \beta_{ii} X_i^2 + \sum_{i=1}^{k-1} \sum_{j=i+1}^k \beta_{ij} X_i X_j + \epsilon \quad (58)$$

Where X_1, X_2, \dots, X_k are the input variables which influence the response Y ; $\beta_0, \beta_i (i=1,2,\dots,k), \beta_{ii} (i=1,2,\dots,k; j=1,2,\dots,k)$ are unknown parameters, and ϵ is random error.

Table 3. The original and coded levels of the input variables for the coagulation/washing process.

Variables		Coded levels				
		-2	-1	0	1	2
pH	X_1	4.1	4.3	4.5	4.7	4.9
Temperature	X_2 (°C)	40	45	50	55	60
Concentration	X_3 (%)	10	20	30	40	50
Time	X_4 (min)	5	10	15	20	25
Mixer speed	X_5 (rpm)	150	200	250	300	350
Wash water ratio	X_6 (g/g)	3	4	5	6	7

3.2.3 Results and Discussion

The analytical data are given in Appendix 2 along with the experimental design. Table 4 presents the regression coefficients obtained for each response, including the coefficients of determination for the equations derived. All the coefficients of determination (R^2) for the regression equations of the responses, with the exception of WPN, were significant at $p < 0.01$. The responses are discussed in relation to the parameters which were shown to be significant ($p < 0.01$).

Table 4. Least squares fit and regression estimates for the responses: Y_1 = Ash(%); Y_2 = Ca(mg/g); Y_3 = Na(mg/g); Y_4 = Lactose(%); and Y_5 = WPN (mg/g)

Parameters	Regression Coefficients				
	Y_1	Y_2	Y_3	Y_4	Y_5
intercept	3.3439**	7.1511**	0.0594**	0.2235**	2.2793**
X_1	0.4898**	2.1128**	-0.0176**	-0.0266	-0.2763**
X_2	-0.0483	0.1738	0.0085*	-0.0135	0.1108
X_3	0.6878**	3.2218**	-0.0466**	0.1010**	-0.2083*
X_4	-0.0963*	-0.4678	-0.0018	-0.0962**	-0.1653
X_5	-0.0793	-0.3183	-0.0026	-0.0477*	-0.1843
X_6	-0.0343	-0.3483	-0.0078*	-0.0535*	-0.1743
X_1X_1	-0.3218**	-1.5963**	0.0310**	0.0185	-0.0158
X_2X_2	-0.0868	-0.2738	0.0024	0.0001	-0.0371
X_3X_3	-0.0593	-0.2063	0.0198**	-0.0222	0.0479
X_4X_4	-0.1018*	-0.3113	0.0051	0.0268	0.1567
X_5X_5	-0.1106*	-0.7738*	0.0058	-0.0154	-0.0321
X_6X_6	-0.0506	-0.1076	0.0078	0.0257	0.2654
X_1X_2	0.0122	0.1972	0.0164**	0.0906**	0.1041
X_1X_3	0.1847**	2.3434**	0.0153**	-0.0315	-0.0772
X_1X_4	-0.0603	-0.1209	-0.0028	0.0040	0.0772
X_1X_5	-0.0072	-0.1491	-0.0089*	0.0033	-0.1059
X_1X_6	-0.0047	-0.1959	0.0003	0.0099	-0.0734
X_2X_3	0.0372	0.1947	-0.0034	-0.0299	-0.1453
X_2X_4	0.0497	0.1728	-0.0066	0.0155	-0.0247
X_2X_5	0.0266	0.0672	0.0024	0.0114	-0.0803
X_2X_6	-0.0134	0.0428	0.0006	0.0057	-0.0078
X_3X_4	-0.0253	-0.1484	0.0006	-0.0618*	0.0891
X_3X_5	-0.0822	-0.3141	0.0011	-0.0299	0.1447
X_3X_6	-0.0522	-0.1559	0.0018	-0.0041	0.0572
X_4X_5	-0.0009	-0.1397	-0.0041	0.0188	-0.0647
X_4X_6	-0.0234	-0.0753	-0.0046	-0.0034	-0.0247
X_5X_6	-0.0303	-0.1172	0.0108**	-0.0481	0.1522*
R^2	0.96**	0.94**	0.96**	0.81**	0.70

* Significant at $p < 0.05$, ** Significant at $p < 0.01$

Minerals

The most important parameters for ash and calcium were pH, concentration, $(\text{pH})^2$ and the interaction $\text{pH} \times \text{C}$. Minimum ash and calcium occurs at low pH values and low concentrations, with a good correlation ($R^2 = 0.95$) being obtained between calcium and ash. Figure 11 presents a surface response plot of ash as a function of pH and concentration. The maximum ash at any specified concentration lies near the isoelectric pH (4.6), but shifts toward higher pH values as the concentration increases. The calcium content of casein has been shown to increase with pH (Jablonka & Munro, 1985; Brulé & Fauquant, 1981) and is considered to be due to an increase of calcium binding to casein. Thus, the quadratic effect of pH on ash and calcium cannot be related to solubility, but may be due to low diffusion. Poor diffusion near the isoelectric point may be due to larger particle size, a low level of hydration, low porosity, and/or gelation of the curd. Figure 11 also illustrates that the ash content (including calcium) increases linearly with concentration. This effect may be expected since colloidal calcium is less soluble as SMP concentration increases (Brulé et al., 1974; Brulé & Fauquant, 1981). At low concentrations ($< 20\%$), a low ash content ($\leq 2\%$) can be obtained over the pH range of 4.1-4.9. If the concentration of SMP is increased beyond 20%, the pH should be reduced below the isoelectric point to obtain a casein with a low ash content.

The same factors influencing ash and calcium content influence sodium content, but also includes $(\text{C})^2$, $\text{pH} \times \text{T}$ and $\text{rpm} \times \text{WWR}$. Figure 12 shows that minimum sodium content occurs close to isoelectric point and a concentration of 42%, while maximum sodium occurs at low concentrations and pH's. Sodium has an inverse relationship relative to calcium ($R^2 = 0.88$) and indicates that the solubility of sodium salts may be affected by the solubility of calcium salts. Some absorption of sodium ions by casein and/or calcium phosphate may take place (Gueurts et al., 1974), with the degree of this absorption depending on several factors including pH and calcium ion concentration.

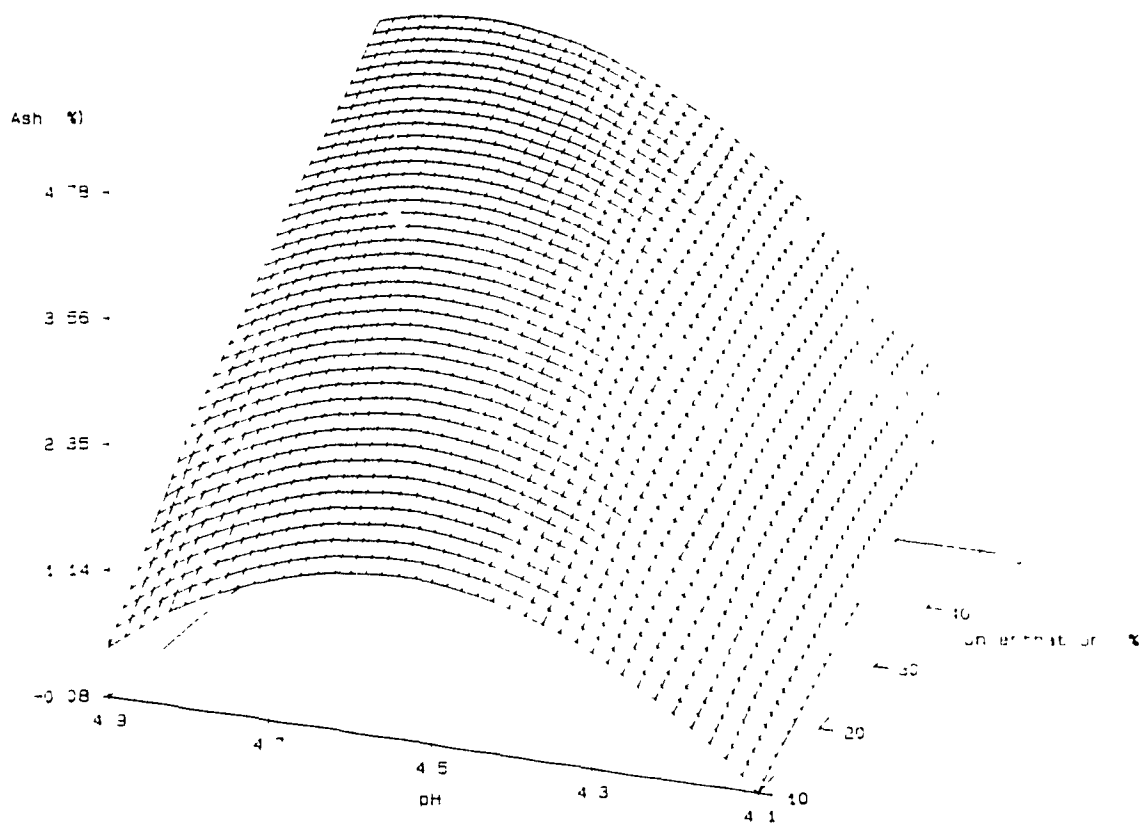


Figure 11. A surface response plot of predicted residual ash (%) as a function of coagulation pH and SMP concentration.

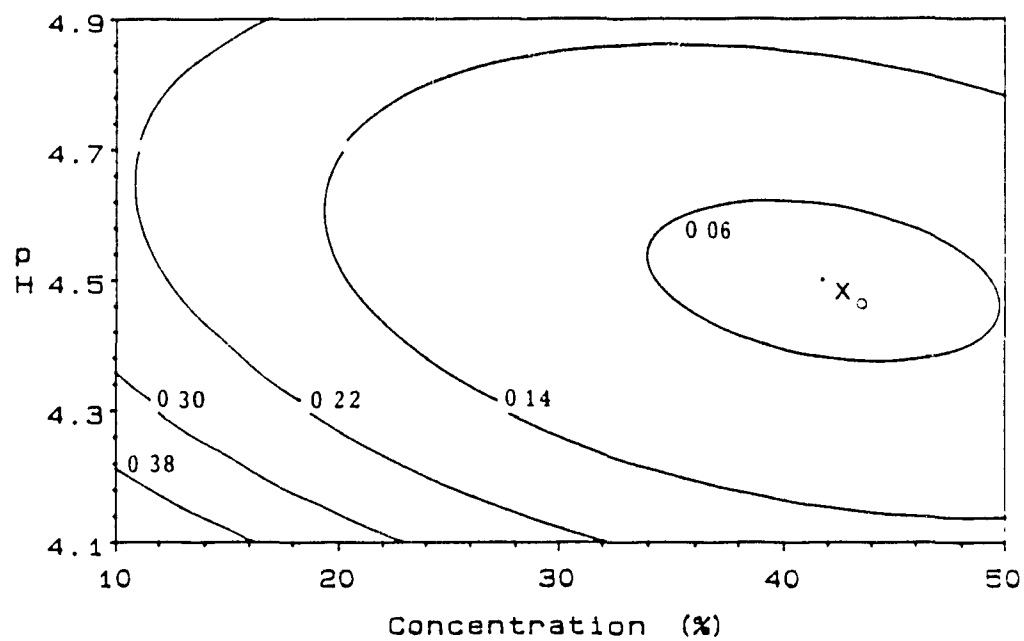


Figure 12. Contour plot of the predicted residual sodium (mg/g) as a function of coagulation pH and SMP concentration. The stationary point (X_0) is located at a pH of 4.51 and a concentration of 42%.

Lactose

The most important parameters affecting lactose removal are concentration, time and pH x T. The linear positive effect of concentration may be explained by the effect of concentration on subsequent curd properties, including gelation, particle size and reduction in the porosity of the curd. Furthermore, the efficiency of separation at the coagulation step decreases when the concentration is increased, due to less water being present. The negative effect of time is related to diffusion, with the approach to equilibrium between lactose entrapped within the casein and in solution, depending on contact time. Figure 13 shows that minimum lactose content occurs at lower concentrations, while maximum lactose is present when minimum times and maximum concentrations are used. The interaction pH x T is an indirect effect, where pH affects the curd characteristics and therefore the diffusion/temperature relationship associated with lactose removal. Figure 14 presents a contour plot of lactose as a function of pH and temperature, and illustrates a saddle point (X_0). Taking X_0 as a reference point, lactose can be minimized by either increasing the pH and decreasing the temperature, or decreasing the pH and increasing the temperature.

Whey Protein Nitrogen

WPN as a variable in the multiresponse model was not significant ($R^2 = 0.70$) although the coagulation/washing process clearly did have some effect on the whey proteins. pH is the only variable which significantly affected the residual WPN ($p < 0.01$) and Figure 15 presents a surface plot of WPN as a function of pH and concentration. Minimum residual WPN occurs at the maximum SMP concentration (50%) and pH (4.9). This may be explained by the fact that β -lactoglobulin, over the pH range of 4 to 5, has reduced solubility at low salt concentrations (de Wit, 1981). Since the salt concentration increases with pH and SMP concentration, β -lactoglobulin content in the curd decreases. Denaturation does not play a part in this process because the wash water temperatures were limited to $\leq 60^\circ\text{C}$.

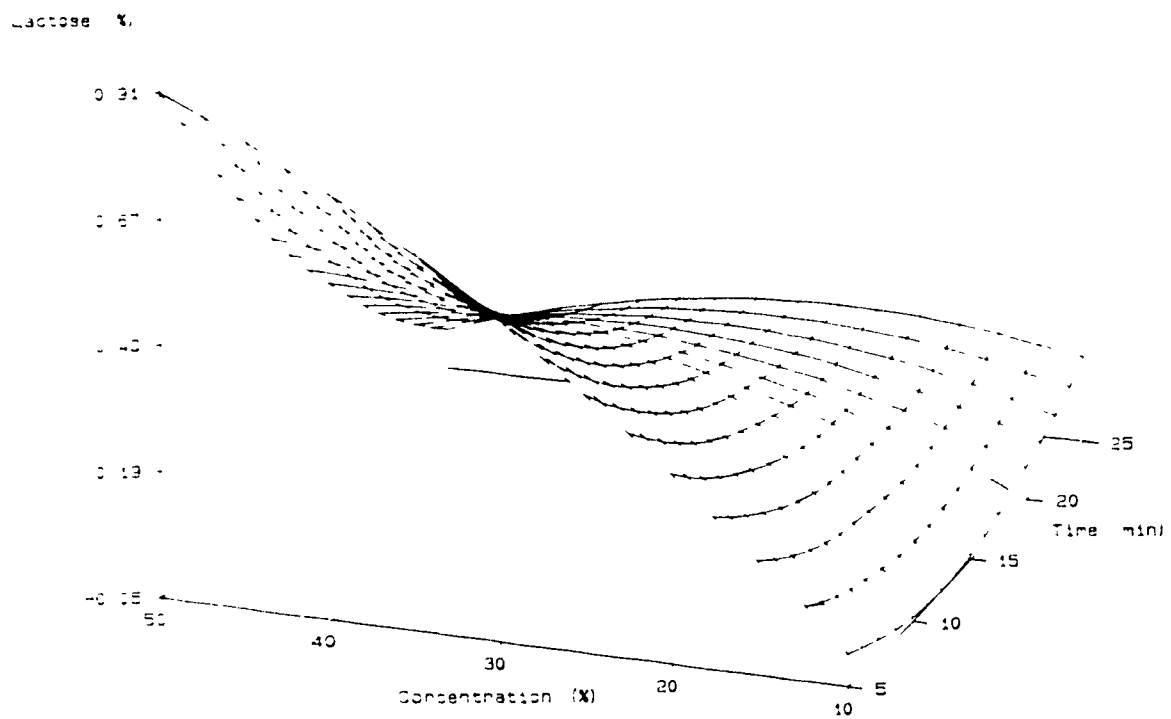


Figure 13. A surface response plot of predicted residual lactose (%) as a function of SMP concentration and washing time.

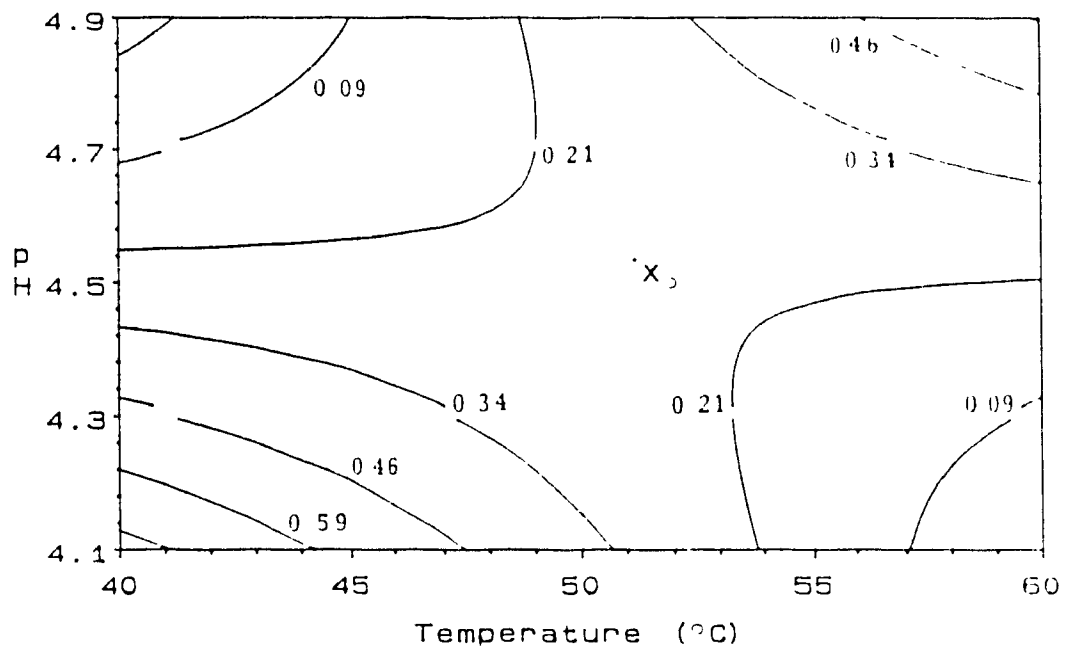


Figure 14. A contour plot of predicted residual lactose (%) as a function of coagulation pH and washing temperature. The saddle point (X_s) is located at pH 4.54 and 51°C.

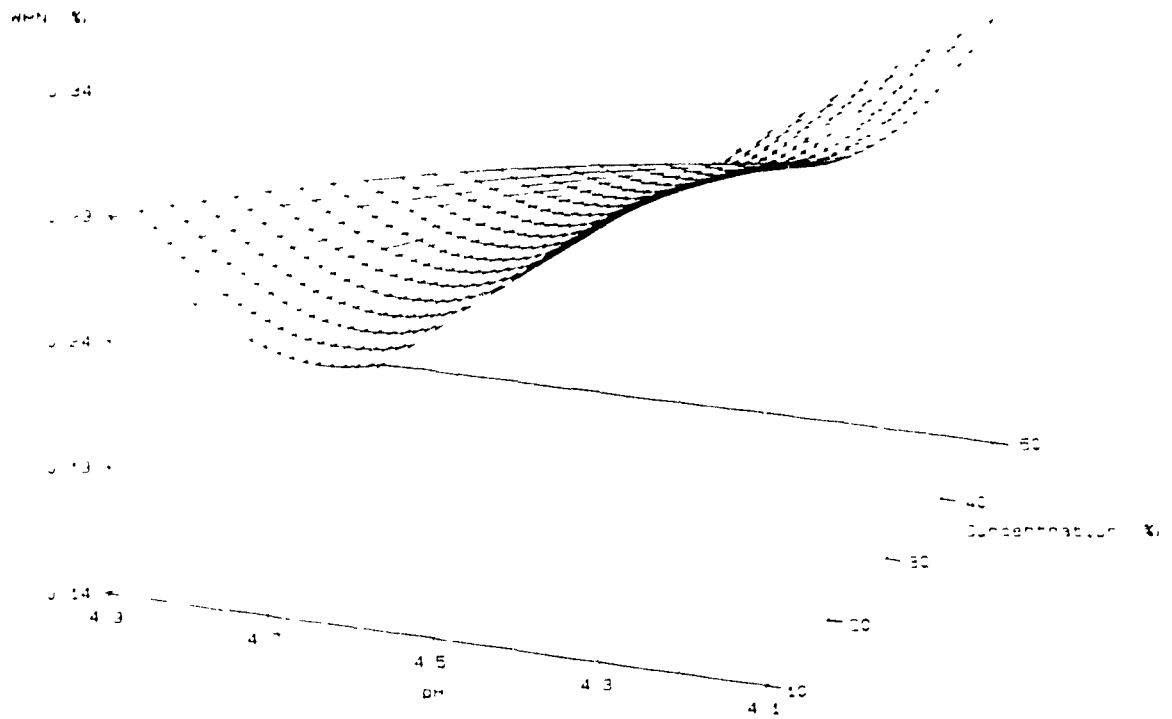


Figure 15. A surface response plot of predicted residual WPN (%) as a function of coagulation pH and SMP concentration.

Simultaneous Optimisation of the Responses

By superimposing the contour plots of the response variables of interest, one can determine a region where conditions will be "near" optimal for all responses. Figure 16 illustrates composite contour plots for predicted lactose and ash (%) as a function of coagulation pH and concentration, with the other parameters fixed (see Figure legend). The shaded regions indicate the conditions which would meet international acid casein standards, with the lowest pH and concentrations being the minimum point for both ash and lactose. Increasing the washing temperature of the second and third wash from 55°C (Figure 16a) to 60°C (Figure 16b), all other parameters being kept constant, leads to a significant extension of the concentration under the shaded area. Thus, high temperature washing may be practical when dealing with high SMP concentrations (> 20%) such as the case of extrusion. This approach is simple and permits the optimization of more than one response at a time, but for obvious reasons is limited to considering only two independent variables simultaneously. The mathematical determination of a multiresponse optimum considering more than two variables is possible by more sophisticated methods and will be discussed in Chapter 3.4.

Effect of washing stages

The experimental design provides a means to optimise the parameters under consideration within the framework of the experimental design. In the main design, the number of washes was limited to four for practical purposes. To further investigate the behaviour of the individual washing stages on ash, lactose, and WPN (Figure 17), a separate coagulation study was carried out with a high SMP concentration (30%), which can be related to SMP extrusion. All the components in question decrease as a function of the number of washing stages, with most of ash and WPN being removed by the first three washes, while lactose in the curd and in wash water continued decreasing significantly until the 5th wash. Some type of binding mechanism or restricted diffusion is evident by the fact that the lactose content in the curd is still about 10 times greater than that in the wash water after the 5th and 6th wash. After the 4th wash both ash and

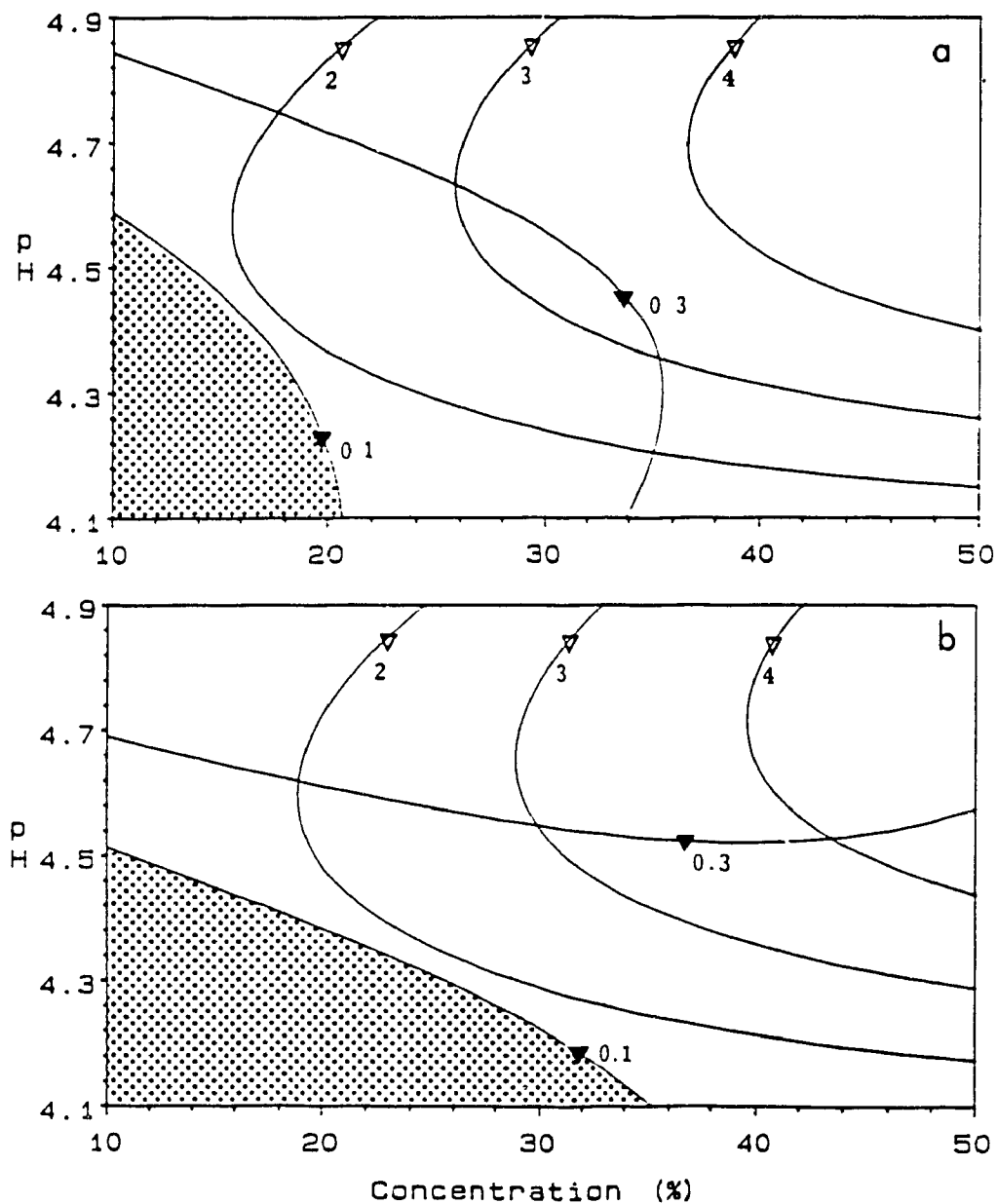


Figure 16. Superimposed contour plots of predicted percent ash (∇) and percent lactose (\blacktriangledown) as a function of coagulation pH and SMP concentration. (a) temperature = 55°C and (b) temperature = 60°C. Agitation, time and WWR were fixed at , 250 rpm, 15 min and 4:1 respectively.

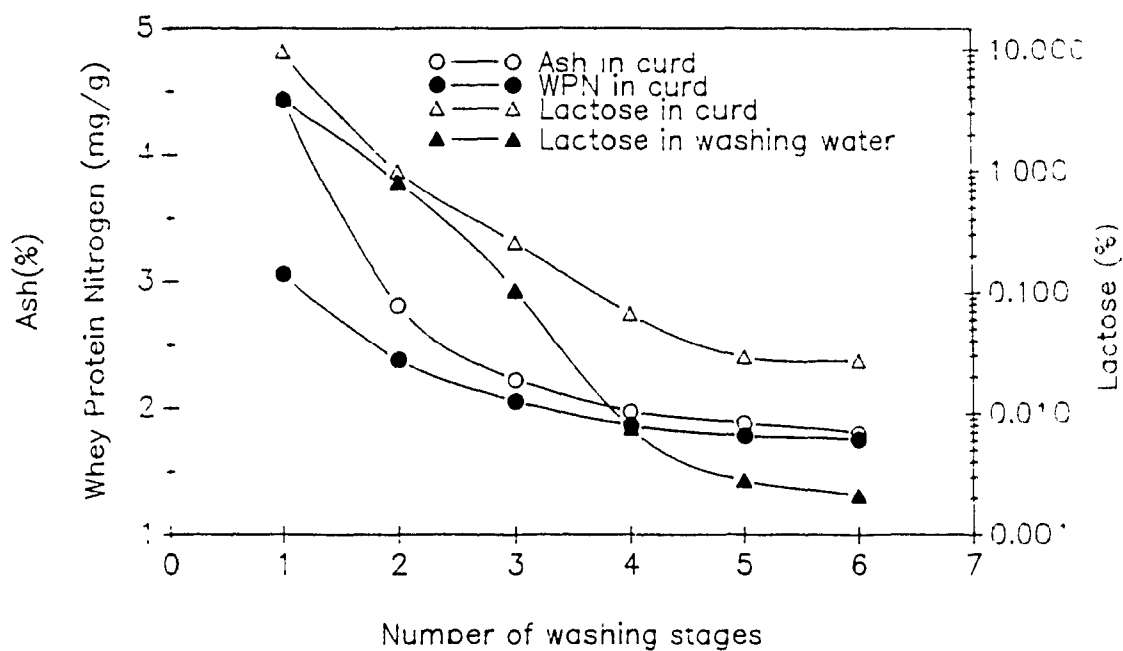


Figure 17. Effect of the number of washing stages on residual ash, lactose, whey protein nitrogen, and lactose in wash water at a pH of 4.5, temperature of 50°C, SMP concentration of 30%, agitation at 300 rpm, WWR of 5:1, and washing time of 15 min.

lactose levels meet international standards, even though the starting concentration was much higher (30 vs 10%) than the conventional fluid skim milk process.

The washing efficiency for lactose can be measured by the Murphree Stage Efficiency coefficient (MSE) which indicates the approach to equilibrium at each stage. The MSE can be computed using the following relation (Hobman, 1978; Jordan, 1983):

$$\text{MSE} = (X_0 - X)/(X_0 - X_1) \quad (59)$$

where: X_0 = uniform lactose concentration in the solid at zero time (i.e. in the incoming curd), X = average lactose concentration in the solid (curd) at time t (i.e. in the outgoing curd), X_1 = Constant concentration of lactose in the solid at equilibrium and in the bulk of the solution at all times. All lactose concentrations are expressed as "casein-free" mass fractions, where:

$$\text{Lactose concentration} = (\text{mass lactose})/(\text{mass lactose} + \text{mass water})$$

Table 5 gives the MSE for up to 6 washes for the data illustrated in Figure 17. The MSE decreases fairly consistently from the second to the fifth stage, after which it drops tenfold. A typical industrial MSE is ~ 0.75 (Hobman, 1978) which was maintained until the fourth wash. It may be concluded that the 6th stage is not necessary and the MSE of washes 4 and 5 could be increased significantly by either increasing washing time and/or dewatering before entering the next washing stage (Pearce et al., 1987). The latter technique can have a major effect on the MSE and may also lead to a reduction in the number of washing stages and in the WWR (Hobman, 1978; Bressan & Hobman, 1985; Pearce et al., 1987).

Table 5. Murphree stage efficiency (MSE) for successive washing stages.

Washing stage	X0	X	X1	MSI:(%)
2	0.115720	0.013530	0.008060	94.9
3	0.013530	0.003505	0.001030	80.2
4	0.003505	0.000906	0.000075	75.8
5	0.000906	0.000372	0.000028	60.8
6	0.000372	0.000351	0.000021	6.0

3.2.4 Conclusion

Coagulation and washing conditions clearly affect the residual whey components in the casein curd. The response surface approach provided a unique means of studying the coagulation/washing process and provided insight into the factors affecting acid casein production. The multivariate relationships generated allow one to predict the expected response (residual lactose, ash, minerals, and WPN) in relation to concentration, pH, agitation, temperature, time and WWR. Furthermore, the superimposition contour plots of responses helped in determining a region of interest for more than one response and might be useful as a multiresponse optimization technique. Previous work on washing efficiency has only considered lactose (Hobman, 1978; Bressan & Hobman, 1985; Pearce et al., 1987), assuming that its removal reflected the concomitant loss of minerals and whey proteins. This study shows that conditions minimizing lactose do not necessarily minimize the remaining whey components, however such conditions were found using RSM. Conditions for well washed casein produced from concentrated milk solutions (>20%) could be found for application to extrusion process. Although the system used in this study does not simulate the coagulation in the extruder reactor, the results can be used to assist in determining the operating conditions for SMP extrusion considered in a succeeding chapter.

3.3 EFFECT OF COAGULATION AND WASHING CONDITIONS ON FINES, WATER HOLDING CAPACITY AND MICROSTRUCTURE OF ACID CASEIN CURD

ABSTRACT

Acid casein prepared under various conditions of pH, concentration and wash regimens was analyzed for water holding capacity and loss of fines, and the structure of the curd was assessed by scanning electron microscopy. Concentration, pH and temperature were the major factors in terms of influencing fines, water holding capacity and the microstructure of the curd. Fines could be minimized by selecting appropriate pH, concentration and agitation conditions. The final moisture content of the curd was mainly controlled by pH, concentration and temperature and these variables may be selected to obtain good dewatering and drying efficiencies. Microstructural analysis visualized the effects of pH, concentration, temperature and their interactions on the casein structural network and the effects of the process parameters are discussed in relation to those changes. Response surface methodology was shown to be an effective tool for examining which of the variables used in the process were significant and provided guidance as to the physico-chemical mechanisms which affected the system.

3.3.1 Introduction

The effect of precipitation and washing conditions on residual whey components such as lactose, minerals and whey proteins have been assessed by RSM (Fichtali et al., 1990a) and are reported in Chapter 3.2. The models obtained using RSM allowed the optimization of selected responses for the significant variables affecting them. Parameters such as the loss of fines and curd moisture affect the efficiency of the process and require optimization, while curd microstructure is also of interest in relation to the functional

properties of the end product. This chapter discusses the results obtained from a RSM study of acid casein production based on concentrated SMP solutions in relation to fines, water holding capacity (WHC) and curd microstructure.

3.3.2 Material and Methods

Details of the material and methods are presented in Chapter 3.2. An apparatus was designed to allow the control of the shear rate, coagulation pH and temperature of SMP solutions and the washing of the curd under controlled conditions (Figure 10). The coagulum was separated from the whey using a 100 mesh (150 μm) stainless steel screen, the whey set aside and the coagulum returned to the holding vessel for washing. This process was repeated a total of four times with the whey/wash water collected each time, collated, and then centrifuged at 10,000 $\times g$ to isolate the fines. The fines were oven dried (80°C for 12 h) and weighed to determine their proportion of the starting material. After washing, the curd was drained for one hour on a 60 mesh screen and representative samples taken for moisture analysis (AOAC, 1984) and freeze drying. The freeze dried samples were examined by scanning electron microscopy using a Nanolab LE2100 scanning electron microscope (Vickers Instruments Inc.). Separate titration and temperature studies of SMP solutions were carried out to investigate the effects of concentration on the buffering capacity of the system, and temperature on the amount of fines produced. The experimental design and regression model have been discussed in Chapter 3.2 and the data used for the analysis are given in Appendix 2.

3.3.3 Results

Table 6 presents the regression equations parameters and coefficients, with most significant coefficients denoted with asterix. This data provides basic relationships of how SMP behaves under the given experimental conditions and both coefficients of determination (R^2) are significant at $p < 0.01$. Although many variables and their

interactions are included in the model, only those which were significant at $p < 0.01$ were considered in our analysis.

Table 6. Least squares fit and regression estimates for WHC (Y_1) and percent fines (Y_2).

Parameters	Regression Coefficients	
	Y_1	Y_2
Intercept	67 7847**	1 3010*
X_1	-2 3888**	1.6475**
X_2	-1 3483**	-0 4205
X_3	-0 5338	2.1970**
X_4	0 8913*	0 4435*
X_5	0 5938	0 5435*
X_6	0 3833	0 1385
X_1X_1	2 9096**	2 9788**
X_2X_2	0 3721	0.0213
X_3X_3	2.2096**	1 5875**
X_4X_4	0.6596	0 0563
X_5X_5	0 5596	0 1913
X_6X_6	0 1846	0 0688
X_1X_2	-0 8203	0.1675
X_1X_3	0 3416	-0 8713**
X_1X_4	0 5228	0 0538
X_1X_5	0 4884	-0 5413*
X_1X_6	0 5503	-0 2088
X_2X_3	0 0859	-0 6325*
X_2X_4	0 2222	-0.3338
X_2X_5	0 2353	0.1925
X_2X_6	-0.1541	0.0263
X_3X_4	0 1991	0 2950
X_3X_5	0 8359	1 0813**
X_3X_6	0 0503	0 1175
X_4X_5	-0.5790	-0.0775
X_4X_6	0.2578	0 0950
X_5X_6	-0.2766	-0 2675
R^2	0 88**	0 95**

* Significant at $p < 0.05$, ** Significant at $p < 0.01$

Titration of SMP

A basic understanding of the pH behavior of SMP as a function of concentration is important to this work, since extrusion requires the use of higher concentrations (i.e. >20%). Titration of reconstituted SMP (5-25%) at 45°C with HCl illustrated three major trends (Figure 18) as a function of increasing concentration; (a) the initial pH of the solution decreases, (b) the pH at which observable coagulation takes place increases (indicated by arrows) and (c) the slope of the titration curve decreases producing an increase in buffering capacity. Similar changes in buffering capacity have been reported for milks concentrated by ultrafiltration (Brulé et al. 1974; Srilaorkul, 1989) and these concentration effects are important because they influence the coagulation process, subsequent aggregation of casein micelles, fines and microstructure.

Factors Affecting Fines

Fines are a key factor in the economics of acid casein manufacture. Concentration (C) and pH, including their squares (pH^2 , C^2) and interactions ($\text{pH} \times C$) plus the interaction between concentration and agitation ($C \times \text{rpm}$) are the most important parameters affecting the loss of fines. Figure 19 presents a contour plot of fines as a function of pH and concentration, with minimum fines occurring at 22% SMP and pH 4.42, well away from the isoelectric pH. At the higher concentrations (> 40%) it was observed that as pH and concentration were increased simultaneously, coagulation was incomplete resulting in a high level of fines. This problem was attributed to poor mixing efficiency and poor hydration of the SMP. The interaction between concentration and agitation is an important factor and indicates that the shear rate should be controlled. Figure 20 presents a contour plot of the resulting fines as a function of concentration and rpm at the optimum pH of 4.42 for reduced fines. The surface response plot shows a stationary ridge indicating that there is an optimum agitation speed associated with each concentration. This can be interpreted to indicate that at high concentrations, increases in agitation lead to particle disruption and increased fines, but at lower concentrations and higher agitation, the increase in collision frequency of smaller particles results in aggregation and a reduction in fines.

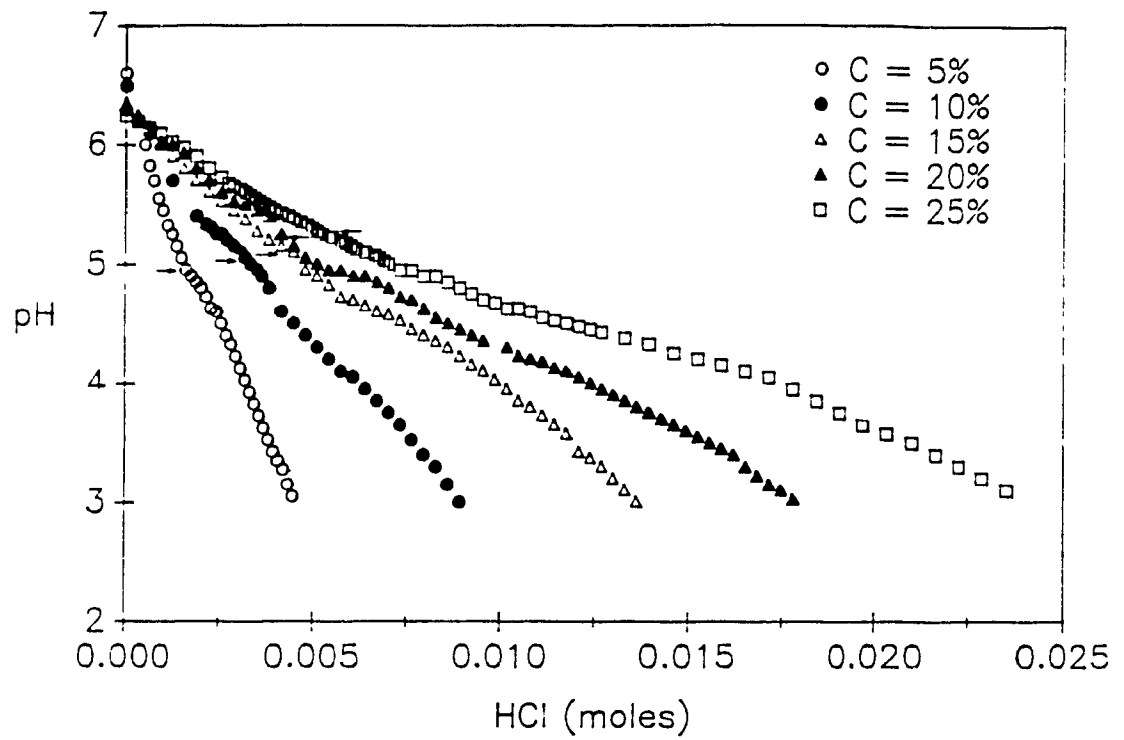


Figure 18. Titration curves of skim milk powder at 45°C and different concentrations. The arrows indicate the pH at which visual coagulation was observed.

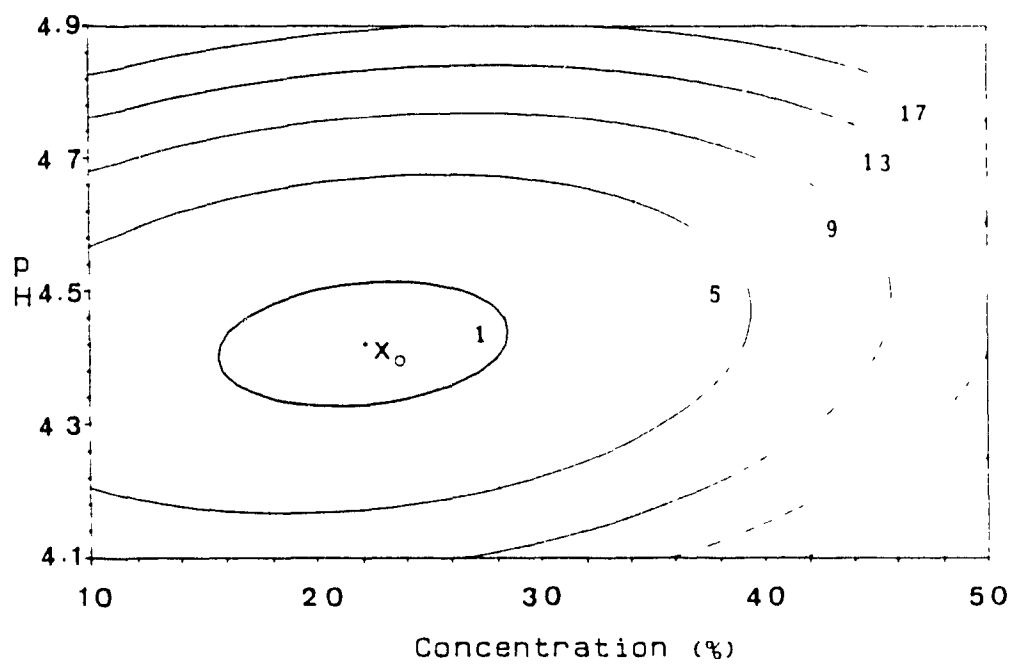


Figure 19. Contour plots of the predicted percent fines as a function of pH and concentration. The stationary point (X_0) is located at a pH of 4.42 and a concentration of 22%.

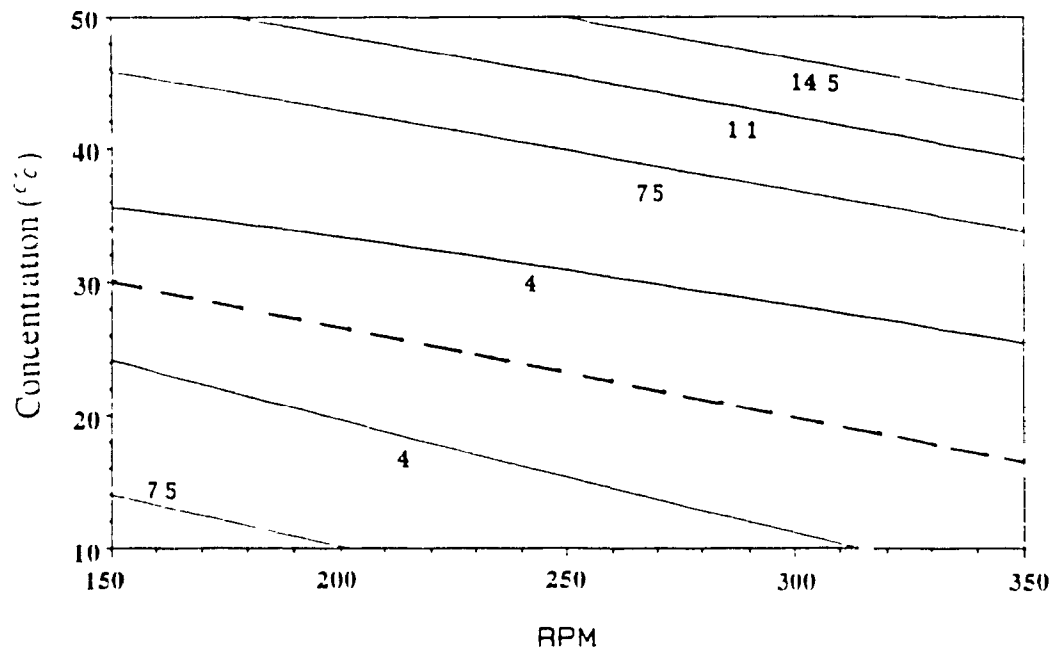


Figure 20. Contour plots of the predicted percent fines as a function of concentration and agitation (rpm) at a fixed pH of 4.42.

Another important variable which can influence the production of fines is the coagulation temperature which was studied at 45 and 60°C using 10% solids. Figure 21 illustrates that increasing the coagulation temperature and maintaining the curd washing temperature at 45°C, led to a reduction in minimum fines and also caused a shift in the pH corresponding to minimum fines from the original isoelectric point of 4.6 to 4.8.

Effect on Water Holding Capacity

Curd moisture and water binding are important parameters associated with the production of acid casein and have a major effect on dewatering, drying efficiency and the physico-chemical characteristics of the end product (i.e., density, dispersibility, water activity and wettability). The most important variables affecting the moisture content of the curd after the last wash are: pH, $(\text{pH})^2$, $(C)^2$ and temperature (T). Figure 22 presents a contour plot of curd WHC as a function of pH and temperature. Minimum WHC occurs at a pH close to the isoelectric point (4.62) and at the maximum temperature studied (60°C). The effect of $(C)^2$ is shown in Figure 23 as a contour plot of WHC as a function of pH and concentration and the minimum WHC once again occurs close to the isoelectric point but at 31% solids.

Microstructure

By studying the microstructure of the curd in terms of size, shape and arrangement of the aggregates, including size and frequency of pores, one can gain some insight into the coagulation and washing process as it relates to the variables considered in the experimental design. Of the parameters studied; only pH, concentration and temperature were shown to affect the microstructure in any visually discernible fashion. In order to compare the effect of a selected input variable (pH, concentration or temperature) each one was evaluated at its extreme value while the rest of the variables were maintained constant. The effect of pH is illustrated in Figure 24 and shows that at pH 4.1 (Figure 24a) the product is friable, porous and more like an aggregate of small particles even though the concentration is relatively high (30%), while at pH 4.9 (Figure 24b) the

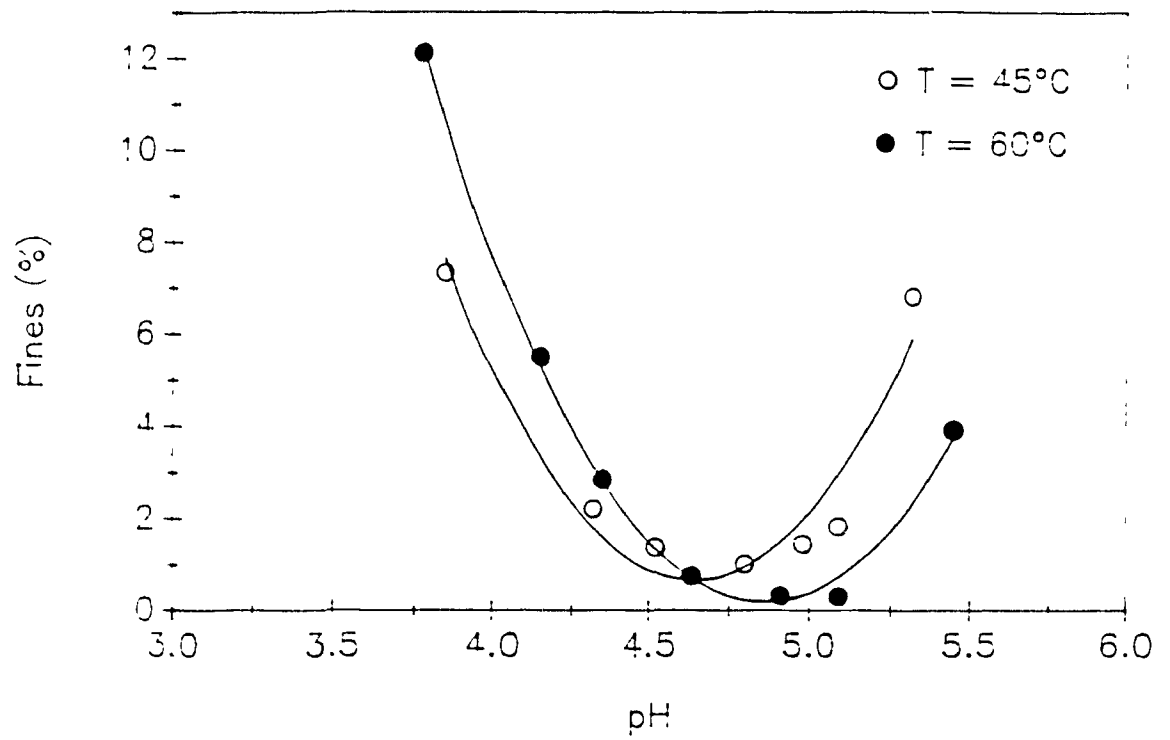


Figure 21. Effect of pH on percent fines at two coagulation temperatures.

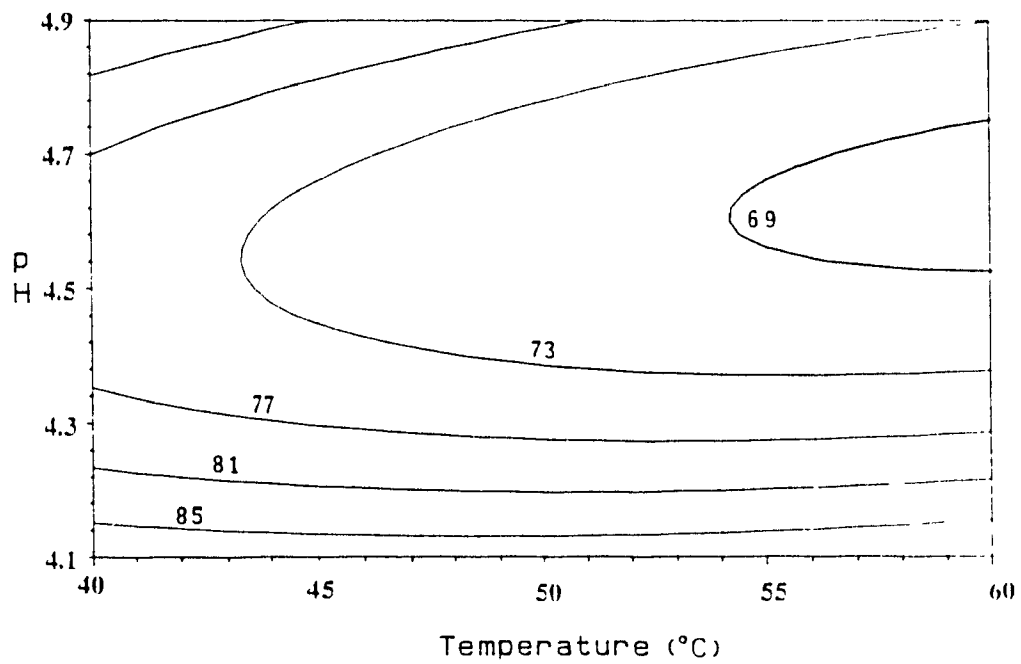


Figure 22. Contour plots of the predicted water holding capacity after the last wash as a function of pH and temperature.

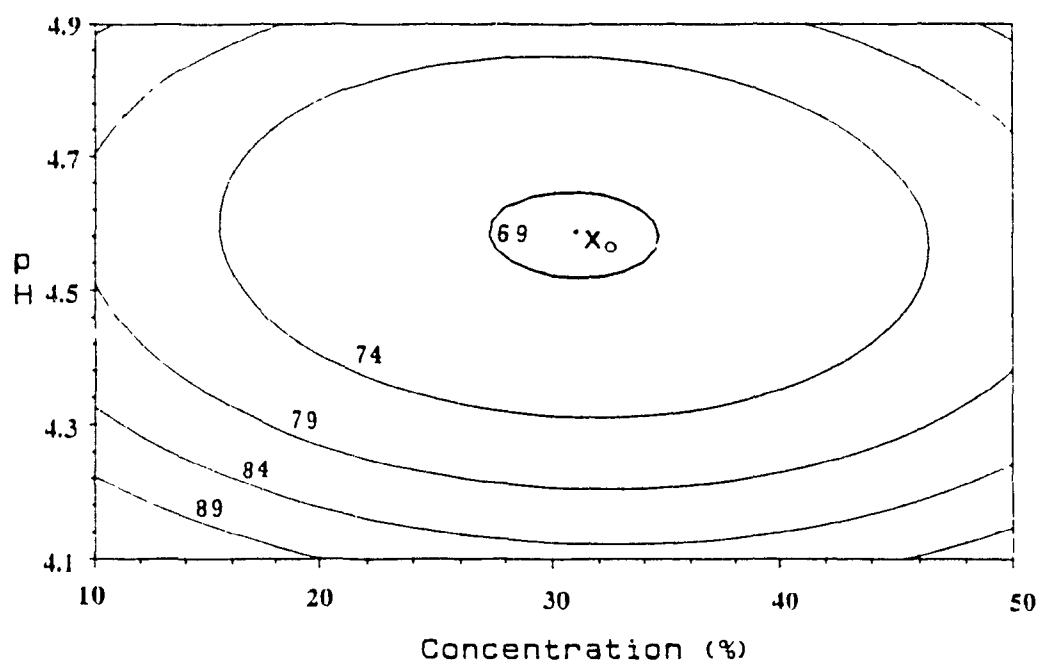


Figure 23. Contour plots of the predicted water holding capacity after the last wash as a function of pH and concentration. The stationary point (X_0) is located at a pH of 4.58 and a concentration of 31%.

casein is porous with some gelatinous character. At 30% and pH of 4.5 (Figure 24c), the product appear to be very firm with a minimum of porosity.

Curds obtained at 10 and 50% solids differ substantially in their structural characteristics (Figure 25). At 10% (Figure 25a), a friable, porous aggregate is obtained, while at 50% (Figure 25b), a porous gelatinous mass with apparent elastic characteristics is observed. The high porosity obtained at 10% indicates that mechanical removal of water may be feasible, while the 50% solids sample would likely trap water, making it difficult to remove. The effect of temperature on curd structure can be seen in Figure 26. As the temperature is increased from 40°C (Figure 26a) to 60°C (Figure 26b), with the other variables held constant, the curd loses most of its porosity and the surface characteristics make a transition from an irregular to a smoother structure.

The interaction effects of pH, concentration and temperature also affect the microstructure of the curd. Because of the experimental design, only specific treatment combinations were available for comparison and subsequent comparisons were made using the most closely related samples. Comparing the microstructure of curds obtained at pH 4.3 and pH 4.7 (Figure 27), an effect similar to that at extreme pH's is observed, with low pH samples (Figure 27a,b,c) being more aggregate-like, while the high pH samples (Figure 27d,e,f) are more gelatinous. Superimposing the concentration effect illustrates that the gelation aspect is enhanced and porosity reduced if the concentration is increased from 20% (Figure 27a,d) to 40% solids (Figure 27b,e). Although temperature is also a factor here, Figure 27 shows it is not significant in this case, as the temperature has only been increased 10°C from 45°C (Figure 27a,d) to 55°C (Figure 27c,f), with only a minor change being observed in porosity.

3.3.4 Discussion

Concentration, pH and temperature are the most important variables in the multivariate process used to produce acid casein and which affect fines, WHC and

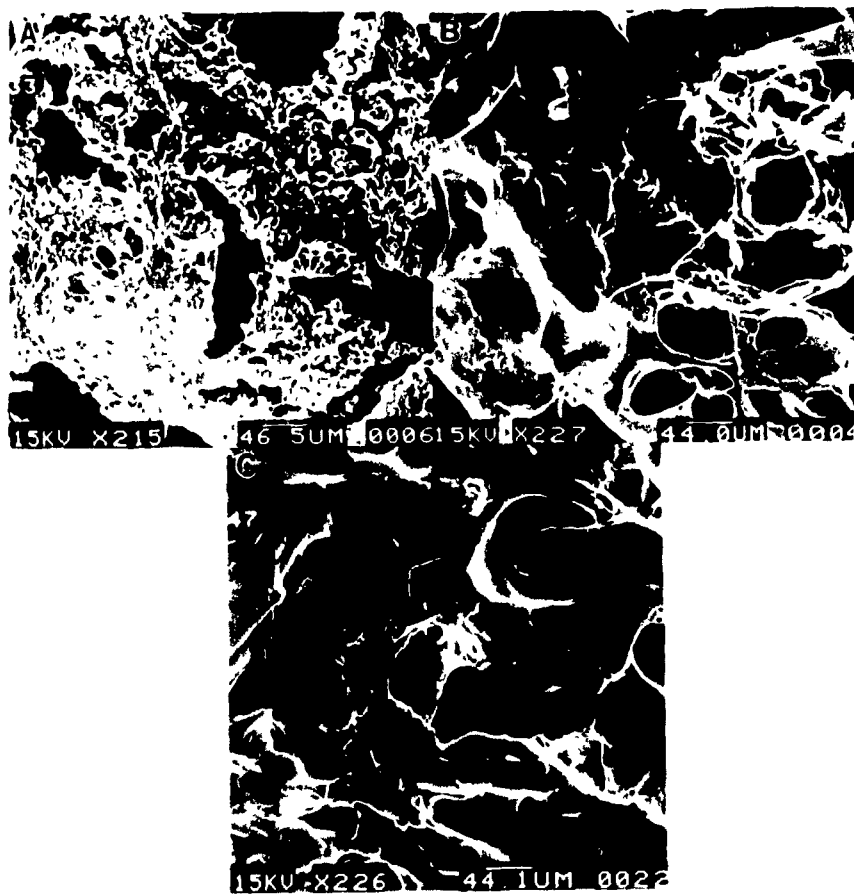


Figure 24. Scanning electron micrographs of acid casein obtained at pH of (A) 4.1, (B) 4.9, and (C) 4.5. Temperature, concentration, washing time, agitation, and WWR were fixed at 50°C, 30%, 15min, 250rpm, 5:1, respectively.



Figure 25. Scanning electron micrographs of acid casein obtained at concentration of (A) 10% SMP and (B) 50% SMP. Temperature, pH, washing time, agitation, and WWR were fixed at 50°C, 4.5, 15min, 250rpm, 5:1, respectively.

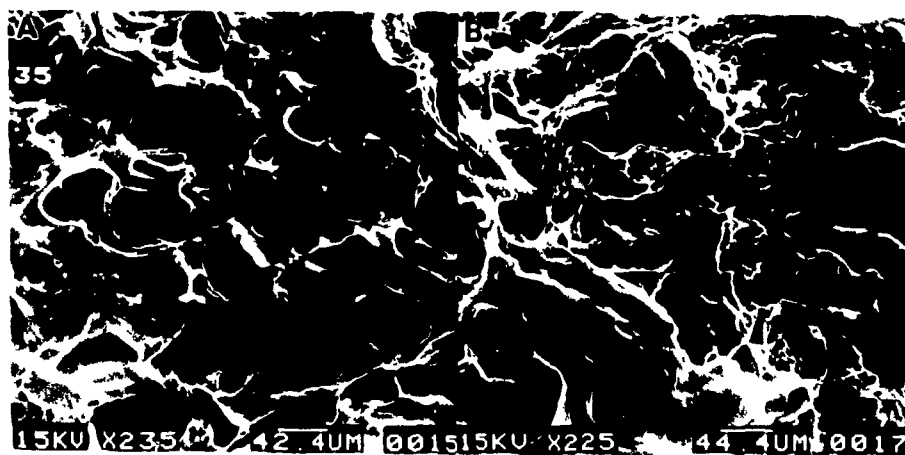


Figure 26. Scanning electron micrographs of acid casein obtained at temperature of (A) 40°C, and (B) 60°C. Concentration, pH, washing time, agitation, and WWR were fixed at 30%, 4.5, 15min, 250rpm, 5:1, respectively.



Figure 27. Scanning electron micrographs of acid casein obtained at various conditions of pH, concentration and temperature: (A) pH=4.3, C=20%, T=45°C; (B) pH=4.3, C=40%, T=45°C; (C) pH=4.3, C=20%, T=55°C; (D) pH=4.7, C=20%, T=45°C; (E) pH=4.7, C=40%, T=45°C; and (F) pH=4.7, C=20%, T=55°C.

microstructure. Concentration induces major changes in the milk system (Fox, 1982), including a closer packing of the casein micelles, a higher concentration of denatured proteins, precipitation of calcium phosphate which decreases the pH, and a reduction in the amount of available free water. At higher concentrations intermolecular interactions and aggregation have a higher probability of occurring and should lead to lower fines. Our results however, indicate that fines increase above concentrations of 22% (Figure 19) and therefore other factors must be involved in the coagulation efficiency of concentrated SMP solutions. Reduction of fines at high concentrations requires a careful choice of pH and agitation (Figures 19,20). In addition, increasing coagulation temperature (Figure 21) in combination with adequate shear may increase the kinetic energy of particles aiding in the agglomeration process, thereby reducing fines. This concurs with observations made by Jablonca and Munro (1985, 1986a) who have noted that particle size and curd strength increased with coagulation temperature. Concentration also has a significant effect on the proteinic network comprising the casein curd as shown by the micrographs in Figures 25 and 27. Intermolecular protein attractions and gelation are accelerated at higher protein concentrations because of the increased probability of intermolecular contacts and the higher calcium content. The dispersibility and coagulation problems associated with high SMP concentrations may be overcome by increasing the rate of shear, adjusting the temperature for optimal dispersion (60°C) or lowering the interfacial tension through the use of surfactants such as lecithin (Kinsella, 1984). Extrusion processing to produce acid casein requires high concentrations (i.e. >20%) and provides both shear and temperature control. Surfactants could also be incorporated into the process if needed to aid in producing a more dispersible product.

Other reactions which may occur during the manufacture of SMP (i.e., denaturation of whey proteins, increases in colloidal/soluble calcium ratio, decreases in solubility) may also affect, to some extent, the coagulation of highly concentrated solutions of reconstituted SMP. Heat precipitated calcium phosphate can associate with casein micelles and form a surface layer on the micelle (Fox, 1982) and the formation of a complex between denatured β -lactoglobulin and κ -casein can affect the zeta potential

and subsequent hydration of micelles, thereby reducing their coagulability. If such factors do have an effect, they will tend to be more pronounced at higher concentrations. Fox (1982) has emphasized that the coagulation behavior of concentrated milk is quite complex and that the factors affecting such coagulation processes have not been well established.

pH strongly affects the attractive and repulsive forces between proteins and their ability to associate with water (Chou and Morr, 1979; Cheftel et al., 1985). At the isoelectric point protein-protein interactions are maximized and this association leads to minimum hydration (Figures 22,23). These conditions should also lead to minimum fines which occurs at a pH of 4.42, somewhat away from the isoelectric point. This result runs counter to the fact that particle size is known to increase with the pH even above the isoelectric point (thereby reducing fines) because of increased calcium binding with pH (Jablonca and Munro, 1985). It may be possible that at higher SMP concentrations (22%) hydrophobic and disulphide bonds may compensate for the reduction in electrostatic repulsive forces at pH's away from the isoelectric point (Cheftel et al., 1985) and hence lead to minimum fines at a pH other than the isoelectric point. The concentration zone over which visible gelation occurs in the micrographs increases with increasing the pH. At pH 4.7 gelation occurs at both 20 and 40% SMP (Figure 27d,e) while at pH 4.3 it is limited to the 40% SMP and is less pronounced (Figure 27a,b). At a concentration of 30%, gelation occurs at a pH 4.9 and 4.5 but not at a pH 4.1 (Figure 24). Based on the physical characteristics discernable from by the micrographs, it becomes apparent that the extent of gelation of SMP is a combined effect of pH and concentration.

Temperature is one of the many factors affecting the water holding capacity of proteins, aside from composition, protein conformation, pH, solutes and surface area (Chou and Morr, 1979; Kinsella and Fox, 1986). High temperatures favour protein-protein interactions to the detriment of protein-water interaction and Figure 22 shows that minimum hydration occurs at the maximum temperature (60°C) studied. Increasing temperature leads to a reduction in hydrogen bonding and usually to the aggregation of

particles (Cheftel et al., 1985), reducing the overall availability of polar groups to bind water. Curd shrinkage observed with higher washing temperatures may be due to such an aggregation mechanism which results in decreased curd porosity and the expulsion of more capillary water (Figure 26b). Similar shrinkage and firming of curd has also been observed with increasing coagulation temperature (O'Meara and Munro, 1982; Jablonca and Munro 1986a).

One final observation is that the effect of concentration on the WHC resulted in a minimum occurring at 31% SMP (Figure 23) which corresponded with the minimum porosity being observed at 30% SMP in the microstructural survey (Figure 24c). Hydration is affected by the aggregation of the micelles which may reduce the total surface area of the protein and their subsequent ability to bind water. On the other hand, hydration may be enhanced by gelation by trapping water in the structural network formed. Both aggregation and gelation are dependent upon concentration and the interaction of these two opposing phenomena on hydration, at a pH close to the isoelectric point, may be the reason that an intermediate solids concentration results in minimum hydration properties.

3.3.5 Conclusion

Coagulation and washing conditions have been shown to influence the microstructure of the acid casein curd, the loss of fines therefrom and the water holding capacity of the curd. RSM was an effective tool for examining which of the variables used in the process were significant and provided guidance as to which mechanisms may affect the system. Fines could be minimized by selecting appropriate pH, concentration and agitation conditions while the moisture content of the final curd was mainly controlled by pH, concentration and temperature, and these parameters will likely affect the dewatering properties and drying efficiencies of the curd. Microstructural analysis demonstrated the effects of pH, concentration, temperature and their interactions on the casein structural network. Thus, the coagulation pH and concentration affect not only the

efficiency of the acid casein production process but also the functional properties of the end product. This study indicates that the careful assessment of the coagulation/washing process can yield information which may be useful in obtaining a better understanding of casein coagulation and applicable to both conventional casein manufacture and the development of an extrusion based process.

3.4 MULTIRESPONSE OPTIMIZATION OF ACID CASEIN PRODUCTION

ABSTRACT

A multivariate dependent process, designed to produce an acid casein from skim milk powder was studied in terms of minimizing residual lactose, ash and fines. Compromise optimum conditions were derived using the Generalized Distance Approach (GDA) and an Extended Response Surface Procedure (ERSP) which made use of the SAS RSREG procedure with and without constraints. The GDA procedure produced good results in terms of providing an optimum for a general acid casein process, while the ERSP allowed more extensive analysis of the data in terms of assessing specific processing conditions. Although more computing intensive, the ERSP conferred additional flexibility in determining optimal conditions for special situations such as extrusion processing. Both approaches are useful for process engineering, with the GDA being a more general tool while the ERSP is advantageous when the GDA procedure becomes limiting

3.4.1 Introduction

The manufacture of acid casein from skim milk is a primary industrial process which serves to provide the base material for the further processing of milk proteins into soluble caseinates, mainly used by the food industry (Muller, 1971; Richert, 1975; Muller, 1982; Southward, 1985, Fichtali et al., 1990a). The overall quality of acid casein depends on the conditions associated with the coagulation and washing of the curd, with residual lactose and ash being important quality attributes, and the minimization of fines being a major economic consideration.

It was clear from our initial work (Chapter 3.1) that a more detailed investigation was required of the coagulation and washing procedures in relation to the extrusion process. These procedures involve a number of variables, including pH and concentration for the coagulation step; and, temperature, time, agitation and wash water ratio (WWR) for the washing step. An experimental model system was utilized to simulate the extrusion processing conditions and evaluated using response surface methodology (RSM) to assess the relationships between the responses (fines; microstructure; and residual lactose, WPN, and minerals) and the process variables (Fichtali et al., 1990a,b) as discussed in Chapters 3.2 & 3.3.

RSM provided a useful means for studying such a complex multivariate coagulation/washing system. This approach has been enhanced by the availability of multiresponse optimization routines (Khuri and Conlon, 1981), specifically the Generalized Distance Approach (GDA). This procedure was assessed in relation to obtaining a multivariate compromise optimum for the coagulation/washing process for acid casein in general and compared to an Extended Response Surface Procedure (ERSP) through the use of the SAS RSREG procedure with and without constraints as devised by the author.

3.4.2 Material and Methods

The details of the experimental protocol and analyses, and the experimental design have been described in Chapters 3.2 & 3.3. In essence SMP was coagulated under various conditions of pH and concentration (C), and subsequently washed under variable conditions of temperature (T), agitation (rpm), time (t) and WWR according to a central composite design. The casein fines were separated from the wash water by centrifugation and the product was freeze dried and analyzed for lactose and ash.

Generalized Distance Approach

Contour plots of individual responses can be used to optimize one response at a time against two selected independent variables. When two or more response variables are considered simultaneously, the optimization problem becomes substantially more complex and conditions which are optimal for one response may not be optimal for another, or may be physically impractical. In addition, the optimum may be a function of more than two independent variables. Optimization of the multiresponse function can be achieved using the Generalized Distance Approach (Khuri and Conlon, 1981; Khuri and Cornell, 1987). This method permits one to find compromise conditions for the input variables that are somewhat favourable to all responses. This implies that the multiresponse function deviates as little as possible from the individual optima and the deviation is formulated as a distance function which is minimized over the experimental region. Mathematically, if the responses are considered to be correlated, this distance function can be expressed as:

$$\rho[\hat{y}(x), \phi] = \left[\frac{(\hat{y}(x) - \phi)' \hat{\Sigma}^{-1} (y(x) - \phi)}{z'(x)(Z'Z)^{-1} z(x)} \right]^{1/2} \quad (60)$$

where: x is defined as a $1 \times k$ vector of the coded input variables,

$z(x)$ is a vector of order $p \times 1$ of the same form as a row of Z , but is evaluated at the point x ,

$\hat{y}(x)$ is the vector of predicted r responses at the point x ,

ϕ being the vector of individual optima, and

$\hat{\Sigma}$ is an estimate of the variance-covariance matrix of the responses given by:

$$\hat{\Sigma} = \frac{Y' [I_n - Z(Z'Z)^{-1} Z'] Y}{(n-p)} \quad (61)$$

where Y is the $n \times r$ multiresponse data matrix. It is to be noted that the matrix Z is such that all the responses are represented by the models:

$$y_i = Z\beta_i + \epsilon_i \quad i = 1, 2, \dots, r$$

and Z is assumed to be of order $n \times p$ and rank p .

The minimization of the ρ function with respect to x over the experimental region will produce a compromise optimum for the multivariate system under consideration. The input data for the Multiple Response (MR) program developed by Conlon and Khuri (1988) are the design and response matrix, which are used to calculate the regression equations and the optima for each response. Once the individual optima have been obtained, the GDA is used to calculate the compromise optimum. A variable which can be adjusted in this search is the design radius (the extreme limits of the coded variables), which can be reduced to narrow the search. Since our design is not rotatable, the radius is a required parameter in the program. The details of the search method and convergence criteria used in the program have been discussed by Khuri and Conlon (1981).

Extended Response Surface Procedure (ERSP) for Multiresponse Optimization

An alternative approach to finding a multiresponse optimum is to use an ERSP with constraints. Because of practical experimental considerations, the original experimental RSM design is restricted to 50 variable combinations. A search for an optimum under these conditions is limited because the grid comprising the variable combinations is quite crude and the optimum may be missed. By writing a small subroutine, one can generate a much finer grid using second order regression equations by reducing the interval between the coded variables (i.e., 0.25 instead of 1.00). The expanded data set considers all the variable combinations and an extensive new set of responses values is calculated. If the computing power is available, even more combinations can be generated by reducing the coded level interval to even smaller values

to increase the precision of the search. The response of interest is then sorted in ascending order using a sort routine which is part of the RSREG procedure. The maximum or minimum of the sorted response can be determined with or without constraints on the remaining responses. In addition to this, the search in the design space can also be limited by constraining the input variables to selected ranges. Assuming the relations originally derived from the experimental data are sufficiently precise, this approach allows one to optimize a selected variable with constraints on either input variables or the remaining responses. The end result is an optimum with constraints, which may also be considered a type of multivariate response optimum. The SAS program used for computation is given in Appendix 3.

3.4.3 Results and Discussion

The complete experimental design in terms of coded values and their respective responses is presented in Appendix 2. The regression equations and their estimated regression coefficients are presented in Table 4 for lactose and ash, and in Table 6 for fines. Figure 28 illustrates in graphical form the type of problem to be solved. Here pH and concentration are the variables under consideration, with the remaining variables fixed and the responses are presented as overlapping contour plots. In this circumstance, one can visually estimate a multiresponse optimum in relation to fines, lactose content and ash. The shaded region in Figure 28 can be considered the best conditions meeting the criteria of minimal fines, lactose and ash. Khuri's procedure uses a mathematical approach to find a more general solution, which is not restricted in terms of the number of variables under consideration, as in the case of the surface response plot.

For the calculations, the design matrix and the data matrix for lactose, ash and fines (Appendix 2) were entered into the MR program and a search implemented for the compromise minimum using design radii of 2.00 and 1.75. The output of the program provides optima for the factors investigated and computes the corresponding responses from them (Table 7).

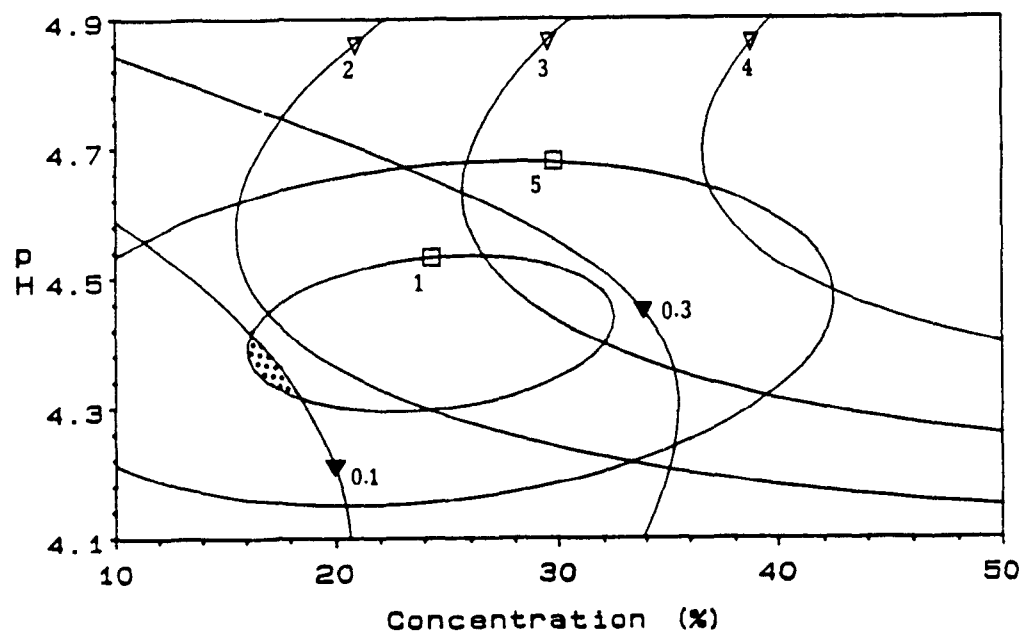


Figure 28. Superimposed multiple response contour plots of predicted percent ash (∇), lactose (\blacktriangledown), and fines (\square) as a function of pH and concentration. Temperature = 55°C; time = 15 min; rpm = 250; and WWR = 4:1.

Table 7. Multiresponse factor optima calculated using the Generalized Distance Approach and their subsequent predicted responses for two radii (r).

Variables	Optimal Values	
	$r=2.00$	$r=1.75$
pH	4.33	4.34
Temperature (°C)	45	46
Concentration (%)	12.3	14.9
Wash Time (min)	14.4	15.8
rpm	263	259
Wash water ratio	4.8	4.9
Responses	Optimal Values	
Fines	1.70	1.11
Ash	1.55	1.76
Lactose	-0.029	0.011

The compromise optima obtained for searches for both radii were similar and it is likely that the narrower search is slightly more accurate as more error can accumulate when extreme design values are used. The compromise optimum response conditions provide a very useful solution, defining six variables leading to a product which meets international specifications for acid casein in terms of lactose (<0.1%), ash (<2.0%), while minimizing fines, the latter being important from an economic viewpoint. This is clearly a valuable solution in relation to defining and developing a process for the production of acid casein.

One can foresee circumstances where the compromise optimum may not provide a solution which meets specifications or where one may be forced to work outside these optimal values. Extrusion processing, which requires solids content of 20% or more cannot be carried out using the calculated compromise optimum conditions. In this situation, the additional capability of adding constraints would be useful to allow a search

for a solution which defines or limits specific criteria. Such an approach was devised by making use of an ERSP based on the SAS RSREG procedure and a routine to generate a more detailed surface for the search (Appendix 3). To do this, the program was first instructed to minimize fines but to simultaneously restrict lactose and ash to $< 0.05\%$ and $< 1.5\%$, respectively. A variety of additional constraints were then imposed in relation to the extrusion process. Specifically, optimization was studied within the data set using the following criteria: Run 1, the use of a selected pH range; Runs 2-5, specific pH values; Runs 6-11, selected concentrations; and Run 12, a specialty high ash product.

Table 8 presents the constraints placed on the variables for runs 1-12 and the resulting optimal solutions. Thus, the solution for Run 1, which mimics extrusion conditions, is slightly better than the compromise solution (Table 7) obtained using the Multiple Response program in terms of minimizing each response, but still allowing the use of higher SMP concentrations. For Runs 2-5, the effect of increasing pH forces a reduction of the concentration but also results in an increase in minimum fines. In the case of increasing concentration from 25 to 50% (Runs 6-11), the pH required decreases, however, minimum fines reach unacceptable levels. For the manufacture of a specialty high ash casein with low lactose content (Run 12), the key factor appears to be the use of high concentrations. The ERSP is a broader tool in that it allows one to explore an experimental data set more fully and assess basic trends as a function of selected constraints.

Table 8. Minimization of fines using the Extended Response Surface Procedure (ERSP) using defined constraints on responses and input variables. F=Fines, A=Ash, and L=Lactose.

Constraints						
Run#	pH	T (°C)*	C (%)	t (min)	rpm	WWR
1	4.3-4.5	40-60	10-25	10-20	200-250	4-5
2	4.3-4.3	40-60	10-25	10-20	200-250	4-5
3	4.4-4.4	40-60	10-25	10-20	200-250	4-5
4	4.5-4.5	40-60	10-25	10-20	200-250	4-5
5	4.6-4.6	40-60	10-25	10-20	200-250	4-5
6	4.1-4.6	40-60	25-25	10-20	200-250	4-5
7	4.1-4.6	40-60	30-30	10-20	200-250	4-5
8	4.1-4.6	40-60	35-35	10-20	200-250	4-5
9	4.1-4.6	40-60	40-40	10-20	200-250	4-5
10	4.1-4.6	40-60	45-45	10-20	200-250	4-5
11	4.1-4.6	40-60	50-50	10-20	200-250	4-5
12	4.3-4.7	40-60	10-50	10-20	200-250	4-5

Solutions									
Run#	pH	T	C	t	rpm	WWR	F (%)	A (%)	L (%)
1	4.32	59	22	20.0	200	4.0	-0.44	1.48	0.016
2	4.30	60	23	20.0	200	4.0	-0.43	1.42	0.003
3	4.40	60	18	20.0	205	4.0	0.31	1.46	0.050
4	4.50	59	15	16.5	200	4.6	3.26	1.48	0.050
5	4.60	40	11	16.5	250	4.0	4.07	1.49	-0.120
6	4.28	60	25	20.0	200	4.0	-0.32	1.47	0.005
7	4.22	60	30	20.0	200	4.0	1.17	1.44	0.005
8	4.18	60	35	20.0	200	4.0	3.51	1.43	0.013
9	4.16	60	40	20.0	200	4.0	6.20	1.50	0.024
10	4.14	60	45	20.0	200	4.4	10.23	1.50	0.001
11	4.12	60	50	19.5	200	4.0	14.37	1.50	0.037
12	4.35	60	45	20.0	200	4.7	4.01	3.11	0.047

Full range

An attempt was made to compare the two methods more directly by using a totally unconstrained input variables ERSP search with lactose and ash restricted to <0.05% and <1.5%, respectively. The results of the unconstrained input variables search are presented in Table 9 and can be compared to the compromise optima presented in Table 7.

Table 9. Computation of minimum fines with unconstrained input variables and lactose and ash under constraints using the Extended Response Surface Procedure for two design radii.

(a) Radii = 2.00

I	N	pH	T	C	t	rpm	WWR	F (%)	A (%)	L (%)
1	15625	4.5	40	10.0	5	350	7	-3.6	1.10	-0.39
0.5	531441	4.5	40	15.0	5	350	7	-3.7	1.40	-0.25
0.25	24137569	4.45	40	12.5	5	350	7	-3.9	1.18	-0.28

(b) Radii = 1.75

1	4096	4.35	58.8	12.5	6.3	313	6.3	-1.6	1.34	-0.06
0.5	262144	4.45	58.8	12.5	6.3	338	6.8	-2.9	1.41	-0.24
0.25	11390625	4.45	58.8	12.5	6.3	338	6.8	-2.9	1.41	-0.24

I = Interval between coded levels, N = Number of predicted data points generated by SAS, F = Fines, A = Ash, L = Lactose

The solutions are quite different, with the ERSP results being at the limits of the design values for the majority of input variables. Most of the optima are impractical to implement, but do result in improved minimization of fines, lactose and ash. The ESRP solutions also indicate that the effect of the design interval between the coded levels appears to be negligible, but that the design radius does affect the results. These differences can readily be explained in terms of the search approach. In the Generalized Distance Approach, the compromise optimum depends on individual optima of the

responses and how far they are from each other in the design space, and as a result, the compromise optimum may be far from the 'ideal' optimum (Khuri and Cornell, 1987). Using ERSP, the search for minimum fines under the defined constraints will be closer to the optimum, which in turn can be further localized by increasing the number of data points in the design space.

The ERSP approach requires a large number of data points and considerable computing time, i.e., Run # 1 consumed 40 minutes of CPU time (~ \$375/hour). The GDA on the other hand can be run on an IBM PC at negligible cost on readily available hardware. The computing costs for the ERSP are high because the number of variables considered in this study were exceptionally large. In general, most problems of this nature would normally consider only between 2 to 4 variables, which would reduce computing time exponentially and make such calculations much more viable.

Both calculation procedures have merit, the GDA being useful for obtaining a generalized compromise optimum, while the ERSP is useful in specific situations where constraints are a necessity, as in the case of extrusion. The GDA optimum has been shown to be a very workable solution for the conventional acid casein process which is run on a relatively low solids basis. Extrusion processing requires high solids and hence optimal conditions can only be found using constraints. This ability to set constraints is certainly an advantage in such circumstances, providing the flexibility to explore the experimental data in relation to producing a tailor made end product.

3.4.4 Conclusion

An attempt has been made to extend the basic information available from standard multivariate response surface data in terms of optimizing a skim milk coagulation/washing process. It was shown that the GDA program developed by Conlon and Khuri (1988) could be applied to obtain a useful compromise optimum for a standard acid casein process. The GDA result may in fact not provide a viable compromise optimum and in

such circumstances an useful alternate solution can be obtained by an ERSP search as long as the models under consideration are second order. ERSP presents a useful way of deriving additional information from the experimental data set, especially where constraints are likely to be a prerequisite. Both procedures are useful tools to the process engineer and should be considered as adjuncts to standard RSM techniques.

3.5 AN EXTRUDER DIE DESIGN FOR WHEY SEPARATION

ABSTRACT

A special die was designed as an attachment to an extruder in order to assist in whey separation from casein curd as the extrusion process proceeded. The die was tested under various operating conditions and design parameters and the end product analyzed for moisture, ash and lactose. Although the die did not provide satisfactory results due to plugging problems, the results indicate that there is potential for extruder solid-liquid separation in processes where syneresis occurs.

3.5.1 Introduction

Dewatering, including dewheying technology in the food industry relies on solid-liquid separation equipment such as vacuum filters, centrifuge or belt presses which are capable of removing bulk water. Other than these mechanical separation techniques, new methods have been developed such as electro-acoustic dewatering processes (Muralidhara et al., 1988). In the food industry, many processes involve reactions under heat and shear resulting in phase separation, i.e., the rendering of meat. The extruder may be useful for such applications by combining several unit operations in a single process, resulting in equipment and energy savings.

After the conversion of SMP to an acid precipitate, dewheying is required which has a direct effect on the washing efficiency (Hobman, 1978; Pearce et al., 1987). Screen separation is the most commonly used procedure in casein industry, however, its efficiency is lower compared to other mechanical separation techniques such as centrifuges and roller presses. The objective of this study was to design a special die for continuous dewheying and test it to determine whether it could assist in: (1) continuous dewheying

leading to a reduction of the cost associated with conventional dewheying process, and (2) reducing the subsequent washing steps of the casein curd.

3.5.2 Material and Methods

Low heat SMP (section 3.2.2) was continuously coagulated in a Baker Perkins co-rotating twin screw extruder which is described in Appendix 4. The barrel was configured in a 15:1 L/D ratio (barrel length to screw diameter ratio) and the screw profile was designed to generate efficient pumping action and includes 225 mm feed screws, 50 mm short pitch screws and 475 mm single lead screws. The die efficiency was tested under various conditions of moisture, feed rate, screw speed and temperature and the dewheyed samples were assessed for moisture, ash and lactose (section 3.2.2), with pH of the coagulum measured before separation (section 3.2.2).

Die design

Figure 29 is a schematic diagram of the extruder die used for continuous dewheying. It was made of stainless steel and consists of the following parts: (1) a die plate to be fixed to the extruder barrel; (2) a cylindrical screening section made of three layers of stainless steel screens (40, 100 and 40 mesh respectively); (3) a perforated pipe to hold the cylindrical screen and prevent the tearing of screens under pressure; (4) a die orifice holder which can be connected to the screen section; (5) rubber rings to seal the screen section between the die plate and the die orifice holder; and (6) a die orifice which could be changed as required to restrict or to enlarge the opening. Additional drawing details for each part of the die are given in Appendix 5.

3.5.3 Results and Discussion

The die was tested under various extrusion operating conditions (Table 10), using two screen heights, 65 and 150 mm and for three die exit openings, 5; 10 and 15 mm. The small orifice (5 mm) did not work as it plugged easily. Using the larger orifices (10 and

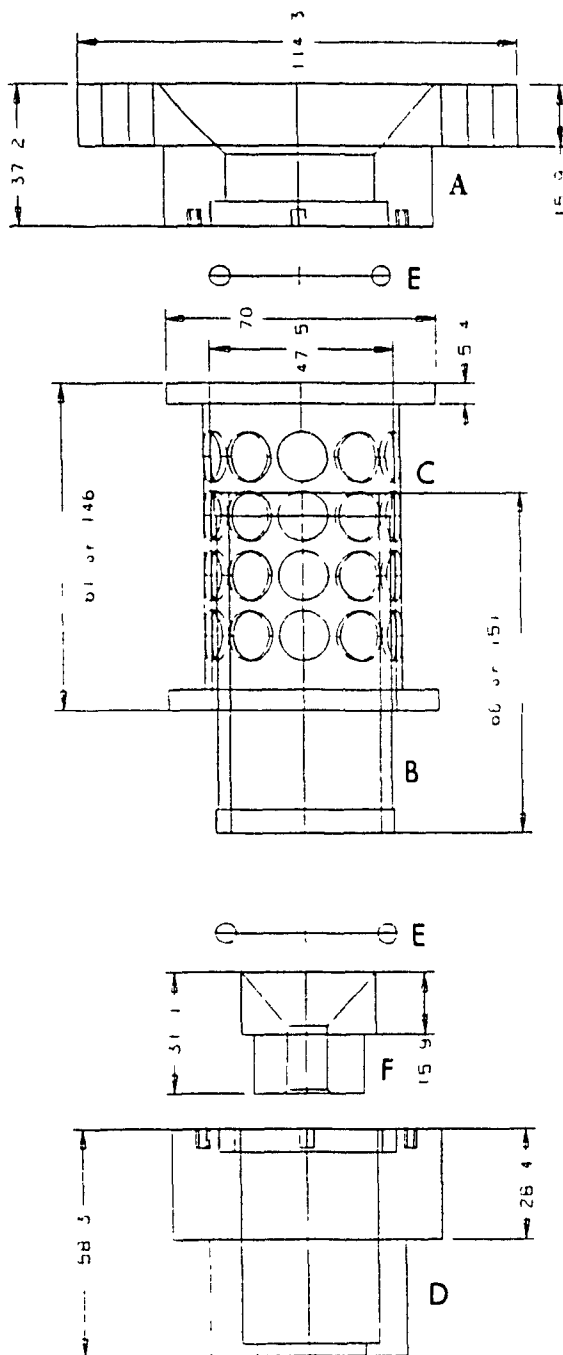


Figure 29. Schematic diagram of the die used for extrusion dewheying process. A = die plate, B = cylindrical screen, C = perforated pipe, D = die orifice holder, E = rubber ring, and F = die orifice.

15 mm), dewheyed samples were collected under some operating conditions. However, in general the pressure generated by the screws was not sufficient to ensure continuous separation over a long period of time due to relatively high moisture content of the curd. The low viscosity of the product plus the screws, which were designed for more viscous materials, led to product backing up in the extruder. The operating conditions and design parameters under which dewheying was possible, and for which analytical results were obtained are given in Table 10.

Table 10. Extrusion conditions and analytical results obtained for dewheyed products. H=cylindrical screen height (mm) , D=die orifice diameter (mm), T= barrel temperature setting (°C), FdR=feed rate (kg/hr), FwR=flow rate (l/hr), M_i=initial moisture of the curd before separation, M_f=final moisture of the curd after separation.

Conditions							Results			
H	D	T	FdR	FwR	rpm	M _i (%)	pH	M _f (%)	Ash (%)	Lactose (%)
65	10	55	13.5	34.4	100	71.8	3.80	68.0	5.0	31.3
65	10	55	14.9	28.0	100	65.3	4.36	58.6	7.1	37.9
65	10	60	18.9	28.0	150	59.7	4.60	51.5	7.3	34.5
65	15	60	18.9	28.0	150	59.7	4.50	55.6	7.3	34.1
65	15	60	22.9	30.0	150	56.7	4.66	55.2	7.7	42.8
150	15	60	18.9	28.0	150	59.7	4.60	52.5	7.3	29.3

Table 10 shows that adequate separation equal to the one which can be obtained by centrifugation (50-60% moisture) may be achieved using the die. The success of using the die depended on operating conditions and design parameters of the die. It has been shown (see Chapters 3.2 & 3.3) that particle size and firmness of the coagulum are largely dependent on pH, concentration and temperature of coagulation. Larger particles having rubbery structure immediately plug the die, while a soft coagulum with small

particles may exit from the die orifice without any significant degree of separation. The longer screen (150 mm) was more difficult to use as more material accumulated at the die requiring more pressure to push the product through the orifice. Most of the samples analyzed may be not representative of the process, as steady state operating conditions were not achieved. The results preclude drawing any accurate conclusions about the performance of the die or the operating conditions required for partial on line separation during the extrusion process.

Further evaluation of using the die for dewheying requires screws which generate enough pressure when low viscosity products are being run, however, such screws are not available. A single screw extruder acting as a screw pump with some mixing elements sealed from each side by pumping screws, may also serve the purposes.

3.5.4 Conclusion

A special die for partial dewheying of SMP coagulum was designed, however, continuous separation without plugging of the die was not possible although, several operating conditions and design parameters were tested. The data obtained for the more workable conditions showed that separation as efficient as centrifugation may be obtained using the dewheying die. Despite the poor results obtained due to screw limitations, the concept of using an extruder die for dewatering may have applications in a number of processes such as, hydrolysed vegetable protein, meat rendering, corn gluten slurry, sugar beets, orange pulp, apple pomace, corn fiber and others. Since the screws were not available to further evaluate the die separation efficiency, the dewheying concept using the die was not considered in subsequent experimentation.

3.6 RHEOLOGICAL BEHAVIOUR OF SODIUM CASEINATE

ABSTRACT

The rheological behaviour of commercial sodium caseinate was determined at various temperatures (25-65°C) and concentrations (10-16%) and was shown to be most adequately described by the Bingham model. The effect of temperature on the viscosity followed an Arrhenius-type relationship while the effect of concentration followed an exponential-type relationship. A model to predict the viscosity as a function of temperature and concentration is presented, which also considers the effect of concentration on the activation energy. The model developed will be useful for sodium caseinate manufacturing and applications.

3.6.1 Introduction

Intensive studies have been carried out to produce acid casein from SMP (Fichtali et al., 1990a,b,c) which are described in Chapters 3.2, 3.3, & 3.4. Acid casein is insoluble and should be neutralized to sodium caseinate which is widely used in various formulated foods because of its desirable physico-chemical, nutritional and functional properties. The major problem associated with sodium caseinate manufacturing lies in its high, viscous glue-like texture, increasing its dissolving time and limiting its concentration for spray drying to ~20% total solids even at higher temperatures of 90-95°C (Southward, 1985).

Towler (1974) studied the effect of shear rate, temperature and concentration on the viscosity of sodium caseinate, however, no rheological model was developed. Such a model would be useful to predict the range of shear, concentration and temperature which may be used to prepare sodium caseinate dispersions with predictable viscosities

which can be handled in agitated tanks, by colloid mills, pumps and spray driers. Furthermore, such a model would aid in understanding the flow behaviour in an extruder and assist in the modelling and hence control of extrusion processes. Viscosity models can also be useful in studying and predicting effects of process conditions on end product quality attributes, as caseinates are widely used for their rheological functional properties.

The objective of this study was to develop a model which adequately describes the effect of shear, temperature and concentration on the viscosity of commercial sodium caseinates, which will be useful for interpreting observations provided by casein neutralization process and characterizing sodium caseinate produced by extrusion.

3.6.2 Material and Methods

Preparation of Samples

Commercial sodium caseinate was obtained from Champlain Industries (Cornwall, Ontario) and served to develop the viscosity model. Selected concentrations (10-16%) were dissolved by agitation in water bath at 60°C, for 20-30 min after which the samples were cooled to ambient temperature and any foam removed from the surface of the solutions prior to making viscosity measurements. Each set of conditions was coded, i.e., CnTm, where C is the concentration; n is the concentration value in percent solids; T is the temperature and m is the temperature value in °C.

Rheology

Rheological measurements were carried out using a Haake Rotovisco RV 20 viscometer, equipped with a M5-Osc measuring system used in the rotational mode and programmable via a computer controlled Rheocontroller RC20 module. An MV2 sensor was used and the temperature controlled to within $\pm 0.1^\circ\text{C}$ using a circulating water bath. The shear rate was programmed to increase continuously from 0 to 200 s^{-1} over 2 minutes giving 50 readings over the time period. Five temperatures (25-65°C) and three concentrations (10-16%) were studied, although in some cases it was not possible to

reach shear rates of 200 s⁻¹ because of high viscosities (i.e., at C₁₃T₂₅, C₁₆T₂₅ and C₁₆T₃₅). Three rheological models were assessed and fitted using regression analysis by the least-squares method.

3.6.3 Results and Discussion

Rheological behaviour

To determine the rheological behaviour, the data obtained under each set of conditions were fitted to each of Bingham, Power Law and Casson models, described by the following equations (Rao, 1986):

(a) Bingham:

$$\tau = \tau_0 + \eta \dot{\gamma} \quad (62)$$

where τ is the shear stress, $\dot{\gamma}$ is the shear rate, η is the coefficient of viscosity and τ_0 is the yield stress.

(b) Power law:

$$\tau = m \dot{\gamma}^{n-1} \quad (63)$$

where m is the consistency index and n is the flow behaviour index.

(c) Casson:

$$\tau^{1/2} = \tau_0^{1/2} + (\mu_0 \dot{\gamma})^{1/2} \quad (64)$$

where μ_0 is the casson plastic viscosity.

The model which best fit the caseinate data was the Bingham model, producing coefficients of determination (R^2) greater than 0.999 and Table 11 gives τ_0 , η , and R^2 values for each set of conditions. A slightly better fit was obtained with the power law model at higher concentrations and lower temperatures (i.e., C₁₃T₂₅, C₁₆T₂₅ and C₁₆T₃₅), but did not fit well for the remaining conditions. Similar trends were observed using the Casson model. Figures 30 and 31 graphically illustrate typical data and show the general

tendency to Bingham behaviour (Newtonian with yield stress) at selected temperatures and concentrations, respectively. Towler (1974) described sodium caseinate solutions as showing pseudoplastic behaviour, with the degree of pseudoplasticity decreasing as the concentration was dropped from 15 to 7.5% total solids, while Newtonian behaviour was observed by Baomy and Brulé (1986) for 8% solids concentration at 25°C. In our study the Bingham model, a yield stress variant of the Newtonian model, produced satisfactory fit ($R^2 > 0.999$) for all the conditions studied.

Table 11. Yield stress, coefficient of viscosity and correlation coefficient obtained at different conditions of temperature and concentration using eqn (62).

C (%)	T (°C)	τ_0 (Pa)	η (Pa s)	R^2
10	25	1.00	0.071	0.9999
10	35	0.92	0.044	0.9999
10	45	0.89	0.028	0.9996
10	55	0.96	0.018	0.9994
10	65	0.84	0.015	0.9994
13	25	13.61	3.674	0.9991
13	35	4.45	1.266	0.9998
13	45	1.34	0.516	1.0000
13	55	1.15	0.242	0.9999
13	65	1.05	0.126	0.9999
16	25	13.88	18.164	0.9995
16	35	11.79	4.180	0.9993
16	45	4.57	1.421	0.9999
16	55	2.19	0.566	1.0000
16	65	1.26	0.271	0.9998

Effect of temperature

The effect of temperature on the viscosity of caseinate solutions may be described by an Arrhenius-type equation (Towler, 1974):

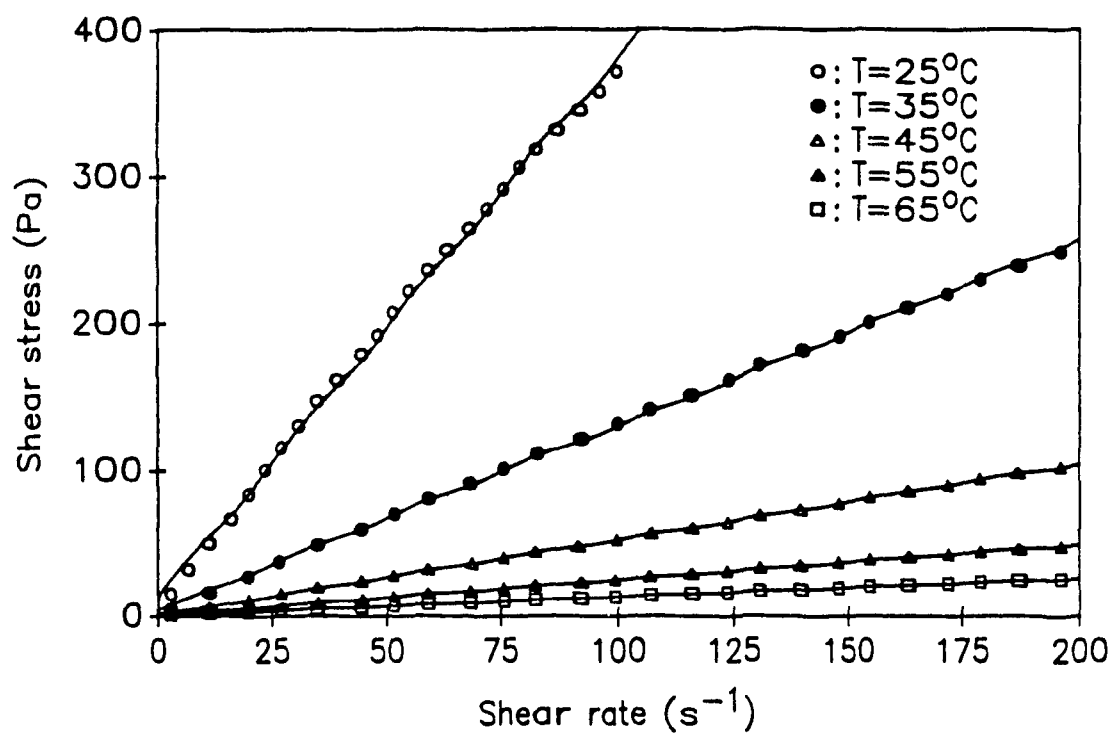


Figure 30. Flow curves for sodium caseinate at 13% solid concentration as a function of temperature and shear rate.

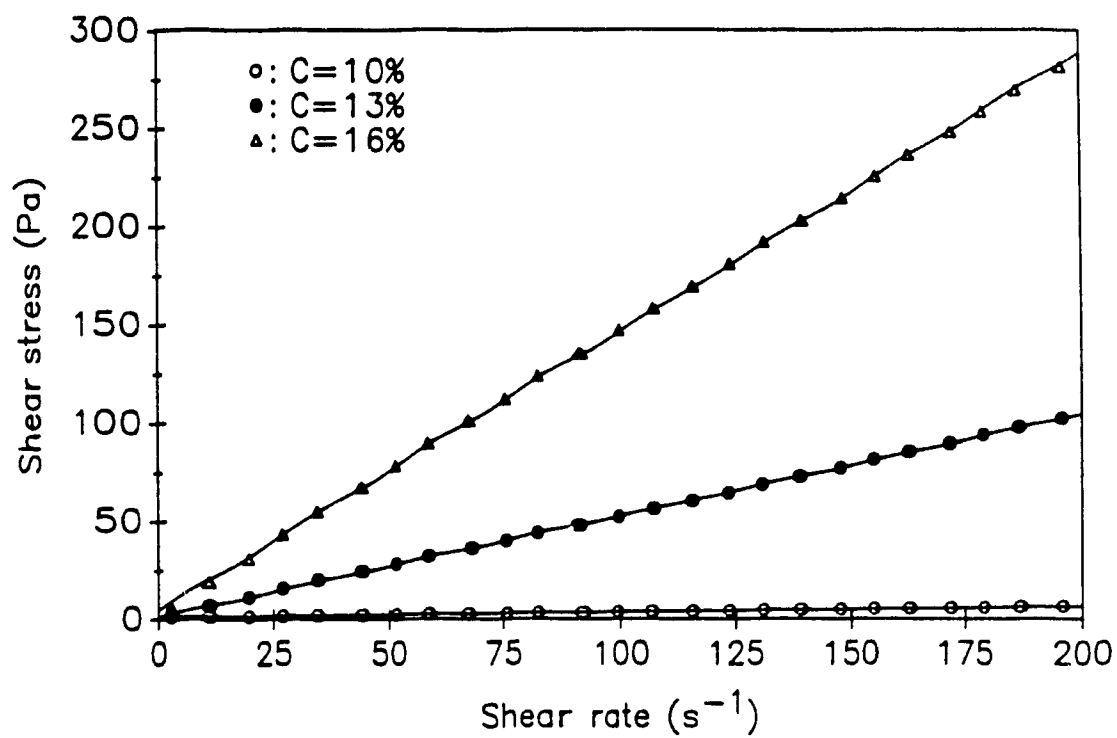


Figure 31. Flow curves for sodium caseinate at 45°C as a function of concentration and shear rate.

$$\eta = \eta_0 \exp (E_a/RT) \quad (65)$$

where η_0 is a constant, E_a is the activation energy for flow, T is the absolute temperature and R is the gas constant (1.987 cal g mol⁻¹ K⁻¹).

Figure 32 shows the effect of temperature on the viscosity of sodium caseinate according to eqn (65). Linear plots are obtained when the log the viscosity at a particular concentration is plotted against $1/T$. The activation energy (slope of the curves) tends to increase with the solid content of the solutions with values of 3.49, 7.32 and 9.09 Kcal/g.mol for 10, 13 and 16% solids concentration, respectively. This implies more energy is required to shear higher concentrations of sodium caseinate.

Effect of concentration

Generally the effect of concentration can be described by either an exponential or a power type of relationship (Rao, 1986) which are given by eqns (66) and (67) respectively:

$$\eta = \eta_1 \exp(A_2 C) \quad (66)$$

$$\eta = \eta_2 \exp(C)^{A_1} \quad (67)$$

where C is the concentration in percent solids and η_1 , η_2 , A_1 , and A_2 are constants. These relations have been used to describe the effect of concentration on viscosity for various food materials (Clark, 1978; Rao, 1986; Morgan et al., 1989; Khalil et al., 1989). Neither of these relations fit our data, as a consequence an exponential-type equation was tried.

$$\eta = \eta_3 \exp(B_1 C + B_2 C^2) \quad (68)$$

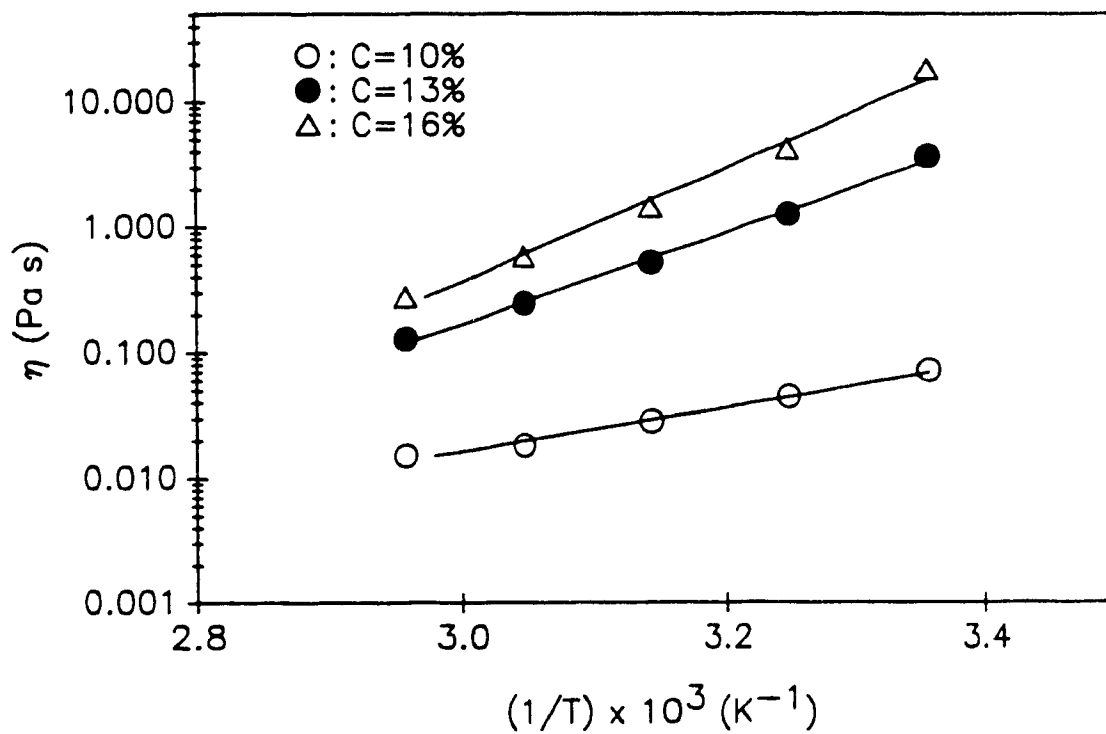


Figure 32. Effect of temperature on viscosity of sodium caseinate at various concentrations.

where η_0 , B_1 and B_2 are constants. This equation has been successfully applied to clarified pear juice concentrates (Ibarz et al., 1989) and Figure 33 presents the logarithmic viscosity vs concentration plots with the data fitted to a second order regression model according to eqn (68), for different temperatures.

The combined effect of temperature and concentration

For practical purposes, it would be very useful to describe the effect of temperature and concentration by a single equation. Combining eqns (65) and (68) and considering the effect of concentration on the activation energy (E_a), the following equation is obtained:

$$\eta = \eta^* \exp \left[(K_1 + K_2 C) \frac{1}{T} + K_3 C + K_4 C^2 \right] \quad (69)$$

where η^* is a constant. The viscosity coefficients from Table 11 were related to temperature and concentration by multiple linear regression using eqn (69). The resulting constants are given in Table 12 and a good fit as indicated by the coefficient of determination ($R^2=0.996$) was obtained. Eqn (69) can be rewritten in terms of E_a as:

$$\eta = \eta^* \exp \left[\frac{E_a}{RT} + K_3 C + K_4 C^2 \right] \quad (70)$$

where,

$$E_a = R(K_1 + K_2 C)$$

In this form, eqn (70) considers the fact that the activation energy increases with increasing the solids concentration. Figure 34 illustrates the combined effect of temperature and concentration on the logarithmic of viscosity as predicted by eqn (69).

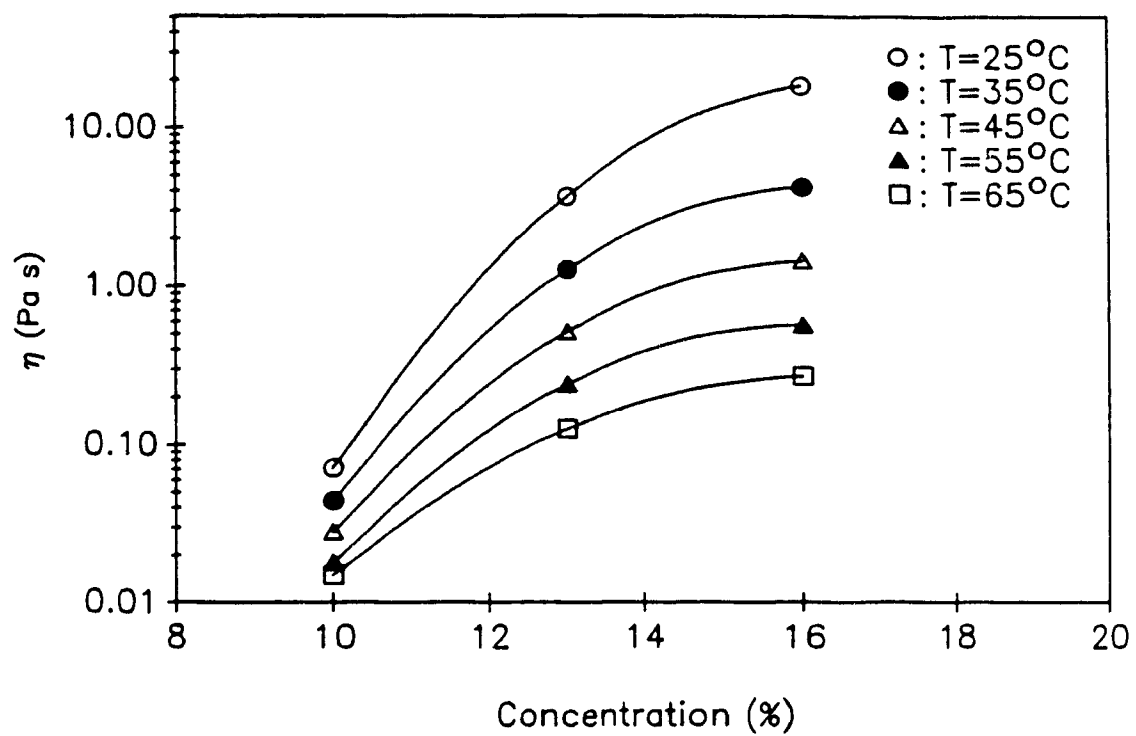


Figure 33. Effect of concentration on viscosity of sodium caseinate at various temperatures.

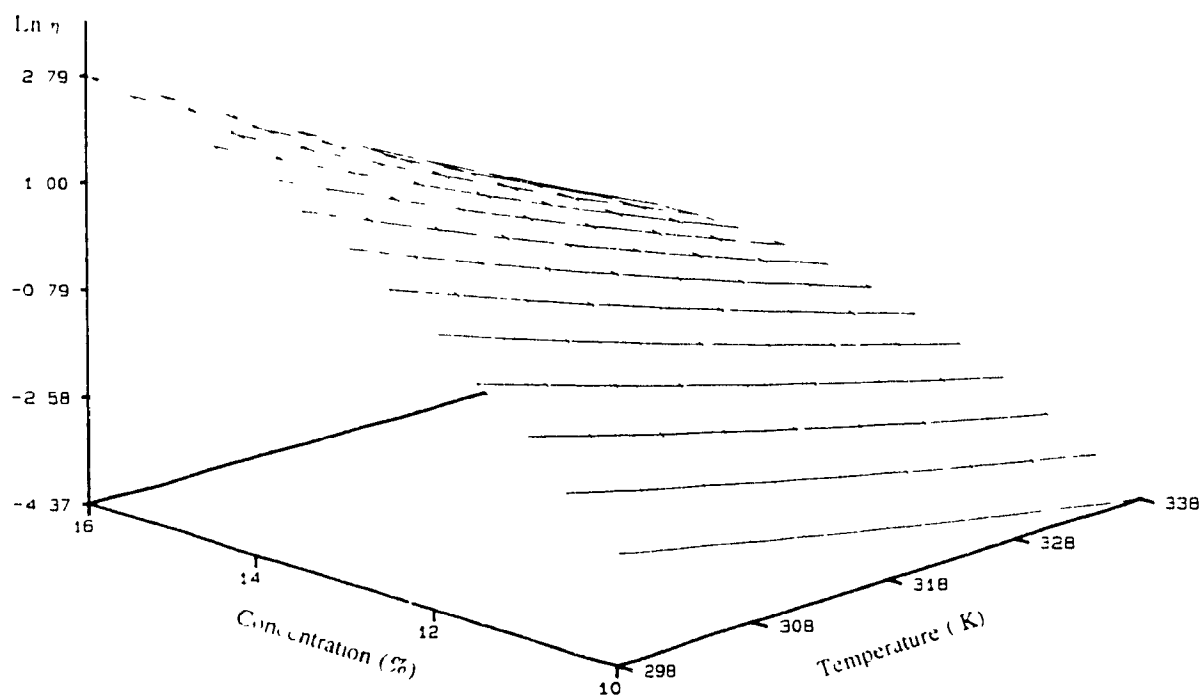


Figure 34. Combined effect of temperature and concentration on the logarithmic of viscosity of sodium caseinate.

Table 12. Model constants and regression estimates according to eqn (69) for sodium caseinate (Champlain Industries).

Parameter	Regression estimate
η^* (Pa s)	7.960×10^{-4}
K_1 (K)	-6384.725
K_2 (K)	1082.029
K_3 (dimensionless)	0.02426
K_4 (dimensionless)	-0.10595
R^2	0.996

It should be emphasized that the constants of eqn (69) are limited to the ranges of temperature and concentration studied and cannot be extrapolated to other conditions or other commercial sodium caseinates. In addition to temperature and concentration, other factors can affect the viscosity of sodium caseinates such as pH, calcium content, type of alkali used for casein neutralization plus seasonal and genetic factors (Southward, 1985)

3.6.4 Conclusion

The rheological behaviour of sodium caseinate was adequately described using Bingham model. Thus shear rate has little or no effect under the conditions studied, however, sodium caseinate exhibits yield stress and hence some energy will be required for caseinate mass deformation. Temperature and concentration have a dramatic effect on the viscosity coefficient of sodium caseinate and the viscosity can be decreased by either decreasing concentration or increasing the temperature, however, both of them may affect the end product characteristics. The model developed will be useful for the manufacture and applications of sodium caseinate.

3.7 EVALUATION OF THE TWIN SCREW EXTRUDER PERFORMANCE FOR ACID CASEIN NEUTRALIZATION

ABSTRACT

Extruder performance for acid casein neutralization to produce sodium caseinate was evaluated in terms of mixing, conveying, specific energy consumption, pressure generated, product temperature and end product characteristics. The effect of selected operating parameters such as, screw speed, temperature and feed rate was investigated and showed that operating conditions have minimal effect on end product characteristics although they can affect the extruder dependent variables, flow behaviour and the residence time distributions (RTD) in the extruder. The results obtained for RTD analysis were compared to theoretical models to assist in describing the extruder as a chemical reactor.

3.7.1 Introduction

The use of the extruder as a chemical and biochemical reactor may offer interesting possibilities in developing novel food applications. Although only few applications have been exploited up to now in the food sector (Linko, 1989), interest is growing in this area due to a better understanding of practical and fundamental aspects of twin screw extrusion (Fichtali & van de Voort, 1989). The conversion of acid casein into sodium caseinate by extrusion is one of these new applications (Boullé, 1986; Tossavainen, 1986), however, no published work evaluates twin-screw extruder performance in carrying out the acid casein conversion to sodium caseinate. A thorough understanding involves establishing relationships between extruder operating conditions, internal process variables and product properties (Fichtali & van de Voort, 1989) which as schematically presented in Figure 2 (Chapter 2.2).

Conventional processes for sodium caseinate manufacture are rather complex and energy consuming, mainly due to high viscosity of the slurry. Furthermore, localized high pH's due to low mixing efficiency when base is added and Maillard reaction due to long time held at high temperatures, may occur. These phenomena are responsible for reductions in the nutritional quality of sodium caseinate and off-flavour development during caseinate storage (Southward, 1985). As an HTST unit, an extruder can handle highly viscous materials, improve mixing and minimize reaction time as a continuous unit operation, resulting in high productivity and product homogeneity.

Preliminary work (Chapter 3.1) indicated that acid casein produced from SMP could be neutralized in the extruder, however, it was clear that substantial work would be required to understand and control the neutralization process. The aim of this study was to analyze the performance of the Baker Perkins twin screw extruder for acid casein neutralization in terms of mixing and conveying through mathematical description of residence time distribution (RTD), and to assess the effect of operating conditions (i.e. screw speed, temperature, feed rate) on: (1) extruder dependent variables (i.e. torque, pressure, product temperature), (2) RTD parameters (i.e. mean residence time, variance, Peclet number), and (3) product properties (i.e. bulk density, expansion ratio, protein nitrogen, colour).

Theory

The theory of RTD has been discussed in detail in Chapter 2.3 including the models available to describe flow, mixing and the methods for determining the RTD in an extruder (Fichtali & van de Voort, 1990a).

3.7.2 Material and Methods

Dried acid casein was obtained from Champlain Industries (New Zealand Import) which had the following proximate analysis: 11% moisture, 93% protein, 2.1% ash, 0.1% lactose and 1.1% fat, on dry basis.

The Baker Perkins twin screw extruder, described in Appendix 4, was used for acid casein neutralization. The barrel was configured in 20:1 L/D and a die with two circular orifices of 9 mm diameter each was used. The temperature is controllable over 9 zones along the barrel, however for this experiment the first two zones were not used, thus, the thermocouples for temperature control shown in Figure 35 were numbered from 3 to 9. The screw configuration (Figure 35) was designed to obtain good dispersive and distributive mixing and conveying capabilities. Good mixing is very important to obtain homogeneous conversion and is mainly achieved through the use of paddles located at different sections of the screw profile, but also through leakage flow, back pressure and simple diffusion. The paddles also generate heat by viscous dissipation of mechanical energy, increase the residence time in the extruder in high shear zones and increase new surface generation. Single lead screws were used between paddle sections to maintain good conveying performance and to act as steam lock in the high temperature zones to avoid chaotic fluctuations in process characteristics and product quality (Fichtali & van de Voort, 1989). Experiments were carried out to investigate the effect of operating conditions on: (1) extruder dependent variables, (2) RTD, and (3) end product properties.

Sample preparation and, tracer irradiation and detection for RTD analysis

As a tracer, manganese dioxide was used in the form of a uniform mixture of casein (3g) and MnO₂ (2g). The reasons for choosing this particular tracer were its reasonable radiation energy level for detection purposes and its relatively low half-life (2.576 hr) which avoids prolonged radiation pollution problems (Wolf and White, 1976). When the extruder attained steady state operation, indicated by a constant torque, pressure and product temperature, the tracer was introduced instantaneously downstream in the middle of the feed port (see Figure 6). The extrudate was collected as one continuous strand over a period of 5 min following the introduction of the tracer. The extruded

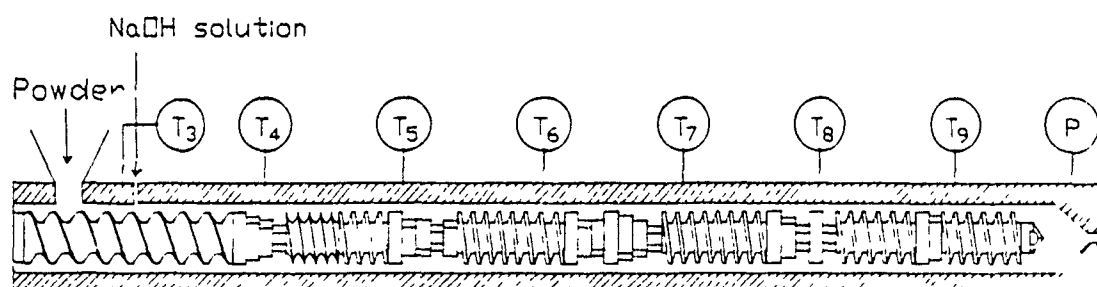


Figure 35. Pressure and temperature control zones, and screw configuration used for casein neutralization. The screw configuration comprises (from left to right): 300 mm, feed screw; 50 mm, 30° forwarding paddles; 50 mm, short pitch screw; 50 mm, single lead screw; 37.5 mm, 60° forwarding paddles; 25 mm, 30° reversing paddles; 100 mm, single lead; 50 mm, 60° forwarding paddles; 37.5 mm, 30° reversing paddles; 100 mm, single lead; 37.5 mm, 45° forwarding paddles; 25 mm, 90° paddles; 75 mm, single lead; 25 mm, 60° forwarding paddles and 75 mm, single lead.

product was then cut into ~30 cm, labelled segments and the original weight recorded for each segment. The corresponding time for each segment was determined based on the weight of the segment plus the weight of prior segments relative to the total weight of the extruded material over 5 min. The segments were dried at 100°C in an oven and then ground to 40 mesh using a Brinkmann centrifugal grinding mill (type ZM 1). Samples (4.5 g) from each ground segment, placed in polyethylene vials, were irradiated in the SLOWPOKE reactor at the university of Toronto. The irradiation time was 30 sec at a neutron flux of 2×10^{11} neutrons $\text{cm}^2 \text{sec}^{-1}$. The irradiation time is a function of the neutron flux available, the activity required and the amount of MnO_2 in the samples. The γ -rays emitted by the ^{56}Mn isotope was measured using a Canberra Ge detector and a 8180 Multichannel Analyzer after a delay time (time between end of irradiation and starting of computing) of 1 min. Two energy levels, 847 and 1811 KeV, were measured and corrections were made for background levels. These conditions were determined based on a preliminary experiment which was used also to verify the reproducibility of the results. The data obtained at 847 KeV were used and the concentrations were converted from counts/g to mg of MnO_2 /g through the use of a standard curve obtained by irradiating standards of MnO_2 /casein mixtures.

Physico-chemical analysis

Samples required for expansion ratio measurements were extruded in chilly water to keep the extruded strand uniform and smooth in shape. All the samples were dried in tray dryer (National Drying Machinery CO. Philadelphia, Type TY-2) at a temperature of 55°C for 2 days. The expansion ratio was determined by calculating the ratio of the diameter of the dried extrudate to the die orifice diameter. Samples were ground to 40 mesh for density, protein nitrogen and colour analysis. Bulk density was measured using a 10 ml cylinder and taping the wall (18 times) with a spatula. Taping is the method used by Niro Atomizer for dairy dried products (Niro Atomizer, 1976). Protein nitrogen was determined by kjeldahl (AOAC, 1984) using a Tacator, Kjeltec Auto 1030 Analyzer. The colour of milled extrudate in 3.5 cm diameter petri plates, was measured using L,a,b Opponent colour scales under illuminant D65 (daylight) with a Hunter Labscan II spectro

colorimeter. Only L values (lightness, 100 for perfect white) and b values (yellowness when positive) were considered. The pH was measured based on 5% solids according to a method outlined by Towler (1978) and the moisture determined after drying over night at 100°C. Measurements were made as follows; 6 replicates for the expansion ratio, 4 replicates for density, 2 replicates for protein nitrogen, and 5 replicates for colour and the average for each analysis was reported. A sample of the commercial acid casein used as a feed material was ground to 40 mesh (originally 30 mesh) and analyzed for bulk density, protein nitrogen and colour for comparison.

Calculations

The specific energy consumption (SEC) was calculated as follows:

$$\text{Net HP} = (\% \text{ Torque}) \times (\text{operating speed} / \text{maximum speed}) \times (\text{Machine HP}) \quad (71)$$

$$\text{SEC (HP.hr/kg)} = \text{Net HP} / \text{Feed rate} \quad (72)$$

$$\text{SEC (KJ/kg)} = \text{SEC (HP.hr/kg)} \times 0.7457 \times 3600 \quad (73)$$

where the maximum speed is equal to 500 rpm, and the machine HP is equal to 25.

The exit age distribution, $E(t)$, the cumulative RTD, $F(t)$, the mean resident time, (t) and the dimensionless time (θ) were computed according to eqns (40-42) and (34), respectively. To normalize the RTD, the amount of tracer left in the extruder after the sampling period has to be determined. A plot of tracer concentration as a function of time (Figure 36) shows an exponential decay at the tail portion. This portion tends to tail off as a straight line on a semi-logarithmic plot. The slope of each line was determined for each experiment and the truncation error (area under the tail after sampling period) calculated using eqn (39). The variance of C-distribution was calculated based on equation (33) which can be approximated as:

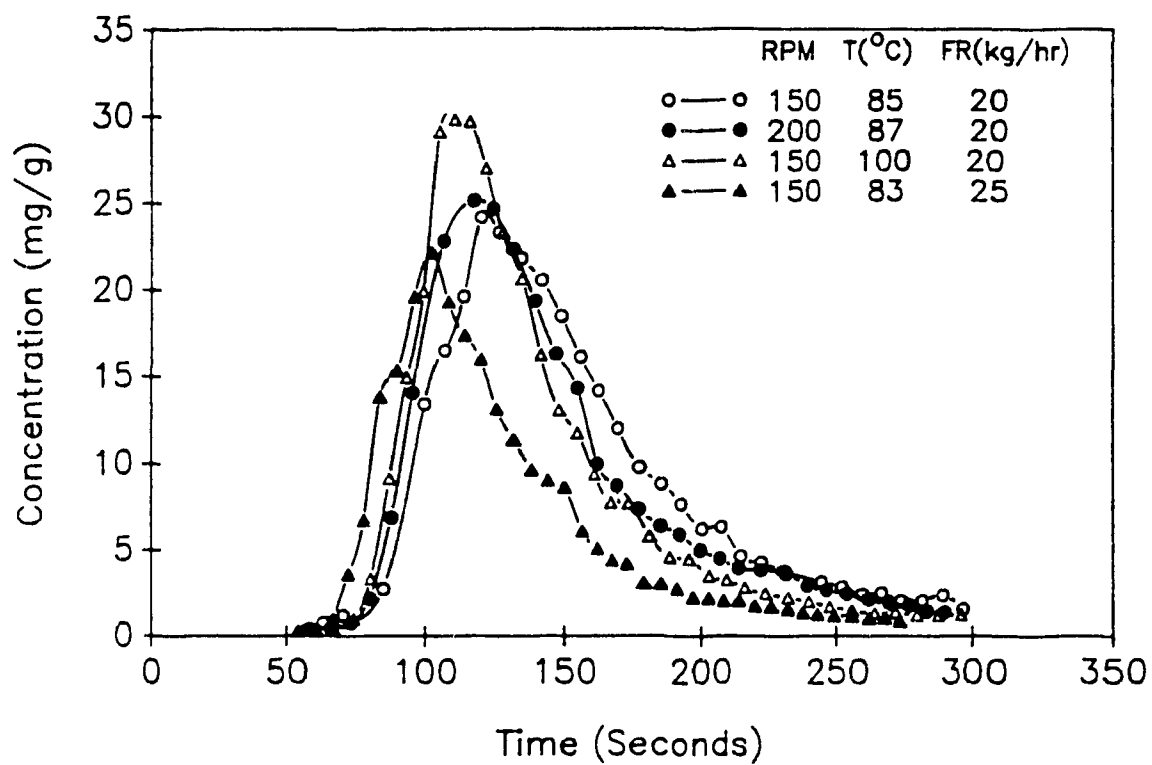


Figure 36. Residence time distribution of caseinate under various conditions.

$$\sigma^2 = (\Sigma t^2 C / \Sigma C) - (\Sigma t C / \Sigma C)^2 \quad (74)$$

and Peclet number (Pe) determined by solving numerically eqn (49) using the MathCAD computing package (MathSoft, Inc. Cambridge, Massachusetts).

A nonlinear regression procedure was used to fit the experimental $F(\theta)$ distributions to an appropriate model. The parameters of the model were estimated by the modified Gauss-Newton method (Hartley, 1961) using SAS (SAS Institute, Inc. Cary, North Carolina).

3.7.3 Results and Discussion

Effect on extruder dependent variables

The standard extrusion conditions used were: 150 rpm screw speed, 30% moisture, 20 kg/hr feed rate and a temperature profile from the feed zone to the die of: 40, 50, 55, 60, 70, 80, and 80 (°C). For this experiment the cooling system of the extruder was not used so that the heat generated by the dissipation of mechanical energy could be investigated. The effect of the barrel temperature setting profile on product temperature profile is given in Figure 37 and shows that the product temperature is higher than the barrel set temperature except in the feed zone. This difference is due to the input mechanical energy by viscous dissipation and a greater difference is obtained when a lower temperature setting is used because of reduced viscosity and a concomitant increase in break down force. This is elucidated by an increase in SEC and pressure when the setting temperature is reduced (Figure 38) due to an increase in viscosity. It should be noted that the x-axis of Figure 38 only represents the temperature in the last two zones of the barrel. The complete temperature profile is given in Figure 37.

Viscosity at the die (μ_d) is related to the pressure drop (ΔP) at the die and to flow rate (Q) by the following equation (Harper, 1981):

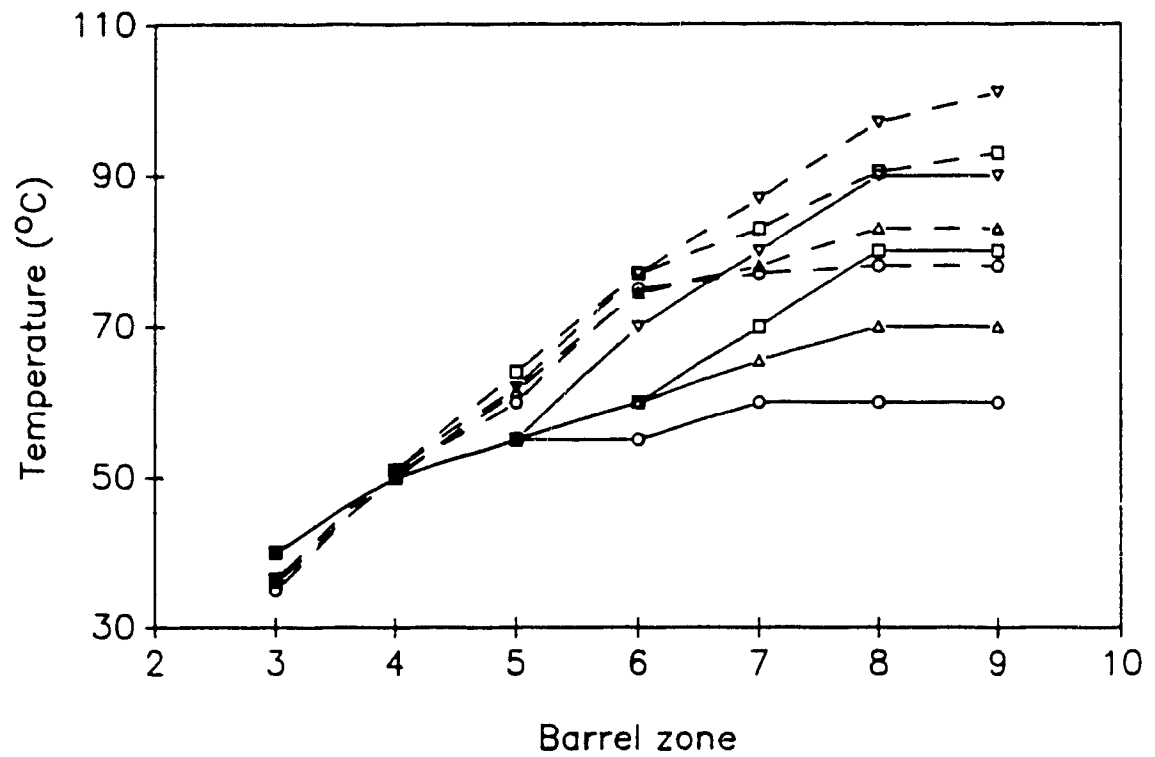


Figure 37. Effect of barrel setting temperature profile (continuous lines) on product temperature profile (dashed lines). (o)=experiment 1, (Δ)=experiment 2, (□)=experiment 3, (∇)=experiment 4. Screw speed, moisture and feed rate were fixed to 150, 30% and 20 Kg/hr, respectively.

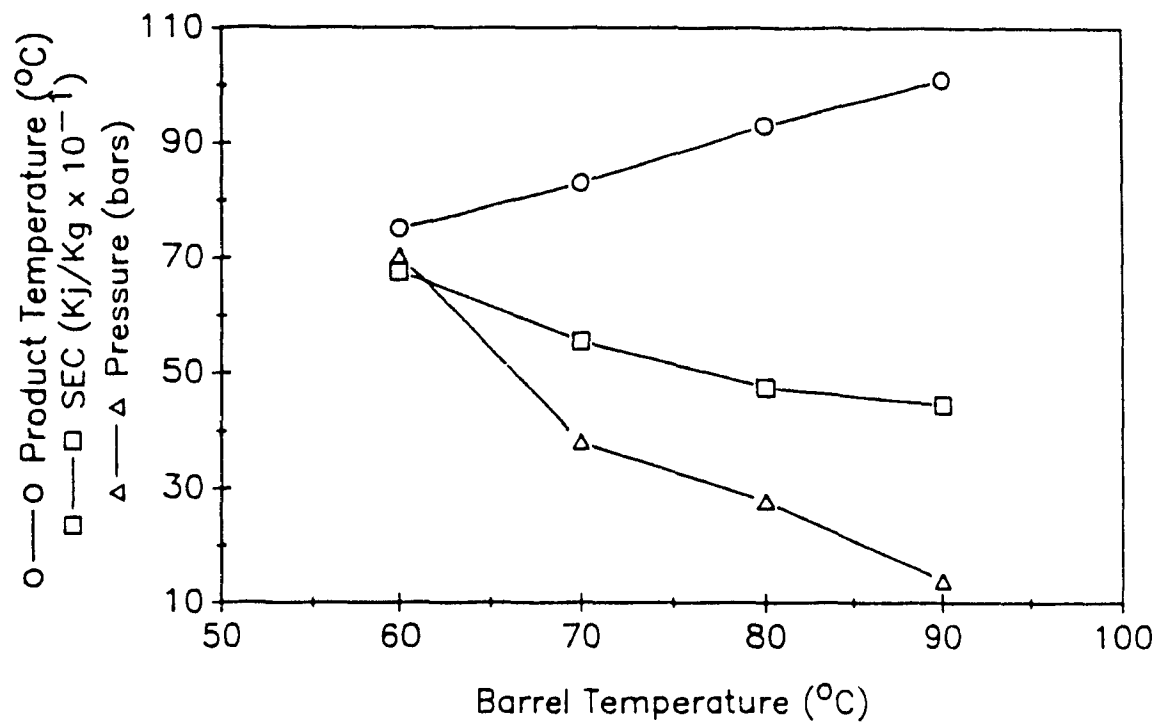


Figure 38. Effect of last zones barrel temperature setting on product temperature at the exit, SEC, and pressure at the die.

$$\mu_d = K(\Delta P/Q) \quad (75)$$

where K is the die geometric constant. Thus, an increase in viscosity (i.e., decreasing temperature and/or moisture) at constant screw speed, will increase the pressure at the die. This will also lead to an increase in SEC as the percent torque is proportional to the viscosity.

Increasing screw speed from 100 to 250 rpm (Figure 39) leads to an increase in product temperature which will reduce the viscosity, and as a consequence the pressure generated at the die dropped when the screw speed was increased. Although the viscosity decreases when increasing the screw speed, resulting in less percent torque, the SEC increases significantly. With increasing feed rate (Figure 40) an inverse effect of what was observed for screw speed is obtained for pressure and SEC, while the product temperature at the exit remained constant. The increase of temperature with screw speed indicates that the heat energy supplied by friction is greater than the heat lost by convection from the barrel wall due to a decrease in residence time of the product in the barrel. The degree of fill and flow rate (Q) increase when increasing feed rate. This in turn, according to eqn (75), will lead to a decrease in pressure as the viscosity remains constant.

The SEC is an important extrusion parameter in that it can be viewed as a measure of the energy required to deform the material in the extruder screw channels, e.g., the total deformation times the average shear stress (Agur, 1986):

$$\text{SEC} \sim \tau_{av} \times \gamma_{av} \quad (76)$$

$$\text{SEC} \sim \tau_{av} \times \dot{\gamma}_{av} \times \bar{t}$$

where τ_{av} is the average shear stress, γ_{av} is the average shear strain, and $\dot{\gamma}_{av}$ is the average shear rate. Shear stress and shear rate increases with screw speed and are practically

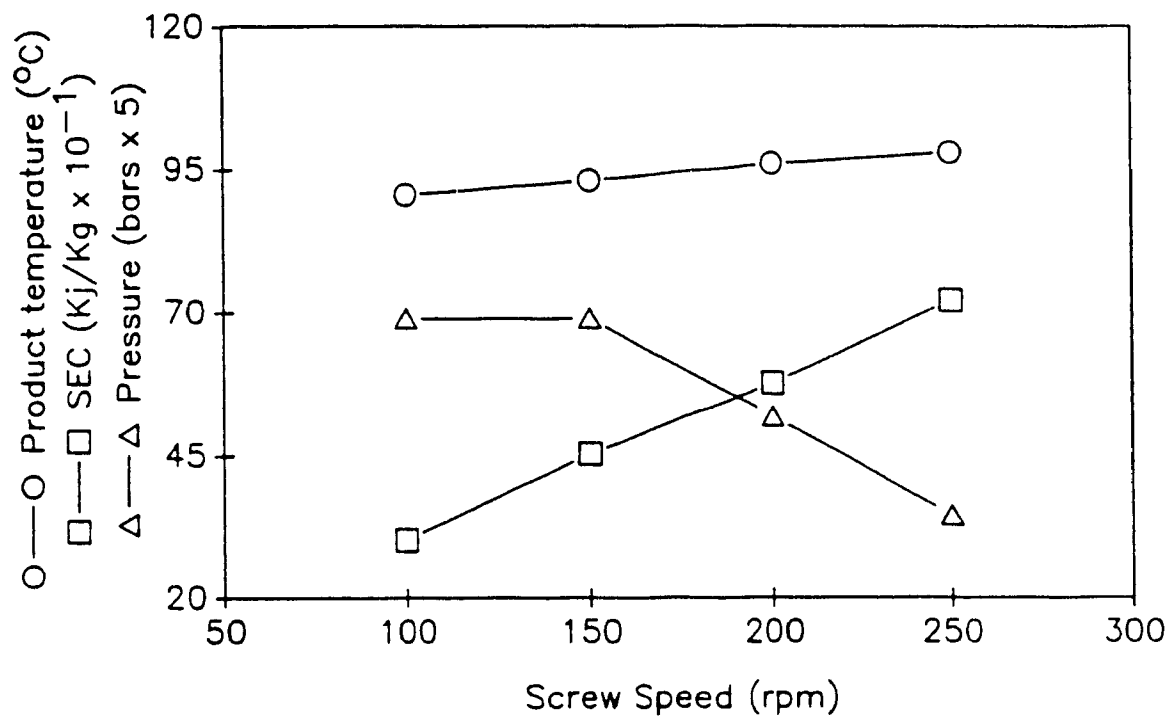


Figure 39. Effect of screw speed on product temperature at the exit, SEC, and pressure at the die.

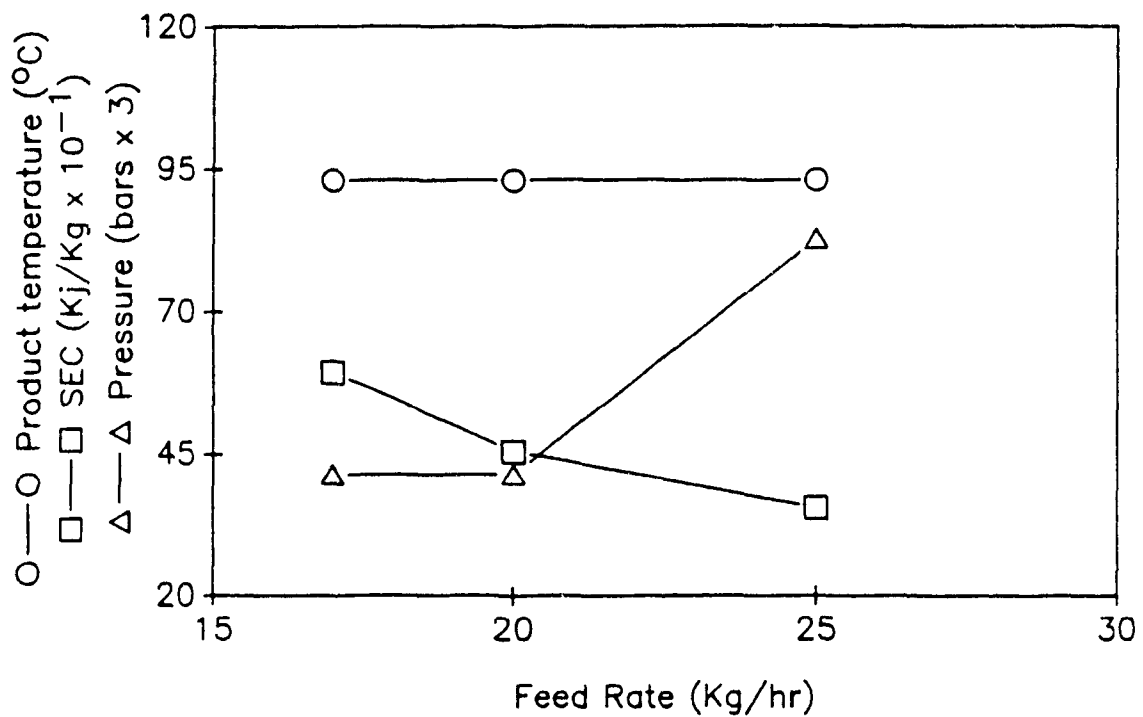


Figure 40. Effect of feed rate on product temperature at the exit, SEC, and pressure at the die.

independent of feed rate, while the mean residence time (\bar{t}) decreases with screw speed and feed rate. Thus, one would expect that SEC should increase with an increase in screw speed, but drop with an increase in throughput rate, which is reflected in our results (Figures 39 and 40).

Similar trends have generally been observed in other studies dealing with extrusion of food materials from plant origin (Bhattacharya & Hanna, 1987; Della Valle et al., 1987; Fletcher et al., 1985), although, no increase in SEC was observed by Bhattacharya & Hanna (1987) when increasing screw speed. This difference may be due to the fact that the material used was strongly pseudoplastic and a significant reduction in viscosity may occur when increasing shear rate (i.e. screw speed). Thus, the increase in screw speed may be balanced by a decrease in percent torque in eqn (71), and as a consequence, SEC may not change appreciably. Sodium caseinate was shown to behave as a Newtonian fluid with yield stress up to a concentration of 16% total solids (Chapter 3.6). If one can assume this flow behaviour does not change drastically at higher solids concentration, then the shear rate will have only a small effect on the viscosity and the SEC would increase with screw speed.

Effect on RTD

The C-distributions are plotted in Figure 36 and Table 13 gives the computed data for each experiment. The mean residence time decreases with increasing screw speed, temperature, or feed rate. Feed rate and temperature also affect the shape of the distribution as indicated by the variance, while the effect of screw speed is negligible. Increasing feed rate or temperature will likely narrow the RTD. Similar observations have been obtained for feed rate and screw speed (Biral, 1979; Mosso et al., 1982; Altomare & Ghossi, 1986; Kao & Allison, 1984), while the effect of temperature may be due to changes in viscosity, which will likely affect the velocity profile and mixing patterns in the extruder.

Table 13. Operating conditions and computed data for mean residence time (\bar{t}), variance, Pe, truncation error (R'), and percent tracer left in the extruder after the sampling period (ΔMnO_2). The moisture content was kept constant at 29%.

Experiment	RPM	T(°C)	FeR(kg/hr)	\bar{t} (s)	σ^2 (s ²)	Pe	R'	ΔMnO_2 (%)
1	150	85	20	153	2053	21.9	115.3	5.2
2	200	87	20	148	2102	19.8	93.5	4.5
3	150	100	20	135	1640	21.1	108.5	5.2
4	150	83	25	128	1775	17.4	62.2	4.2

No major differences were obtained for Pe values in terms of an axial mixing analysis. Pe is an indication of the extent of axial mixing with little axial mixing being obtained when $Pe > 25$ and excessive axial mixing being obtained when $Pe \sim 2.5$ (Todd & Irving, 1969). Axial mixing is more affected by screw configuration than by operating conditions (Todd, 1975) and the average Pe obtained (~ 20) could be considered as a characteristic of the screw configuration used. This value indicates that no excessive axial mixing has been resulted using the screw configuration given in Figure 35, producing good product homogeneity. The slight decrease of Pe number when increasing the feed rate may be due to an increase in the degree of fill of the barrel (Todd & Irving, 1969).

Table 13 also gives the values of truncation error estimates (R') which were used to normalize the RTD's, and the percent tracer left in the extruder after sampling period. Less tracer is left in the extruder when increasing screw speed or the feed rate. To assess the effect of operating conditions on the tail portion (Janssen et al., 1979), the internal age distribution given by eqn (35), was plotted against the dimensionless time in Figure 41. For clarity, only tail portions were plotted for experiments 2-4 (Table 13) as no major difference was observed in the remaining part of the distribution. It can be seen, from

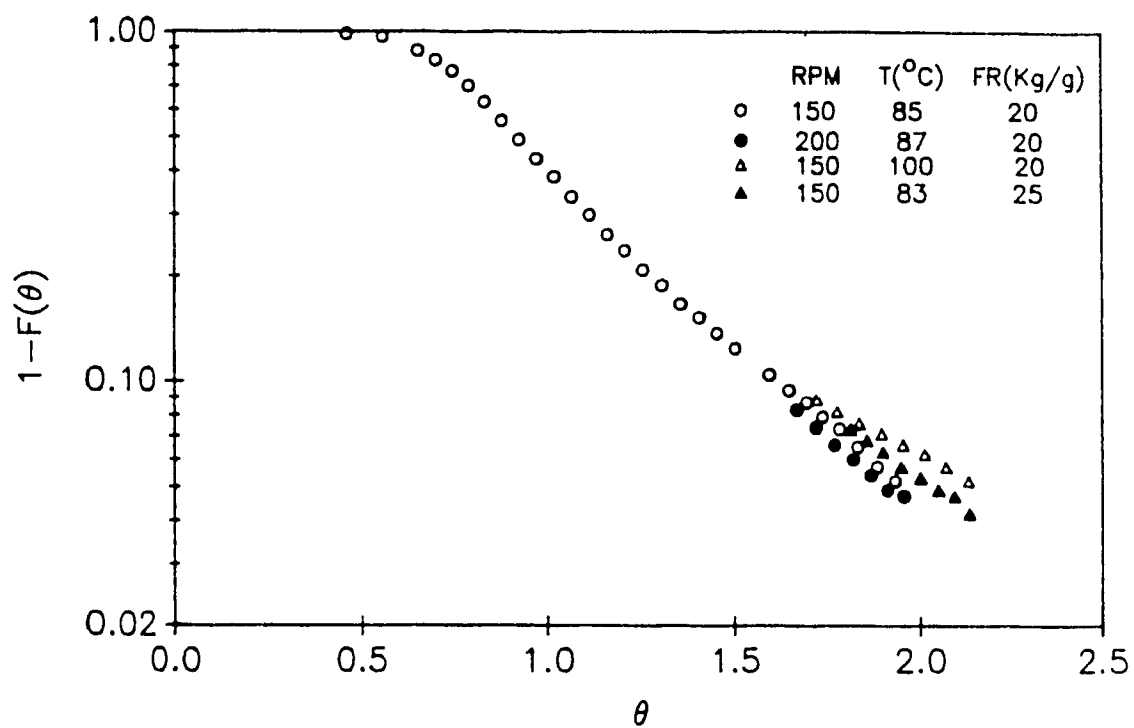


Figure 41. Integral age distribution of caseinate under various conditions

Figure 41, that there is a tendency of the tail to become longer at high temperature (100°C), while the effect of screw speed and feed rate is negligible. This is in accordance with the results obtained by Janssen et al., (1979) which indicate that increasing die pressure will shorten the tail of the RTD in a counter-rotating TSE. Die pressures can be increased by reducing temperature as shown in Figure 38. One has to keep in mind that 4 to 5% of the tracer is still in the extruder after sampling period which may exit under different regimens and it is precisely this tail which may be the factor which eventually limits the performance characteristics of the extruder. Protracted residence time may lead to product degradation and non homogeneity and this is why any analysis of RTD should consider the tail portion. The deviation of Figure 41 from straight vertical line indicates deviation from positive displacement behaviour, as a truly positive displacement device has an internal age distribution of straight vertical line through $\theta = 1$ (Rauwendaal, 1981).

Comparison with theoretical models

It is useful to compare the data obtained with theoretical models to assess the behaviour and the performance of the extruder as a chemical reactor. Two interesting models have been presented by Levenspiel (1972) which are the dispersion model and the tanks in series model given by eqns (46) and (47), respectively. An attempt to fit both models to the experimental points by theoretical curve matching is presented in Figure 42 for the dispersion model, and in Figure 43 for the tanks in series model. No satisfactory fit was obtained and as a consequence the flow behaviour in the extruder cannot be described considering a simple diffusion law (dispersion model) or n perfectly mixed tanks in series. These models are actually adequate when the flow in the extruder does not deviate too much from plug flow behaviour, a condition which counter-rotating extruders approach more closely than the co-rotating ones.

The velocity profile in a twin screw extruder having the screw configuration given in Figure 35 is very complex. Mixed models which consider different sections in the extruder having different flow regimens could be more realistic in describing RTD. A simple model could be derived by considering the flow in the extruder as a combination

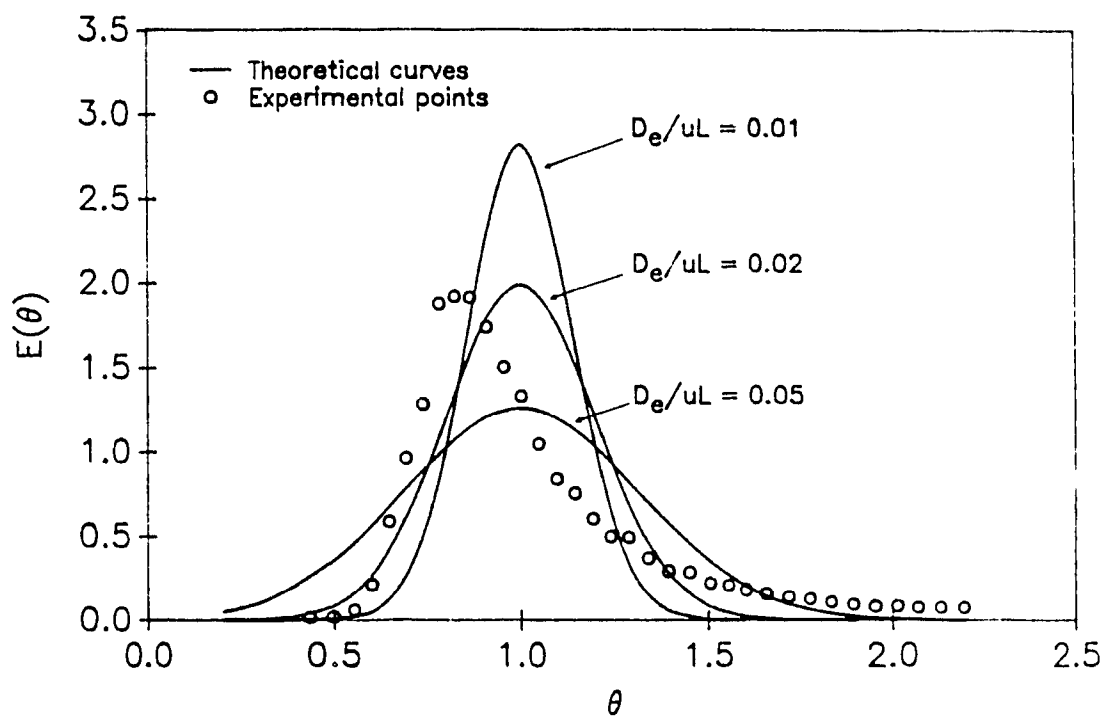


Figure 42. Typical experimental $E(\theta)$ distribution function for casein neutralization process compared to the dispersion model.

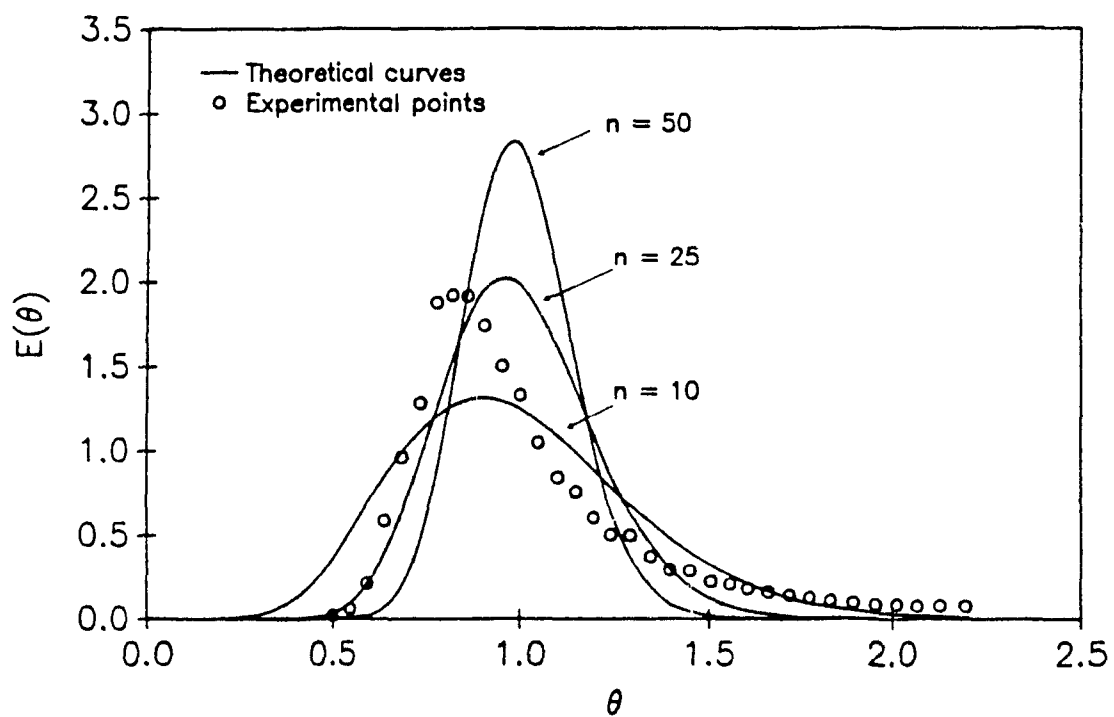


Figure 43. Typical experimental $E(\theta)$ distribution function for casein neutralization process compared to the tanks in series model.

of plug flow and perfect mixing, which was given by eqn (53). This model has been shown to be adequate in describing the RTD in a TSE (Altomare & Ghossl, 1986; Balke, 1985; Agur, 1986) and Figure 44 shows that a good fit is obtained specifically at P value (fraction of plug flow) equal to 0.6. The P value can be considered as a measure of the conveying performance, while the 1-P value can be considered as a measure of the mixing performance of the extruder. This is equivalent to saying that ~60% of the mass moves under a plug flow regimen and ~40% of the mass moves under a perfect mixing regimen.

The deviation of the data from theoretical curves using the plug flow/perfect mixing model (Figure 44) indicates that other phenomena such as, recirculation and dead space may be present in the extruder. To assess the presence of such phenomena, a more powerful model, the multistage Wolf and Resnick (1963) model, was considered, described by eqn (54). This equation was solved using nonlinear regression analysis and the parameters of the model are given in Table 14 along with asymptotic standard errors and 95% interval confidence limits. The parameter n is the number of stages in series, and b can be considered to be a measure of the efficiency of mixing, being equal to unity for perfect mixing and tending to infinity for plug flow. The deviation of the b parameter from unity indicates that perfect mixing is not obtained in the entire extruder due to the presence of plug flow and/or dead space. The parameter ϵ is a measure of the phase shift in the system, and the fact that $\epsilon/t > 0$ indicates that the system response lags behind that expected for perfect mixing due to plug flow and/or a lag in response caused by any delay in the system that would affect its measured response characteristics.

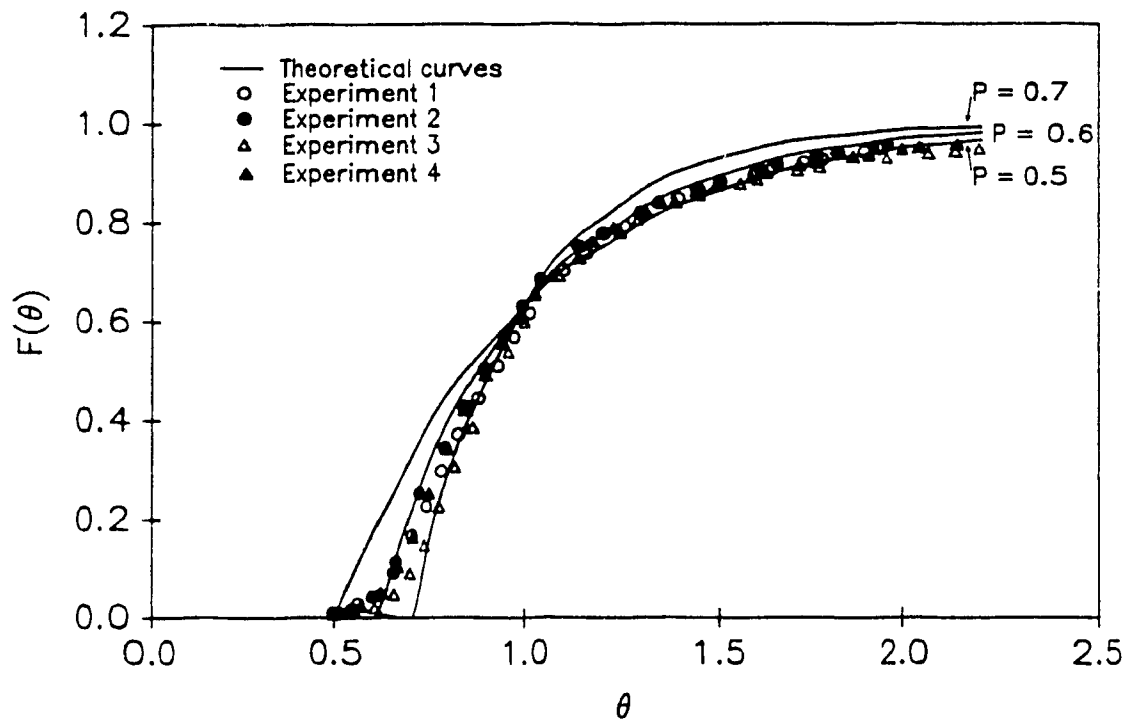


Figure 44 Experimental $F(\theta)$ distribution functions for the casein neutralization process compared to the Wolf and Resnick model.

Table 14. Wolf and Resnick model parameters estimates to fit the RTD data. Conditions of experiments 1-4 are given in Table 13

Experiment	n	b	ϵ/t	Standard Error		95% confidence	
				b	ϵ/t	b	ϵ/t
1	3	4.20	0.161	0.09	0.004	4.02-4.38	0.153-0.168
2	3	4.34	0.158	0.11	0.004	4.12-4.56	0.150-0.166
3	3	4.41	0.177	0.15	0.005	4.11-4.71	0.167-0.189
4	3	4.27	0.161	0.11	0.004	4.05-4.50	0.152-0.170

Screw speed and feed rate seem to have negligible effect on the model parameters, while only a minor effect is observed with the temperature (Table 14). The calculated $F(\theta)$ is plotted in Figure 45 along with experimental data for experiment 1. The agreement is evident with similar fitting quality being obtained with the other operating conditions.

Effect on product characteristics

The physico-chemical analysis of sodium caseinate produced under different operating conditions, are given in Table 15, including moisture content and pH for each sample. The pH was found to increase linearly with the amount of NaOH added to the casein. For pH 6.25-7.40, the regression equation was: $\text{pH} = 2.157 \times C + 3.512$ ($R = 0.999$), where C is the NaOH concentration (g/l). It was difficult to keep the pH exactly at the same value while changing operating conditions and the results are based on using different NaOH concentrations in an attempt to balance the effect of feed rate on pH. The temperatures reported in Table 15 are the product temperature at the die exit.

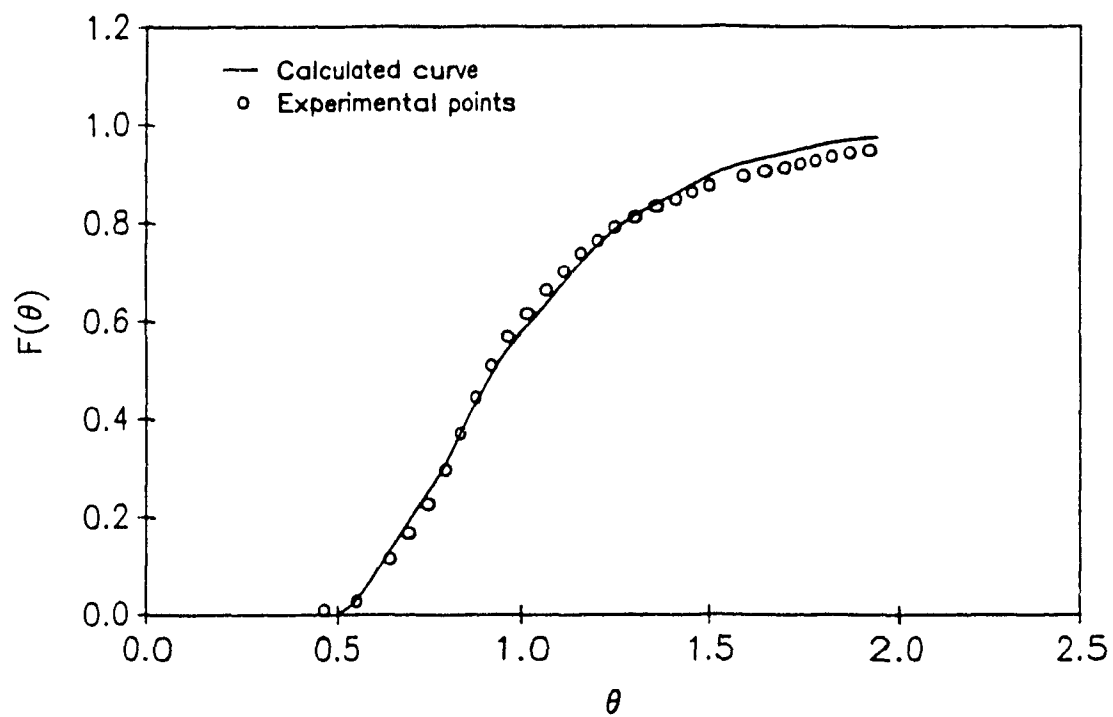


Figure 45. Typical fit of experimental $F(\theta)$ distribution function to the multistage Wolf and Resnick model.

Table 15. Properties of sodium caseinate obtained by neutralization of acid casein under various extrusion conditions. FeR = Feed Rate (kg/hr), M = Moisture (%), ER = Expansion Ratio, BD = Bulk Density (g/cm^3), N = protein nitrogen (% dry basis), L and b are the colour parameters which stand for lightness and yellowness, respectively.

Sample	rpm	T(°C)	FeR	M	pH	ER	BD	N	L	b
1	100	91	20	2.9	7.5	2.0	0.61	91.1	85.3	15.6
2	150	93	20	3.6	7.3	2.0	0.59	92.4	85.5	15.0
3	200	96	20	2.3	7.4	2.0	0.67	92.1	87.0	14.0
4	250	96	20	3.2	7.3	1.9	0.63	92.2	86.7	14.3
5	150	83	20	3.0	7.3	2.0	0.67	93.8	85.6	15.7
6	150	101	20	3.6	7.3	2.0	0.69	94.5	86.0	15.8
7	150	93	17	3.0	6.8	1.9	0.69	94.6	85.4	15.8
8	150	93	25	3.0	7.1	2.1	0.65	93.7	84.8	16.7
AC*				2.5	-	-	0.69	93.0	87.5	13.1

* Acid casein used for neutralization which was dried to 2.5% moisture content

Table 15 shows that no major changes are affected on product properties when varying the extruder operating conditions, with the exception of a small difference in whiteness. Average values of 2, $0.65 \text{ g}/\text{cm}^3$, and 93% were obtained for expansion ratio, density, and protein nitrogen, respectively, for all the conditions. Tossavainen et al. (1986) however, indicated that the expansion ratio decreases with increasing temperature (65 to 112°C) which may be due to their use of sodium bicarbonate as a neutralizing agent, as opposed to the sodium hydroxide used in our experiments. The slight decrease in whiteness and increase in yellowness is insignificant which indicates that no Maillard browning has occurred. A sharp yellowness can result from poor mixing due to localized regions of high pH and one can conclude from our results that good mixing has been obtained in the extruder as also elucidated from the RTD analysis.

3.7.4 General Discussion and Conclusion

The basic mechanism of mixing is the induction of physical motion of mass particles. The types of motion that can occur are molecular diffusion, turbulent motion, and convective motion (Rauwendaal, 1986), the latter being the predominant motion in high viscosity liquids. Mixing in our case could be considered as convective which is generally the type of mixing occurring in polymer melt extrusion. The sodium caseinate exhibits a yield stress and thus screw configuration and barrel temperature profile should be designed to allow effective dispersive mixing before distributive mixing becomes dominant. Thus, the temperature should be much lower in the early zones to increase the viscosity and then the break down force, with some mixing elements incorporated in the low temperature zone to aid in dispersive mixing. The mixing zones substantially increase the interfacial area generation which randomises the minor components.

Laminar mixing action can only be analyzed if the exact flow patterns are known. This can be done reasonably well for simple rectangular flow channels in a single screw extruder (Chapter 2.3). However, in TSE's with mixing sections incorporated, flow patterns become very complex. In one respect, this is desirable because complex velocity profiles tend to improve the mixing effectiveness. On the other hand, the mathematical description of the velocity profiles becomes very involved. Even so, the study of RTD's provided a useful mean for evaluating mixing and conveying for acid casein neutralization. The flow in the barrel can be considered as a combination of plug flow and perfect mixing according to Figure 44, resulting in good mixing and conveying performance. Other phenomena such as recirculation and dead space could be considered as minor, however, their inclusion in any RTD model will improve the fit as shown in Figure 45. In addition, no excessive axial mixing was obtained as indicated by the Peclet number, which contributes to good product homogeneity. The increase in product yellowness was negligible compared to the original feed material, which is also reinforces the conclusion that good mixing behaviour is obtained in the extruder. No major

fluctuations in pressure or torque were observed during the process after the steady state operation was attained. No surging or plugging occurred under the operating conditions used, however, decreasing the temperature below 60°C would drastically increase the viscosity and a shut down or seizing of the extruder may occur.

Operating conditions have an effect on SEC, pressure, product temperature and RTD's. The mechanical energy is transformed in the extruder into heat by friction and viscous heat generation. Thus, the higher the SEC the high will be the temperature rise of the material. The increase in SEC at low throughput is primarily caused by the sharp increase in residence time at low feed rates. Minimization of SEC could be achieved through the use of a lower screw speed and/or higher feed rate, or by reducing the viscosity of the mass by increasing temperature and/or moisture. However, increasing temperature seems to increase the tail portion of the RTD (Figure 41) and might lead to Maillard browning for the proportion of the mass which spends a longer time in the barrel. Thus, it might be preferable to decrease viscosity through increasing moisture rather than increasing temperature, which might also lead to an improvement in product solubility (Tossavainen, 1986). This is practical for neutralization of freshly prepared casein which contains (~50%) moisture.

This study demonstrates the effects of processing parameters of a Baker Perkins TSE for acid casein neutralization to produce sodium caseinate. It is clear that there are defined relationships between the operating conditions (barrel temperature setting, screw speed, feed rate); dependent extruder variables (SEC, pressure, product temperature), and RTD's. However, in this process, no major effect was observed on the product properties within the range of operating conditions studied. In one respect, this is desirable because no rigorous control in operating conditions will be required and the optimization may be concentrated on economics rather than product quality. On the other hand it will be more difficult to produce a product with specific characteristics as usually done in extrusion of proteins from plant origin.

It is clear that RTD analysis of an extruder can yield very interesting information about its conveying and mixing behaviour, that would be very difficult to obtain by any other method. In conclusion, the twin screw extruder, with judicious choice of screw configuration and operating conditions can produce a high quality sodium caseinate, mainly due to its good mixing and conveying characteristics and control over the process parameters.

3.8 PILOT PLANT PRODUCTION OF CASEINS USING EXTRUSION PROCESSING. I. ACID CASEIN PRODUCTION

ABSTRACT

Coagulation of skim milk powder was carried out in a twin screw extruder and a four stage washing process, previously optimized on a laboratory scale, was carried out. Various batches were produced to investigate the effect of coagulation pH and SMP concentration, and the dewatering system on washing efficiency. Lactose, ash, fines and the water holding capacity of the curd were compared to predictions from response surface models determined from previous studies on model systems. Two methods of dewatering were investigated, screening and centrifugation, the latter producing lower residual lactose and ash, but a greater loss of fines. The resulting washed curd was used as a feed for the conversion of acid casein to sodium caseinate by extrusion, discussed in the succeeding chapter.

3.8.1 Introduction

Preliminary research indicated that an acid co-precipitate could be produced from SMP by extrusion (Chapter 3.1). The resulting product was difficult to wash in order to reduce the residual lactose and ash to an acceptable level (i.e., 0.1% lactose and 2% ash). As a consequence, studies were implemented to determine appropriate coagulation and washing conditions to be applied to an extruded product. Experiments were designed to model and optimize the coagulation/washing process to remove lactose and ash, and minimize fines (Chapters 3.2 & 3.3) using Response Surface Methodology (RSM). The models obtained using RSM allowed multiresponse optimization of acid casein production using optimization techniques (Chapter 3.4). The study of microstructure and water

holding capacity provided additional guidance as to which physico-chemical mechanisms may affect the system (Chapter 3.3). These studies are already published or in press (Barraquio et al., 1988; Fichtali et al., 1990a,b,c). A special die was designed and tested for dewheying process using a twin screw extruder, however, a complete re-design of the barrel and screws is required to render it practical. This study showed that efficient coagulation occurs in the extruder and that a coagulum with a moisture of up to 80% may be obtained.

The objective of this study is to integrate the knowledge and experience gained from the previous work and apply it to production of acid casein on a pilot plant scale using extrusion technology and assess the end product.

3.8.2 Material and methods

Commercial low heat SMP (see section 3.2.2) was used for this experiment.

Coagulation of SMP

A Baker Perkins MPF-50D co-rotating intermeshing twin screw extruder (see Appendix 4) was used to carry out the extrusion process. No restrictive die insert was used and the barrel was configured in a 15:1 L/D ratio. The screw profile was designed to have a good balance of conveying and mixing action and is shown in Figure 46 along with the barrel temperature profile. The temperature setting was lower in the first zones to allow some mixing of the powder with acid solution before coagulation occurs in the subsequent higher temperature zones, which otherwise might result in reduced fines (Muller, 1971). Reagent grade HCl was used as the acidulant with the pH of the coagulum measured every 3-4 minutes using a Corning Model 140 digital pH meter and the pH maintained within ± 0.02 during the process. The product temperature at the exit was monitored using a digital thermocouple, screw speed was 100 rpm and the other extrusion conditions used are tabulated in Table 16 for each batch produced, along with coagulation pH and concentration. Batches 1 and 2 differ only in the separation technique

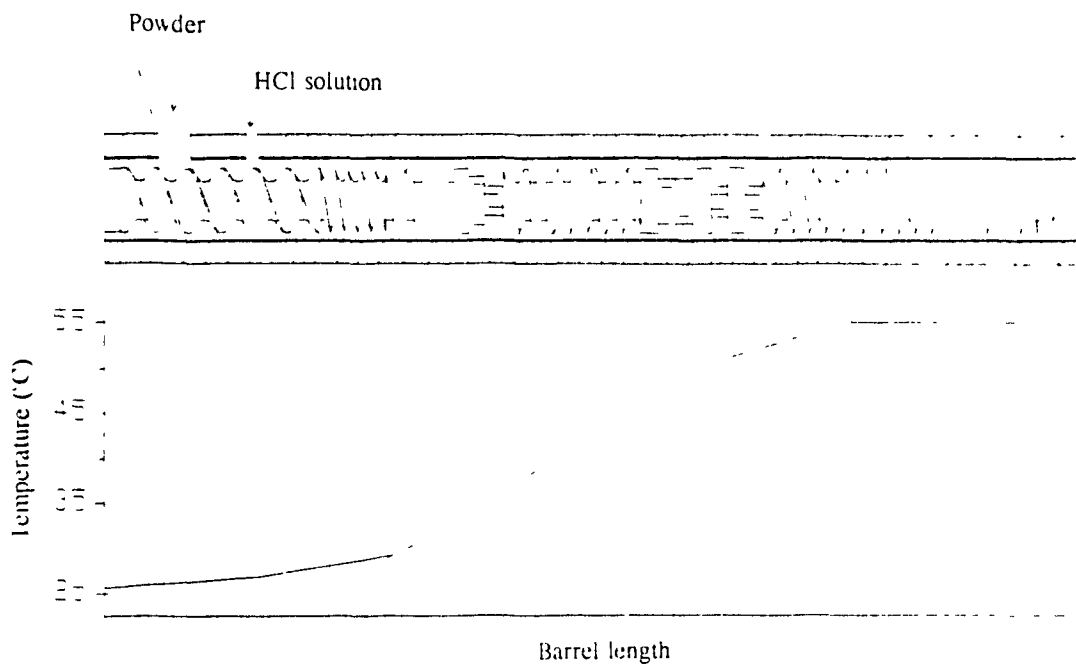


Figure 46. Screw configuration and barrel temperature profile used for SMP coagulation. The screw configuration comprises (from right to left): 225 mm, feed screw; 50 mm, short pitch screw; 50 mm, single lead screw; 37.5 mm, 45° forwarding paddles; 100 mm, single lead screws; 50 mm, 60° forwarding paddles, 37.5 mm, 90° paddles and 200 mm, single lead screws.

used for dewatering the curd and will be compared, while batches 2, 4, and 5 differ in the coagulation conditions (pH and concentration) and will be the subject of another comparison. Batch 3 was obtained by centrifugation of batch 1 after the last wash. The coagulation pH of batches 1-3 was very close to the optimal predicted coagulation pH (4.28) at 25% concentration required to obtain reduced lactose, ash and fines (see run #6 in Table 8, Chapter 3.4).

Table 16. Coagulation conditions of SMP and separation technique used for each batch. FdR=Feed Rate (kg/hr), FwR=Flow Rate (l/hr), C=Concentration, the screw speed was fixed at 100 rpm and the barrel temperature profile is presented in Figure 46.

Batch #	FdR	FwR	pH	C(%)	Separation technique
B1	15	45	4.31	25	Screen
B2	15	45	4.31	25	Centrifuge
B3	15	45	4.31	25	Screen/Centrifuge*
B4	15	45	4.56	25	Centrifuge
B5	20	30	4.35	40	Centrifuge

*Centrifuge was used only after the last wash

Washing and Dewatering

Washing of the coagulum was carried out in a 100l temperature controlled tank fitted with a variable speed propeller calibrated using a tachometer. Four washing stages were used, the water adjusted to the same pH used for coagulation with a wash water ratio of 4:1, an agitation speed of 200 rpm and an average residence time of 20 min. To disperse the coagulum after each dewatering, the agitation speed was higher for the first min (~400 rpm). The wash water temperature was 45°C for the first and last wash and 60°C for the second and the third wash. The washing conditions were determined from previous washing optimization studies (Chapter 3.4), except for batch 4 for which the optimized washing temperature for the second and the third wash is normally lower than

60°C. A basket centrifuge (Model STM-1000, Western States Machine Company, Ohio) was used for the dewheying and dewatering steps and was connected to the washing tank through a positive variable speed pump (ALBIN, model 107SLP). The centrifuge was operated at 911 x g for the 3 first washing stages and 1615 x g for the last washing stage. Conventional screening (100 mesh) was also used for dewatering (batch 1) and its efficiency compared to centrifugation. A flow diagram of the whole process, up to caseinate production, is given in the next chapter (Figure 53).

Analysis

Samples of dewatered curd were taken after the whey off stage and after each washing stage, freeze dried and analyzed for lactose, ash, moisture (Fichtali et al., 1990a,b) and total protein nitrogen (see section 3.7.2). Representative samples from the wash water were used for fines analysis and water holding capacity of the curd determined before the last centrifugation (Fichtali et al., 1990b). Lactose in the wash water was analyzed by HPLC according to a method recommended by LKB Biochrom where the 5-sulphosalicylic acid was used (50mg/ml sample) to precipitate the proteins and the samples were mixed and kept at 4°C for one hour in a pyrex tube, centrifuged for 15 min at 5000 rpm and filtered through Nalgen 4-mm syringe filters. The samples were then injected into the HPLC (Waters, WISP model 710B) equipped with a Mandel Scientific column (model 10N-300). The lactose in the wash water was also analyzed by the standard phenol-sulphuric method (International Standard, 1980). HPLC analysis resulted in more reproducible results when the lactose concentration was higher or equal to 0.1%, while the phenol sulphuric method was more accurate at lower concentrations.

3.8.3 Results and Discussion

Production of Acid Casein

The conversion of SMP to an insoluble coagulum in the presence of HCl is a straight forward process as the extruder is operated at low temperatures (55°C) and no pressure gradient was developed due to the high moisture conditions and large die orifice

used. Under these conditions mixing is mainly due to molecular diffusion and the turbulence induced by the paddles and screws rather to convective motion as is generally the case in extrusion. Preliminary experiments showed that a good mixing was achieved at both concentrations studied (25 and 40%), using the screw configuration given in Figure 46 and a barrel L/D ratio of 15:1. Only 3% net torque was registered leading to very low specific energy consumption of 27 kJ/kg determined from eqns (71-73). The product temperature at the die exit was $46.5 \pm 1^\circ\text{C}$ and the minimum residence time was ~ 40 seconds as measured by dye injection. All extruded products were white, although texturally each set of conditions produced products which differed in their overall characteristics. A fine, friable coagulum was obtained by precipitating at a low pH (batches 1, 2, and 5 in Table 16), while a firm product with larger particle size was produced at the higher pH (batch 4).

Washing and Dewatering

Because the coagulum contains substantial amounts of lactose, ash and whey protein, the curd needs to be washed to bring the product to within international standards. A number of washing steps are required to remove the whey components and the conditions selected had been predetermined based on earlier optimization studies of model systems (Fichtali et al., 1990c). Batch 4 (Table 16) presented the most problems during the washing as the curd firms and shrinks, specifically after the high temperature washes (second and third wash) and the cake has to be broken up before the next washing stage, otherwise washing efficiency will be reduced. After each washing step, the product has to be dewatered, which can be carried out by screening or centrifugation. Dewatering by centrifugation was shown to be more efficient than conventional screen separation. The moisture content of the final curd from batch 1 (screen) was 75.7% while it was 52.6% for batch 2 (centrifuge), however, with concomitant increased loss of fines ($\sim 5x$ higher). Centrifugation was also substantially more effective in terms of lactose removal (Figure 47), however, the difference in terms of ash was not very significant (Figure 48). To elucidate the effect of coagulation pH and concentration on curd characteristics, batches 2, 4, and 5 (Table 16) were compared. Batch 2 gave the lowest lactose and ash contents

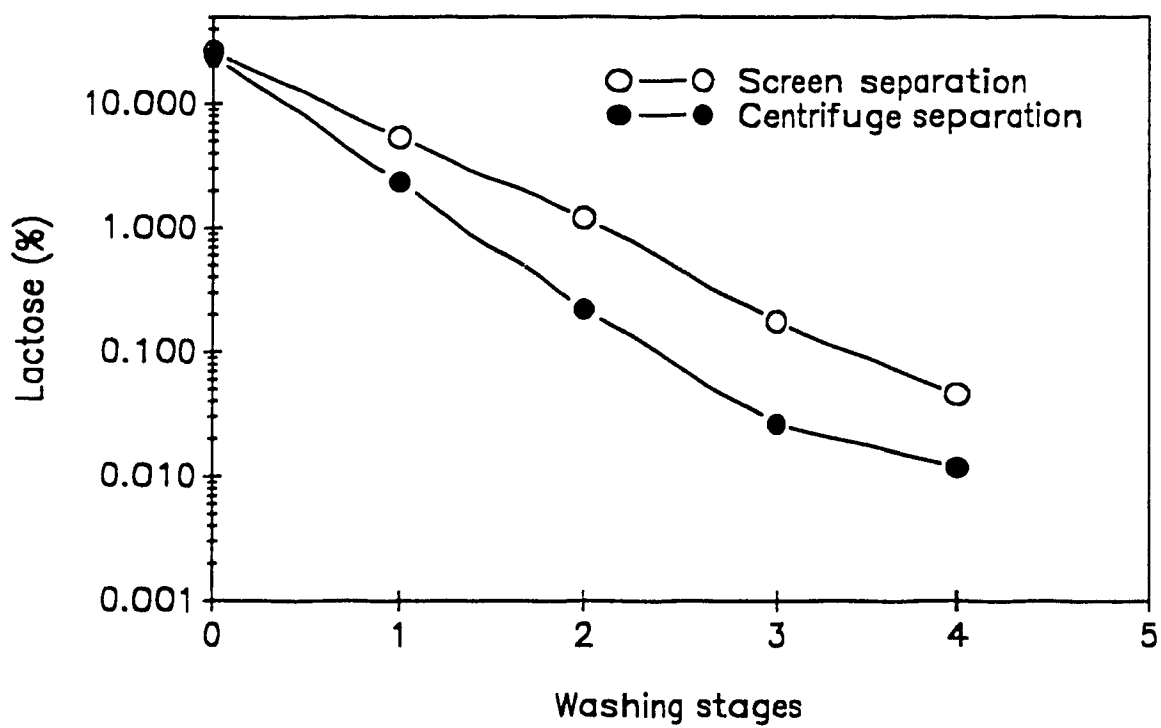


Figure 47. Effect of separation technique on lactose removal for the whey off stage and each washing stage.

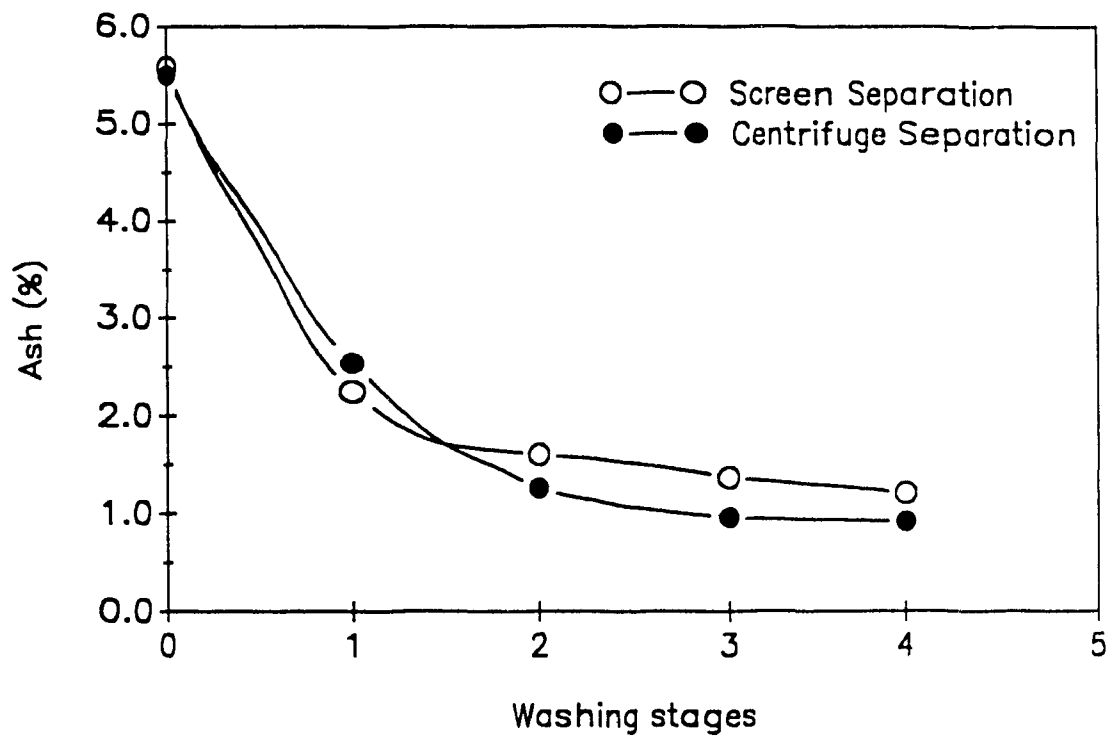


Figure 48. Effect of separation technique on ash removal for the whey off stage and each washing stage.

of the three batches, however, only lactose could be considered to be significantly different (Figures 49 and 50). This result concurs with our previous laboratory scale work (Chapter 3.2), where the effect of pH and concentration on whey components removal was elucidated.

Values of lactose, ash, fines and water holding capacity for each batch were compared to the values predicted from the response surface models in previous laboratory scale studies (Chapters 3.2 & 3.3) which were based on screen separation. The pilot scale experimental results for batch 1 produced by screen separation (Table 17) are in excellent agreement with our earlier RSM predictions, with the exception of fines.

Table 17. Experimental values for lactose (L), ash (A), fines (F) and water holding capacity (WHC) against predicted values.

Batch #	Experimental values				Predicted values ¹			
	L(%)	A(%)	F(%)	WHC(%)	L(%)	A(%)	F(%)	WHC(%)
B1	0.045	1.21	1.22	75.7	0.050	1.42	0.00	76.5
B2	0.012	0.92	6.50	75.5	0.050	1.42	0.00	76.5
B3	0.038	0.83	-	-	-	-	-	-
B4	0.043	1.38	0.95	66.9	0.242	2.07	0.65	68.1
B5	0.055	1.16	2.01	73.5	0.088	2.86	1.09	74.2

¹Predicted based on response surface models (Chapters 3.2 & 3.3) using screen separation

The main difference between the laboratory scale and the pilot plant experiments lies in the type of mixer used at the coagulation step. The continuous mixing in an extruder is substantially different than the batch mixing with a vessel and blade stirring used on the laboratory scale. In addition the residence time in an extruder was much shorter than the mixing time used on the laboratory scale. Even so, the laboratory models

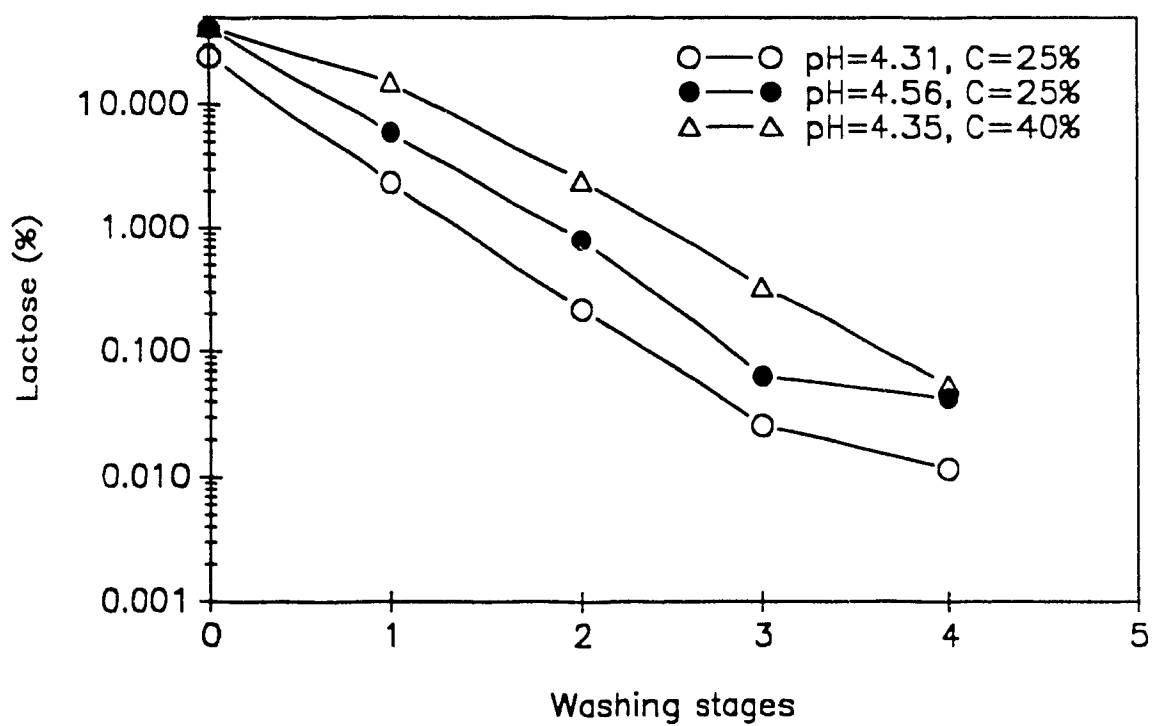


Figure 49. Effect of coagulation pH and SMP concentration (C) on the lactose removal for the whey off stage and each washing stage.

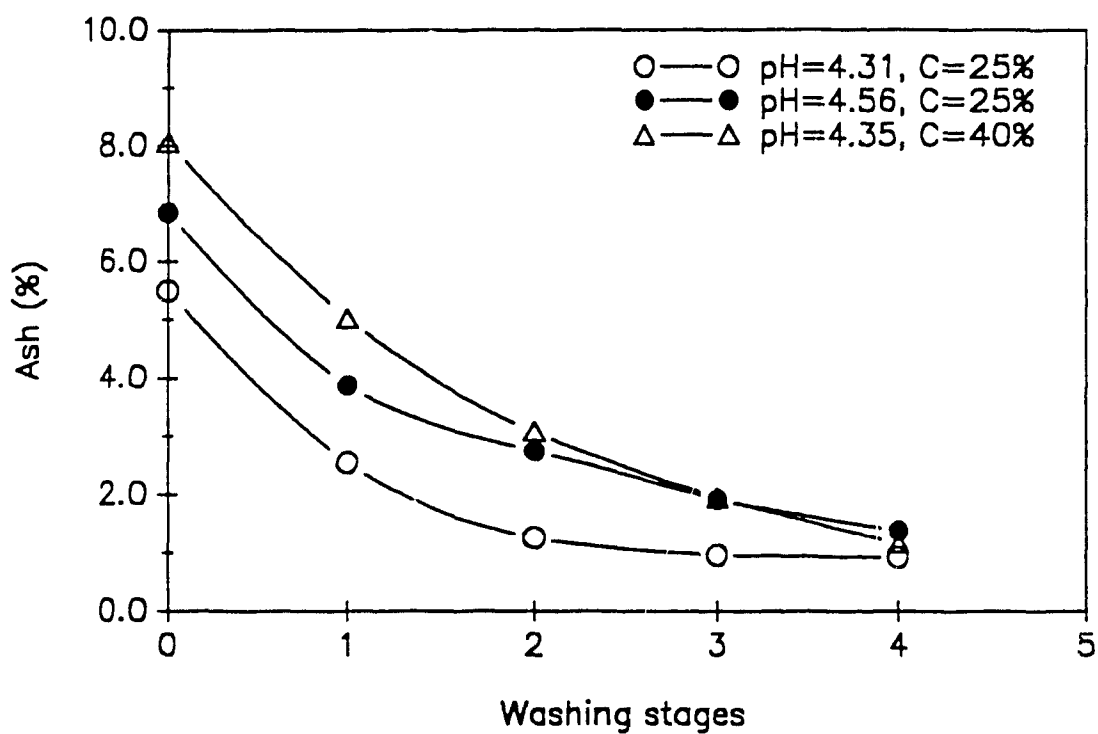


Figure 50. Effect of coagulation pH and SMP concentration (C) on the ash removal for the whey off stage and each washing stage.

provided sufficient direction to determine the extrusion parameters. Ash and lactose were not affected much by the shear rate at the coagulation step and this may be the reason that good agreement was obtained between experimental and predicted values. Fines however, may be affected by the shear forces and contact time during coagulation and the magnitude of this effect is a function of the coagulation conditions (pH and concentration).

Centrifugal separation (batches 2, 4 and 5) resulted in lower lactose and ash contents, but a general increase in fines, especially in batch 2, as compared to the predicted values based on screen separation (Table 17). This was expected based on a higher separation efficiency of the centrifuge which will likely drain more fines with wash water. The water holding capacities were in good agreement with the predicted values. The differences obtained in end product characteristics, illustrate the substantive effect coagulation conditions can have on the washing process efficiency.

The washing efficiency for lactose removal can be measured by the Murphree Stage Efficiency (MSE) coefficient (eqn 59), which indicates the approach to equilibrium of lactose at each stage in the washing process. Table 18 gives the moisture contents of the curd after the whey off stage and after each washing/dewatering step for the different batches produced and their MSE's. MSE values obtained under the same coagulation conditions but with different dewatering systems (batch 1 and 2) show that higher MSE's are obtained by centrifuge dewatering except for the last wash because of reduced lactose concentration at this stage. Higher MSE's were generally obtained for batch 2 than batch 4 or 5 which was expected based on the optimized coagulation and washing conditions used for batch 2. Batch 4 is the most efficiently dewatered product and this is likely due to the high coagulation pH which is close to the isoelectric point, resulting in a firmer curd with a lower water holding capacity (Fichtali et al., 1990c).

Table 18. Moisture content of the curd after the whey off stage and after each wash and the Murphree Stage Efficiency (MSE) of lactose removal for different batches.

Wash #	Moisture (%)				MSE (%)			
	B1	B2	B4	B5	B1	B2	B4	B5
Whey off	66.9	66.8	65.1	55.1	83.1	85.0	70.6	72.7
1	74.6	61.3	57.9	63.2	86.3	95.5	83.6	72.2
2	71.5	58.9	53.3	59.2	83.0	94.1	86.9	85.2
3	70.3	57.5	53.4	58.4	88.4	89.3	88.6	89.0
4	75.7	52.6	48.8	57.0	82.4	51.3	55.4	85.1

Samples of wash water were taken every 5 minutes during the washing to elucidate the effect of contact time on lactose diffusion. The results for batch 1 (screen separation) and batch 2 (centrifuge separation) are plotted in Figure 51. The lactose concentrations in the wash water from screen separation are, as expected, higher than what was obtained using centrifuge dewatering. The lactose concentration during washing however, does not increase much over 5 to 20 minutes and thus, the majority of lactose has diffused out during the first 5 minutes. Similar trends were obtained with batches 4 and 5, and Table 19 gives the percent lactose diffused in the first 5 minutes of washing time based on the total lactose diffused over 20 minutes. The rate of diffusion depends on the washing stage and on the coagulation conditions (i.e., curd characteristics) and in certain cases washing time can be decreased without affecting lactose removal. However, data are needed during the first 5 minutes of washing to derive a kinetic model for lactose diffusion from which washing time could be determined. More work is needed to accurately elucidate the effect of coagulation and washing conditions on lactose diffusion.

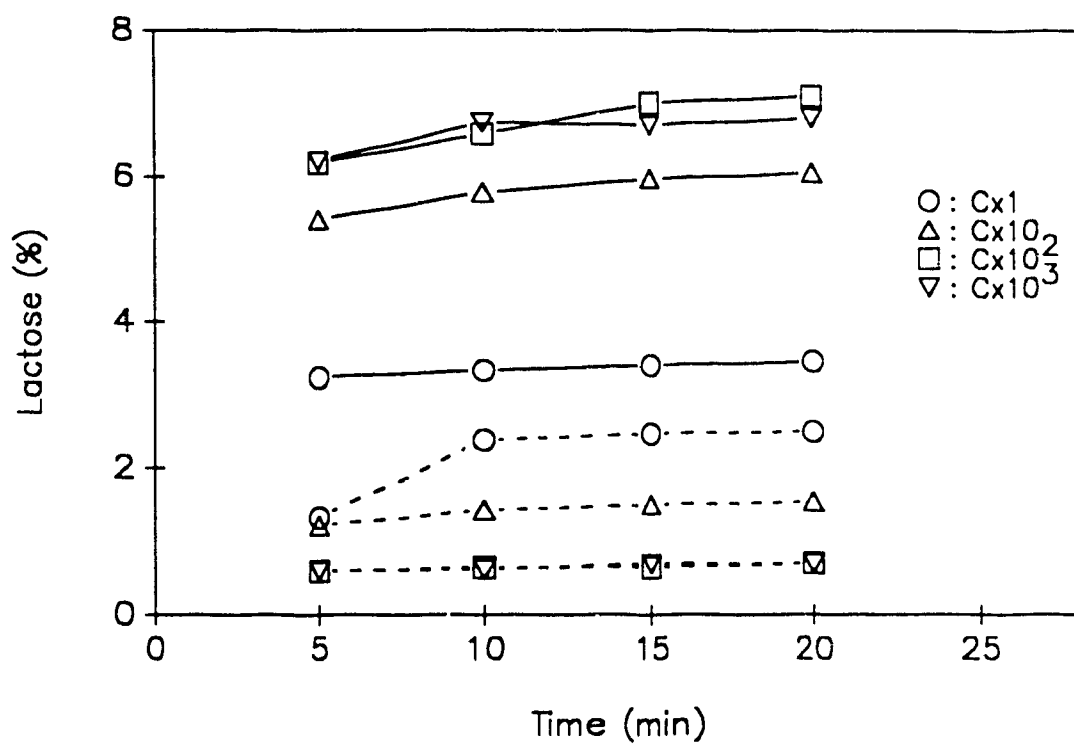


Figure 51. Lactose concentration in the wash water as a function of contact time using screen for dewatering (solid lines) and centrifuge for dewatering (dashed lines) for each washing stage; (o)=first wash, (Δ)=second wash, (\square)=third wash and (∇)=fourth wash.

Table 19. Percent lactose diffused for the first 5 minutes washing time based on the total lactose diffused over 20 minutes for each washing stage and for batches 1-5.

Washing stage	B1	B2	B4	B5
1	94.0	53.3	93.4	96.5
2	89.4	73.9	93.6	66.8
3	87.2	84.6	88.7	78.7
4	91.3	86.1	92.0	85.0

The acid casein produced was analyzed and compared (Table 20) to a commercially available product (Champlain Industries, a New Zealand import). The pilot plant produced casein has lower lactose and ash than the commercial casein and this is due to the high efficiency of the coagulation/washing system used at the pilot plant. Acceptable amounts of lactose and ash may well be obtained using only 3-stage washing which would reduce the production costs.

Table 20. Proximate analysis of caseins produced using extrusion and their comparison to commercial casein (Champlain, a New Zealand Import).

Analysis (dry basis)	B1	B2	B4	B5	Commercial
Protein (Nx6.38)	92.1	95.7	96.5	93.6	93.0
Ash	1.21	0.92	1.38	1.16	2.09
Lactose	0.045	0.012	0.043	0.055	0.12

3.8.4 Conclusion

Our initial work on the production of an acid curd from SMP by extrusion processing indicated that significantly more effort had to go into developing the process to produce a quality product. By modifying the extrusion process conditions, studying high solids coagulation and optimizing the coagulation and washing steps, acid casein of an acceptable quality can be produced by extrusion. Major improvements in the process were accomplished relative to the preliminary study (Chapter 3.1) largely based on laboratory research results. This process is continuous, controllable, uses high solids SMP and may reduce labour and floor space requirements relative to conventional processes. The acid casein produced in this manner can serve as a feed for further conversion by extrusion to sodium caseinate, discussed in the next chapter.

3.9 PILOT PLANT PRODUCTION OF CASEINS USING EXTRUSION PROCESSING II: SODIUM CASEINATE PRODUCTION

ABSTRACT

Extrusion processing was used to neutralize an acid casein produced from SMP by extrusion. Neutralization was achieved at a high moisture content (70%) and the products were adjusted to 87% moisture before spray drying. A commercial acid casein was also neutralized by extrusion but at lower moisture level (29%) and spray dried under similar conditions. The physico-chemical characteristics of the end products were determined and compared to commercially available sodium caseinates. The results indicated that a product similar to commercial caseinate can be obtained from SMP by extrusion processing. A flow diagram of the whole process from coagulation up to spray drying is presented, and a plant layout is proposed which could be used to produce sodium caseinate from SMP.

3.9.1 Introduction

Acid casein is an insoluble product with limited applications in food formulations and should be neutralized by alkali to yield a soluble and functional caseinate. Manufacturing methods and uses of caseinates have been reviewed in Chapter 2.1. Caseinates may be produced from freshly precipitated acid casein curd or from dried casein. The manufacture of caseinate from fresh casein curd is preferred as it gives a blander product and reduces the production cost associated with drying and storage prior to its conversion to sodium caseinate (Cayen and Baker, 1963, Southward, 1985).

Neutralization of high moisture casein (~75%) by extrusion was shown to be possible in our preliminary work on SMP conversion (Chapter 3.1) and may result in high mixing efficiency and good product homogeneity when appropriate operating conditions and screw configuration are used (Chapter 3.7). The rheological behaviour of sodium caseinate was described by a Bingham model for concentrations up to 16% and the effect of shear rate was considered negligible, however, temperature and concentration dramatically affected the viscosity of sodium caseinate (Chapter 3.6).

The objective of this study was: (1) to produce sodium caseinates by neutralizing commercial and SMP based acid caseins, and then drying; (2) to assess the end products and compare them to commercially available sodium caseinates; and (3) to conceive a plant layout of a process which could be applied to dairy industry.

3.9.2 Material and Methods

Acid casein produced using extrusion processing (Fichtali & van de Voort, 1990b), and described in Chapter 3.8, was used as a feed material for the second extrusion neutralization step. Commercial dried casein (see section 3.7.2) was also served as a feed material for the neutralization process. Various commercial sodium caseinates were obtained for comparison purposes and are listed in Table 21 and coded P4-P7.

Table 21. Origin and drying technique for different commercial sodium caseinates.

Caseinate	P4	P5	P6	P7
Origin	ChAMPLAIN (Canada)	Farbest (USA)	Farbest (USA)	Farbest (France)
Drying	spray	roller	spray	spray

Neutralization of acid casein

The dewatered fresh casein curd obtained from the first part of this study (Chapter 3.8) was ground using a Comil-mill model 196 S (Quadro Eng. Inc., Waterloo, Canada) fitted with a 0.31 cm sieving screen. A free flowing mass was obtained which did not present any problems for the feeder or its calibration, thus a wet curd (50-55% moisture) could be fed into the extruder without significant fluctuations during the process.

The same co-rotating intermeshing twin screw extruder (see Appendix 4) used to produce acid casein, was used to carry out the second extrusion neutralization step. Reagent grade NaOH was used for the acid casein conversion in a quantity of 2.5-2.8% by weight of casein solids to obtain a pH between 6.7 and 6.9. The quantity of NaOH required was higher than the value reported in the literature, which is 1.7-2.2% (Southward, 1985) and this could result in a sodium caseinate with a higher sodium content than commercial caseinates. The barrel configuration, die and screw profile were identical to the previous study (Chapter 3.7). The screw profile is given in Figure 52 along with the barrel temperature profile which was very similar to the set temperature profile. The screw speed was 100 rpm, the feed rate was 15 kg/hr, the NaOH flow rate was adjusted to give 70% moisture and the product temperature at the exit was 95°C.

The dry commercial acid casein was also neutralized using the same screw configuration and die, but at 20 kg/hr feed rate, 150 rpm screw speed producing a final moisture content of 29%. Lower barrel setting temperatures were used, however, a barrel temperature profile similar to Figure 52 was obtained. These operating conditions were determined based on the work described in Chapter 3.7. The product temperature at the exit was 95.5°C, similar to the temperature obtained for neutralizing SMP caseins (95°C).

Spray drying

Industrial spray drying generally uses solutions with 20% solids and a temperature of 90-95°C, however, using this concentration and a temperature of 80°C presented some problems with the atomizer disc of the Niro Atomizer (model P6.3) spray dryer used, due

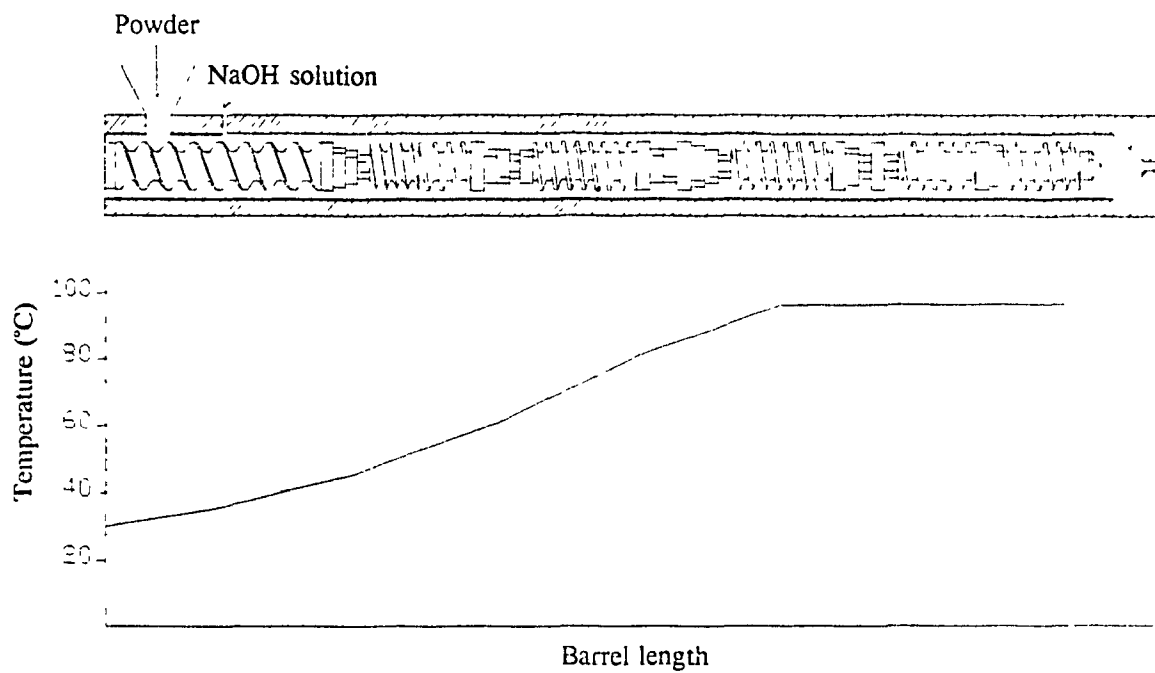


Figure 52. Screw configuration and barrel temperature profile used for casein neutralization. Details of the screw configuration were given in Figure 35.

to high viscosities. To reduce the viscosity, the extruded caseinate solutions were adjusted to 13% solids in a 50l agitated tank maintained at 80°C and then pumped into the spray dryer at a feed rate of 32 l/hr, having an inlet temperature of 195°C and outlet temperature of 87°C. Two solutions obtained from acid casein batches 2 and 4 (see Chapter 3.8) and the solution obtained from commercial casein were spray dried. A flow diagram representing the whole process used to produce acid casein and sodium caseinate, is given in Figure 53.

Analysis

The three end products and commercial sodium caseinates (Table 19) were analyzed for moisture, protein nitrogen, ash (AOAC, 1984) and lactose (International Standard, 1980). The pH was measured based on 5% solids and the solubility assessed at 40°C according to the methods outlined by Towler (1978). The water absorption capacity was measured by a Brabender farinograph (type FA-R/2) using a method specifically developed for caseins and caseinates (Knightbridge & Goldman, 1975) which was adapted to the 80g bowl. Bulk density (see section 3.7.2), viscosity (see section 3.6.2), and calcium and sodium (Fichtali et al., 1990a) were also determined and the microstructure of the caseinates assessed by scanning electron microscopy (Fichtali et al., 1990b).

3.9.3 Results and Discussion

Neutralization and drying

For acid caseins produced from SMP using extrusion, torque and pressure during neutralization by extrusion were negligible due to their high moisture contents (70%). The specific energy consumption calculated using eqns (71-73) was only about 54 kJ/kg. Commercial acid casein, extruded at a lower moisture level (29%) required about ten times energy (526 kJ/kg) and generated measurable pressures (~400 psi). A lower barrel temperature setting was used to have a product temperature at the die exit of 95.5°C

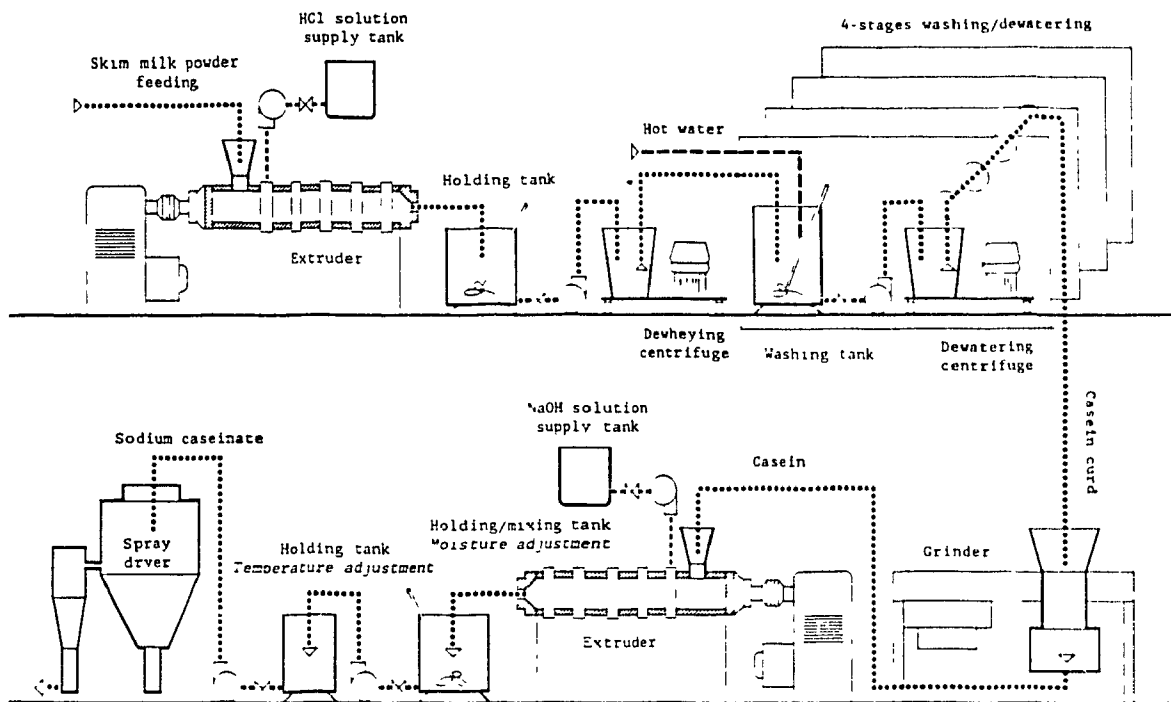


Figure 53. Pilot plant flow diagram used to produce acid casein and sodium caseinate.

because of heat generated by mechanical energy dissipation. These findings were expected based on the results of Chapter 3.7.

Spray drying required adjustment of the moisture to 87% to decrease the caseinate solution viscosity. Adjustment of the 70% moisture SMP caseinates at 80°C did not present a problem, however, adjusting the 29% moisture caseinate required substantial mixing time (~ 4 hrs) at 80°C to obtain an homogeneous solution. Hence spray drying is not the best method for drying when extruding at low moisture levels because the extruder specific energy consumption is much higher and the dilution process for spray drying takes an overly long time, both steps increasing the cost of the process and may affect the quality of the end product. Spray drying may be the method of choice when extruding fresh casein, but when extruding dried acid casein, roller or attrition drying (see section 2.2.3) would likely be better. The yields obtained after spray drying were 96.2% and 98.6% for caseinates originated from batches 2 and 4 (see Chapter 3.8) respectively with similar yield obtained for caseinate from commercial casein (~ 98%), the balance lost due to handling and as loss of fines in the process.

Physico-chemical properties

Table 22 provides typical analytical results for the pilot scale spray dried products in relation to commercial sodium caseinates. Lower lactose contents were obtained for the SMP caseinates (P2 and P3), likely due to the selected optimized conditions and high washing efficiency used in the pilot plant (Figure 53). Lactose is responsible for Maillard browning and off-flavour development during storage and should be minimized. No major differences were obtained in protein nitrogen or water absorption characteristics, and the moistures contents are generally less than the 5% required for satisfactory storage (Southward, 1985) with the exception of the roller dried caseinate (P5). The roller dried caseinate (P5) also had higher ash, calcium and sodium contents, and a higher pH, and bulk density. The density is similar to what was obtained in Chapter 3.7 for tray dried caseinates (see Table 15) and this high density is economical in terms of packaging and transport, however, the high pH of 7.55 may be a cause of off-flavours. The very low

calcium content obtained for SMP caseinate P2 is likely because of the low coagulation pH and washing conditions used to produce the base casein material which in turn resulted in a slightly higher sodium content due to increased amounts of sodium hydroxide required for neutralization. All the products tested are ~100% soluble at 40°C with the exception of the commercial extruded casein (P1).

Table 22. Typical analysis of sodium caseinates produced by extrusion of commercial acid casein (P1), batch 2 (P2) and batch 4 (P3) and their comparison with commercial sodium caseinates (P4-P7) listed in Table 21. Protein, ash, Ca and Na data are on dry basis; and water absorption data are on as is basis.

Analysis	P1	P2	P3	P4	P5	P6	P7
Protein (%) (Nx6.38)	93.9	90.4	90.5	89.4	89.9	91.4	93.1
Moisture (%)	4.5	2.1	1.9	2.7	9.8	4.1	5.2
Ash (%)	3.7	4.0	3.9	3.6	6.6	3.6	3.7
Lactose (%)	0.10	0.012	0.04	0.11	0.12	0.12	0.15
Calcium (%)	0.064	0.004	0.060	0.049	0.081	0.065	0.053
Sodium (%)	1.33	1.73	1.40	1.37	2.50	1.07	1.27
pH	6.45	6.72	6.85	6.85	7.55	6.36	6.62
Solubility at 40°C (%)	99.8	~100	100	100	~100	~100	~100
Water absorption (%)	274.4	273.8	275.4	274.7	274.4	273.5	274.2
Bulk density (g/cm ³)	0.14	0.14	0.16	0.28	0.68	0.36	0.41

One major difference between the pilot plant produced caseinates (P1-P3) compared to commercial spray dried caseinates, lies in their low bulk density. The bulk density is directly related to the solids content of the caseinate solution prior to spray drying (Johnson, 1970), and due to atomizer problems at 20% solid contents we were obliged to reduce the solids concentration. Economic considerations, however, require that the total solids content of the caseinate solution be as high as possible, e.g., a decrease in total solids from 20 to 15% could increase drying costs by approximately 40% because of reduced spray drier throughput (Johnson, 1970). Higher concentrations

may however be tolerated by using an more appropriate atomizer disc having larger holes and increasing the temperature beyond 80°C to further reduce the viscosity.

The viscosities of the seven caseinates were measured at 25°C and 10 % solids using a shear rate varying from zero to 200 s⁻¹. The viscosity data were fitted to Bingham model as described in Chapter 3.6. Table 23 gives viscosity coefficients, yield stresses and coefficients of determination for each of the different caseinates.

Table 23. Viscosity coefficients (η) and yield stresses (τ_0) using Bingham model, at T=25°C and C=10% solids, for sodium caseinates produced from commercial acid casein (P1), batch 2 (P2), and batch 4 (P3) and their comparison to commercial caseinates (P4-P7) listed in Table 21.

$$\tau = \tau_0 + \eta\dot{\gamma}$$

Caseinate	τ_0	η	R ²
P1	2.147	0.1400	0.9991
P2	1.159	0.0459	0.9999
P3	1.135	0.0445	0.9999
P4	1.002	0.0708	0.9999
P5	1.108	0.0541	0.9997
P6	1.048	0.0334	0.9998
P7	1.097	0.0804	1.0000

Although Bingham model proved to be adequate in describing the flow behaviour of a wide range of sodium caseinates (R² > 0.999), the viscosity coefficients vary from one product to an other (Table 23). In addition to temperature and concentration, other factors may affect the viscosity of sodium caseinate such as pH, calcium content, type of alkali used and seasonal and genetic factors (Southward, 1985). No clear relationship can be drawn between the viscosity coefficients given in Table 23, and the pH and/or calcium

contents tabulated in Table 22. Thus the variations in viscosity may be also related to the process itself and/or to genetic factors. The viscosity of P1 is clearly much higher than the other products. This may be due to the lower pH obtained for this product (Towler, 1976) and to more severe thermal and shear treatment required for moisture adjustment for spray drying. Figure 54 presents some typical flow curves and shows that the viscosity is much higher at low shear rates due to yield stress and becomes constant at shear rates of $> 50 \text{ s}^{-1}$.

The microstructure of typical pilot plant produced SMP caseinate and commercial caseinates is illustrated in Figure 55. The roller dried caseinate (Figure 55C) is clearly different from the spray dried products (Figure 55A,B,D,E) in particle size, shape and surface properties. Roller dried caseinate, as noted in section 2.2.3, is of limited use and is of poorer quality than the spray dried products. Spray dried caseinates generally appear as spherical particles of heterogeneous size which may follow a normal distribution. Some filamentous particles are however present in the caseinate illustrated in Figure 55D. The particles of the SMP caseinate produced (Figure 55A) have the smoothest surface, while rougher particles observed in the commercial samples may be due to packaging and/or more severe drying conditions.

The functional properties of SMP caseinates are not considered here, however, they have been studied by V. Barraquio and are discussed elsewhere. Sensory analysis of the caseinates was conducted in the Food Research and Development Centre of St-Hyacinthe and will be published elsewhere, however, the main difference was in a taste which can be described as soapy, where the SMP caseinate lacked this attribute, being significantly blander than the commercial products (J. Fortin, private communication).

3.9.4 Plant Layout Concept

Based on our results and experience, a simplified plant layout is proposed and presented in Figure 56 which could be adapted to dairy industry. A lower cost single

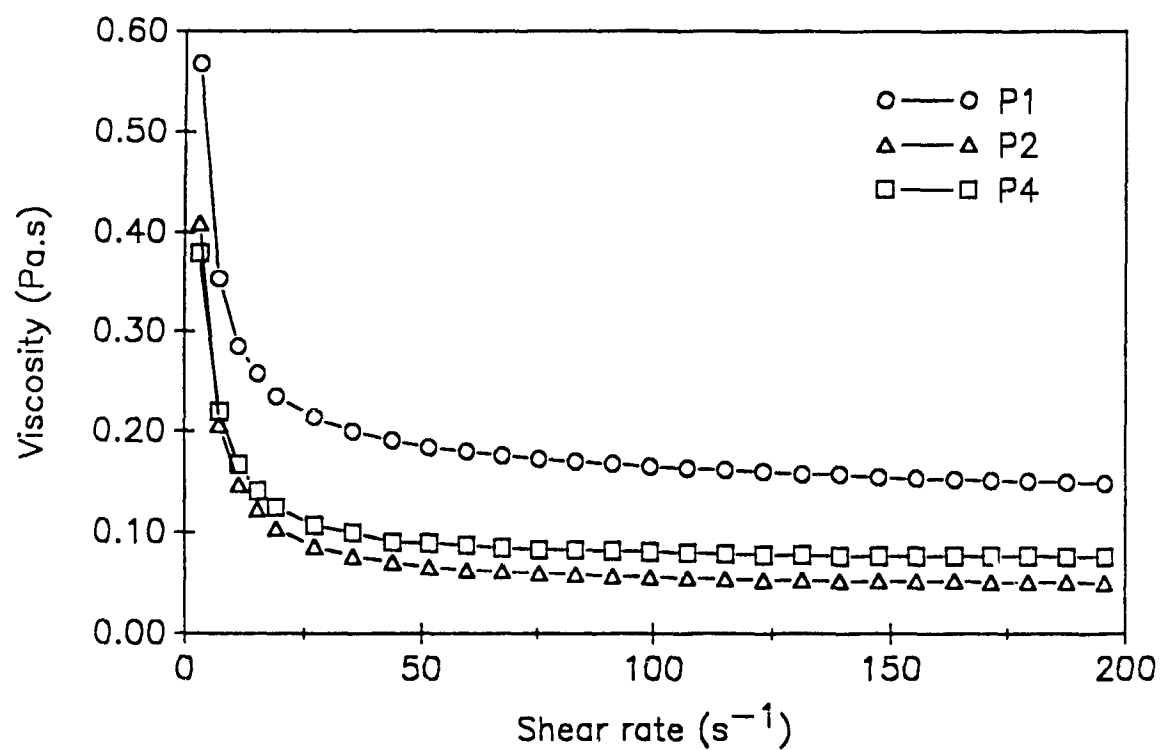


Figure 54. Viscosity curves of sodium caseinates P1, P2 and P4 listed in Table 22 at 25°C and 10 % solids content.



Figure 55. Scanning electron micrographs of sodium caseinate obtained from SMP using extrusion (A) and its comparison to a commercial roller dried sodium caseinate (C) and commercial spray dried caseinates (B, D, and E).

screw extruder could be designed to carry out the coagulation step using a screw which acts as a pump, but should also have some mixing elements. The inner barrel and screws surfaces should be covered with an acid resistant polymer (i.e., teflon) to avoid corrosion caused by the acid overtime. This is possible since the coagulation temperature is generally low (45°C). A holding tank after the extruder allows for an increase in contact time of the curd with the whey to increase its firmness. After dewheying by pumping the coagulum through an inclined screen, three or four washing stages are envisaged using heated tanks fitted with agitators and screens for separation. A con-current or counter-current washing system could be used with the latter being more economical. The dewatered curd which should have about 70% moisture can be pumped to a twin screw extruder equipped with a feeder capable of delivering a slurry. Alkali can be injected to the extruder to neutralize the casein and simultaneously bring the moisture up to about 80%. A tank fitted with an agitator can be used for viscosity adjustment (moisture/temperature) and then the caseinate can be pumped to a holding tank prior to spray drying. On line pH and viscosity measurement and control can be used and a panel controlling the whole process can be adapted to make the process automated.

3.9.5 Conclusion

Neutralization of fresh casein (50-55% moisture) was shown to be possible by extrusion processing, requiring minimal specific energy, providing good mixing and homogeneity of the product, and allows ready adjustment of moisture, viscosity, or pH of the extruded solutions. Spray drying may be the method of choice when extruding high moisture caseinate, however, solids content should be kept as high as possible to obtain a product with a higher bulk density.

Sodium caseinate with physico-chemical properties equal to or better than commercial caseinates may be produced by a two step extrusion process. These caseinates may differ in their physico-chemical characteristics as a function of the process conditions and as a consequence, in their functional and sensory properties. SMP caseinate obtained

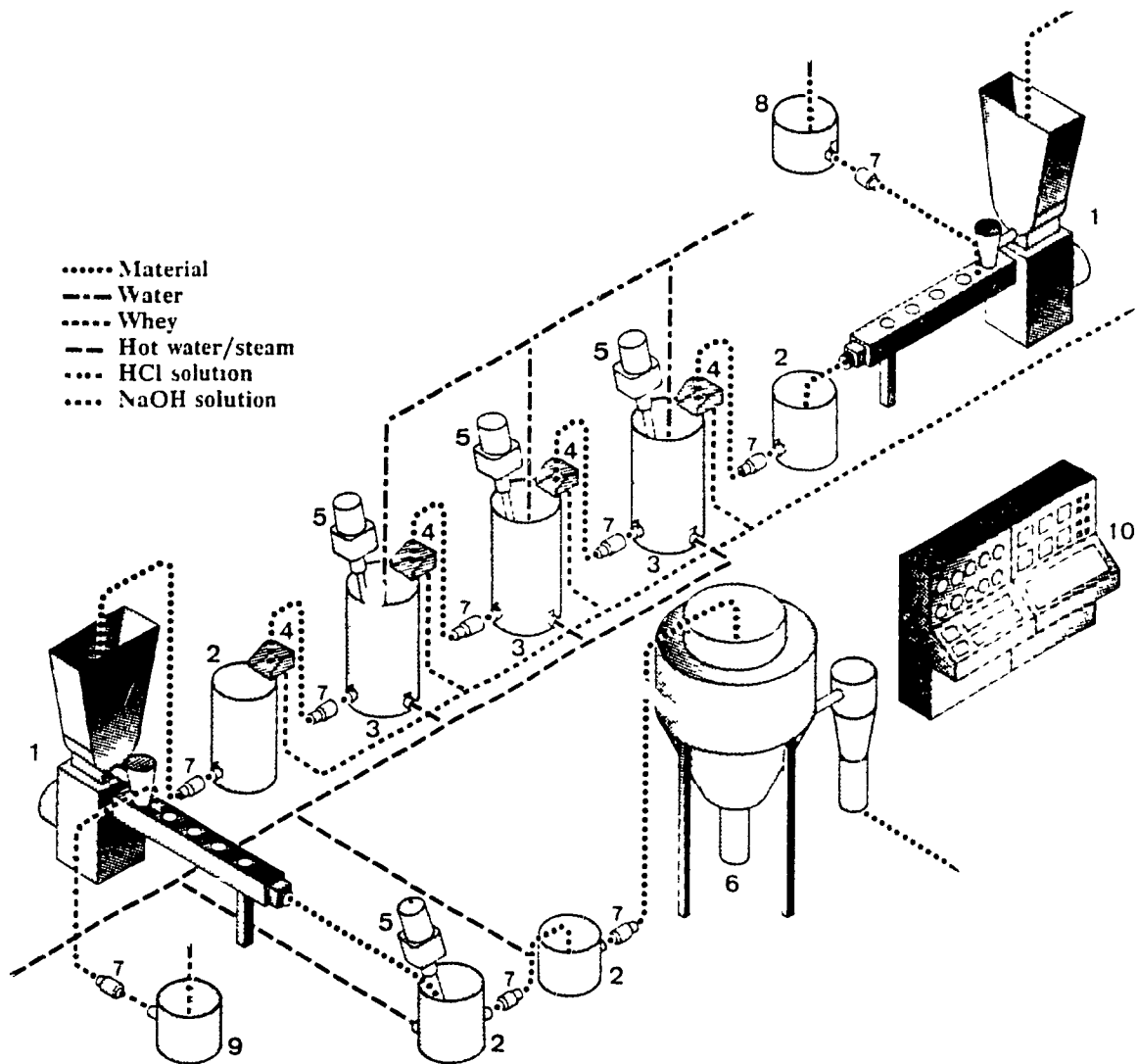


Figure 56. Plant layout concept for caseinate production using extrusion technology
 1=extruder, 2=holding tank, 3=washing tank, 4= inclined screen for separation,
 5=agitator, 6=spray dryer, 7=pump, 8=supply tank for HCl solution, 9=supply tank
 for NaOH solution, 10=panel control.

by this new process has a very low lactose content, adequate pH and ash content. The product is homogeneous, produced from fresh casein has undergone a mild time-temperature history during the process which may be the reasons it has a very blander flavour.

4 GENERAL CONCLUSION

A new process was developed capable of converting surplus skim milk powder into added value acid casein and sodium caseinate. The process includes several unit operations which are: coagulation, dewheying, washing, dewatering, neutralization and drying. All of these steps were studied, evaluated and/or optimized to determine operating conditions and suitable equipment. The study of the coagulation/washing process using response surface methodology (RSM) provided insight into the factors affecting coagulation of concentrated milks and the subsequent whey removal through the washing process. The results indicated that the careful assessment of the coagulation/washing process can yield useful information relative to improving our understanding of the coagulation mechanism and the factors affecting the process. The use of new optimization techniques such as the Generalized Distance Approach (GDA) and the Extended Surface Response Procedure (ESRP) permitted an extended analysis of the response surface models in terms of multiresponse optimization of acid casein production. Both approaches were shown to be useful for process engineering applications, with GDA being a more general tool while the ERSP is advantageous when specific constraints on either process variables or responses are required.

In order to simplify the process and reduce its cost, a study was implemented to design and test an extruder die for dewheying purposes. Despite the inconclusive results obtained due to screw design limitations, the concept of using an extruder die for dewatering may have application in a number of food processes. Neutralization of casein by a second extrusion step required rheological and extruder performance determinations. The flow behaviour of caseinate was assessed by developing a rheological model as a function of temperature and concentration which could be used for caseinate production and applications purposes. The engineering aspects of the twin screw extruder for casein

neutralization were analyzed in terms of residence time distributions, mixing, conveying, energy consumption, temperature profiles and pressures generated at the die. This study provided a clear understanding of the extruder system and the neutralization process.

The understanding gained in each step of casein/caseinate production and about the extruder as a chemical reactor, was integrated to design a process and to select the operating conditions capable of producing quality caseins and caseinates. The physico-chemical characteristics of acid caseins and caseinates produced were assessed and compared to commercially available products and the results indicated that similar or better quality products could be obtained from skim milk powder using this new extrusion based process.

This new process potentially provides a number of advantages, including: (1) it is a continuous process which can be controlled and maintained to produce a consistently high quality product, (2) it is not based on a perishable product (i.e., raw milk) minimizing storage and contamination problems, (3) has inherent flexibility, control and can be automated, (4) uses high solids for coagulation and casein neutralization, resulting in higher throughput and energy efficiency, (5) reduced heat treatment as the mean residence time in the extruder is about 2-2.5 min as opposed to 30-60 min using tanks, colloid mills and stirrers, (6) reduced cost in terms of labour and floor space requirements per production unit, (7) has lower capital investment relative to conventional processes, and (8) provides for the ability to manufacture on demand as opposed to when milk is produced.

Additional work which could be considered, would be the fine tuning of our understanding of the process to improve it. Lactose removal is very important in the process and developing a kinetic model for lactose diffusion in wash water may be very useful in defining washing time and to improve the washing efficiency. The extruder die designed for whey separation was shown to have a potential (Chapter 3.5) and studies should be concentrated on designing a special screw having sufficient pumping action and

further improving the die design. This work may open a new area in food extrusion applications which is to add a separation unit operation to extrusion processes where high moisture products are processed. An other area which deserves more work is related to rheological modelling of sodium caseinate. The rheological model developed in Chapter 3.6 was restricted to 13% solids because of the high viscosity of sodium caseinates solutions. Higher concentrations could be studied using a capillary rheometer with an Instron or using the extruder itself fitted with a capillary die and pressure transducers. The design of a capillary die for the extruder is not a very difficult task and relatively cheap (~ 2000\$), however, the experimental work is very tedious. With a model describing the rheological behaviour of high solids concentrations (20-50%), it could be used for modelling acid casein conversion by extrusion. The rheological model could also include the effect of pH and calcium content to make it applicable to a wide range of sodium caseinates.

Clearly all the advantages of SMP extrusion have not been elucidated in every detail, however, the basic concept has been developed to the point where others can evaluate the economical feasibility of the process and determine whether the process warrants scale-up to the industrial level.

LITERATURE CITED

- ACP Marketing. (1978). Should the CDC subsidize the production of casein in Canada? A report of the ACP Marketing, Montreal, Canada.
- Agur, E.E. (1986). Extruder scale-up in a co-rotating twin screw extrusion compounding process. *Advances in Polym. Technol.*, 6:225-232
- Altomare, R.E. & Ghossi, P. (1986). An analysis of residence time distribution patterns in a twin screw cooking extruder. *Biotechnology Progress*, 2:157-163.
- Antila, J., Pipatti, R. & Linko, P. (1984). Process control and automation in extrusion cooking. In: *Thermal Processing and Quality of Foods*. P. Zeuthen, J.C. Cheftel, C. Eriksson, M. Jul, H. Leniger, P. Linko, G. Varela & G. Vos eds, Elsevier Applied Science, London, pp. 44-48.
- AOAC. (1984). *Official Methods of Analysis*, 14th ed. Arlington, Virginia: Association of Official Analytical Chemists, pp 303.
- Balke, S.T. (1985). Predicting component concentration fluctuations in extruded polymer composites. *S.P.E. ANTEC Tech. papers*, April, 49-53.
- Barraquero, V.L., Fichtali, J., Ng-Kwai-Hang, K.F. & van de Voort, F.R. (1988). Acid coagulation of skim milk powder by extrusion processing. *Can Inst. Food Sci. Technol. J.*, 21:305-311.
- Barraquero, V.L. & van de Voort, F.R. (1988). Milk and soy proteins: Their status in review. *Can Inst. Food Sci. Technol. J.*, 5:477-493.
- Bhattacharya, M. & Hanna, M.A. (1986). Viscosity modelling of dough in extrusion. *J. Food Technol.*, 21:167-174.
- Bhattacharya, M. & Hanna, M.A. (1987). Influence of process and product variables on extrusion energy and pressure requirements. *J. Food Technol.*, 6:153-163.
- Bigg, D. & Middleman, S. (1974). Mixing in a screw extruder. A model for residence time distribution and strain. *Ind. Eng. Chem. Fundam.*, 13:66-71.
- Baomy, J.J. & Brulé, G. (1986). Etude comparée de la solubilité et de la viscosité des solutions de caséinate et paracaseinate de sodium en présence de calcium. *Lait*, 66:65-77.
- Biral, F. (1979). Etude de la distribution des temps de séjour dans une extrudeuse à double vis. Mémoire d'ingénieur, Université de Louvain, Belgium.
- Blais, J.A., Boulet, M. & Julien, J-P. (1984). Laits concentrés et lait en poudre. In: *Science et Technologie du Lait*. J-P Julien, J.P. Nadeau & R. Dumais eds, La Fondation de technologie laitière du Québec Inc., Québec, pp. 289-324.
- Boissonnat, P., Mangé, C., Bouvier, J.M. & Gelus, M. (1987). Modelling a twin screw extruder by residence time distribution. *7th World Congress of Food Science and Technology*, Singapore, sept/oct.

- Booy, M.L. (1978). Geometry of fully wiped twin screw equipment. *Polym. Eng. Sci.*, 18:973-984.
- Booy, M.L. (1980). Isothermal flow of viscous liquids in co-rotating twin screw devices. *Polym. Eng. Sci.*, 20:1220-1228.
- Boullé, M.A. (1987). New caseinate manufacture process for high concentration caseinate. In: *Extrusion Technology for the Food Industry*. C. O'Connor ed., Elsevier Applied Science, London, pp.96-108.
- Bounie, D. (1988). Modelling of the flow pattern in twin-screw extruder through residence time distribution experiments. *J. Food Eng.*, 7:223-246.
- Bounie, D. & Cheftel, J.C. (1986). The use of tracer and thermosensitive molecules to assess flow behaviour and severity of heat processing during Extrusion-Cooking. In: *Pasta and Extrusion Cooked Foods: Some Technological and Nutritional Aspects*. Ch. Mercier & C. Cantarelli eds, Elsevier Applied Science Publishers, London, pp. 148-158.
- Box, G.E.P. & Draper, N.R. (1987). *Empirical Model Building and Response Surfaces*. John Wiley and Sons, New York, pp. 502-527.
- Bressan, J.A., Carroad, P.A., Merson, L. & Dunkley, L. (1981). Temperature dependence of effective coefficient for total solids during washing of cheese curd. *J. Food Sci.*, 46:1958-1959.
- Bressan, J.A. & Hobman, P.G. (1985). Stage efficiency in continuous countercurrent casein washing systems. *N.Z. J. Dairy Sci. Technol.*, 20:117-127.
- Bruin, S., van Zutlichem, D.J. & Stolp, W. (1978). A review of fundamental and engineering aspects of extrusion of biopolymers in a single-screw extruder. *J. Food Process Eng.*, 2:1-37.
- Brulé, G., Maubois, J.L. & Fauquant, J. (1974). Etude de la teneur en éléments minéraux des produits obtenus lors de l'ultrafiltration du lait sur membrane. *Lait*, 54:600-615.
- Brulé, G. & Fauquant, J. (1981). Mineral balance in skim-milk and milk retentate: effect of physicochemical characteristics of the aqueous phase. *J. Dairy Res.*, 48:91-97.
- Burkhardt, K., Herrmann, H. & Jakopin, S. (1978). Plasticizing and mixing principles of intermeshing co-rotating and counter-rotating twin screw extruders. *S.P.E. ANTEC Tech. Papers*, 24:498-506.
- Canadian Dairy Commission. (1983). *The Dairy Research Program*. Ottawa, Ontario.
- Canadian Dairy Commission. (1986). *The Annual Report 1985/86*. Ottawa, Ontario.
- Cayen, M.N. & Baker, B.E. (1963). Some factors affecting the flavour of sodium caseinate. *Agricultural and Food Chemistry*, 11:12-14.
- Cheftel, J.-C. (1985). *Protéines Alimentaires*. TEC and DOC Lavoisier, Paris.
- Chen, A.H.; Jao, Y.C.; Larkin, J.W. & Goldstein, W.E. (1978). *J. Food Process Eng.*, 2:337-342.
- Chou, D.H. & Morr, C.V. (1979). Protein-water interactions and functional properties. *Journal of American Oil Chemist's Society*, 56:53A-62A.

- Chouikhi, S.M., Ferdinand, J.M. & Smith, A.C. (1989). The application of a microwave attenuation sensor to study mixing in an extruder cooker. In: *Process Engineering in the Food Industry*. R.W. Field and J.A. Howell eds, Elsevier Applied Science, London, pp. 211-222.
- Chung, J.T. (1983). Counter-rotating, partially intermeshing, conical twin-screw extruder. *Plastics compounding*, **6**:59-60,62,64,67.
- Clark, J.P. (1978). Dough rheology in extrusion cooking. *Food Technol.*, **23**:73-76.
- Cochran, W.G & Cox, G.M. (1957). *Experimental Designs*. John Wiley and Sons, Inc., New York.
- Conlon, M. & Khuri, A. (1988). MR Multiple response optimization. *Technical report number 322*. Department of statistics, University of Florida.
- Colonna, P., Melcion, J.P., Vergnes, B. & Mercier, C. (1983). Flow, mixing and residence time distribution of maize starch within a twin-screw extruder with a longitudinally split barrel. *J. Cereal Sci.*, **1**:115-125.
- Dagleish, D.G. & Law, J.R. (1988). Sodium caseinates - composition and properties of different preparations. *Journal of the Society of Dairy Technology*, **41**:1-4.
- Dankwerts, P.V. (1953). Continuous flow systems. Distribution of residence times. *Chem. Eng. Sci.*, **2**: 1-13.
- Date, A.R. & Gray, A.L. (1989). *Applications of Inductively Coupled Plasma Mass Spectrometry*. Chapman and Hall, New York.
- Davidson, V.J., Paton, D., Diosady, L.L. & Spratt, W.A. (1983). Residence time distributions for wheat starch in a single screw extruder. *J. Food Sci.*, **48**:1157-1161.
- Della Valle, G., Tayeb, J. & Melcion, J.P. (1987). Relationship of extrusion variables with pressure and temperature during twin screw extrusion cooking of starch. *J. Food Eng.*, **6**:423-444.
- Denson, C.D. & Hwang, B.K. (1980). The influence of the axial pressure gradient on flow rate for newtonian liquids in a self wiping co-rotating twin screw extruder. *Polym. Eng. Sci.*, **20**:956-971.
- de Wit, J.N. (1981). Structure and functional behaviour of whey proteins. *Netherland Milk and Dairy J.*, **35**:47-64.
- Eise, K., Herrmann, H., Jakopin, S., Burkhardt, U. & Werner, H. (1981). An analysis of twin-screw extruder mechanisms. *Advances in Plastic Technol.*, **2**:18-39.
- English, A. (1981). Future uses of skimmed milk-texturizing processes. *Journal of the Society of Dairy Technology*, **34**:70-73.
- Ess, J.W., Hornsby, P.R., Lin, S.Y. & Bevis, M.J. (1984). Characterisation of dispersion in mineral-filled thermoplastics compounds. *Plastics and Rubber Processing and Applications*, **4**:7-14.
- Ess, J.W. & Hornsby, P.R. (1986). Characterisation of distributive mixing in thermoplastics compositions. *Polymer Testing*, **6**:205-218.

- Ess, J.W. & Hornsby, P.R. (1987). Twin screw extrusion compounding of mineral filled thermoplastics: dispersive mixing effects. *Plastics and Rubber Processing and Applications*, **8**:147-156.
- Ferry-Wilczek, H., Melcion, J.-P., Gaborit, T., & Della Vallé, G. (1988). Recherche d'un traceur d'intensité de traitement en relation avec le temps de séjour dans un cuiseur-extrudeur bi-vis. *Sciences des Aliments*, **8**:133-148.
- Fichtali, J. & van de Voort, F.R. (1989). Fundamental and practical aspects of twin screw extrusion. *Cereal Foods World*, **34**:921-930.
- Fichtali, J., van de Voort, F.R. & Toupin, C. J. (1990a). Coagulation and washing conditions for acid casein production from skim milk powder. *Int. J. Food Sci. Technol.*, (in press).
- Fichtali, J., van de Voort, F.R. & Toupin, C. J. (1990b). Effects of coagulation and washing conditions on water holding capacity, fines and microstructure of casein curd. *J. Dairy Res.*, (in press).
- Fichtali, J., van de Voort, F.R. & Khuri, A.I. (1990c). Multiresponse optimization of acid casein production. *J. Food Process Eng.*, **12**:247-258.
- Fichtali & van de Voort, F.R. (1990a). Flow behaviour, mixing and residence time distribution in relation to twin screw extrusion: A review. *J. Food Eng.*, (submitted).
- Fichtali, J. & van de Voort, F.R. (1990b). Pilot plant production of caseins. I. Production of acid casein. *Milchwissenschaft*, (in press).
- Fletcher, S.I., Richmond, P. & Smith, A.C. (1985). An experimental study of twin screw extrusion cooking of maize grits. *J. Food Eng.*, **4**:291-312.
- Fox, P.F. (1982). Heated-induced coagulation of milk. In: *Developments in Dairy Chemistry-1*. P.F. Fox, ed. Elsevier Applied Science Publishers, London and New York, pp.189-228.
- Fox, P.F. (1989). The milk protein system. In: *Developments in Dairy Chemistry-4*. P.F. Fox, ed. Elsevier Applied Science Publishers, London, pp. 1-53.
- Geurts, T.J., Walstra, P. & Mulder, H. (1974). Water binding to milk protein, with particular reference to cheese. *Netherlands Milk and Dairy Journal*, **28**:46-72.
- Griffith, R.M. (1962). Fully developed flow in screw extruders. *Ind. Eng. Chem. Fundam.*, **1**:180-187.
- Guzman-Tello, R. & Cheftel, J.C. (1987). Thiamine destruction during extrusion cooking as an indication of the intensity of thermal processing. *Int. J. Food Sci. Technol.*, **22**: 549-562.
- Gwozdz, M. (1983). Fabrication de caséines et caséinates, procédés procalex. *Techniques Laitières*, **23**: 19-23.
- Harper, J.S., Rhodes, T.P. & Wanninger, L.A. (1971). Viscosity model for cooked cereal doughs. *American Inst. Chem. Eng.*, **67**:40-43.
- Harper, M. H. (1978). Extrusion processing of food. *Food Technol. J.* **23**:67.
- Harper, J.M. (1981). *Extrusion of Foods*. Vol. 1. CRC Press, Florida.

- Hartley, H.O. (1961). The modified Gauss-Newton method for the fitting of non-linear regression functions by least squares. *Technometrics*, **3**:269-280.
- Herrmann, H. & Burkhardt U. (1978). Geschwindigkeits- und schubspannungsverteilungen in dicht kammenden gleichdrall- und gendrall-doppelschnecken. *Kunststoffe*, **68**:753-758.
- Hobman, P.G. (1978). A model for predicting the water required to wash casein curd. *N.Z. J. Dairy Sci. Technol.*, **13**:229-235.
- Hornsby, P.R. (1987). Flow and mixing phenomena in a co-rotating intermeshing twin screw extruder. *Plastics and Rubber Processing and Applications*, **7**:237-240.
- Ibarz, A., Pagan, J., Gutiérrez, J. & Vicente, M. (1989). Rheological properties of clarified pear juice concentrates. *J. Food Eng.*, **10**:57-63.
- International standard ISO-5548, (1980). Caseins and caseinates. Determination of lactose content - Photometric method. *International Organization for standardization*, ISO, Genève.
- Jablonka, M.S. & Munro, P.A. (1985). Particle size distribution and calcium content of batch-precipitated acid casein curd: effect of precipitation temperature and pH. *Journal of Dairy Research*, **52**:419-428.
- Jablonka, M.S. & Munro, P.A. (1986a). Development of an objective method for assessing the mechanical strength of casein curd. *J.Dairy Res.*, **53**:61-68.
- Jablonka, M.S. & Munro, P.A. (1986b). Effect of precipitation temperature and pH on the continuous pilot-scale precipitation of casein curd. *N.Z. J. Dairy Sci. Technol.*, **21**:111-123.
- Jablonka, M.S. & Munro, P.A. (1987). Mechanical properties of lactic, mineral acid and rennet casein curds from commercial plants. *N.Z. J. Dairy Sci. Technol.*, **22**:67-74.
- Jager, T., Zuulichem, D.J.v., & Stolp, W. (1988). Residence time distribution in extrusion cooking. Part IV: The Feed zone of a conical, counter-rotating, twin screw extruder processing maize grits. *J. Food Eng.*, **8**:157-172.
- Jager, T., Zuulichem, D.J.v., Stolp, W. & van't Riet, K. (1989). Residence time distribution in extrusion cooking. Part V: The compression zone of a counter-rotating, twin screw extruder feed with maize grits. *J. Food Eng.*, **9**:203-218.
- Janssen, L.P.B.M. (1978). *Twin Screw Extrusion*. Elsevier Scientific Publishing Company, New York.
- Janssen, L.P.B.M., Hollander, R.W., & Smith, J.M. (1979). Residence time distribution in a plasticating twin screw extruder. *AIChE Journal*, **25**:345-351.
- Janssen, L.P.B.M. & Smith, J.M. (1980). Comparison of different classes of extruders. *Plastics and Rubbers:Processing*, Sept/Dec, 115-122.
- Janssen, L.P.B.M. (1986). Models for cooking extrusion. In: *Food Engineering and Process Applications*. Vol.2. M. Le Maguer and P. Jelen Eds. Elsevier Applied Science Publishers., London and New York.
- Jao, Y.C. & Chen, A.H. (1978). Engineering analysis of soy dough rheology in extrusion. *J. Food Process Eng.*, **2**:97-112.

- Jasberg, B.K.; Mustakas, G.C. & Bagley, E.B. (1981). Effect of extruder retention time on capillary flow of soy dough. *J. Food Process Eng.*, **5**:43-56.
- Johnson, R.K. (1970). Sodium caseinate, a production challenge overcome. *Food Technology in New Zealand*, **5**:465-467.
- Jordan, P.J. (1983). A vertical vat for washing of casein curd. *N.Z. J. Dairy Sci. Technol.*, **18**:27-33.
- Kao, S.V. & Allison, G.R. (1984). Residence time in a twin screw extruder. *Polymer Eng. Sci.*, **24**:645-651.
- Khalil, K.E., Ramakrishna, P., Nanjundaswamy, A.M. & Patwardhan, M.V. (1989). Rheological behaviour of clarified banana juice: Effect of temperature and concentration. *J. Food Eng.*, **10**:231-340.
- Khuri, A.I. & Colon, M. (1981). Simultaneous optimization of multiple responses represented by polynomial regression function. *Technometrics*, **23**:363-376.
- Khuri, A.I. & Cornell, J.A. (1987). *Response Surfaces, Designs and Analysis*. Marcel Dekker, Inc., New York.
- Kim, W.S., Skatschkow, W.W. & Jewmenow, S.D. (1973). Theoretisch beschreibung des mischprozesses in den schneckenkanalen von doppelschneckenextrudern. *Plaste und Kautschuk*, **20**: 696-702.
- Kim, B.Y. & Kinsella, J.E. (1989). Effect of temperature and pH on the coagulation of casein. *Milchwissenschaft*, **44**:622-625.
- Kinsella, J.E. (1984). Milk proteins: physicochemical and functional properties. *CRC Critical Reviews in Food Science and Nutrition*, **21**:197-262.
- Kinsella, J.E. & Fox, P.F. (1986). Water sorption by proteins: Milk and whey proteins. *CRC Critical Reviews in Food Science and Nutrition*, **24**:91-139.
- Kinsella, J.E., Whitehead, D.M., Brady, J. & Bringe, N.A. (1989). Milk proteins: Possible relationships of structure and function. In: *Developments in Dairy Chemistry-4*. P.F. Fox, ed., Elsevier Applied Science Publishers, London, pp. 55-95.
- Knightbridge, J.P. & Goldman, A. (1975). Water absorptive capacity of dried milk products. *N.Z. J Dairy Sci. Technol.*, **10**:152-157.
- Kudra, T., Raghavan, G.S.V., van de Voort, F.R. & Ramaswamy, H.S. (1989). Microwave heating characteristics of rutile. *American Society of Agricultural Engineers*, paper No. 893542.
- Kurmato, S., Jenness, R., Coulter, S.T. & Choi, R.P. (1959). Standardization of the Harland-Ashworth test for whey protein nitrogen. *J. Dairy Sci.*, **42**:28-38.
- Levenspiel, O. (1972). *Chemical Reaction Engineering*. John Wiley and Sons, New York.
- Levich, V.G., Markin, V.S. & Chismadzhev, Yu. A. (1967). On hydrodynamic mixing in a model of a porous medium with stagnant zones. *Chem. Eng. Sci.*, **22**:1357-1367.
- Levine, L., Symes, S. & Weimer, J. (1987). *Biotechnology progress*, **3**:221.

- Levine, L. (1988). Understanding extruder performance. *Cereal Foods World*, **33**:963.
- Lim, J.K., Wakamiya, S., Noguchi, A., & Lee, C.H. (1985). Effect of reverse screw elements on the residence time distribution in twin-screw extruder. *Korean J. Food Sci. Technol.*, **17**:208-212
- Linko, P. (1989). Extrusion cooking in bioconversions. In: *Extrusion Cooking*. C. Mercier, P. Linko and J.M. Harper, eds, American Association of Cereal Chemists, Inc. St. Paul, Minnesota, pp. 235-245.
- Lohrey, E.E. & Humphries. (1976). The protein quality of some New Zealand milk products. *N.Z. J. Dairy Sci. Technol.*, **11**:147-154.
- Luxenburg, L.A., Baird, D.G. & Joseph, E.G. (1985). Background studies in the modeling of extrusion cooking processes for soy flour doughs. *Biotechnology Progress*, **1**:33-38.
- Mackey, K.L.; Ofoli, R.Y.; Morgan, R.G. & Steffe, J.F. (1989). Rheology modeling of potato flour during extrusion cooking. *J. Food Process Eng.*, **12**:1-11.
- Maheshri, J.C. & Wyman, C.E. (1979). Mixing in intermeshing twin screw extruder chambers: streamlines and strain for down channel circulation. *Ind. Eng. Chem. Fundam.*, **18**:226-233.
- Maheshri, J.C. & Wyman, C.E. (1980). Mixing in an intermeshing twin screw extruder chamber: combined cross and down channel flow. *Polym. Eng. Sci.*, **20**:601-607.
- Mangé, C., Boissonat, P., & Gélus, M. (1987). Distribution of residence times and comparison of three twin-screw extruders of different size. In: *Extrusion Technology for the Food Industry*. C. O'Connor, ed, Elsevier Applied Science, London, pp.117-131.
- Martelli, F.G. (1983). *Twin Screw Extruders: A Basic Understanding*. Van Nostrand Reinhold Company, New York.
- McKelvey, J.M. (1962). *Polymer Processing*. Wiley and Sons, New York.
- Meuser, F., Pfaller, W. & van Lengerich, B. (1987). Technological aspects regarding specific changes to the characteristic properties of extrudates by HTST extrusion cooking. In: *Extrusion Technology for the Food Industry*. Colm O'Connor, ed., Elsevier Applied Science, London, pp. 35-70.
- Meuser, F., & Wiedmann, W. (1989). Extrusion plant design. In: *Extrusion Cooking*. C. Mercier, P. Linko & J.M. Harper, eds. American Association of Cereal Chemists, Inc. St. Paul, Minnesota, pp. 91-155.
- Millauer, C. (1986). The monitoring and control of an extrusion system. In: *Extrusion Technology for the Food Industry*. C. O'Connor, ed. Elsevier Applied Science, London, pp. 54-70.
- Morgan, R.G.; Suter, D.A. & Sweat, V.E. (1979). Modeling the effects of temperature-time history, temperature, shear rate and moisture on apparent viscosity of defatted soy flour dough. paper# 79-6002, presented at ASAE and CSAG meeting, Winnipeg, Canada.
- Morgan, R.G., Steffe, J.F. & Ofoli, R.Y. (1989). A generalized viscosity model for extrusion of protein doughs. *J. Food Process Eng.*, **11**:55-78.

- Mosso, K., Jeunink, J. & Cheftel, J.C. (1982). Température, pression et temps de séjour d'un mélange alimentaire dans un cuiseur-extrudeur bi-vis influence des paramètres opératoires. *Ind. Aliment. Agric.*, **99**:5-18.
- Muller, L.L. (1971). Manufacture and uses of casein and co-precipitate. *Dairy Science Abstracts*, **33**:659-674.
- Muller, L.L. (1982). Manufacture of casein, caseinate and co-precipitates. In: *Developments in Dairy Chemistry-1*. P.F. Fox, ed., Elsevier Applied Science Publishers, London, pp.315-337 London:
- Mulvihill, D.M. (1989). Caseins and caseinate: Manufacture. In: *Developments in Dairy Chemistry-4*. P.F. Fox, ed., Elsevier Applied Science Publishers, London, pp. 131-172.
- Muralidhara, H.S., Chauhan, S.P., Senapati, N., Beard, R., Jirjis, B. & Kim, B.C. (1988). Electroacoustic dewatering (EAD) a novel approach for food processing, and recovery. *Separation Sci. Technol.*, **23**:2143-2158
- Niro Atomizer (1976). *Analytical Methods for Dairy Milk Products*, 3^d ed., Niro Atomizer Ltd., Copenhagen.
- O'Meara, G.M. & Munro, P.A. (1982). The precipitation and shrinkage of acid casein curd: a preliminary study. *N.Z. J. Dairy Sci. Technol.*, **17**:147-159.
- Olkku, J., Hassinen, H., Antila, J., Pohjanpalo, H. & Linko, P. (1980a). Automation of HTST-extrusion cooker. In: *Food Process Engineering*. Vol.1. P. Linko, Y. Malkki, J. Olkku and J. Larinkari eds., Applied Science Publishers, London, pp. 777-790.
- Olkku, J., Antila, J., Heikkinen, J. & Linko, P. (1980b). Residence time distribution in twin-screw extruder. In: *Food Process Engineering- Vol. 1*. P. Linko, Y. Malkki, J. Olkku and J. Larinkari, eds., Applied Science Publishers, London, pp. 791-794.
- Owusu-Ansah, J., van de Voort, F.R. & Stanley, D.W. (1982). Effects of extrusion variables on moisture and extrusion crystallinity of corn starch. *Can. Inst. Food Sci. Technol. J.* **15**:257.
- Owusu-Ansah, J., van de Voort, F.R. & Stanley, D.W. (1983). Physico-chemical changes in cornstarch as a function of extrusion variables. *Cereal Chem.* **60**:319.
- Owusu-Ansah, J., van de Voort, F.R. & Stanley, D.W. (1984). Textural and microstructural changes in corn starch as a function of extrusion variables. *Can. Inst. Food Sci. Technol. J.* **17**:65
- Pearce, K.N., Johnstone, R.J. & Maccoll, A.J. (1987). Computer simulation of continuous multi-stage countercurrent washing of casein curd. *N.Z. J. Dairy Sci. Technol.*, **22**:49-66.
- Pinto, G. & Tadmor, Z. (1970). Mixing and residence time distribution in melt screw extruders. *Polym. Eng. Sci.*, **10**:279-288.
- Rao, M.A. (1986). Rheological Properties of fluid foods. In: *Engineering Properties of Foods*. M.A. Rao & S.S.H Rizvi, eds, Marcel Dekker, New York, pp. 1-47.
- Rauwendaal, C.J. (1981). Analysis and experimental evaluation of twin screw extruders. *Polym. Eng. Sci.*, **21**:1092-1100.

- Rauwendaal, C.J. (1986). *Polymer Extrusion*. Hanser Publishers, New York.
- Remsen, C.H. & Clark, J.P. (1978). A viscosity model for cooking dough. *J. Food Process Eng.*, **2**:39-64.
- Richert, S.H. (1975). Current milk protein manufacturing processes. *J. Dairy Sci.*, **58**:985-993.
- Roberts, S. A. & Guy, R. C. E. (1987). Metastable states in a food extrusion cooker. *J. Food Eng.* **6**:103.
- Roberts, S. A. & Guy, R. C. E. (1986). Instabilities in an extrusion-cooker: a simple model. *J. Food Eng.* **5**:7.
- Roeper, J. (1982). Recent experiences with a new drying technique resulting in casein products with improved physical and bacteriological qualities. *Bulletin, International Dairy Federation*. Doc. #147, 21-22.
- Rossen, J. L. & Miller, R. C. (1973). Food extrusion. *Food Technol. J.* **27**:46.
- Schenkel, G. (1966). *Plastics Extrusion Technology and Theory*. Iliffe, London.
- Schmidt, D.G. (1982). Association of caseins and casein micelle structure. In: *Developments in Dairy Chemistry-1*. P.F. Fox, ed., Elsevier Applied Science Publishers, London, pp. 61-86.
- Segalen, P. (1982). Caséines et caséinates, fabrication et utilisation. In: *Proteines Animales. Extraits, Concentrés et Isolats en Alimentation Humaine*, C.-M. Bourgeois et P. Leroux eds., Technique and documentation Lavoisier, Paris, pp. 155-171.
- Singh, R.P. (1983). Numerical techniques. In: *Computer-Aided Techniques in Food Technology*. I. Saguy ed., Marcel Dekker, New York.
- Southward, C.R. (1985). Manufacture and applications of edible casein products. I. Manufacture and properties. *N.Z. J. Dairy Sci. Technol.*, **20**:79-101.
- Southward, C.R. (1986). Utilization of milk components: casein. In: *Modern Dairy Technology Vol. 1. Advances in Milk Processing*. R.K. Robinson, ed., Elsevier Applied Science Publishers, London, pp.317-368.
- Srilaorkul, S.; Ozimek, L.; Wolfe, F. & Dziuba, J. (1989). The effect of ultrafiltration on the physicochemical properties of retentate. *Can. Inst. Food Sci. Technol. J.*, **22**:56-62.
- Stevens, M.J. (1985). *Extruder Principles and Operation*. Elsevier Applied Science Publishers, London.
- Stults, B. (1978). Food process instrumentation and control. *Food Technol. J.* **23**:22.
- Swaigood, H.E (1982). Chemistry of milk protein. In: *Developments in Dairy Chemistry-1*. P.F. Fox, ed., Elsevier Applied Science Publishers, London, pp. 1-59.
- Szpendowski, J., Smietana, Z. & Zuraw, J. (1983). Production of extrusion texturized protein preparations. *Milchwissenschaft*, **38**:577-581.
- Szydłowski, W. & White, J.L. (1987). An improved theory of metering in an intermeshing co-rotating twin-screw extruder. *Advances in Polymer Technol.*, **7**:177-183.

- Tayeb, J., Vergnes, B. & Della Valle, G. (1988a). Theoretical computation of isothermal flow through the reverse screw element of twin screw extrusion. *J. Food Sci.*, **53**:616-625.
- Tayeb, J., Vergnes, B. & Della Valle, G. (1988b). A basic model for a twin screw extruder. *J. Food Sci.*, **53**:1047-1056.
- Todd, D.B. & Irving, H.F. (1969). Axial mixing in a self-wiping reactor. *Chem. Eng. Progress*, **65**:184-89.
- Todd, D.B. (1975a). Mixing in twin screw extruders. *Polym. Eng. Sci.*, **71**:81-82.
- Todd, D.B. (1975b). Residence time distribution in twin screw extruders. *Polym. Eng. Sci.*, **15**:437-443.
- Tossavainen, O., Hakulin, S., Kervinen, R., Myllymäki, O. & Linko, P. (1986). Neutralisation of acid casein in a twin-screw cooking extruder. *Lebens.-Wiss. u.-Technol.*, **19**:443-447.
- Towler, C. (1974). Rheology of casein solutions. *N.Z. J. Dairy Sci. Technol.*, **9**:155-160.
- Towler, C. (1976). Conversion of casein curd to sodium caseinate. *N.Z. J. Dairy Sci. Technol.*, **11**:24:29.
- Towler, C. (1978). The manufacture and reconstitution characteristics of granular sodium caseinate. *N.Z. J. Dairy Sci. Technol.*, **13**:71-76.
- van de Voort, F.R. (1980). Evaluation of milkoscan 104 infrared milk analyzer. *J. Assoc. Off. Anal. Chem.*, **63**:973.
- van de Voort, F.R., Stanley, D.W. & Edamura, R. (1984). Improved utilization of dairy proteins: Coextrusion of casein and wheat flour. *J. Dairy Sci.* **67**:749.
- Walk, C.J. (1982). Residence time distribution of a counter-rotating non-intermeshing twin screw extruder. *S.P.E. ANTEC Tech. paper*, **28**:423-426.
- Werner, H. & Eise, K. (1979). An analysis of the conveying characteristics of twin-screw, co-rotating extruders. *S.P.E. ANTEC Tech. paper*, **25**:181-187.
- Wolf, D. & Resnick, W. (1963). Residence time distribution in real systems. *Ind. Eng. Chem Fundam.*, **2**:287-293.
- Wolf, D. & White, D.H. (1976). Experimental study of the residence time distribution in plasticating screw extruders. *AIChE Journal*, **22**:122-131.
- Wolf, D., Holm, N., & White, D.H. (1986). Residence time distribution in a commercial twin screw extruder. *Polym. Eng. Sci.*, **26**:640-646
- Wyman, C.E. (1975). Theoretical model for intermeshing twin screw extruders. *Polym. Eng. Sci.*, **15**:606-611
- Yacu, W.A. (1985). Modelling a twin screw co-rotating extruder. *J. Food Process Eng.*, **8**:1-21.

Zadow, J.G. (1971a). Some theoretical aspects of casein washing: Part I. *Australian J. Dairy Technol.*, **26**:9-13.

Zadow, J.G. (1971b). Some theoretical aspects of casein washing: Part II. *Australian J. Dairy Technol.*, **6**:14-17.

Zuilichem, D.J.v., de Swart, J.G. & Buisman, G. (1973). Residence time distributions in an extruder. *Lebensm.-Wiss. u.-Technol.*, **6**:184-189.

Zuilichem, D.J.v., Jager, T., Stolp, W. & de Swart, J.G. (1988a). Residence time distribution in extrusion cooking. Part I: Coincidence detection of radiotracer. *J. Food Eng.*, **7**:147-158.

Zuilichem, D.J.v., Jager, T., & Stolp, W. (1988b). Residence time distribution in extrusion cooking. Part II: Single screw extruders processing maize and soya. *J. Food Eng.*, **7**:197-210.

Zuilichem, D.J.v., Jager, T., Stolp, W. & de Swart, J.G. (1988c). Residence time distribution in extrusion cooking. Part III: Mathematical modelling of the axial mixing in a conical, counter-rotating, twin screw extruder processing maize grits. *J. Food Eng.*, **8**:109-127.

APPENDICES

Appendix [1]

A: Basic Program for data transfer from tape recording to IBM PC and conversion to APL readable format

```
10 PRINT "PROGRAM NAME:DATALOG.BAS"
20 PRINT "THIS PROGRAM TRANSFERS FROM TAPE THROUGH THE C20 AT 2400 BAUD"
30 PRINT " "
40 PRINT "SET C20 SWITCHES TO 1 0 0 0 1 1 FROM LEFT TO RIGHT"
50 PRINT " "
60 PRINT "CR7 DATA LOGGER DATA TRANSFER PROGRAM"
70 PRINT " "
80 INPUT "HOW MANY MEASUREMENTS IS THE DATA LOGGER RECORDING?";N
90 N=N*10
100 REM - A VALUE OF 10 IS USED BECAUSE EACH DATA POINT USES 10 BYTES
110 DIM A$(N)
120 PRINT "TEST PROGRAM FOR COMMUNICATION BETWEEN DATA LOGGER AND
COMPUTER"
130 A=0
140 OPEN "COM1:2400,E,7,2" AS #2
150 REM COMMUNICATION WITH C20 DATA TRANSFER UNIT ESTABLISHED
160 INPUT "ENTER FILENAME IN WHICH DATA IS TO BE PLACED";F$
170 PRINT " "
180 PRINT "RESET C20 -TURN ON TAPE RECORDER -CAN ABORT DATA TRANSFER"
190 PRINT "WITH A CTRL BREAK AND TYPING RUN 710"
200 OPEN F$ FOR OUTPUT AS #1
210 REM OPEN A FILE FOR DATA TO BE PLACED
220 PRINT #2,A$
230 REM READS DATA FROM C20 UNIT
240 A=A+1
250 LINE INPUT #2, A$
260 REM WRITES DATA TO FILE #2
270 PRINT A$
280 PRINT #1, A$
290 GOTO 220
300 PRINT #2, CHR$(27)
310 REM SHUTS OFF CASSETTE PLAYER AUTOMATICALLY
320 CLOSE #1
330 CLOSE #2
340 PRINT "DATA LOADING TERMINATED"
350 INPUT "ENTER NAME OF FILE TO BE CONVERTED TO APL";F$
360 INPUT "HOW MANY MEASUREMENTS WAS THE DATA LOGGER RECORDING?";N
370 N=N*10
380 REM BEGIN PROCESS OF REMOVING REDUNDANT DATA (I.E., CHANNEL#)
390 OPEN F$ FOR INPUT AS #1
400 OPEN F$+".DAT" FOR OUTPUT AS #2
410 REM ADD EXTENSION ".DAT" TO THE FILE FOR APL PROGRAM RECOGNITION
420 LINE INPUT #1, A$
```

```
430 IF EOF(1) GOTO 500
440 FOR I=1 TO N STEP 10
450 B$=MID$(A$,I+3,6)
460 REM CUT OFF EXTRANEIOUS DATA
470 PRINT #2,B$
480 NEXT I
490 GOTO 420
500 CLOSE #1
510 CLOSE #2
520 PRINT "DATA CONVERTED TO APL READABLE FORMAT"
530 INPUT "DO YOU WANT TO INSPECT THE DATE (Y/N)";ANSW$
540 IF ANSW$="n" GOTO 640
550 IF ANSW$="N" GOTO 640
560 INPUT "NAME OF THE FILE TO BE INSPECTED";F$
570 OPEN F$+".DAT" FOR INPUT AS #1
580 A=1
590 LINE INPUT #1,C$
600 A=A+1
610 PRINT C$
620 IF A=20 GOTO 640
630 GOTO 590
640 CLOSE #1
650 PRINT " "
660 INPUT "DO YOU WISH TO CONVERT ANY MORE FILES";ANSW$
670 IF ANSW$="y" GOTO 60
680 IF ANSW$="Y" GOTO 60
690 PRINT "END OF PROGRAM - GOING INTO STATGRAPHICS PROGRAM"
700 GOTO 790
710 REM -SHUTTING DOWN ROUTINE AFTER CTRL BREAK
720 OPEN "COM1:2400,E,7,2" AS #2
730 PRINT #2,CHR$(27) 'TELLS C20 TO STOP TAPE'
740 CLOSE #2
750 CLOSE #1
760 PRINT "DATA TRANSFER HALTED BY CTL BRK"
770 GOTO 350
780 PRINT "TO APL FORMAT"
790 SYSTEM
```

B: APL Program to convert the data to matrix form for plotting and analysis

```

[0] CONVERT
[1] 'PROGRAM CONVERT - USED TO CONVERT VECTOR DATA FROM AN UNFORMATTED'
[2] 'READ OF DATA OBTAINED FROM C20 CONVERTER USING A BASIC PROGRAM'
[3] , ,
[4] 'ENTER THE VARIABLE NAME OF DATA GIVEN IN THE UNFORMATTED READ'
[5] □PP+6
[6] V←□
[7] , ,
[8] 20ρV
[9] , ,
[10] 'THESE ARE THE FIRST 20 DATA POINTS IN THE VECTOR'
[11] , ,
[12] 'ENTER THE NUMBER OF ELEMENTS TO BE DROPPED FROM THE FRONT END OF
VECTOR'
[13] D←□
[14] V←D↓V
[15] , ,
[16] 'THE REVISED FRONT OF THE VECTOR IS'
[17] 20ρV
[18] , ,
[19] , ,
[20] 'THESE ARE THE LAST 20 DATA POINTS IN THE VECTOR'
[21] , ,
[22] REVERSE←ϕV
[23] REVERSE←20ρREVERSE
[24] REVERSE←ϕREVERSE
[25] REVERSE
[26] , ,
[27] 'ENTER THE NUMBER OF ELEMENTS TO BE DROPPED (NEGATIVE NUMBER)'
[28] D←□
[29] V←D↓V
[30] , ,
[31] REVERSE←ϕV
[32] REVERSE←20ρREVERSE
[33] REVERSE←ϕREVERSE
[34] 'THE REVISED BACK END OF THE VECTOR IS:'
[35] , ,
[36] REVERSE
[37] , ,
[38] 'THE NUMBER OF ELEMENTS IN THE CONVERTED VECTOR IS:'
[39] ρV
[40] , ,
[41] 'ENTER THE NUMBER OF MEASUREMENTS MADE WITH DATA LOGGER'
[42] , ,
[43] COL←□
[44] ROW←(ρV)÷COL
[45] FIX←ROW,COL
[46] M←FIXρV

```

```

[47] , ,
[48] , ,
[49] , ,

[50] 'CONVERTING TIME (CHANNEL 3 & 4) TO DECIMAL FORMAT'
[51] '-----'
[52] M3←M[;3] M4←[;4]
[53] M2←100 100 τM3
[54] M21←M2[1;] M22←M2[2;]
[55] M21←M21x60
[56] M4←M4÷60
[57] 'DECIMAL TIME IN MIN'
[58] M1←M22+M21+M4
[59] , ,
[60] M1
[61] R←ρM1 MI←⌊/M1
[62] MF←RρMI
[63] M34←MI-MF
[64] , ,
[65] 'CHANGE OF SCALE, ORIGIN AT 0 MIN'
[66] M34
[67] , ,
[68] 'THE DATA IS STORED AS A MATRIX CALLED \M\
[69] 'ONE CAN ACCESS A SPECIFIC VECTOR X FROM \M\ BY ASKING FOR \M[;X]'
[70] M[;3]←M34
[71] 'THIS WILL TAKE A MOMENT - - BE PATIENT'
[72] , ,
[73] 'F0.3' FMT M
[74] , ,
[75] , ,
[76] 'THE DATA IS STORED IN A VARIABLE "M" '
[77] 'RENAME THE VARIABLE TO AVOID FUTURE CONFLICTS'
[78] , ,
[79] , ,
[80] 'ANY MORE CONVERSION REQUIRED? (Y/N)'
[81] ANS←□
[82] →(ANS='Y')ρ1
[83] , ,
[84] 'END OF PROGRAM'
[85] ▽

```

Appendix [2]

Experimental design and the multiresponse experimental data obtained for skim milk coagulation/washing process.

X_1 =pH, X_2 =Temperature ($^{\circ}$ C), X_3 =Concentration(%), X_4 =Washing time (min), X_5 =Mixer speed (rpm), X_6 =Wash water ratio (g/g), Y_1 =Fines (%), Y_2 =Ash (%), Y_3 =Lactose (%), Y_4 =Calcium (mg/g), Y_5 =Sodium (mg/g), Y_6 =Whey protein nitrogen (mg/g), Y_7 =Water holding capacity (%).

X_1	X_2	X_3	X_4	X_5	X_6	Y_1	Y_2	Y_3	Y_4	Y_5	Y_6	Y_7
-1	-1	-1	-1	-1	-1	1.48	1.53	0.300	11.50	0.086	1.920	66.9
1	-1	-1	-1	1	-1	3.97	2.58	0.114	9.26	0.054	1.745	76.0
-1	1	-1	-1	1	-1	1.36	1.27	0.182	8.61	0.057	1.920	73.3
1	1	-1	-1	-1	-1	7.47	2.40	0.334	8.96	0.050	1.809	73.1
-1	-1	1	-1	-1	1	6.27	2.91	1.050	0.40	0.210	4.267	74.9
1	-1	1	-1	1	1	8.41	3.87	0.123	0.72	0.158	2.293	74.1
-1	1	1	-1	1	1	7.84	2.62	0.159	0.61	0.147	1.880	74.2
1	1	1	-1	-1	1	5.54	4.23	0.680	0.45	0.210	2.150	73.9
-1	-1	-1	1	-1	1	1.73	1.85	0.103	0.26	0.232	3.244	79.5
1	-1	-1	1	1	1	4.64	2.29	0.086	0.44	0.197	2.657	78.8
-1	1	-1	1	1	1	1.59	1.40	0.103	0.31	0.217	1.975	79.6
1	1	-1	1	-1	1	8.41	2.09	0.101	0.34	0.223	2.895	79.8
-1	-1	1	1	-1	-1	6.94	2.81	0.532	1.44	0.071	2.570	75.6
1	-1	1	1	1	-1	12.20	3.80	0.134	2.10	0.062	2.586	76.3
-1	1	1	1	1	-1	8.67	2.66	0.248	2.06	0.085	2.372	78.0
1	1	1	1	-1	-1	4.90	4.10	0.288	2.26	0.083	2.705	73.9
0	0	0	0	0	0	1.63	3.45	0.197	2.74	0.107	3.300	77.1
0	0	0	0	0	0	1.24	3.25	0.270	3.28	0.074	3.109	75.8
-1	-1	-1	-1	1	1	3.00	1.72	0.087	2.51	0.087	3.633	77.9
1	-1	-1	-1	-1	1	6.86	2.49	0.108	0.99	0.106	2.697	77.1
-1	1	-1	-1	-1	1	1.89	1.33	0.120	0.34	0.233	3.617	77.7
1	1	-1	-1	1	1	5.97	2.17	0.132	0.43	0.178	3.443	77.5
-1	-1	1	1	1	-1	9.37	2.57	0.888	0.47	0.226	3.260	78.9
1	-1	1	-1	-1	-1	7.72	4.52	0.433	0.19	0.197	2.705	78.8
-1	1	1	-1	-1	-1	3.30	2.50	0.352	0.53	0.187	3.221	77.3
1	1	1	-1	1	-1	10.50	3.89	0.559	0.89	0.104	2.150	74.2
-1	-1	-1	1	1	-1	2.80	1.57	0.172	1.83	0.084	1.904	74.3
1	-1	-1	1	-1	-1	1.75	1.51	0.097	0.55	0.106	1.825	74.6
-1	1	-1	1	-1	-1	1.75	1.51	0.157	12.15	0.126	2.943	67.2
1	1	-1	1	1	-1	6.30	2.11	0.126	11.37	0.118	2.332	64.3
-1	-1	1	1	1	1	12.40	1.94	0.134	11.18	0.104	1.738	72.5
1	-1	1	1	-1	1	11.60	4.06	0.136	9.06	0.071	1.975	74.4
-1	1	1	1	-1	1	6.39	2.43	0.207	0.30	0.226	2.602	80.5
1	1	1	1	1	1	9.16	3.66	0.122	1.86	0.128	2.427	76.1
0	0	0	0	0	0	1.22	3.10	0.236	5.42	0.055	2.031	70.4
0	0	0	0	0	0	1.26	3.25	0.234	7.32	0.070	2.832	65.9
-2	0	0	0	0	0	8.05	1.64	0.257	0.47	0.206	3.823	73.9

2	0	0	0	0	0	18.20	2.70	0.312	12.81	0.058	1.722	77.1
0	-2	0	0	0	0	1.24	3.10	0.179	9.02	0.084	4.014	67.0
0	2	0	0	0	0	1.38	3.12	0.242	3.42	0.063	2.396	71.6
0	0	-2	0	0	0	1.44	1.95	0.055	5.41	0.066	2.309	69.6
0	0	2	0	0	0	13.7	4.49	0.188	3.33	0.086	2.586	68.2
0	0	0	-2	0	0	1.34	3.39	0.548	8.90	0.095	4.220	65.1
0	0	0	2	0	0	1.56	2.71	0.087	5.17	0.073	3.062	69.7
0	0	0	0	-2	0	0.88	3.19	0.205	7.58	0.044	2.039	69.7
0	0	0	0	2	0	3.10	2.84	0.092	7.28	0.097	2.158	69.9
0	0	0	0	0	-2	1.18	3.45	0.473	7.51	0.050	1.872	69.6
0	0	0	0	0	2	1.82	3.06	0.153	6.02	0.061	2.078	66.6
0	0	0	0	0	0	1.41	3.29	0.227	6.32	0.066	1.967	67.3
0	0	0	0	0	0	1.35	3.27	0.230	6.94	0.064	2.356	68.1

Appendix [3]

General SAS program used for the Extended Surface Response Procedure (ESRP) for multiresponse optimization.

```

OPTIONS LINESIZE=72
        PAGESIZE=66;

DATA CAS;
  INFILE DATA;
  INPUT X1 X2 X3 X4 X5 X6 Y1 Y2 Y3 @@;

DATA B; SET CAS END=EOF; OUTPUT;
  IF EOF THEN DO; Y1=.; Y2=.; Y3=.; *Y1=FINES Y2=ASH Y3=LACTOSE*;
    DO X1=-2 TO 2 BY V1;
      DO X2=-2 TO 2 BY V2;
        DO X3=-2 TO 2 BY V3;
          DO X4=-2 TO 2 BY V4;
            DO X5=-2 TO 2 BY V5;
              DO X6=-2 TO 2 BY V6;
                OUTPUT;
              END;
            END;
          END;
        END;
      END;
    END;
  END;

PROC RSREG DATA=B OUT=C;
  MODEL Y1 Y2 Y3=X1 X2 X3 X4 X5 X6/PREDICT;

DATA D; SET C;
  IF Y2<K1; IF Y3<K2;

PROC SORT DATA=D; BY DESCENDING Y1;
PROC PRINT DATA=D;
RUN;
ENDSAS;

```

Remarques:

- $0 < V_n$ ($n=1,2,\dots,6$) < 1
- K_1 and K_2 are minima tolerated for ash and lactose, respectively.
- X_1 - X_6 could be restricted to smaller interval, i.e. $[-1,0.5]$ instead of $[-2,2]$. X_1 - X_6 definitions are given in Appendix [2].

Example: Program used for run #1 in Table 8 (section 3.4.3).

```
OPTIONS LINESIZE=72
        PAGESIZE=66;
```

```
DATA CAS;
  INFILE DATA;
  INPUT X1 X2 X3 X4 X5 X6 Y1 Y2 Y3 @@;
```

```
DATA B; SET CAS END=EOF; OUTPUT;
  IF EOF THEN DO; Y1=.; Y2=.; Y3=.; *Y1=FINES Y2=ASH Y3=LACTOSE*;
  DO X1=-1 TO 0 BY 0.1;
    DO X2=-2 TO 2 BY 0.2;
      DO X3=-2 TO -0.5 BY 0.1;
        DO X4=-1 TO 1 BY 0.1;
          DO X5=-1 TO 0 BY 0.1;
            DO X6=-1 TO 0 BY 0.2;
              OUTPUT;
            END;
          END;
        END;
      END;
    END;
  END;
END;
```

```
PROC RSREG DATA=B OUT=C;
  MODEL Y1 Y2 Y3=X1 X2 X3 X4 X5 X6/PREDICT;
```

```
DATA D; SET C;
  IF Y2<1.5; IF Y3<0.05;
```

```
PROC SORT DATA=D; BY DESCENDING Y1;
PROC PRINT DATA=D;
RUN;
ENDSAS;
```

Appendix [4]

Description of the twin screw extruder

The extruder used for coagulation and neutralization is a Baker Perkins MPF-50D with co-rotating and intermeshing screws. The drive system is 25 HP, 1750 rpm, constant torque, and with electrical and mechanical over-torque protection. The gearbox is designed to reduce the rpm from 1750 to 500 through a speed reducer/splitter and to have easy access to bearings, gears and shafts. The power rating is 25 HP at 500 rpm maximum output speed and the maximum operating pressure is 2000 psi. The extruder is equipped with a variable speed volumetric feeder, a variable speed and adjustable die-face cutter, three-headed injection pump to deliver liquids or slurries into the barrel, and a heat exchanger unit pre-assembled with all controls for the nine zones of barrel cooling. The independent heating/cooling zones offer precise control over the process temperature gradient. A panel control provides control of the barrel temperature profile, liquids flow rate, material feed rate, screw speed and gives readings about barrel and product temperatures at different zones, pressure at the die and percent torque.

The screws and the barrel are made from carbon steel No 4140. The MPF-50D can be dead-stopped at any stage and the horizontally split barrel permits rapid access examination of internal product conditions and changes in screw configuration. Five alternative main feed port locations provide effective barrel process lengths of 25:1, 20:1, 15:1, 10:1, and 5:1 L/D, enabling the user to determine optimum chamber length for his particular application. Side feeder ports, allow separate downstream incorporation of heat or shear sensitive ingredients which could be damaged by exposure to the full heat history of the main substance. Injection ports are located in a number of points along the barrel for direct incorporation of liquids or slurries and the barrel temperature may be controlled in nine zones along the barrel.

The screws can be configured in various ways depending of the particulate process, using feed screws, bi-lobal paddles, short pitch screws, and single lead screws. The function of feed screws are to convey the material downstream to the mixing zone. These screws have a double lead with a pitch of one diameter. Paddles are the primary working component of an agitator assembly. These provide very good mixing and generate the interparticulate friction within the product which converts the mechanical energy into heat. Several relative orientations are possible to have forwarding or reverse actions with different degrees of conveying ability. The conveying ability is from best to least: 30°F > 45°F > 60°F > 90°F > 60°R > 45°R > 30°R (F=forward, R=reverse). The short pitch screws are generally used at the beginning of mixing zone after the feed screws which help to cut the material and improve the subsequent mixing. The single lead screws (discharge screws) are designed to have good

positive conveying action and high pressures at the die exit, but also contribute to the mixing action. Because of their importance in modelling, the dimensions of single lead screws are given below along with some barrel characteristics:

Variable	Symbol	value
Major diameter	(D_1)	50.2 mm
Root diameter	(D_r)	28.6 mm
Channel depth	(H)	11.1 mm
Tip width	(e)	2.6 mm
Channel bottom width	(E)	5.3 mm
Distance between screw shafts	(C_L)	40.0 mm
Helix angle	(ψ)	4.6°
Tip area	(A_t)	16.7 cm ²
Root area	(A_r)	18.0 cm ²
Volume	(V_s)	51.5 cm ³
Barrel diameter	(D)	50.8 mm
Barrel volume*	(V_b)	322 cm ³
Barrel surface area*	(A_{bs})	213 cm ²

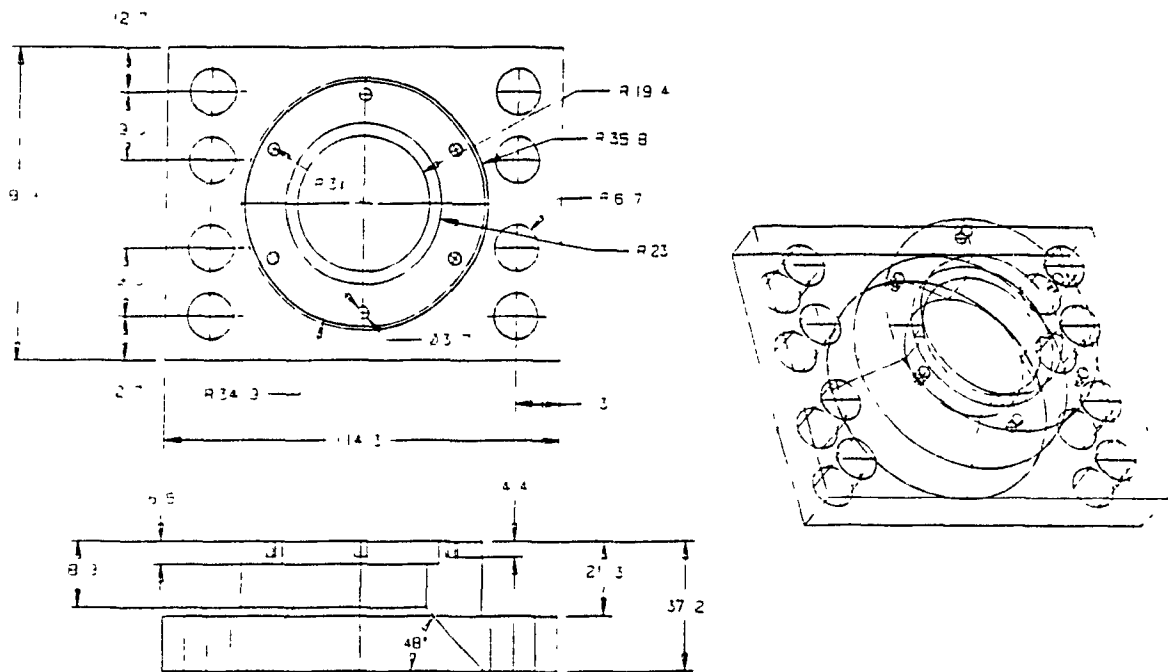
* For a barrel having 25:1 L/D

Within the screw profile, orifice plugs may be used to hold product in the cooking section. The orifice plug diameter determines the relative filled length within the section immediately upstream of the orifice plug. The filled length influences the amount of work done on the feed material (i.e. the larger the orifice plugs, the greater the filled length resulting in increased residence time in the paddles section and, therefore, greater energy input). In conjunction with orifice plugs, the barrel valve assembly must be used which allows the external adjustment of the filled length. Opening the barrel valve vane allows material to flow over and between orifice plugs. This adjustment is continuously variable for fine tuning, whereas the orifice plug size is a stepwise, more coarse adjustment. A die plate should be attached to the barrel which has a combined product temperature and pressure sensing port and allows cooling of the product at the exit, if necessarily, by an independent water circulation. Die orifices with different geometries may be inserted in the die plate.

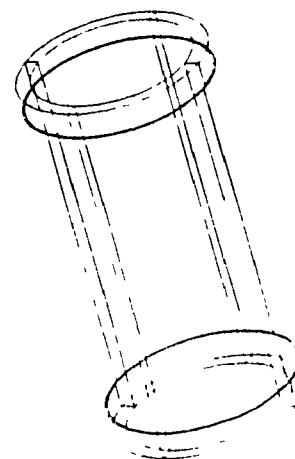
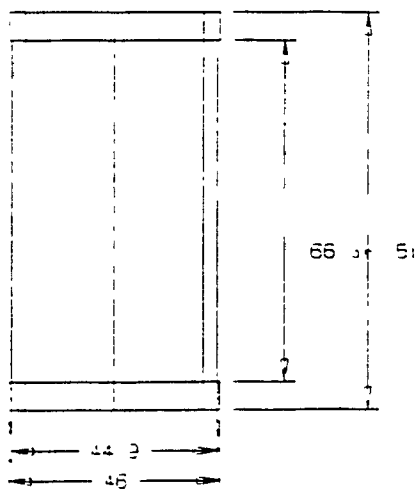
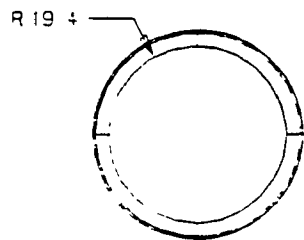
Appendix [5]

Schematic drawing of each part of the extruder dewheying die given in Figure 29 and discussed in Chapter 3.5 (dimensions are in mm)

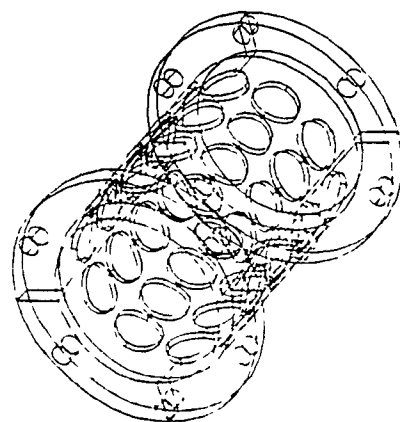
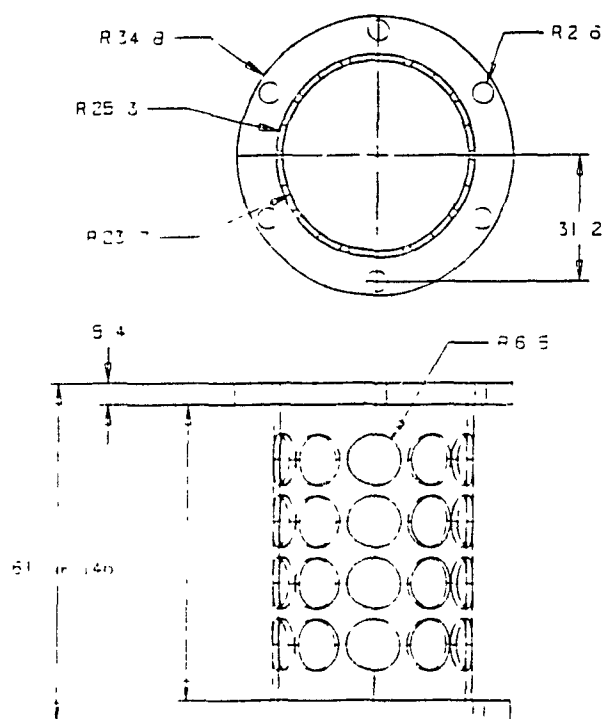
A: Schematic drawing of the die plate



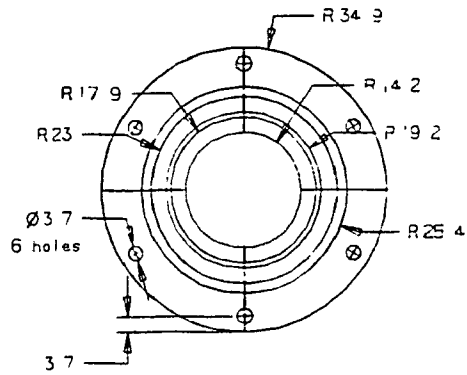
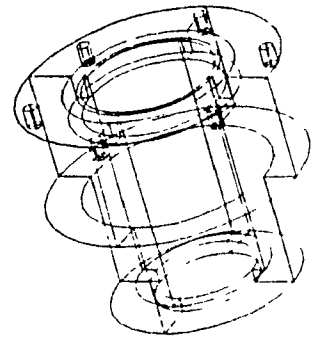
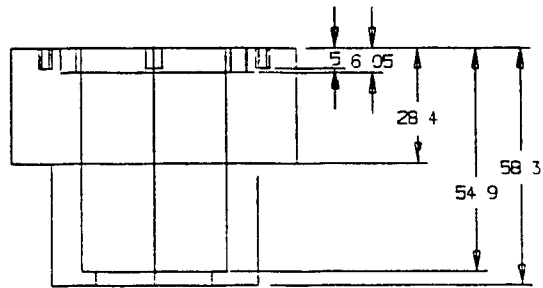
B: Schematic drawing of the cylindrical screen



C: Schematic drawing of the perforated pipe



D: Schematic drawing of the die orifice holder



E: Schematic drawing of the die orifice

